Tsunami impact analysis in Coquimbo Bay

Multidisciplinary approach to mitigate future tsunami hazards

I. van den Berg
R.J. Daals
C.E.M. Heuberger
S.P. Hildering
B.E. van Maris
C.M. Smulders

TU Delft UCSC

Tsunami impact analysis in Coquimbo Bay

Multidisciplinary approach to mitigate future tsunami hazards

by

I. van den Berg	4178300
R.J. Daals	4090381
C.E.M. Heuberger	4166272
S.P. Hildering	4159438
B.E. van Maris	4143450
C.M. Smulders	4211855

to carry out a multidisciplinary project
at Universidad Católica de la Santísima Concepción,
supervised by the Delft University of Technology.

Project duration:	September 3, 2016 – October 28, 2016	
Project committee:	Ir. H.J. Verhagen,	TU Delft
	Dr. ir. M.A.N. Hendriks,	TU Delft
	Prof. dr. ir. R.E. Aránquiz M.,	UCSC
	Dr. ir. C.A. Oyarzo V.,	UCSC

Preface

Before you lies the report of our multidisciplinary project in Chile; 'Tsunami impact analysis in Coquimbo Bay'. We conducted a research to improve the Coquimbo Bay welfare and safety. This project was carried out as part of our masters program at the Delft University of Technology. From the 3rd of September until the 28th of October 2016 we worked at Universidad Católica de la Santísima Concepción, where extensive knowledge about earthquakes and tsunamis is present.

In Concepción we were well guided by our supervisors Rafael Aránguiz and Claudio Oyarzo. Their thorough knowledge on the subject of earthquake resistant construction and tsunami simulations was our primary guidance. Fortunately they were always available and willing to answer our pending questions and to point us in the right direction. Likewise our supervisors in the Netherlands, Henk-Jan Verhagen and Max Hendriks, were always quick to answer our questions via email and they gave us wise advice and instruction when necessary.

We would like to thank our Chilean and Dutch supervisors for their time, involvement and support during our project. Furthermore, we would like to thank our sponsors for making this project possible and all our followers on Facebook and our website for their interest. You really motivated us to work on this project even harder to achieve even better results. A special word of thanks goes out to ing. Leo Kuljanski from Tensar for helping us with the design of the reinforced soil.

We especially thank Mary Hayes who helped us get our life in Chile arranged. You helped us manouvre through life in Chile by giving us a hand with housing, sporting, Spanish, places to go and visit and you even lent us your own bicyle to do our groceries.

Of course, we would also like to thank our families for their unconditional love and support, although we had to miss you for so long. Your countless phonecalls, motivating messages and kind words kept us going.

We hope you enjoy reading.

I. van den Berg
R.J. Daals
C.E.M. Heuberger
S.P. Hildering
B.E. van Maris
C.M. Smulders
Concepción, October 2016

Outline of the report

The report consists of 4 main parts; Development Coquimbo Bay, Coastal protection, Altamar highrise and Master plan. In chapter 1 Introduction, the project area and objective is initiated.

Part I, Development Coquimbo Bay, discusses the scope area in its entirety. Chapter 2 analyses all aspects of the project area and the effects of the tsunami of September 2015 on the area. The goal to realise an integral solution for the area as a whole is accomplished by creating 5 different alternatives, which are described in chapter 3. To do so, already different mitigation measures that are discussed later in part II are implemented. Subsequently, by making use of the NEOWAVE software these different alternatives are simulated in order to be able to compare the effects of the alternatives on a possible future tsunami. Chapter 4 describes this process and presents the most relevant results. Additionally, in chapter 5 the alternatives are compared on other aspects as well by using a multi criteria analysis. Also the costs of the different alternatives are estimated. Chapter 6 concludes the first part with the choice of the final alternative.

The second part, Coastal protection, describes the preliminary design of the coastal protection of the best alternative. In chapter 7 different possible mitigation measures for the coastal defense of the specific alternative are proposed. The different options are simulated of which the results are presented in chapter 8 and evaluated in chapter 9. In chapter 10 a proposal for a specific coastal protection is made.

The third part of the report, Altamar highrise, contains a detailed evaluation of the Altamar highrise, that is located in the project area as a possible vertical evacuation refuge. Chapter 11 analyses all relevant aspects of the building and the effects of the previous tsunami of September 2015. A model of the building has been created using the official structural drawings and information complemented with some assumptions, this process is described in chapter 12. The building is loaded by an earthquake followed by tsunami forces, which are described in chapter 13. After evaluation of the results in chapter 14 a conclusion is drawn about the possibility of the Altamar building as a vertical evacuation refuge in chapter 15.

In the fourth part of the report, Master plan, all aspects of the research come together. The chosen alternative, mitigation measure and the conclusion about the Altamar building are combined to make an overall evacuation plan for the area in chapter 16. The final configuration of the whole area is summarised and presented visually in chapter 17. Finally, several recommendations are presented in chapter 18 concerning the different topics of the project.

Summary

Coquimbo is a port city approximately 400 km north of Santiago and lies next to La Serena. Coquimbo was recently hit by a tsunami on the 16th of September 2015. Most damage occurred in Coquimbo Bay, which is the scope area of this project. The area consists of a beach, a damaged seawall, wetlands, and the Altamar highrise. Due to the damage caused by the previous tsunami and the poor socioeconomic background of the surrounding neighborhood called Baquedano, the Chilean authorities are planning to redevelop the area. In front of Coquimbo a large seismic gap exists since 1922, which makes the probability of an earthquake and corresponding tsunami in the near future very high. This situation leads to the attention for the project; to find a new and integrated purpose of the project area, enhancing public values and improve the safety concerning a possible future tsunami.

Functional aspects for the area as improving the safety against tsunamis, redeveloping the ecology of the wetlands, and increasing the welfare of the neighborhood results into 5 alternatives. With the NEOWAVE software a tsunami generation, propagation and impact is modeled. The bathymetry is modified conform the different alternatives for the Coquimbo Bay area and a realistic earthquake scenario is chosen to model the inundation depth and flow velocity of the tsunami impact. Inundation maps and flow velocity data measured at important tide gauges provide information about the tsunami impact in the different alternatives. This information is used to assign a score to the safety criteria in the multi criteria analysis.

Besides safety, also nature & recreation, welfare of the neighborhood, visual hindrance, infrastructure, construction process, and durability & maintenance are criteria that are assessed from the stakeholders point of view. Based on the score from this multi criteria analysis, the costs of the alternatives and a preference for a multifunctional solution alternative II is chosen as the best integral solution. This alternative includes an elevated coastal road with floodgates to reduce overtopping and to control the return flow of a tsunami. The wetlands are to large extend restored to their former configuration and the dynamic behavior of the wetlands is stimulated.

Part of the coastal protection is defined as a multifunctional boulevard. For the remaining part of the coastal area 3 different possibilities are considered: a reflective L-Wall, a ground dam with a natural slope, or a dam of reinforced soil. Using NEOWAVE simulations the economically optimal height of the coastal protection is determined to be 5 m from sea level. With a coastal protection of this height an average maximum inundation of 2,72 m in the Baquedano area is expected. Besides that, the coastal protection retains the first out of 3 incoming tsunami waves which increases the evacuation time. All options for the configuration of the coastal road are conceptually designed, loaded with tsunami forces and checked for several failure mechanisms. It turns out that horizontal stability and rotational stability are the decisive failure mechanisms. Based on the lowest costs and the highest aesthetic implementation the option with reinforced soil is the best solution.

Furthermore the possibility of the Altamar highrise, which is located in the project area, as a vertical evacuation refuge is investigated. A model of the building is created in Etabs using the official structural drawings and information provided by the local authorities. Assumptions on the reinforcement ratios and several structural element dimensions are made due to limitations in project time. A non-linear time history analysis for the earthquake loading is performed using amplified records from the September 2015 earthquake. Subsequently the tsunami forces are modeled and applied.

A mesh refinement study and alpha-variation study are performed. The alpha factor determines the amount of numerical damping applied to solve the equilibrium equation in the non-linear time history analysis. Due to hardware limitations the mesh refinement study is not finished, but fortunately a value of 0 can be used for alpha which implies no numerical damping is necessary. The obtained model results are evaluated in terms of stability, displacements and story drifts. It is concluded that the Altamar building fulfills the structural demands and remains perfectly stable.

With the availability of an additional evacuation building a new evacuation plan for Coquimbo Bay is created. The new coastal protection decreases damage and the probability of loss of life by increasing the evacuation

time. New evacuation routes and a smaller inundation in the Baquedano area increase the safety for the area. It is recommended that further investigation should contain multiple tsunami scenarios with a finer grid size and a probabilistic calculation on the damage in the Baquedano area.

Sponsors

We would especially like to thank our sponsors: Arcadis, BAM, Sweco, Tensar, Fugro, and Bouwen Met Staal. They made this project possible with both financial support and their expertise. We are delighted with their involvement and interest in the project and in us as civil engineering students.

Contents

List of Figures

List of Tables

1 Introduction

The region of Coquimbo lies approximately 400 km north of Santiago. La Serena is its largest city and next to it lies the city Coquimbo with its seaport. The name Coquimbo means “place of calm water” in the native language and the coast is characterised by a long, flat and sandy beach, a good location for a port. However, bordering the Pacific Ocean the region has experienced many earthquakes and tsunamis in the last hundreds of years. The last significant earthquake and corresponding tsunami was on the 16th of September 2015. This tsunami had a maximum inundation height of 6.4 m and an inundation of 700 m. It caused a lot of destruction in the lower parts of the city and the existing seawall was demolished.

Studies (Aránguiz et al. [3]) have shown that the earthquake of September 2015 came from the Coquimbo-Illapel seismic region, which lies south of Coquimbo, and filled the seismic gap that existed since 1943. The seismic region north of this region is called the Copiapó-Coquimbo region, but this region hasn’t experienced significant seismic activity since 1922. In 1922 there was an earthquake of Mw 8,3 in this region, which was felt from Iquique to Concepción. The maximum tsunami height was 7 m and the tsunami had an inundation of 2 km. The lack of a significant tsunami from the Copiapó-Coquimbo region since 1922 suggests the possibility of a large earthquake and tsunami in the near future, which might cause more damage to Coquimbo than the September 2015 tsunami. When this knowledge is combined with the hypothesis that the 2015 tsunami did not release all stored energy along that fault line, the conclusion is that the risk of another big earthquake and accompanied tsunami is alarmingly high.

1.1. The project area

The situation mentioned above led to the attention for the project area, indicated in figure1.1, and its possibilities. Measurements and simulations (Aránguiz et al. [2]) after the September 2015 tsunami have shown that the wetlands have probably served as a buffer zone for the zone behind it. The river and part of the wetlands are a protected natural park at the moment, where birds live and breed. This might be good to preserve, maintain and integrate together with the rest of the area. However, at the moment homeless people have organized small shelters to live there scattered around.

The highrise building that is located in the area near the beach, indicated in figure 1.1, has survived the earthquake and tsunami and might serve as a vertical evacuation possibility in the future. There are plans to realise two more highrise buildings next to the existing Altamar building, but the communication between the different authorities and organizations seems to be lacking. These plans are not definite and the possibilities are plenty.

The demolished seawall needs replacement. This gives the opportunity to design a better and more long lasting one, integrating the area in front of the coastal road and the wetlands behind it. The neighbourhood behind the railway is poor and might have a lot to gain from the future developments in the area.

1.2. The objective

The main objective of the project is to find a new and integrated purpose of the project area, enhancing the public values and improve the safety concerning a possible future tsunami. To achieve this objective the river and its wetlands, the seawall and the possibilities for the Altamar building need to be analysed and new designs will be presented for the area as a whole or for subsections separately.

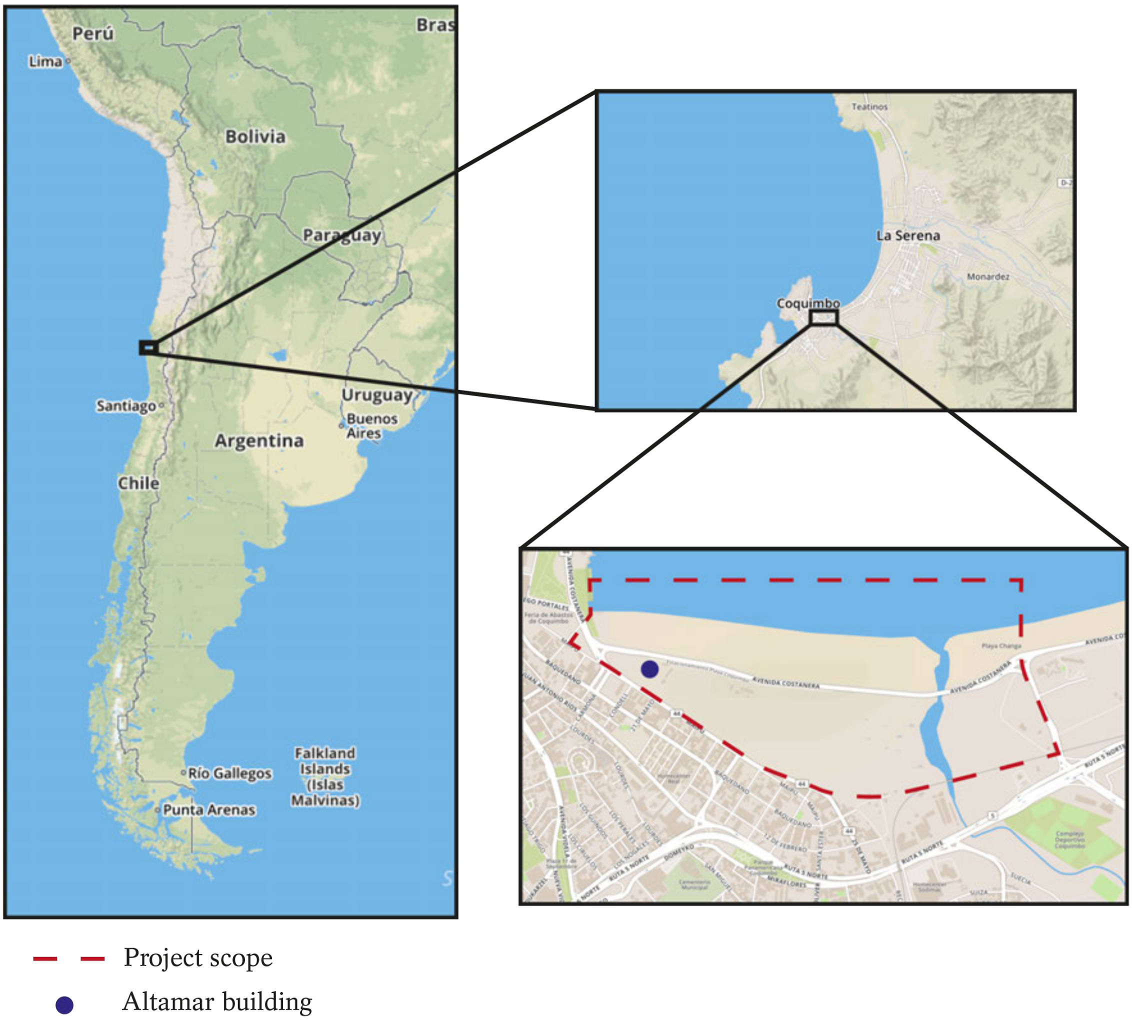

Figure 1.1: The location of the project area, source: Mapbox.com [29]

I

Development Coquimbo Bay

2
Analysis

This chapter describes the analyses of the complete project scope. In section 2.1 the project scope will be defined and the current situation will be explained. In section 2.2 there is an explanation of the generation and propagation of earthquakes and tsunamis. Section 2.3 elaborates on the social and economic aspects of the region. In section 2.4 the remaining boundary conditions are summarised. Finally in section 2.5 the risk analysis can be found.

2.1. Scope

In the problem statement a reference is made to the lower part of Coquimbo Bay as the area of interest. In this section the area of focus is defined. The project scope includes the wetlands, the Altamar highrise building, the coastal road (including primary sea defense), the beach and an area of approximately 100 m offshore. The southern boundary follows the railway that is situated here. In figure 2.1 the boundaries of the scope are displayed.

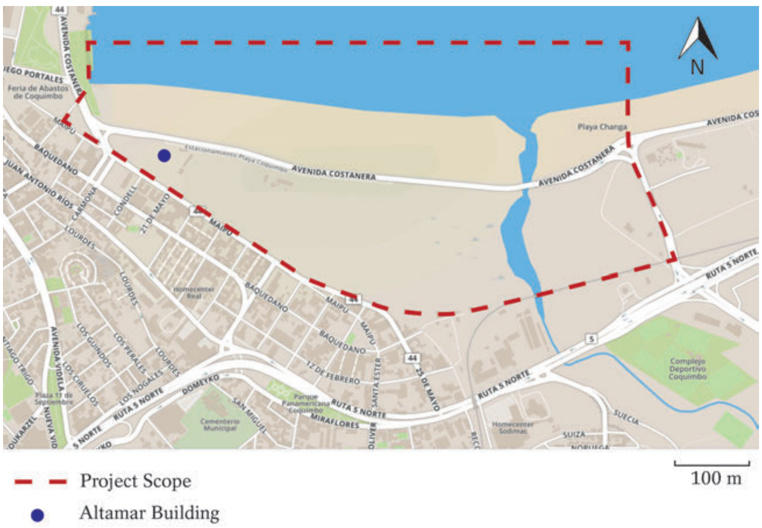

Figure 2.1: Scope area, source: Mapbox.com [30]

2.1.1. Bathymetry

For the analysis of the propagation of the tsunami the bathymetry is important. The bathymetry used in the NEOWAVE model is compiled out of nautical charts. In figure 2.2 the depth profile can be seen and figure 2.3 gives an overview of the exact location.

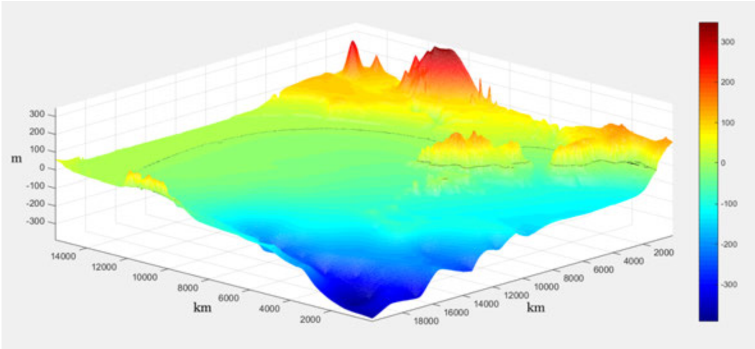

Figure 2.2: Bathymetry exracted from NEOwave model

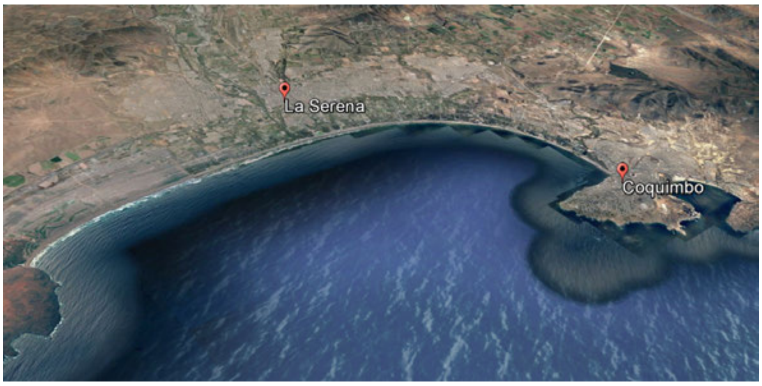

Figure 2.3: Overview Coquimo bay, source: Google Earth [19]

2.1.2. Wetlands

The region of Coquimbo has a very valuable network of coastal wetlands, all in proximity of population and therefore also known as the “urban wetland”. These wetlands are especially important because they are located in a semi-arid region where wetlands are scarce. They generate a biological corridor for a variety of migratory birds and offer a place for resting and nesting.

But for the public the area is perceived as a vacant site without any function. In combination with urban growth and intensified activities in the development of projects along the coastal edge, this has caused deterioration and induced a serious threat for this ecosystem (Claussen [7]).

The 2015 tsunami study (Aránguiz et al. [2]) shows that the wetlands have a buffer function with respect to the impact of the tsunami. The inundation behind the wetlands was evidently lower than in other parts. The full description of the impact of the tsunami of 2015 can be found in appendix C.

2.1.3. Seawall

Along the coastline Av. Costanera is located on an elevated embankment of approximately 1,5 meter. In front of this road there is a seawall constructed out of concrete en rocks. Due to the 2015 tsunami the seawall is significantly damaged. In appendix C the design of the current seawall is further discussed.

2.1.4. Altamar building

At this moment there is only one building located in the project area. This building is named Altamar and has 26 stories. During the most recent tsunami and earthquake the building did not suffer any structural damage. Therefore the building has the potential to become a vertical evacuation building. Whether this is possible will be further discussed in part III.

Currently there are plans to build two additional buildings next to the Altamar building. The construction has not started yet, but the apartments are already on the market to be rented. Therefore we will take these buildings into account during the project.

2.2. Earthquakes and tsunamis

To understand the the current seismic situation at the Chilean coast a short description about the origin of an earthquake and corresponding tsunami is presented. Furthermore, some historic events near the Coquimbo Bay area are analysed to gain insight in a possible future tsunami.

A tsunami is produced by a vertical displacement of a large amount of water. This displacement can be caused by several phenomena, but the most relevant one in the case of the Chilean coastline is earthquakes. In the case of converging tectonic plates, which is the case in Chile, the overriding plate bulges due to friction between the two plates. The location where this happens is called the fault. Faults can have lengths up to 1000 km. During this process the pressure increases until the overriding plate moves suddenly. This movement releases a huge amount of energy. A large volume of water is lifted by this movement and starts propagating as a tsunami. In figure 2.4 this whole process is illustrated.

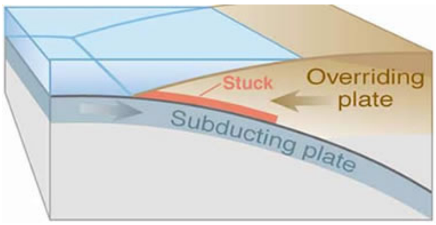

(a) Continental plate shoves beneath the oceanic plate

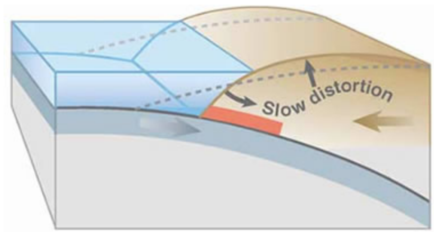

(b) Bulging of the continental plate

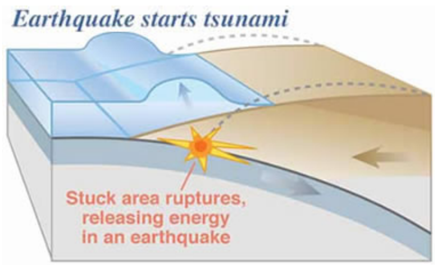

(c) Abrupt movement of the continental plate

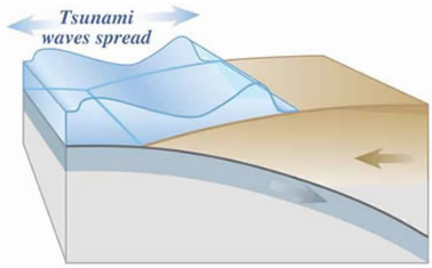

(d) Generation of a tsunam

Figure 2.4: Mechanism of the generation of a tsunami, source: Oregongeology.org [37]

After an earthquake has occurred, aftershocks are to be expected. The whole area in which these aftershocks take place is called the rupture area. It is important to note that the whole rupture area and not only the epicentre can be responsible for the generation of a tsunami. Furthermore, it is possible that a tsunami exists of several waves due to the aftershocks. The magnitude of an earthquake, which is directly related to the size of the tsunami, is defined in the following way:

$$
\begin{aligned}
M_w &= \frac{2}{3} \cdot (Log(M_0) - 9,1) \\
M_0 &= \mu \cdot L \cdot W \cdot D_0
\end{aligned}
\tag{2.1}
$$

Where
L = fault length
W = fault width
$D0$ = fault depth
μ = shear modulus of rock

The length, width, depth and friction modulus of the fault influence the magnitude of the earthquake as can be seen from equation 2.1. The parameters are illustrated in figure 2.5. With a combination of the convergence rate and the date of occurrence of an earlier earthquake, a prediction can be made about when a future earthquake will occur and what magnitude it will have.

In the past 400 years the earthquakes and tsunamis that occurred in front of the coast of Chile were well documented. An overview is given in figure 2.6 and appendix C. It can be observed that the rupture area

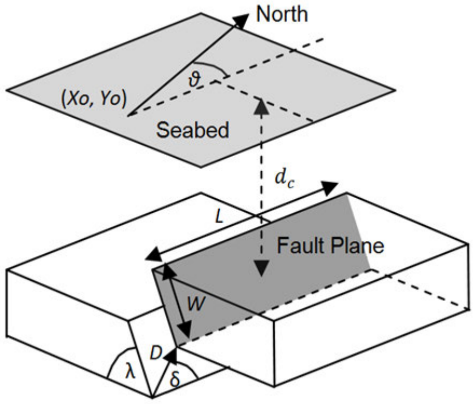

Figure 2.5: Fault plane, source: Aránguiz [1]

.

of earthquakes often partly coincides with the rupture area of a previous earthquake. The different colours indicate geographically different active rupture zones. With this knowledge it is possible to estimate the state of the different possible rupture areas and the probability of the occurrence of an earthquake. The period between earthquakes with the same rupture area is referred to as a seismic gap. The most recent tsunami which occurred in 2015, marked with a yellow star, closed the seismic gap in the region south of Coquimbo. However, it can be perceived that there is still a large seismic gap from the latitude -30° to -26° since the tsunami of 1922. The converging plates have been bulging for almost 100 years. The last seismic gap in this region was also a period of approximately 100 years, so therefore a tsunami of similar size to the one in 1922 could be expected in the upcoming decade.

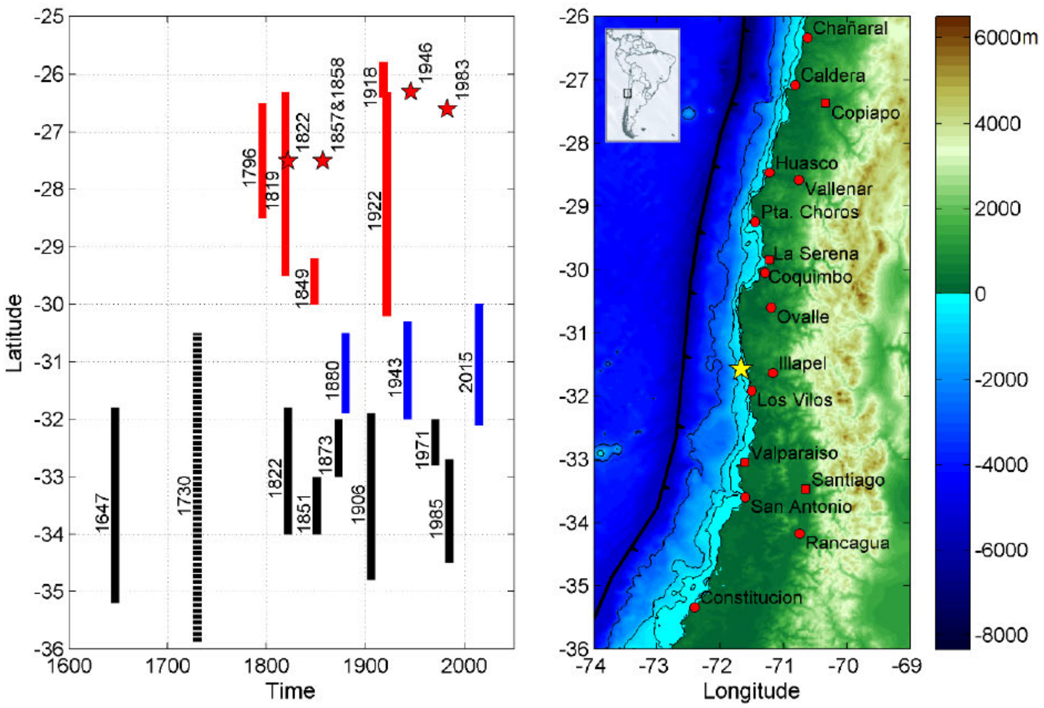

Figure 2.6: Seismic gaps, source: Aránguiz et al. [2]

.

2.3. Socioeconomic aspects

The geographic location enabled Coquimbo to develop as a port city. Because of the booming mining activities around 1840, Coquimbo became an export centre for the growing industry of gold and copper. Main activities in the Coquimbo region are mining, agriculture and fishing (Municipalidaddecoquimbo.cl [34]). The Port of Coquimbo is established as an independent enterprise and is located in the Coquimbo Bay. The port is an important link in the infrastructure.

2.3.1. Economy of Chile

It is estimated that one-half of all Chileans make less than 500 USD per month. According to the Organization for Economic Co-operation and Development (OECD), *"Chile is the OECD country with the greatest difference between the rich and poor, as well as the 4th poorest country of the 34 member states."* The Council on Hemispheric Affair states: *"Nine out of ten workers in Chile make less than the average minimum salary in developed countries"* (Hunziker [21]). According to Dr. R. Aránguiz the neighbourhood directly south of the project scope named Baquedano is a typical area where this poverty is recognizable.

2.3.2. Plan for Remodelling Urban Sector Baquedano

Due to the tsunami of September 2015 and more tsunamis in the past, the ministry of Housing and Urban Development in Coquimbo has developed a plan to renovate the area. The tsunami hazard is not the only reason that the neighbourhood will be renewed. The area has suffered degradation over last decades because of the intensification of industry and deterioration of the buildings. The ministry wants to improve the livability of the neighborhood and thereby also improve the security against tsunamis. A consultation with the local municipalities of La Serena confirms the vision of the government to improve the region of Coquimbo.

For the project there are elements that have to be taken into account in order to comply to the wishes of the government. The part of the plan of the ministry that is relevant to the project is presented below:

Figure 2.7: Overview of masterplan, source: Ministry of Housing and Urban development [32]

Important aspects from the master plan:

- A coastal wall will be built to increase the safety of the region and existing evacuation routes will be improved.
- There are no detailed realisation plans concerning the wetlands and the park. This leaves room to implement new ideas.
- The current houses will be replaced by housing built according to tsunami standards, implying that the first two floors of the buildings will not be used for residential purposes.

2.3.3. Stakeholders

With regard to the future plans of the lower part of Coquimbo Bay area, a renewal of the region can not be established without mapping and considering all the stakeholders. In figure 2.8 the power and interest of the stakeholders is summarised in a matrix. A further elaboration of the stakeholders is given in appendix B. The future plans of the surrounding area that are discussed in section 2.3.2 are the starting point for this analysis.

Figure 2.8 depicts a qualitative assessment of the power vs. the interest of the stakeholders. Since this analysis is partly subjective, this assesment only classifies the stakeholders in 4 global categories.

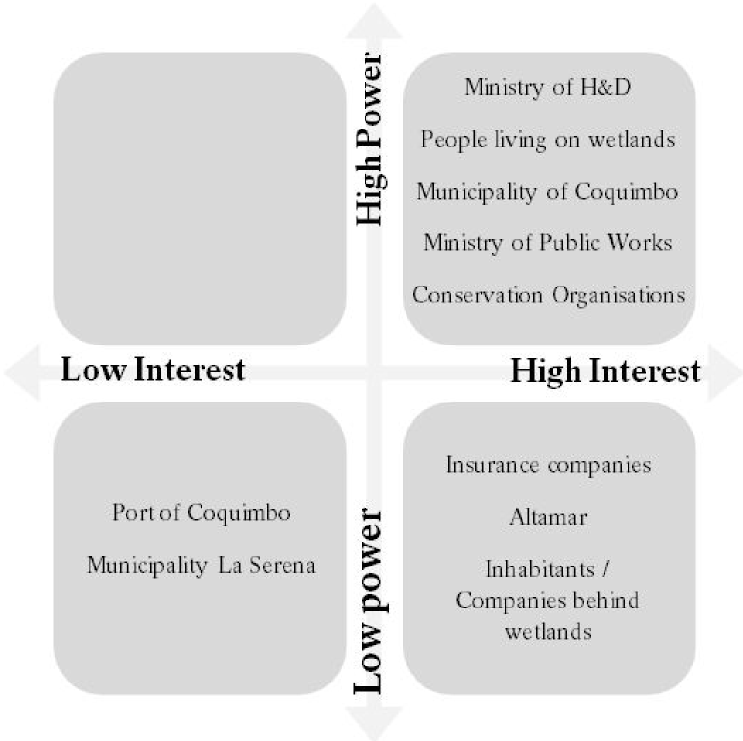

Figure 2.8: Matrix with the stakeholders.

2.4. Boundary conditions

The most important features of the boundary conditions of the area of interest are summarised in table 2.1. A detailed description of the boundary conditions can be found in appendix A.

Boundary condition	Property	Specific value(s) or description	Additional information
Coastal features	Type of coast	Leading edge	Low potential for storm surge
Soil properties	Layers of soil	0-7 m silty sand, 7 - 9,5 m silty clay, > 9,5 m silty sand	-
Tidal conditions	Tidal amplitude	1 m	Mainly semidiurnal
Wave conditions	Significant wave height	1-2 m	Mainly swell waves
Wind conditions	Maximum velocities	Not significant	-
Climate	Average temperature/rainfall	7-18° / 80 mm/y	Semi-desert climate
Morphology	Sediment transport rate	Not significant	-

Table 2.1: Boundary conditions

2.5. Risk analysis

Risk is defined as the damage times the probability (Jonkman et al. [26]). For the probability of the tsunami different studies have made a statistical calculation for the possibility of a future tsunami. In the scope of the project the probability will not be further discussed. Since mitigation measures won't influence the probability of a future tsunami it has no direct influence on the project. The potential damage is more interesting since this is within reach to adjust. The amount of damage can be divided in loss of life and a loss of economical value. Initially this damage will be correlated with the impact of the tsunami. The impact of the tsunami depends on the velocity, the water depth and the location of the tsunami impact. Different scenario's can be analysed to establish the different aspects of these components.

Other risks

Besides the risk of a tsunami which is the main topic of this report, other risks can be of importance. During the design of the alternatives for the scope area, the influence on other risks should be kept in mind. Examples of possible risks are the following:

- Storm surge
- Earthquake
- Social security / Crime
- Terrorism
- Traffic safety

3 Synthesis

In this chapter multiple alternatives will be proposed for the development of the project area. The focus lies on the functions of the different elements in the area. The actual design of the coastal protection is treated in part II. In section 3.1 an elaboration of these functional aspects is given. In the sections 3.2 to 3.6 the outlines of the different alternatives are explained and displayed in figures.

3.1. Functional aspects

It is desirable that a coastal protection contains more functions than only safety. This way the value of the design increases compared to designs which serve only for protection. An example of this can be seen in figure 3.1. The government is trying to improve the area of Coquimbo as can be seen in paragraph 2.3.2. Therefore presenting a multifunctional design is recommended.

Figure 3.1: A multifunctional solution in the form of a raised boulevard, picture made by: Reinier Daals

Multiple alternatives are developed to improve the project area. The main goal is to improve the safety of the lower part of Coquimbo bay. An additional target is to increase the welfare of the neighbourhood.

A potential function which could be included is tourism. In the nearby located city, La Serena, a well developed beach culture prevails and there might be possibilities to extend this to Coquimbo. The wetlands with a natural value should also be taken into account though.

With these function in mind and the applicable mitigation measures for the area, five alternatives were created.

3.2. Alternative I - Heightening of coastal road

A possible solution to protect the area is heightening the coastal road. An establishment of a new multi-functional boulevard could be combined with the heightening of the coastal road. Increasing the safety can this way be combined with a boost for the tourism and thereby stimulating the local economy.

The wetlands will be maintained, but will be further developed into a recognizable recreational area. In case of a large tsunami the coastal road may still be over topped. In this case the wetlands function as a buffer zone and the elevated railway at the end of the wetlands will prevent the water from entering the residential area. Figure 3.2 gives a plan overview of Alternative 1. Figure 3.3 gives the cross section of the alternative.

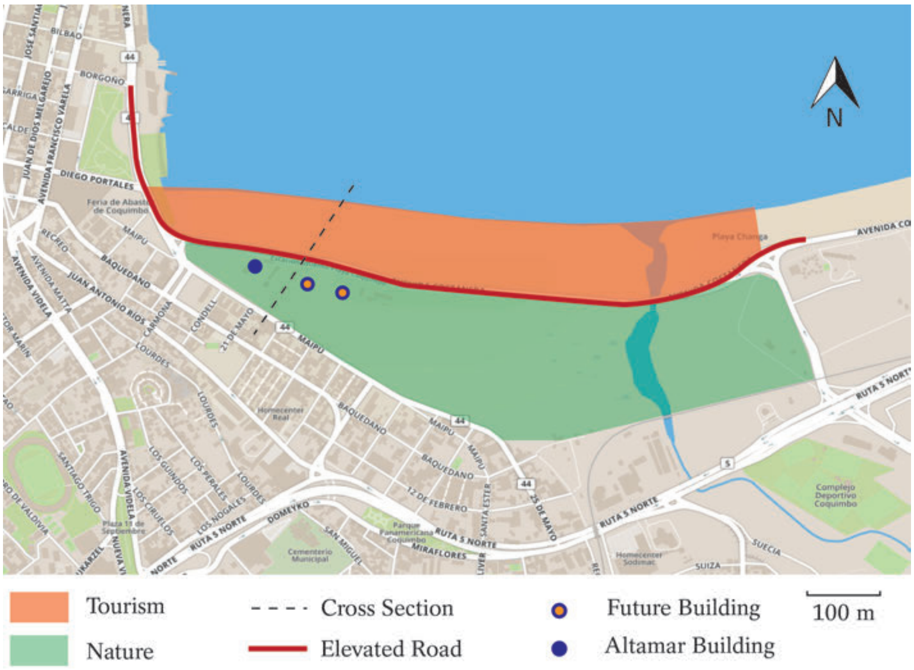

Figure 3.2: Alternative 1, source: Mapbox.com [30]

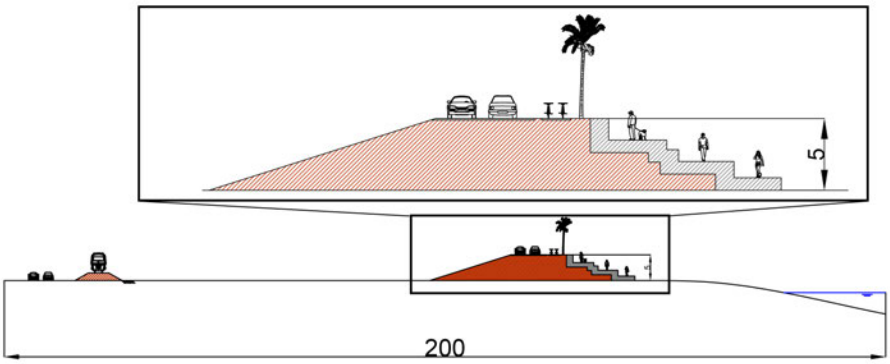

Figure 3.3: Cross section alternative 1, measurements in meters

3.3. Alternative II - Heightening of the coastal road with additional openings

Since the construction of the coastal road the wetlands have deteriorated considerably (Claussen [7]). This deterioration has been caused by the barrier that the road forms between the wetlands and the sea and has caused a decrease of wet surface in the wetlands. An elevation of the road will increase the barrier, but by adding openings in the barrier the amount of wet surface can largely be restored to the way it used to be. More information on this can be found in appendix D. This way the ecological value of the area can be restored which will make it more attractive.

In case of a tsunami water will flow through the openings. This will increase the amount of water that flows into the wetlands, but will decrease the amount of overtopping. Overtopping of the road could be the cause of unexpected scour, which could be prevented this way. Inside the openings the flow velocities will be high, therefore scour protection must be applied in this area. Otherwise the scour will undermine the structure and cause it to fail. However a good estimation of the locations requiring scour protection can easily be made. Additionally the openings will improve the drainage of the water after the tsunami has occurred. Figure 3.4 gives a plan overview of Alternative 2. Figure 3.5 gives the cross section of the alternative.

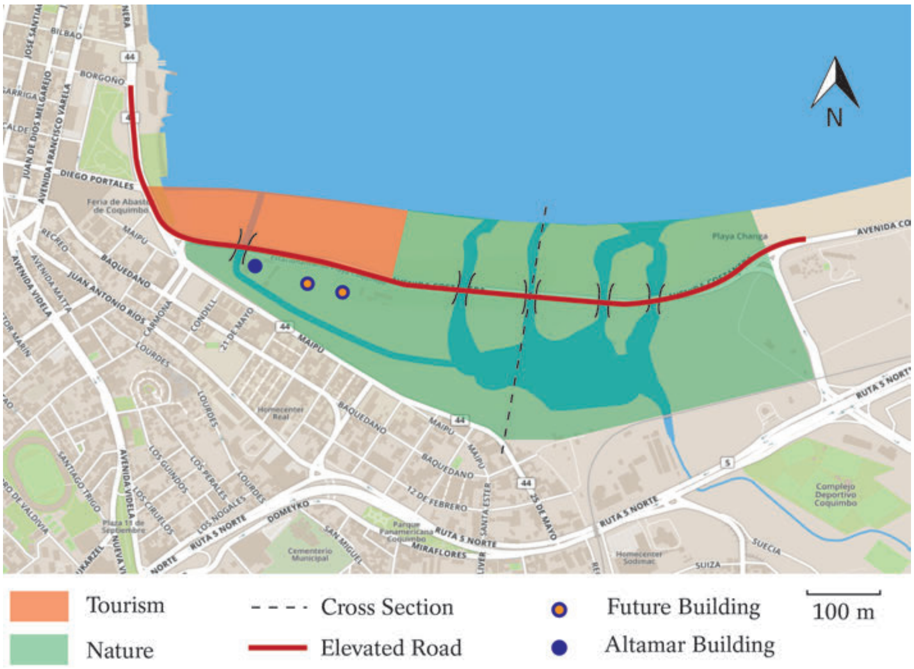

Figure 3.4: Alternative 2, source: Mapbox.com [30]

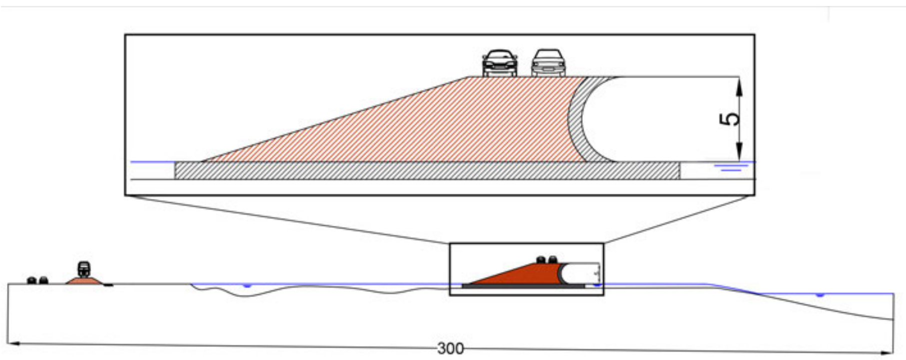

Figure 3.5: cross section alternative 2, measurements in meters

3.4. Alternative III - Protection at the end of the wetlands

In this alternative the road and the wetlands will keep their original shape, but a protection will be added at the end of the wetlands near the railway. When a tsunami arrives, the road will be flooded and the wetland will dissipate a part of the energy of the tsunami. A lower wave will arrive at the protection, which can consist of either a wall or a dam with a natural slope.

Furthermore, the wetlands will be developed into a recognizable recreational area. However it is important that visitors of the area are aware of the vulnerability of the area in case of a tsunami and evacuation possibilities should be provided. Figure 3.6 gives a plan overview of Alternative 3. Figure 3.7 shows the cross section of the alternative.

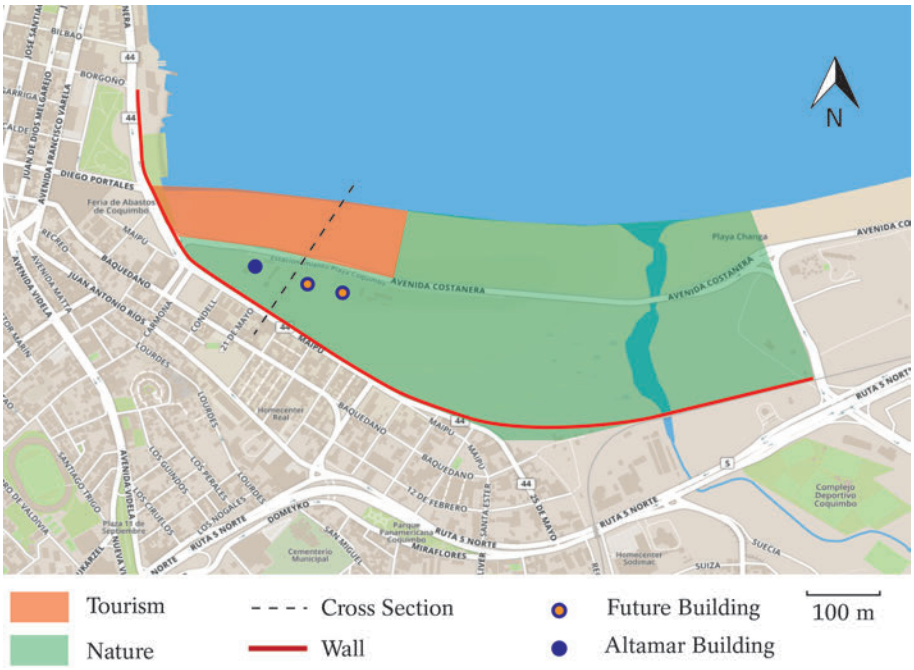

Figure 3.6: Alternative 3, source: Mapbox.com [30]

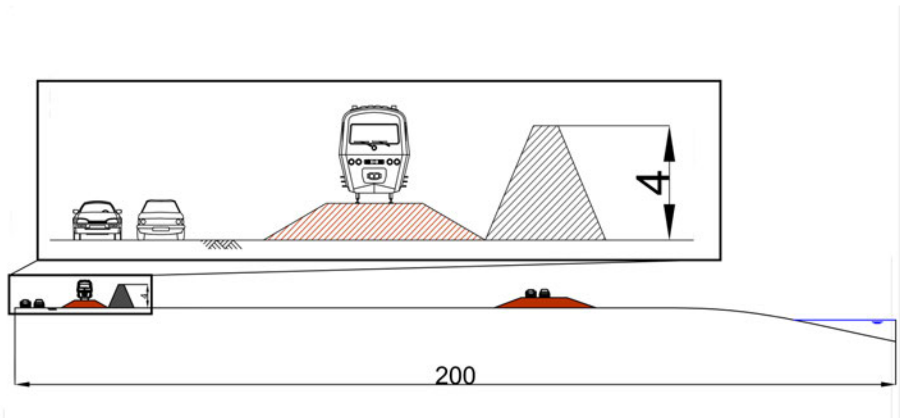

Figure 3.7: cross section alternative 3, measurements in meters

3.5. Alternative IV - Protection at the end of the wetlands and removal of the coastal road

This alternative is to a great extent the same as alternative III. The difference is that in this alternative the coastal road will be removed and a new road will be constructed behind the wetlands. In this case the protection can either consist of a wall, a dam with a natural slope or by elevating the road. Since the wetlands are not cut off anymore by a coastal road, it gives the possibility to blend in a natural way into the coastal zone. Figure 3.8 gives a plan overview of Alternative 4. Figure 3.9 shows the cross section of the alternative.

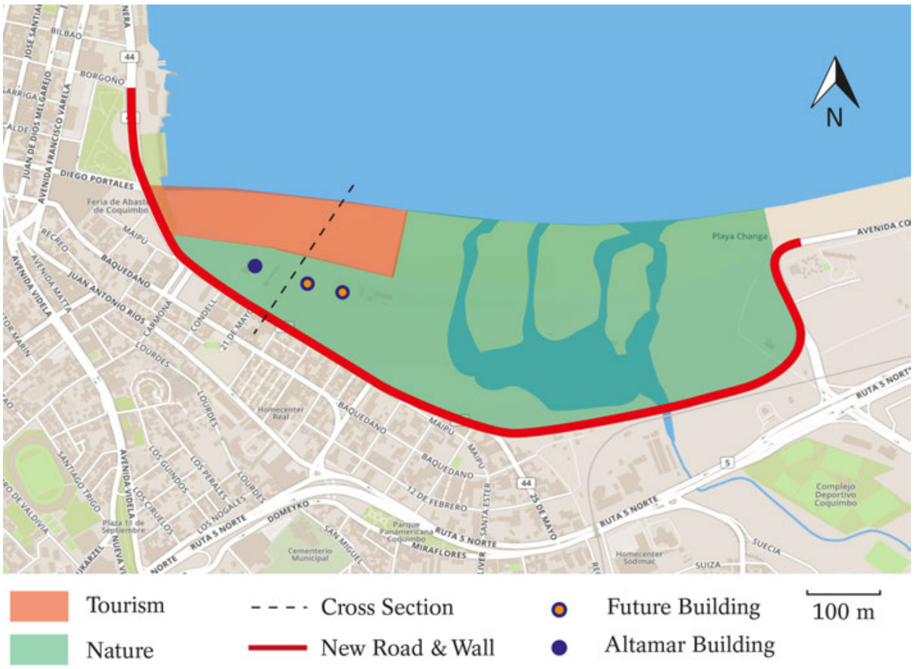

Figure 3.8: Alternative 4, source: Mapbox.com [30]

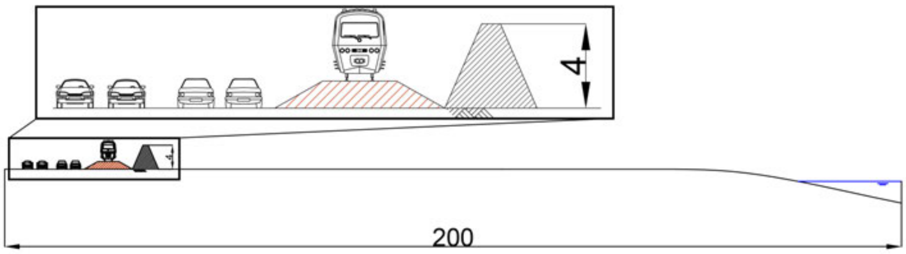

Figure 3.9: cross section alternative 4, measurements in meters

3.6. Alternative V - Creation of dunes

The objective of this alternative is to increase the ecological value of the area, but this will create a new sort of nature and not restore the wetlands as they were. The coastal road will be relocated behind the wetlands and the protection in this alternative will consist of artificial dunes. This way the whole area of the wetlands will only consist of nature and will be used for recreational purposes.

In case of a tsunami the dunes will suffer damage because part of the dunes will be washed away. However, this erosion process will dissipate energy from the tsunami and when the dunes are wide enough the hinterland will still be protected. Figure 3.10 gives a plan overview of Alternative 5. Figure 3.11 gives the cross section of the alternative.

Figure 3.10: Alternative 5, source: Mapbox.com [30]

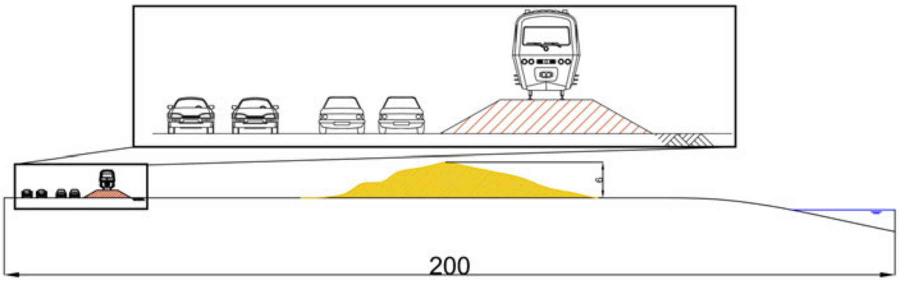

Figure 3.11: cross section alternative 5, measurements in meters

4 Simulation

This chapter contains the simulation of the different alternatives. NEOWAVE was used to perform numerical simulations of tsunamis to determine the effectiveness of the the tsunami protection of the different alternatives.

4.1. Tsunami simulations

The NEOWAVE model uses the shallow water wave equations to model the propagation of a tsunami. A detailed description of this model can be found in appendix E. 6 different earthquake scenarios, which result in different tsunamis, are proposed in appendix E. These earthquake scenarios are from now on referred to as scenario 1 up to scenario 6. A complete overview of the results of the tsunami simulations in the different scenarios can be found in appendix F. Scenario 4 is the worst case scenario with a tsunami leading to inundation heights up to 10 m. In agreement with Dr. R. Aránguiz it is determined that designing a coastal protection to protect Coquimbo Bay from such a tsunami is economically not feasible in Chile. Therefore it is decided to use scenario 1 as a governing scenario resulting in inundation heights up to 6 m. NEOWAVE provides output containing information about inundations heights and flow velocities. To receive specific information about these two parameters, specific tide gauge locations are assigned to the model with coordinates of a location. The model generates data for these specific locations. The locations which are used during the project are given in figure 4.1. Tide gauges at the location corner are used to judge the different alternatives. Simulation results of these inundation heights and flow velocities are presented in appendix F in figures F.4 and F.5.

To be able to simulate a tsunami in the proposed alternatives the original bathymetry is modified. This is done by elevating specific grid points of the most detailed grid with matlab. A detailed description of this process is given in appendix E. A remark should be made that the highest resolution in this grid is 10,27m. Therefore it is only possible to make changes at this scale. This results in modification that do not exactly coincide. Next to that, abrupt changes in bathymetry might produce errors in the model, so the modifications have to be made carefully. Hence, the bathymetry is a lot smoother than originally was intended and thus the simulation results do not give a perfect representation of the different alternatives.

4.2. Modelling results

The maximum inundation heights of the tsunami resulting from scenario 1 with the orginial bathymetry are plotted in figure 4.2. The inundation heights are given in meters. An overview of the impact of the tsunami on alternative I to V is given in figures 4.3a, 4.3b, 4.3c and 4.3d respectively. Results of alternative 4 are missing here due to errors in the simulations. These errors are explained in section E.5. However, because the bathymetry of alternative 3 and 4 are very similar, the results of alternative 3 are used in the evaluation. From the results it can be observed that the buffer zone functions more effectively when the tsunami is partly dissipated and partly reflected in front of the area than when this happens at the back of the wetlands.

Figure 4.1: The locations of the specific tide gauges.

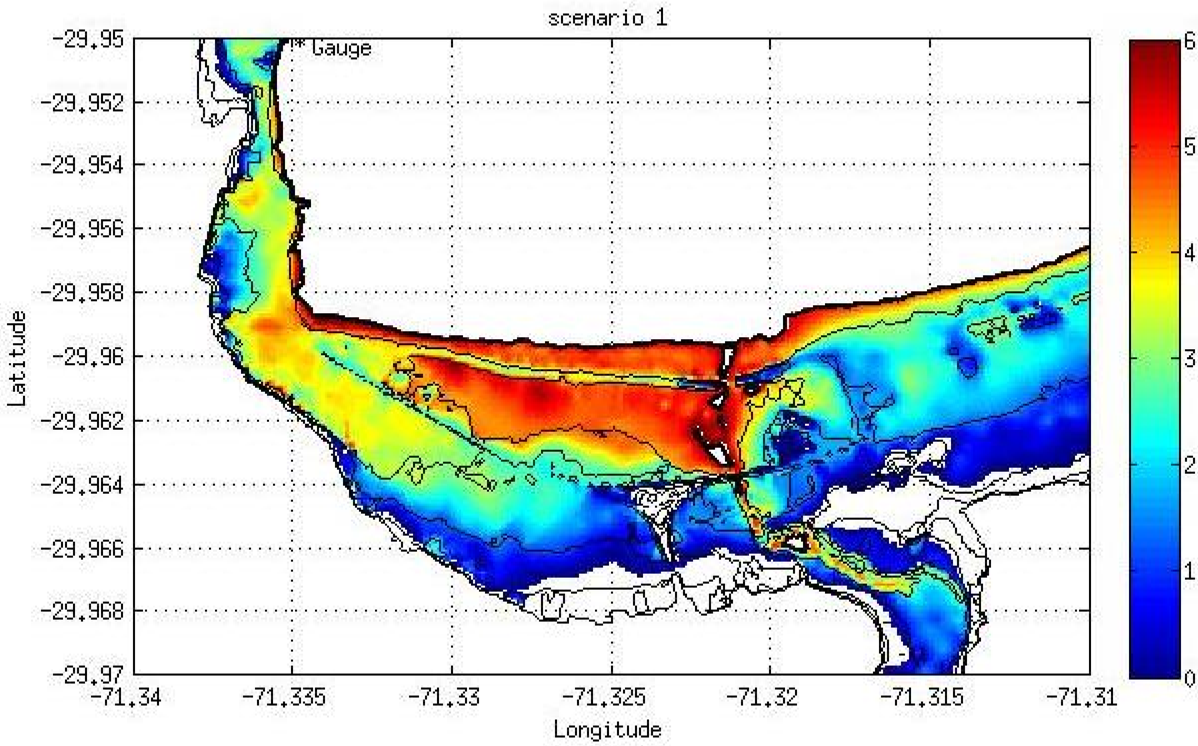

Figure 4.2: Inundation map in meters of scenario 1 with the original bathymetry.

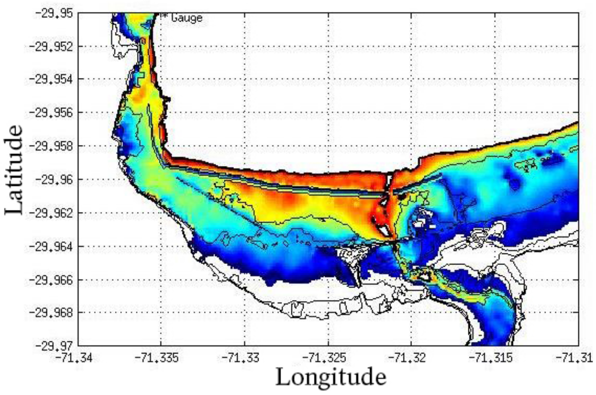

(a) Inundation map in meters of scenario 1 with the bathymetry of alternative I.

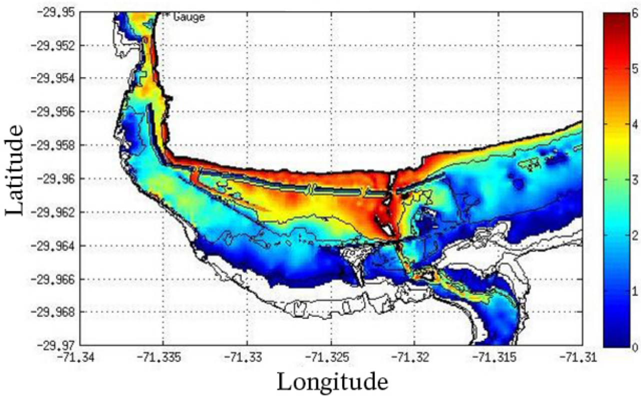

(b) Inundation map in meters of scenario 1 with the bathymetry of alternative II.

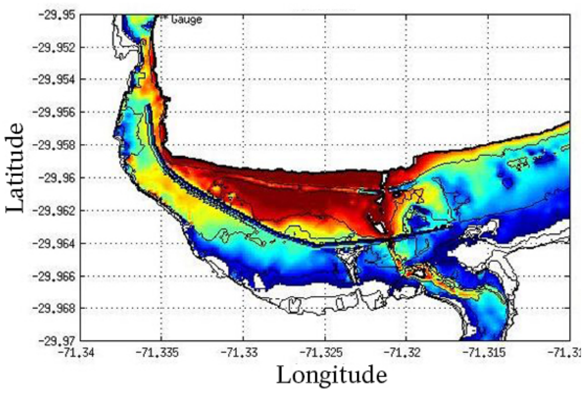

(c) Inundation map in meters of scenario 1 with the bathymetry of alternative III.

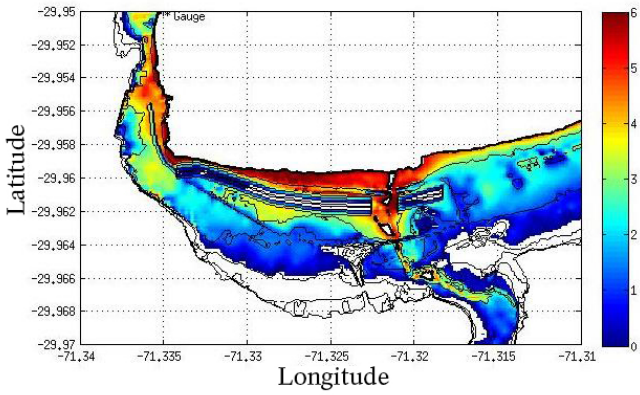

(d) Inundation map in meters of scenario 1 with the bathymetry of alternative V.

Figure 4.3: Different inundation maps in meters of the proposed alternatives.

5 Evaluation

This chapter contains the evaluation of the variants. In section 5.1 the variant with the highest value is determined by means of a Multi Criteria Analysis. This value is determined from the objectives of the stakeholders, see appendix B for the overview of these stakeholders. After this an estimation of the costs is made in section 5.2. With this information a value/costs ratio is determined.

5.1. Multi Criteria Analysis

The different alternatives are compared by means of a multi criteria analysis. The first step in this analysis is to define the criteria and determine the corresponding values. The criteria selected here are safety, nature & recreaction, welfare of the neighbourhood, visual hindrance, infrastructure, construction process and durability & maintenance. These criteria are given a weight factor based on how imporant they are in relation to each other. Finally all alternatives are scored on the different criteria. This score multiplied with the weight factor gives the total score of the alternative. The full process of this analysis is more elaborately explained in appendix G. This is a subjective method as the weight factors and scores of the different alternatives are estimated subjectively.

5.1.1. Criteria

The criteria are choosen such that all important aspects are considered. To prevent certain aspects to be taken into account multiple times it is stated which aspects should be taken into account in which criteria. The summery of this is given in table 5.1. Each criteria also got a weightfactor designated which can be seen in table 5.2. A more elaborated explanation can be found in appendix G.

Criteria	Aspects
Safety	Judged on the amount of inundation height and flow velocities that occur in the neighbourhood Baquedano. Also the retreat of the water after the tsunami event is taken into account and the risk of failure of the structure.
Nature & recreation	Represents the application of building with nature and the redevelopment of the wetlands. This redevelopment consists of restoring the ecosystem and creating a park for recreation.
Welfare neigbourhood	Can be increased by making the area more attractive for tourists.
Visual hindrance	Depends on the height, the exterior and the location of the protection.
Infrastructure	Impact of the solution on the local infrastructure and accessibility of Coquimbo.
Construction process	Judged by the length of the building time and the hindrance for the surroundings.
Durability & maintenance	Depends of the lifetime of the structure and the amount of maintenance that is required.

Table 5.1: Multi criteria analysis criteria

5.1.2. Result

After assessing scores to the alternatives the total scores can be determined. Table 5.2 gives an overview of the scores for each alternative. From this can be concluded that alternative II is the alternative with the highest value. In appendix G the process of obtaining these scores is described.

Criteria	WF	I		II		III		IV		V	
Safety	0,24	75	17,8	85	20,2	40	9,5	40	9,51	50	11,9
Nature & recreation	0,13	40	5,38	70	9,41	50	6,72	85	11,4	75	10,1
Welfare neigbourhood	0,20	90	18,1	75	15,1	50	10,1	25	5,03	15	3,02
Visual hindrance	0,16	45	7,23	45	7,23	55	8,84	70	11,3	50	8,04
Infrastructure	0,14	65	9,11	65	9,11	65	9,11	50	7,01	50	7,01
Construction process	0,05	50	2,26	50	2,26	90	4,07	50	2,26	15	0,68
Durability & maintenance	0,08	75	6,05	65	5,24	75	6,05	75	6,05	25	2,02
Total score			**66,0**		**68,5**		**54,4**		**52,5**		**42,7**

Table 5.2: Multi criteria analysis scores

5.2. Costs

The costs of the different alternatives are based on the cost rates of a construction project of a fishing pier in Tongoy [14]. According to Raúl Oberreuter Olivares from the ministry of public works, project costs are fluctuating a lot within the regions of Chile. Since Tongoy lays within the Coquimbo Region the costs of the project are likely to be in the same range. In appendix H the most important cost drivers are stated.

For each of the alternatives the different costs are summed up. Also general costs and overhead costs that are applicable in all variants are taken into account. In appendix H the costs per alternative are elaborated in more detail.

With this information, the final costs are calculated and presented in table 5.3. In the right column the score of the Multi Criteria Analysis is divided by the corresponding costs in million Chilean pesos. This gives the value/costs ratio, which might determine which alternative will be chosen.

Alternative	Costs (in million Chilean pesos)	Costs (in million euros)	Ratio value/costs
I	20.976	28,0	3,15
II	15.338	20,3	4,47
III	11.945	15,9	4,57
IV	12.087	16,1	4,34
V	9.089	12,1	4,70

Table 5.3: Overview of total costs and benefit-cost ratio per alternative

6
Conclusion

The results from the Multi Criteria Analysis are graphically presented in figure 6.1. The Multi Criteria Analysis revealed that alternative I and II contribute the most to the total values in Coquimbo, wheareas alternative V scores the worst in this analysis. Especially the values safety and and welfare of the neighbourhood, which are the most important values regarding this neighbourhood get a high score in both alternative I and II. Despite the fact that a Multi Criteria Analysis is a subjective tool to measure values, these results will count considerably since the government desires a multifunctional solution, as mentioned in section 2.3.2.

The overview of the total costs of the alternatives shows that alternative V requires the smallest budget, where alternative I is certainly the most expensive solution. When the total amount of value is devided by the costs, alternative II, III and V are rated the highest.

Based on the earlier given argument that the total value is of great importance it is concluded that alternative II is the best solution for the area. This alternative is the best integral solution for the area by combining the values of safety, welfare of the neighbourhood, infrastructure and nature in the coastal protection.

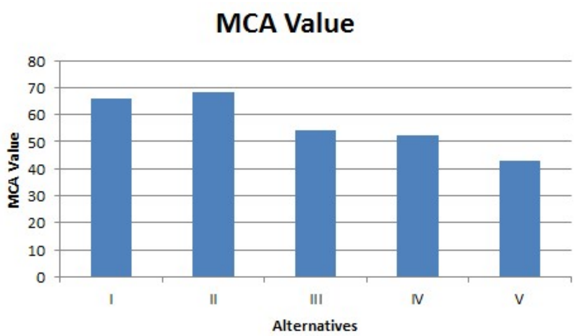

(a) Histogram with MCA values

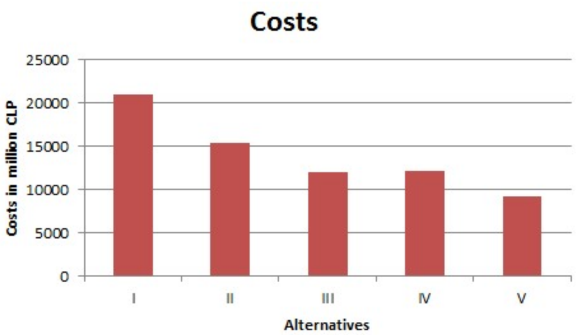

(b) Histogram with costs

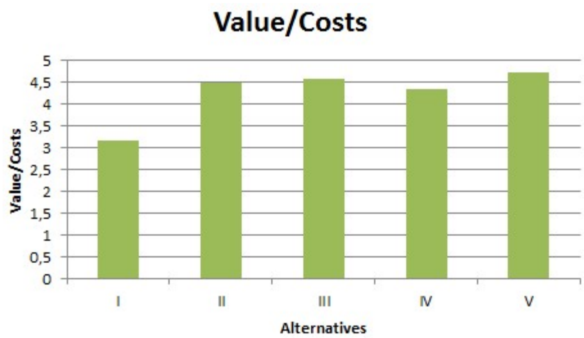

(c) Histogram with value/costs ratio

Figure 6.1: Results evaluation

II

Coastal protection

7 Synthesis

In the previous part (part I) the focus was on the overall development of the area and different options for the actual coastal protection were proposed. In this part these options will be further investigated and designed. In section 7.1 the possible mitigation measures applicable for Coquimbo Bay are discussed. Subsequently, in section 7.2 the mitigations that are applicable for the alternative chosen in part I are selected.

7.1. Mitigation measures

For the design in tsunami prone areas it is often not the incentive to fully protect against the worst-case scenario. This because it is technically challenging and economically unsustainable. Therefore the government chooses to increase the tsunami disaster resilience instead. The resilience is increased by placing mitigation measures. For an overview of all possible mitigation measures see appendix J.

7.1.1. Mitigation measures applicable for Coquimbo Bay

For Coquimbo Bay, only few of the discussed mitigation measures are feasible. The main motives for this selection are the costs, risks and visibility of the measure. In this consideration the reference projects have been taken into account. All the reference projects can be found in Appendix I. Based on the mentioned motives the mitigation measures that are not of interest are:

- A tsunami control forest is not suitable since a tsunami is to be expected in a short time range. The trees will not have time to root themselves strong enough in the ground.
- Innovative structures have a risk of malfunctioning. This because of the fact that they are not tested on big scale and the fact that the systems often come along with mechanisms that are vulnerable for environmental impact.
- Since the wetlands are labeled as a nature reservoir, artificial channels are not preferable.
- Evacuation facilities are available in the region, and there is no need for building new evacuation buildings in this project.
- Big retaining structures are not preferable since this is not beneficial for the tourism of Coquimbo. Besides that, also the local inhabitants do not desire big visible mitigation measures.

Mitigation measures that are of interest are Coastal levees or dunes, floodgates, elevated road, town planning and a multilayer protection model. These are the mitigation measures that are applied for the alternatives in part I. The selected mitigation measures are more elaborated discussed and visualised in appendix J.

7.2. Coastal protection

For the alternative selected in part I there are multiple options for the actual coastal protection. The part in the touristic area will become a multifunctional boulevard. The rest of the protection can consist of a ground dam with a natural slope, a dam of reinforced ground or an elevated road protected by a reflective wall.

7.2.1. Multifunctional boulevard

In the touristic area the seaside of the heightened road will consist of a multifunctional boulevard. This boulevard will contain a large sidewalk and space for businesses to accommodate. The material used for this boulevard is concrete. The backside of the protection will consist of either rubble mound or reinforced soil. This to protect the structure against scour in case of overtopping. Which material is chosen depends on which structure is selected for the rest of the protection. The cross section is shown in figure 7.1.

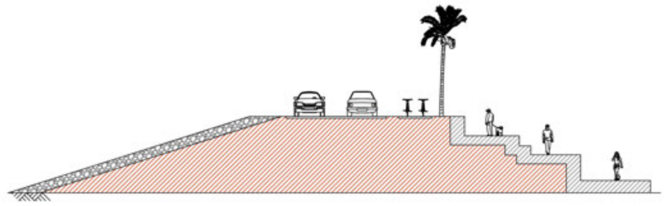

Figure 7.1: Cross section of multifunctional boulevard

7.2.2. Wall

In this alternative the seaside of the protection is protected by a reflective wall. The overall structure is quite similar to the boulevard due to the use of concrete as exterior material. The backside of the protection will consist of rubble mound. The cross section is shown in figure 7.2.

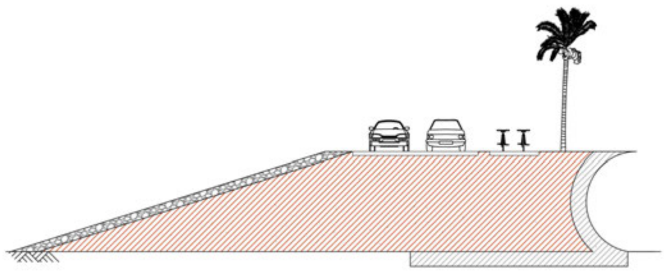

Figure 7.2: Cross section of t-shaped wall

7.2.3. Ground dam with natural slope

Instead of using a steep wall, the protection could be build by using a natural slope. In this case the protection will consist mainly of sand. However because sand will be washed away during a tsunami it is necessary to apply scour protection on the slopes on both sides. Because of the angle of internal friction the maximum slope that can safely be applied is 1:3. The cross section is shown in figure 7.3.

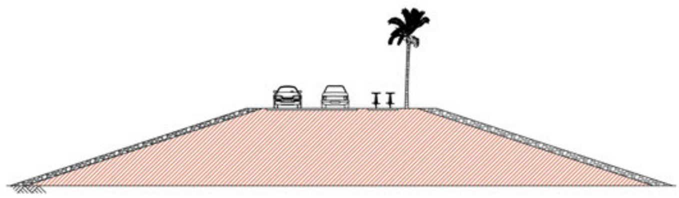

Figure 7.3: Cross section of ground dam with natural slope

7.2.4. Dam of reinforced soil

By using reinforced soil it is possible to create a steeper slope than is possible with normal soil, in this case a slope of 5:2 is chosen. An additional advantage is that the slope does not need to be protected by rubble mound because it is possible to protect the slope with geogrids. This protection is given by wrapping the geogrids around the outer side of the slope with on the inside anti erosion mats (figure 7.5). With this technique it is possible for plants to grow through the mats, this way the slope will keep a natural appearance. The cross section is shown in figure 7.4.

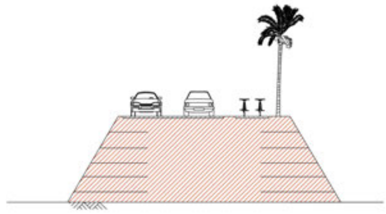

Figure 7.4: Cross section of dam with reinforced ground

Reinforced soil is a method in which soil is combined with geogrids. These geogrids are made of polyethyleen with a high density (HDPE). Because the grids are stretched in one direction they are able to take up high loads due to the reorientation of the molecules. The geogrids are able to withstand the loads and can retain the soil which makes steeper slopes possible. Due to the openings in the geogrids and additional elements that can be added it is still possible to let plants grow on the slope (Tensar [45]).

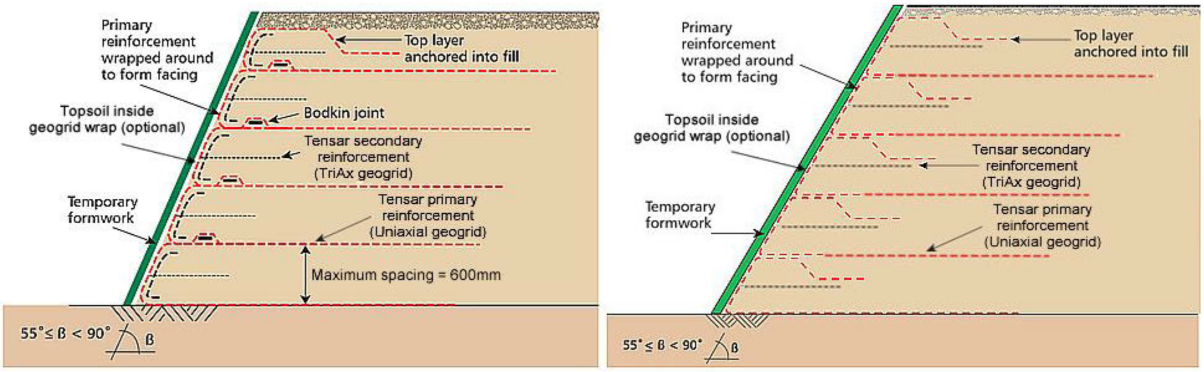

Figure 7.5: Technique to prevent erosion of the slope

8 Simulation

In this chapter the coastal protection is simulated. The mitigation measures that are chosen in the variants are further elaborated. All the coastal protection barriers are onshore barriers with a primary function of dissipating or reflecting the tsunami wave energy. First, the different loads on the barrier are stated in section 8.1. After that, the different options for the structure are schematised in section 8.2. With the numerical simulations from section 8.3 the optimal height of the protection is determined. With this informaition and the magnitudes of the loads the dimensions are defined in 8.4. Finally, section 8.5 will do a check for the maximum inflow of water which is considered as a specific risk for alternative II.

8.1. Loads

In this section an overview is given of all the different loads that are taken into account for designing the hydraulic structure. An overview of all the forces that have to be taken into account according to Federal Emergency Management Agency [17] is given in tabel 8.1. The wind load on the structure is excluded from the table because in the case of a low structure the wind load is negligible and thus will not be taken into account.

The last columns describe which forces have to be applied in the different phases. Phase 1 describes when the surge wave is impacting the structure. Phase 2 is the moment when the waterborne debris impacts on the structure. Phase 3 is the situation where debris damming occurs.

Force	Formula	Phase 1	Phase 2	Phase 3
Weight	$F_g = \rho_g V$	✓	✓	✓
Hydrostatic force	$F_h = \frac{1}{2}\rho_s g b h_{max}^2$	✓	✓	✓
Buoyant Forces	$F_b = \rho_s g V$	✓	✓	✓
Hydrodynamic force	$F_d = \frac{1}{2}\rho_s C_d B (hu^2)_{max}$		✓	✓
Impulsive force	$F_s = 1.5 F_d$	✓		
Debris Impact forces	$F_i = C_m u_{max}\sqrt{km}$		✓	
Debris damming force	$F_{dm} = \frac{1}{2}\rho_s C_d B_d (hu^2)_{max}$			✓
Uplift forces on elevated floors	$F_u = \frac{1}{2} C_u \rho_s A_f u_v^2$	✓	✓	✓
Additional gravity loads	$F_r = \rho_s g h_r A$			✓

Table 8.1: Overview of forces on tsunami retaining structure

The different formulas show that the dimensions and properties of the structure are of high importance. Important input for the forces of the tsunami are h_{max}, u_{max} and $(hu^2)_{max}$. This is to be obtained from the numerical simulations.

Because the design is a coastal protection and not a building, uplift forces on elevated floors do not have to be taken into account. Also the additional gravity load of water on higher floors is not of interest. Additionally the debris damming force is not taken into account, because the length of the coastal protection is larger than the maximum length of the debris. Therefore the hydrodynamic force will not be enhanced due to damming of debris.

According to Federal Emergency Management Agency [17] it is not necessary to apply a safety factor for the sum of the considered tsunami loads for the different phases. For the self weight a factor of 0,9 must be used when it is part of the resistance and thus beneficial. When the self weight is part of the load a factor of 1,2 should be applied.

8.2. Schematisation

For the preliminary design basic calculations are executed to make a first analysis. In order to be able to execute these calculations the structures are schematised. In the next sections it will be explained in which ways the schematisations differ from reality.

8.2.1. Multifunctional boulevard

For the multifunctional boulevard the inside of the structure consist of sand and the outside of concrete, this has a strong resemblance to a caisson construction. Because in Chile everything is constructed in situ the boulevard will not actually consist out of caissons but for the first analysis of the stability this can be used as a representation.

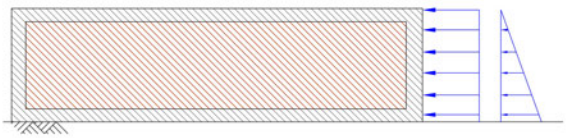

Figure 8.1: Cross section of multifunctional boulevard

8.2.2. Wall

In reality the wall will be curved to better reflect the water. In the first schematisation however it will be modeled as a straight t-shaped wall. The cross section of the schematisation is shown in figure 8.2.

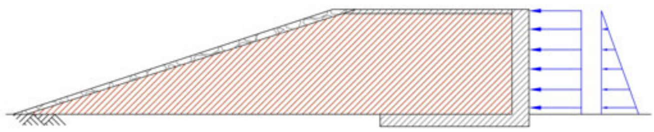

Figure 8.2: Cross section of t-shaped wall

8.2.3. Ground dam with natural slope

For the ground dam with a natural slope failure is most likely to happen due to scour. In order to prevent this the scour protection is of great importance. However for this calculation it is not necessary to schematise the appearance of the dam.

8.2.4. Dam of reinforced soil

For the calculation of the reinforced soil a model program has been provided by the company Tensar. It is not necessary to apply any further simplifications in order to use the model.

8.3. Tsunami simulations

More detailed NEOWAVE tsunami simulations of the chosen alternative II are performed to compare the effect of different heights of the coastal protection on the inundation in the area and the flow velocities in Baquedano. The elevated coastal road is divided in 2 parts, namely a western part (1) and an eastern part (2). The western part (1) is build from the opening at the Altamar building towards the port and the eastern part (2) is build from the floodgate at the Altamar building along the beach towards La Serena. The 2 parts of the wall are illustrated in figure 8.3. The first part respectively is the most important part in protecting Baquedano. Therefore also an extra elevation of this part is taken into consideration.

Figure 8.3: The two different parts of the elevated wall.

The heights of the coastal road mentioned in this section are measured from sea level, because this is more exact than from ground level. To judge the inundation records of NEOWAVE the average of the maximum inundation heights of the 4 tide gauges, depicted in figure 4.1, in Baquedano is calculated. This average of these 4 maxima is from now on referred to as the average height in Baquedano.

Furthermore, an average of the maximum velocities in Baquedano is calculated by taking the square root of the sum of the velocities squared in both x and y direction. This average is called average flow velocity Baquedano.

Next to the inundation height and flow velocity the arrival time of the several tsunami waves is taken into account. The value given in table 8.2 is the arrival time of the first waves with a flow depth of more than 1 meter in Baquedano. The inundation maps of the new modifications and the the specific tide gauges are given in appendix F.

Alternative	Elevation part 1 (m)	Elevation part 2 (m)	Average inundation height Baquedano (m)	Average flow velocity Baquedano (m/s)	Arrival time first wave (min)
Original bathymetry	±3	±2	3,68	2,51	40
Alternative 2.a	5	5	2,72	1,43	40
Alternative 2.b	7	5	3,15	1,07	80
Alternative 2.c	7	6	2,55	1,39	80
Alternative 2.d	8	6	1,95	0,91	80

Table 8.2: Input and output of the different modifications of alternative 2

Table 8.2 shows that heightening of the elevation of part 2 does not result in a significant decrease of inundation unless the elevation of part 1 is at a height of 8 meter, which is considered unacceptable for the local population. A heightening of only part 1 results in even a higher inundation. The only gain is that the first significant wave is blocked by the protection which gives an increase of the evacuation time. However because a heightening of the coastal road with 1 additional meter is significantly more expensive and the gain in inundation height is only 0,20 m the conclusion is that the original alternative, alternative 2.a, is the economically most effective option.

8.4. Calculation results

For all alternatives different calculations had to be performed and different loads are of importance. The conclusions following from these calculations are discussed for the different alternatives. The full calculations can be found in appendix K.

8.4.1. Multifunctional boulevard

The multifunctional boulevard is designed by taking the overall stability into account. For this the horizontal, the vertical, and the rotational stability is checked. With a height of 5 m, this results in a minimum width of 17 m, a thickness of the upper slab of 0,3 m, and a thickness of the side walls of 0,3 m. To compensate for the gross schematisation the bottom slab has not been taken into account for the resistive weight. Also the ground underneath the slope is not taken into account due to the schematisation, by this extra safety is included.

8.4.2. L-wall

Also for the L-wall the stability is leading in the determination of the dimensions. Again the horizontal, the vertical and the rotational stability is checked. With a height of 5 m, this results in a minimum length of the base of 16 m, with a thickness of 1,25 m. The thickness of the wall itself has a minimum of 0,8 m. For the horizontal stability the weight of the ground behind the length of the base has not been taken into account, this induces additional safety.

8.4.3. Ground dam with natural slope

For the ground dam the dimensions are set upfront because of the width of the road and the maximum slope for sand of 1:3. Out of the check of the horizontal stability can be concluded that the weight of the dam is sufficient to resist the tsunami loads.

After the check of the horizontal stability the main part to be designed is the scour protection on the slope. In order to calculate this the velocities measured in the simulation are used. The velocity taken is the maximum positive velocity, which is in the direction of the protection. There are only two measurement points on the beach (see figure 4.1) resulting in the possibility that the velocity is larger. However this velocity only occurs for a small moment in time and for a large amount of the time the velocity is much lower (see figure K.4)

For the calculation the formula of Shield is used (Schiereck [40]):

$$d = \frac{K_v^2 u_c^2}{K_s \psi_c \Delta C^2} \tag{8.1}$$

The factor K_v is to compensate for non-uniform flow. This factor is very uncertain and will vary during the tsunami because it depends on the flow height above and behind the dam. It is empirically determined that the maximum of this factor is 3 (Schiereck [40]), however this factor results in unrealistic large diameters. In another research (De Gunst [10]) it is stated that the value of 1.3 should be applied in the case of a backwards facing step, which is comparable to the flow over the dam. When this is applied a diameter of 1,2 m is found. Because some damage is allowed during the event a shield parameter of 0,06 is applied. To determine how much transport will occur the formula of Paintal is applied for $\psi_c > 0,05$ (Schiereck [40]):

$$q_s* = 13\psi_c^{2,5} \tag{8.2}$$

In which q_s* is the transport per $m^3/m/s$ which is in this case equal to 3 stones per meter dam per tsunami wave of 8 minutes. In this formula there is no correction for the slope and acceleration of the flow, when the correction factors of the shields formula are applied the damage becomes a factor 4 bigger. Because a tsunami is considered a rare event this could be considered acceptable but due to the uncertainty of the factors and the velocity additional research is necessary.

8.4.4. Dam of reinforced soil

Similar to the ground dam with a natural slope the resistance of this dam against the tsunami forces is determined by the weight of the dam. Due to the road and paths on top of the dam a minimum width of the dam is necessary of 14 m, out of the horizontal stability results that this width is sufficient.

To load cases are simulated by the Tensar software, the situation of normal use and the situation after a tsunami has occurred. The situation during the tsunami itself is not simulated because in this situation the tsunami forces work favorable for the geogrids. The situation after the tsunami has occurred results to be governing due to the extra weight of the water inside the dam which results in additional loads on the geogrids. The resulting necessary geogrids are given in figure 8.4. The first three products are geogrids of different strenghts, the bodkins are a method to fix the parts of the geogrids that are wraped around the soil (figure 7.5).

Material quantities	Tensar product	Quantities per linear metre of structure	Material quantities allow for:
	RE510 RE520 RE570 RE500Bodkins	72.3 m² 23.8 m² 19.9 m² 16.0 m	- Length of geogrid turned up face - 0.30m overlap at wraparound - 1.5m return on highest geogrid - no wastage

Figure 8.4: Resulting necessary geogrids

8.4.5. Scour protection

Due to the power of the tsunami it is necessary to apply scour protection around all the structures. Because it is desirable to maintain the natural character of the area this scour protection will be applied underneath a layer of normal soil.

For the calculation of the scour protection the same sheet is used as for the protection on the natural slope (appendix K) and the same uncertainties apply. Because there is no slope in this case the factor K_s is 1, which results in a minimum diameter of 0,7 m and a rock grading of 3000-6000 kg. According to Paintal the damage during a tsunami wave of 8 minutes results in a damage of 6 stones per meter dam. However as mentioned before this is based on a lot of uncertainties and further research is necessary to determine this. Also the necessary filter layers need to be determined in further research.

In order to take the lay-out and the costs for the scour protection into account a design of scour protection is given in table 8.3. Figure 8.5 gives a visual impression of the scour layer.

Weight in kg	D_n in m	Thickness layer in m
10 - 30	0,10	0,2
100 - 300	0,25	0,5
1200 - 2000	0,5	1
3000 - 6000	0,8	1,6

Table 8.3: Design of the scour protection layer

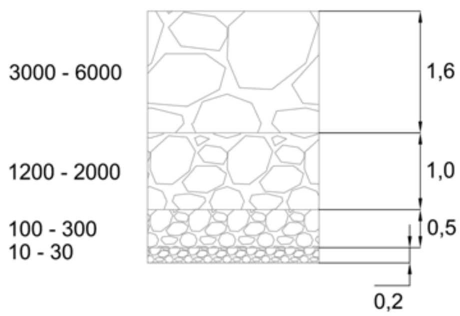

Figure 8.5: Scour layer

In total the scour protection consists of four different layers. The weight in kg is linked to a D_n from figure K.8 from appendix **??**. The minimum thickness of the layer is given by 2 times the D_n [40]. The length of the scour protection is based on the formula from Molenaar and Voorendt [33, p.257]:

$$L = \gamma \cdot n_s \cdot h_{max} \tag{8.3}$$

With safety factor γ taken as 1, n_s = 6 (assuming densely packed sand) and h_{max} is taken as 5 m. This gives for all structures a horizontal scour protection with a length of 30 m at the frontside and backside of the structure. In a final design it is recommended to look deeper into the design parameters of the formula to come to a more exact design of the scour protection.

8.5. Inflow openings in seawall

In total 5 openings will be placed in the coastal protection of alternative II. A risk that has to be considered is the maximum inflow through the channels during tsunami impact. Flooding of the protected area can obstruct evacuation routes. First, the surface of the cross section is approximated. After this, a function for the inflow is composed. The data of the flow velocity and flow depth that can be seen in K.3 in appendix K are extracted from tide gauge beach 2 (see figure 4.1) for the original scenario without adjustments to the bathymetry.

The openings are dimensioned as half circles with a radius of 3 m, see figure 8.6. The sea water level in normal situations is 0,5 m in the channel. With these dimensions the surface of the cross section of one opening is $0,5 * \pi * 3^2 = 14,13 m^2$. This corresponds with a rectangular shape of 6 m by 2,355 m. This latter shape is taken into the calculations for simplification purposes.

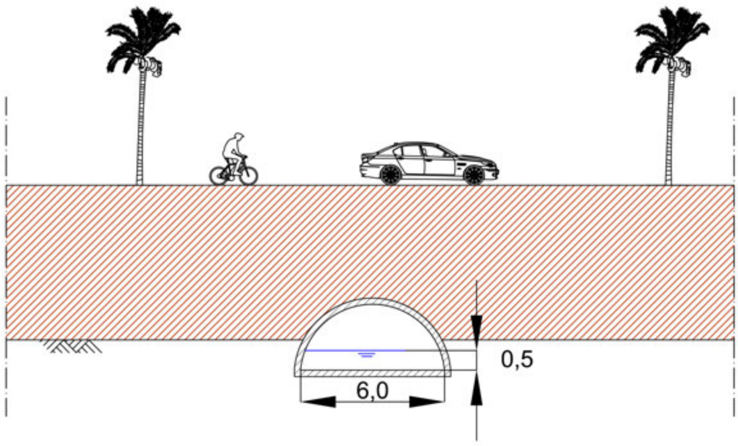

Figure 8.6: Frontview of openings in elevated road

It is possible that in between the tsunami waves water flows out of the wetlands through the floodgates. Due to lack of data this outflow is not taken into account. Fortunately, this is a conservative approach.

Here it is assumed that during the tsunami a uniform and stationary flow over the depth is present in the openings channels. Besides that it is assumed that there is a laminar flow through the channels and there is no friction. This is a conservative approach of calculating the maximum inflow.
Formula of the total inflow is:

$$\text{Volume} = 5 \cdot \int^t Q \cdot dt = 5 \cdot \int^t A(h(t)) \cdot u(t) \cdot dt \tag{8.4}$$

With:

$$\begin{aligned} &A(h(t)) = h(t) \cdot b \\ &h(t) = 0,5 + h_{tidegauge}(t) && \text{for} \quad 0 < h(t) < 2,355 \\ &u(t) = u_{tidegauge}(t) && \text{for} \quad u(t) > 0 \\ &b = 6 \text{ m} \end{aligned}$$

The values $u_{tidegauge}(t)$ and $h_{tidegauge}(t)$ are used as a input in a Matlab script calculating the inflow volume per opening. The result is multiplied by 5 and gives a total inflow volume of 10.723 m^3. The total volume of water inflow can be related to the increase in water level over the scope area, which consist mainly out of wetlands. With Google Maps Area Calculator Tool [9] this is calculated as 408.743,15 m^2. The total increase in water level can now be determined:

$$\Delta h = \frac{\text{Inflow volume}}{\text{basin area}} = \frac{10.723}{408.743,15} = 0,026 \text{ m} \tag{8.5}$$

It can be concluded that this inflow is acceptable as long as the elevation routes are heightened to a level higher as this increase in water level.

9

Evaluation

In this chapter the results of the simulations and calculations of the previous chapter are evaluated in relation to the costs. This leads to the final choice for the coastal protection. In chapter 9.1 the expected damage is elaborated. Chapter 9.2 gives the estimated costs of the different options.

9.1. Damage in Baquedano

A fragility curve was created by Aránguiz et al. [3]. Fragility curves give a probability for the damage due to the tsunami impact and are based on the tsunami impact and damage caused by the tsunami of 2015. In figure 9.1.a the damage that is identified during a survey is plotted against the inundation depth at the respective locations. These data was used to derive the fragilty curve of figure 9.1.c.

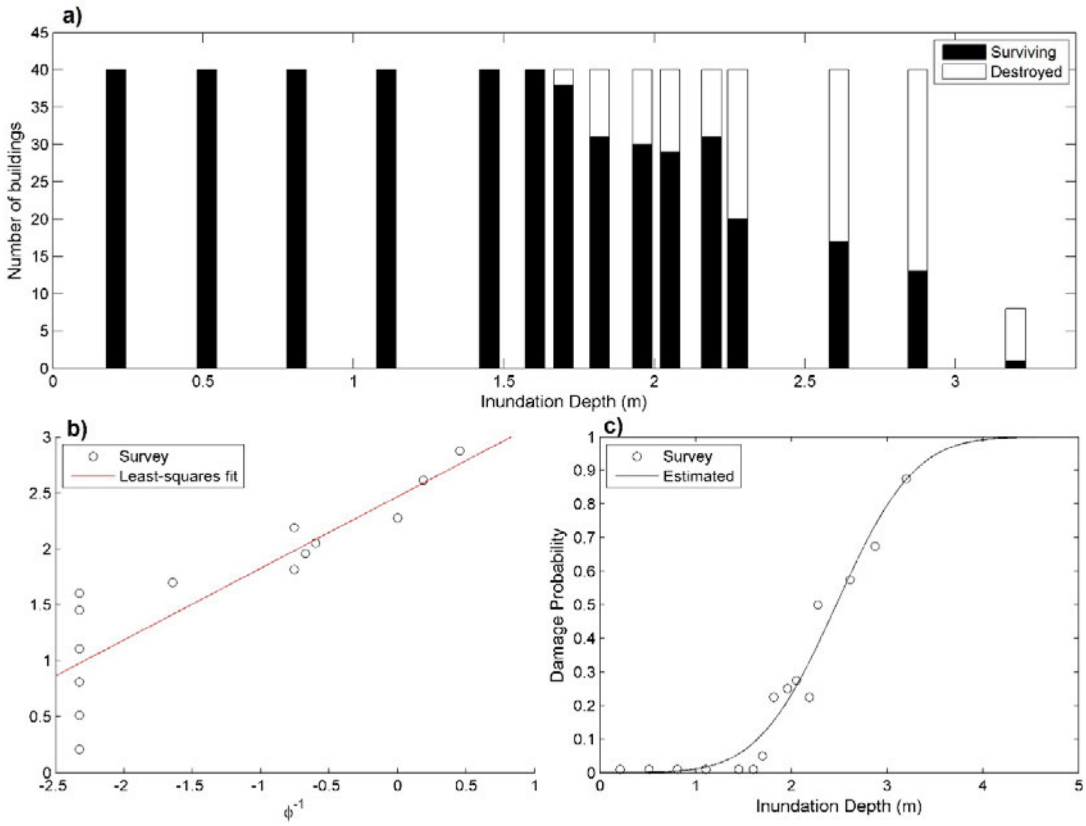

Figure 9.1: Tsunami fragility curve data, source:Aránguiz et al. [3]

In section 8.3 a height of 5 m is chosen, because further elevation does not significantly reduce the inundation. Even with a height of 8 m it is not possible to make the inundation lower than 1,5 m for which no significant damage is noted during the survey. For a height of 5 m, an inundation of 2,72 m is found. This corresponds to a damage probability of 60%, which is quite high. Because there still is a small probability that an even larger tsunami would occur additional research should study the feasibility of rebuilding the Baquedano neighbourhood with elevated houses.

9.2. Costs

In appendix H the costs for the different options within alternative II are further elaborated. The rough estimated design of the necessary scour protection is elaborated and implemented in the total costs. This addition makes the total cost estimation significantly higher that the costs given in section 5.2 from part I. With the given dimensions of the reflective L-Wall, the ground wall, and the reinforced soil the volumes of the materials are more precise determined. For the general costs of all options still the estimated costs of 2 billion CLP is considered. Again, 10% of overhead costs are added. Table 9.1 gives an overview of the costs. In figure 9.2 the cross sections of the different options are given. The horizontal scour layer of 30 m is not shown completely.

Option	Total costs*	Total costs**
L-wall	36.520	48,7
Ground wall	35.344	47,1
Reinforced soil	27.523	36,7

Table 9.1: Total costs overview. *Costs given in million Chilean pesos. **Costs given in million euros

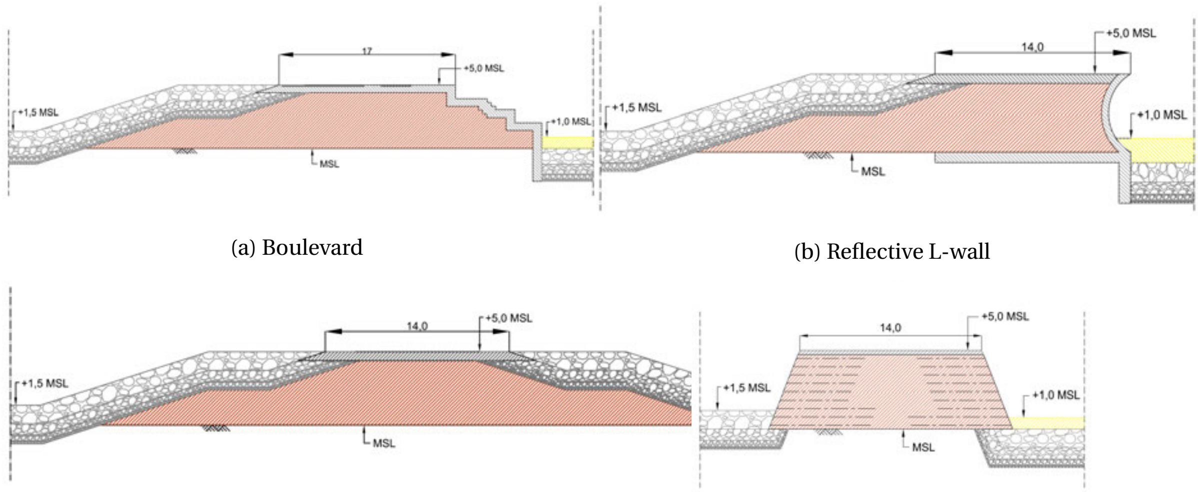

(a) Boulevard

(b) Reflective L-wall

(c) Ground wall

(d) Reinforced soil

Figure 9.2: The different inundation maps in meters of the proposed alternatives.

10
Conclusion

In part I a multi criteria analysis is done but because the options for the coastal protection score the same for almost all the criteria it is not necessary to perform a whole multi criteria analysis again. The only aspect in which the protections differ is the visual hindrance for which the option with the reinforced soil is the only one that scores better than the others.

Out of the costs can be concluded that the dam with the reinforced soil in not only the option with the least visual hindrance but is also the least expensive option. Therefore this is chosen as the coastal protection, a more detailed cross section of the dam is given in figure 10.1. The part of the dam that is in the touristic area will consist of a multifunctional boulevard, the land side of this boulevard will also be made of reinforced soil. The more detailed cross section of this part of the dam is given in figure 10.2.

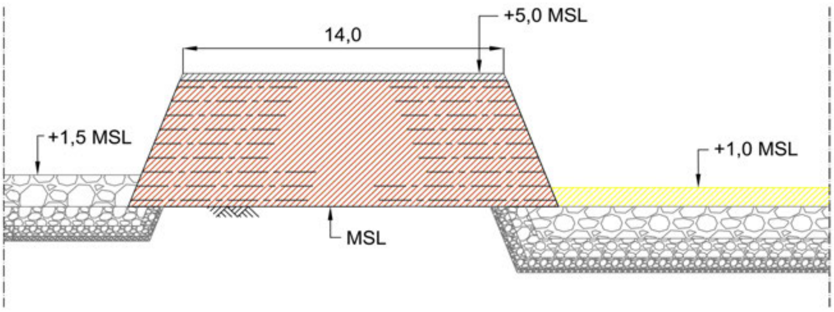

Figure 10.1: More detailed cross section of dam with reinforced soil

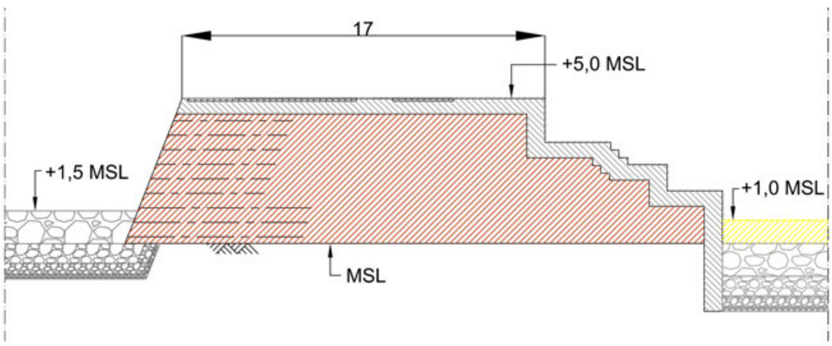

Figure 10.2: More detailed cross section of the multifunctional boulevard

III

Altamar highrise

11

Analysis

This part of the report will look into the possibility of the Altamar highrise as a vertical evacuation location in the project area. In this chapter the building will be analysed; section 11.1 will present the main research question for this part, section 11.2 analyses the location of the Altamar building, section 11.3 describes the effects of the earthquake and tsunami of September 2015 on the building and in section 11.4 the supporting structure of the building is determined.

11.1. Introduction

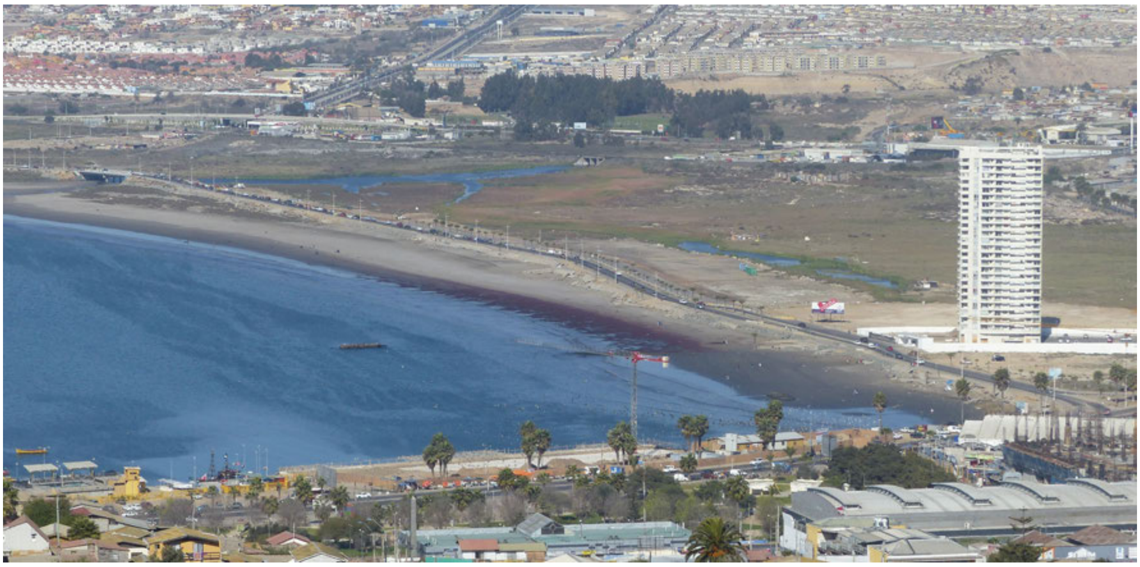

Figure 11.1: The Altamar highrise in the project area

It has been suggested that the Altamar highrise, depicted in figure 11.1, could be used as a vertical evacuation refuge. According to Federal Emergency Management Agency [17, p.1] a vertical evacuation refuge from tsunamis is defined as:

> "*a building or earthen mound that has sufficient height to elevate evacuees above the level of tsunami inundation, and is designed and constructed with the strength and resiliency needed to resist the effects of tsunami waves.*"

A tsunami brings several different hazards that need to be analysed. The building is assumed to be tsunami safe if it posses enough strength and resilience for the different load situations stated in FEMA. Furthermore the building should withstand the antecedent earthquake and remain its function. This brings us to our main research question:

To what extend is the Altamar building capable of resisting a possible future earthquake and tsunami load, such that a vertical evacuation function remains possible?

In order to find an answer to this question a model of the Altamar building is built using finite element software Etabs. Using the worst case tsunami scenario as determined in section 4.1 preceded by an earthquake loading the model of the building is tested. Subsequently, a conclusion is drawn about the possibility of the Altamar highrise as a vertical evacuation refuge.

11.2. Location

The Altamar highrise is located in the corner of Coquimbo bay, as depicted in figure 11.2. The looks of Altamar are quite remarkable since it is the only highrise directly placed next to the shore resulting in a contrasting view with the surroundings, as is clearly shown in figure 11.1. The location and height of this building can be considered as a rendering of the ambition of the local authorities. Coquimbo still has the reputation to be La Serena's ugly little brother but has the potential to grow into a touristic hot spot because of its topographical location and calm bay. The municipality knows this and will try to work towards an increase in tourism for Coquimbo. The building is easily accessed through Avenida Costanera, the road parallel to the beach, which connects Coquimbo with La Serena.

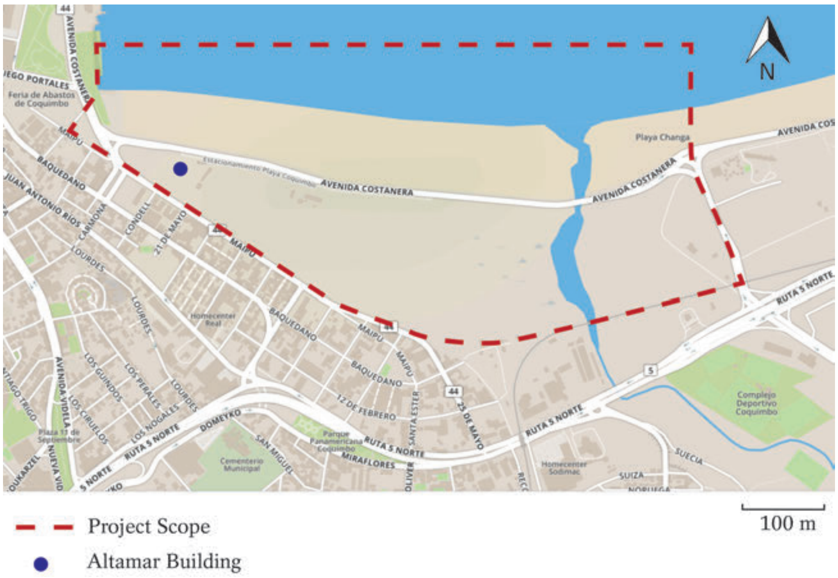

Figure 11.2: Location of Altamar within research area, source: Mapbox.com [30]

With regard to the use of the Altamar building as a vertical evacuation refuge the location is of great importance. Because of the fault line close to the Chilean coast a possible tsunami is considered to have a short warning time according to Federal Emergency Management Agency [17, p.51]. The short warning time is defined as a tsunami arriving within 30 minutes of its initial warning (e.g. an earthquake). The short warning time was even less than 30 minutes for the 2015 Illapel tsunami (Aránguiz et al. [3, p.7]). As a consequence people near the Altamar building should have the oppurtunity to find refuge there. The Altamar building is located close to the road and the surroundings are quite flat thus a quick approach is possible.

The inundation map of the 2015 Illapel tsunami, figure 11.3, shows another interesting fact. The maximum inundation height of 6,41 m was found near the intersection of the coastal road and the railway, this is very close to the location of the Altamar building. The analysis in in appendix C.5 shows that most destroyed buildings were in this area as well, see figure C.4. These facts emphasize the need and potential of this building as a vertical evacuation location.

Cross section A-A is shown in figure 11.4. The red lines are measurement locations of the inundation height and the green line gives the approximate location of the Altamar building. This figure shows that the inundation height at the location of the Altamar building was indeed 6,4 m and that the ground level of the building is at approximately 3,2 m, leading to a flow depth of 3,2 m inside the Altamar building.

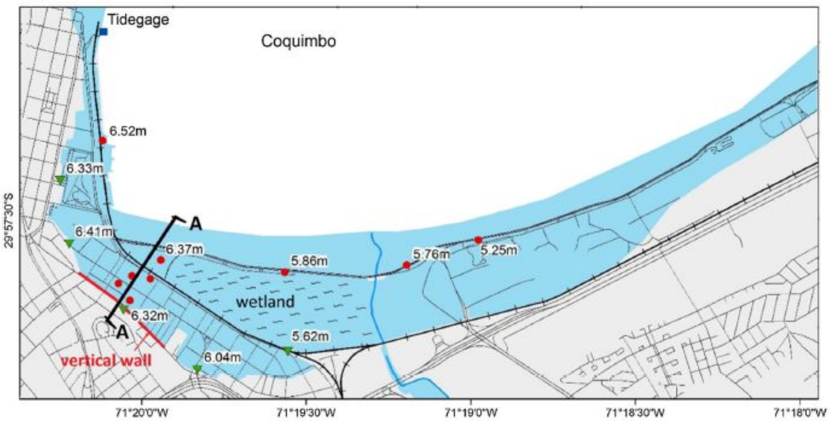

Figure 11.3: Inundation map of the 2015 Tsunami in Coquimbo Bay, source: Aránguiz et al. [2]

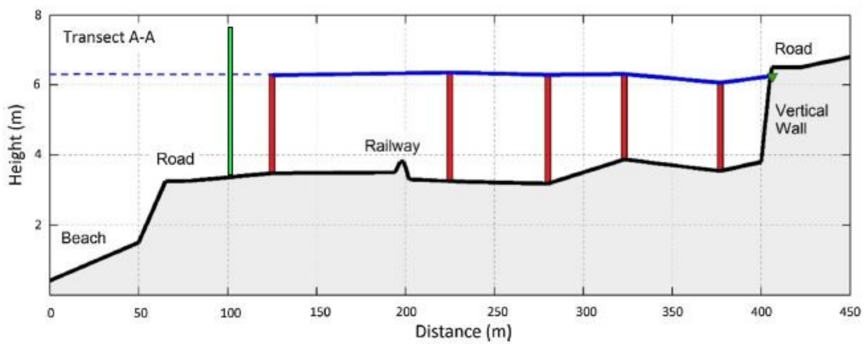

Figure 11.4: Cross section A-A, source: Aránguiz et al. [2]

11.2.1. Seismic region

In Chile, buildings are designed according to NCh433: Seismic Design of Buildings (Bachman and Silva [4]). The code divides Chile in three major vertical earthquake regions and several horizontal regions. The map in figure 11.5 places Coquimbo in the most severe region 3, which stretches along the complete coast of Chile. Furthermore the subregion is IV-R. La Serena/Coquimbo is located in the bottom left of the picture at the location of the red circle.

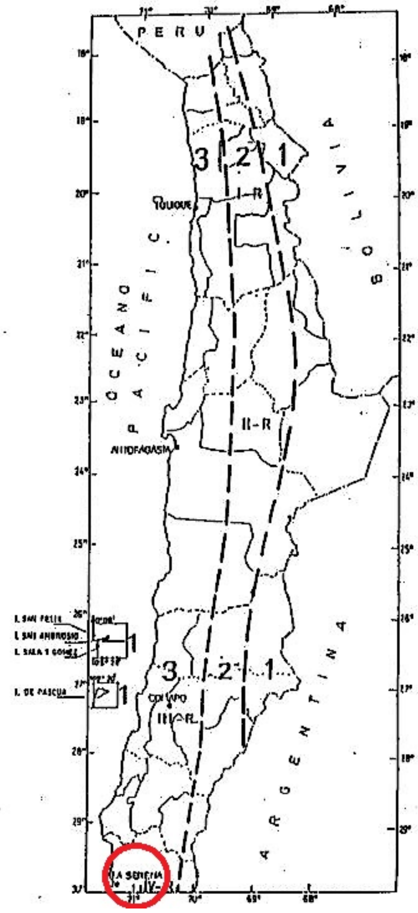

Figure 11.5: Subdivision of Chili according to Chilean seismic design of buildings code NCh433, source: Bachman and Silva [4]

11.3. Tsunami 2015

Analysing the effects of the September 2015 tsunami on the Altamar building might help to predict effects of a future tsunami. This analysis is partly based on an interview with the landlord about the effects of the tsunami of September 2015. The interview was conducted during a visit to the building.

Pictures, as shown in figure 11.6, showed that the inundation height reached up until 20 to 30 cm on the second floor, this corresponds with an inundation height of approximately 3,2 m in the building as was determined in section 11.2.

In Chile there's a long history of seismic activity, which caused their codes to be very detailed about how to design buildings in case of earthquakes. None of the multilevel buildings in the region of Coquimbo collapsed due to the earthquake, which confirms their experienced earthquake resistant designs. Therefore it is very unlikely that the Altamar building will collapse due to the effects of an earthquake.

The Altamar building was build in 2011, after the 2010 event which is mentioned in appendix C. However the structural drawings and calculations are from the 2nd of September 2009. Therefore the building was build according to tsunami building regulations dated from before the alterations that were made after the 2010 event. Recent tsunami building regulations state, amongst others, that the lower 2 levels should not have a residential function and should be as open as possible to provide low resistance to the water that flows through

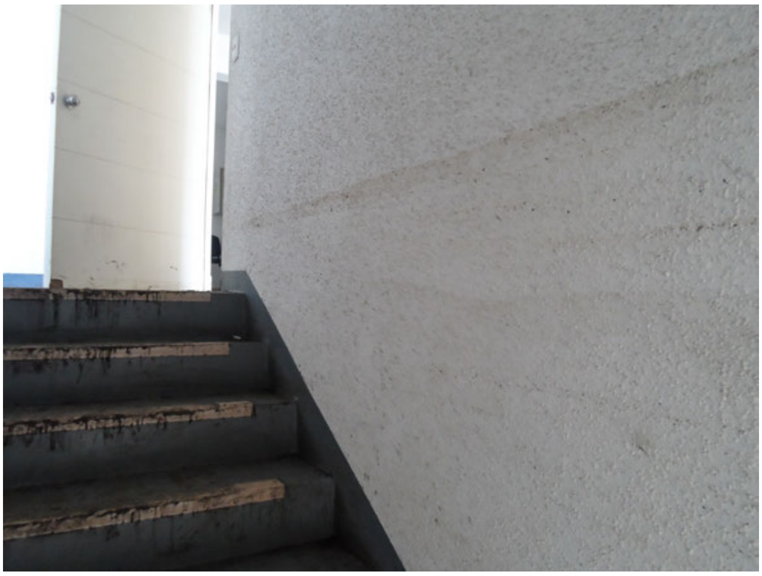

Figure 11.6: The inundation height in the Altamar building, picture taken at second floor

and prevent debris from creating blockages. Fortunately the first 2 floors of the Altamar building are not used for residences. The walls in this part of the building have been made of light materials and are designed to be easily washed away during a tsunami to reduce the resistance. Here the earthquake and tsunami regulations contain a contradiction as earthquake regulations state that soft or weak stories must be avoided.

Figure 11.7 shows some of the destruction on the ground level and the open structure of the ground level. On the ground level several non-supportive walls and other non-structural elements were washed away by the force of the water and debris.

Figure 11.7: Ground level of the Altamar building after the 2015 tsunami

Another effect of the tsunami was scour of the sandy ground around the building, that caused the coastal road to be destroyed. Fortunately, the building is build on a pile foundation that reaches into the rocks deep down, so the building is reasonable save from scour and the 2015 tsunami didn't affect the foundation of the building at all according to the landlord. The tsunami of 2015 clogged the trench that flowed along the side of the building and this hasn't been cleared yet. The clogging of this trench might influence the drainage of the water of a possible future tsunami.

11.4. Structural aspects

Initially we were unable to obtain official structural drawings and information about the Altamar building from the local authorities of Coquimbo. Fortunately on the 7th of October 2016 Dr. Rafael Aránguiz finally received the papers and forwarded them. The following chapters are mainly based on this information. To explain our initial process, our initial models and calculations are elaborated in appendix L. After receiving (a small part of) the structural information a reflective analysis has been performed to check the initial model and, where possible, changes are implemented to create an improved model. The quality of the obtained structural drawings was too limited to include them in this report.

11.4.1. Supporting structure

The Altamar building has a supporting structure mainly consisting of floors and shear walls and is casted in-situ. A relatively small amount of beams connect walls for structural integrity. For the sake of earthquake proof design the stability elements are evenly spread over the floor plans resulting in an almost symmetric configuration. High concentrations of stiff stability elements can cause torsional forces and displacements which are unwanted.

The first 2 floors, which do not fulfill a domestic property, have a different configuration compared to the floors above. The side parallel to the sea is more open at the first 2 floors due to the application of 3 columns in stead of 2 shear walls. These columns support the walls above and create an open space on the first 2 floors. Furthermore, the first 2 floors are joined, which results in high open spaces on the first floor.All stories are 2,55 m high.

The thickness of the shear walls varies between 200 and 400 mm, depending on the location in the building. Floors have a constant thickness of 140 mm. The columns on the first two floors have a diameter of 400 mm.

Reinforcing steel is of quality A630-420h. This is steel with a yield strength of 420 N/mm^2. Unfortunately nothing is known about the applied reinforcement ratios for all structural elements although it is known that the reinforcement ratio range in Chile is 1-8%.

The roof contains a smaller structure to allow the roof to fulfill a recreational function as a rooftop terrace. This structure does not cover the complete roof area.

All elements are formed out of in-situ cast concrete, quality H30. This concrete is denoted as C25/30 in Eurocode 2 term, possessing a characteristic cube compressive strength at 28 days of 30 N/mm^2 or 300 kg/cm^2. This is the most commonly applied concrete quality for highrise buildings like Altamar in Chile.

11.4.2. Construction philosophy

In Chile buildings are designed and constructed to withstand earthquake and/or tsunami loads up to a certain extend. The Chilean people have learned that designing buildings fully earthquake and tsunami proof is way too expensive. The focus has shifted from saving the building to saving lives. This means that they try to let the building be capable of serving its function without failing but damage and deformations are accepted. This results in the situation where the ultimate limit state is always governing over the serviceability limit state.

11.4.3. Soil category

In Bachman and Silva [4] categories are used to define the soil type. The structural information about the Altamar building and its subsoil states that the soil category is B, according to the definition in Instituto Nacional de Normalizacion [23].

12
Model

In this chapter the model of the Altamar highrise is defined. First, section 12.1 describes the software that is used to create the model and section 12.2 describes the uncertainties and assumptions that are made to get to the initial model. Subsequently, section 12.3 describes the verification process of the initial model. Finally the final model is presented in section 12.4.

12.1. Etabs

To analysis the Altamar highrise the building has been modeled using Etabs 2015. Etabs is a structural and earthquake engineering program applying the finite element method. The program is developed by Computers and Structures Inc. (CSI). The software has been provided by Universidad Católica de la Santísima Concepción.

12.2. Assumptions

For the modeling of the building all aspects of a finite element model had to be assumed. Types, dimensions, and properties of concrete elements have initially been assumed using literature (Lagos et al. [28]), pictures, and observations. The main configuration is later on adjusted according to the structural drawings, but there was not enough project time available to adjust the element dimensions.

The concrete quality is initially assumed to be H30, which is the same as C25/30 in terms of Eurocode 2, this was confirmed by the obtained structural information. Even after obtaining of the structural information reinforcement ratios remained unknown. For both the walls and the beams a reinforcement ratio of 1% has been assumed, which is a conservative assumption and in compliance with the opinion of Dr.Ir. Claudio Oyarzo. The structural documents do not give an insight in the applied reinforcement ratios. Etabs lacks the function for the application of reinforcement in shear walls. This has been solved by incorporating the stress-strain diagram of the steel in the tensional non-linear material properties of the concrete for the walls. The floors are modeled without reinforcement since there is no information available so they were left out of the analysis.

Table 12.1 presents the applied dimensions of the structural elements in the model. The decision for not modifying the dimensions has been one with mixed results. A lot of walls posses a higher thickness thus the model here is conservative. Another difference between model and reality occurred in story height. The first two stories are modeled with a height of 3 m whereas the other stories are modeled with a height of 2.4m. The actual building possesses only floors with a height of 2.55 m. This results in the fact that the building is in total a little more than 3 m higher than the model, which is a non-conservative property of the model. The floor thickness is non-conservatively modeled too thick and the beams are conservatively modeled generally too small. The floors have been left out of the in depth analysis because of the great lack of information.

In reality the building possesses a structure to make a rooftop terrace. This structure is not incorporated. However, this will not influence the overall structural behavior of the building.

12.2.1. Finite element elements and mesh

Walls and floors have been modeled as shell elements. Etabs gives the user the choice between the application of thin or thick shell elements. Mindlin-Reissner elements, which are used for thick shell elements, do take

Element	Modeled Dimensions	Real Dimensions
Floors	180 mm	140 mm
Walls	200 mm	200-400 mm
Beams	400 x 200 mm	Several
Columns	400 mm	400 mm

Table 12.1: Modeled dimensions of structural elements

out of plane shear deformation into account. Kirchhof elements for thin shells only take membrane action and bending deformation into account. Considering the horizontal direction of the earthquake loading, this results in an out of plane loading for the walls and an in plane loading for the floors. Therefore it is decided to apply thick shells for the walls and thin shells for the floors.

Etabs meshes structural elements on default. Mesh sizes for walls and floors (shells) are automatically set on 1,25 m. Joints between beams and shell elements are created along the interface and merged by default since meshes have to match alongside the interface. Thus beams, which are considered to be frame elements, are meshed according to the shell mesh. Besides this, Etabs is quite secretive about the finite elements it uses, so no information is available about this.

12.3. Response Spectrum Analysis

To verify the model of the building a response-spectrum analysis was required. First a modal analysis was carried out using Etabs. A modal analysis is necessary to determine the natural mode shapes and eigenfrequencies of a structure during free vibration, for it is assumed that during forced vibrations the mode shape will be a superposition of the natural mode shapes multiplied with a certain unknown time function. The procedure for this analysis is described in the Chilean standard Instituto Nacional de Normalizacion [23] and summarized in appendix M.1.

From the modal analysis the eigenperiods of the modes with the highest mass participation ratios (T^*) were obtained and they are shown in table 12.2.

Direction:	T_1 (s)
x-direction	0,651 s
y-direction	0,996 s

Table 12.2: Eigenperiods of most important modes in both directions

Instituto Nacional de Normalizacion [23] states that the eigenperiods of buildings should be in a range of $N/23 - N/15$, where N is the number of stories. The results shown in table 12.2 are clearly too low and therefore the Altamar building appears to be too stiff. The real building might even be more stiff, as in the model the minimum wall thickness is applied to all walls. Due to lack of time it has been decided that this conservative approach will probably not affect the results too much.

In appendix M.1 all the necessary parameters are given that apply to the Altamar building and which are necessary to determine the design response spectrum. The spectrum is visualized in figure M.1. The generated spectrum and the different scale factors in x and y direction are used as input to create a seismic load case in Etabs. The scale factors are determined in appendix M.1. This load case and its results are used to verify the model.

12.4. Final model

All the information that was obtained during the analysis of the building and the assumptions that were made together led to a model of a structure that's mainly based on shear walls and floors. An impression of the final model can be found in figure 12.1.

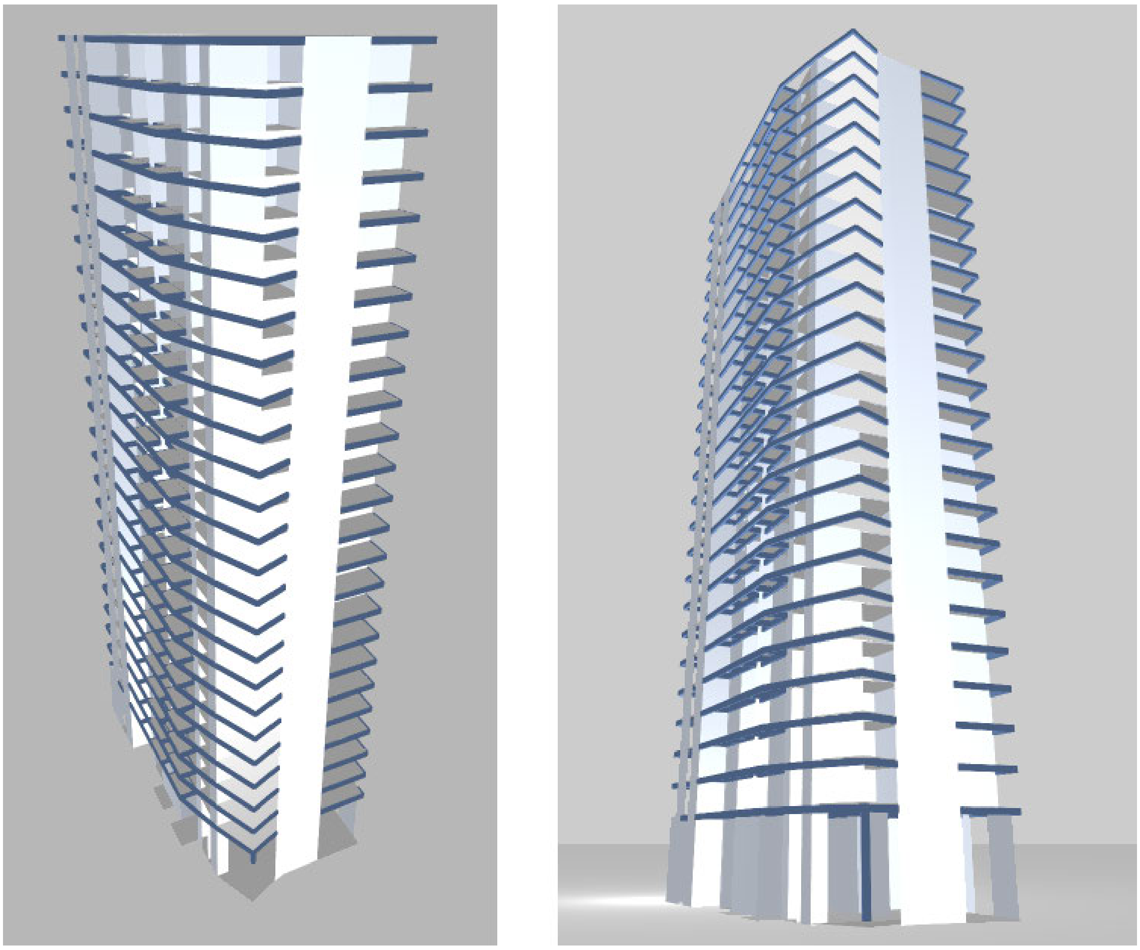

Figure 12.1: The Altamar highrise modeled in Etabs

12.4.1. Floorplans

The configuration of the first 2 floors of the Altamar building differs from the configuration of the other stories, this is shown in figure 12.2. The white-red lines show the positions of the shear walls,the thin blue lines are the beams and the grey dots are the columns.

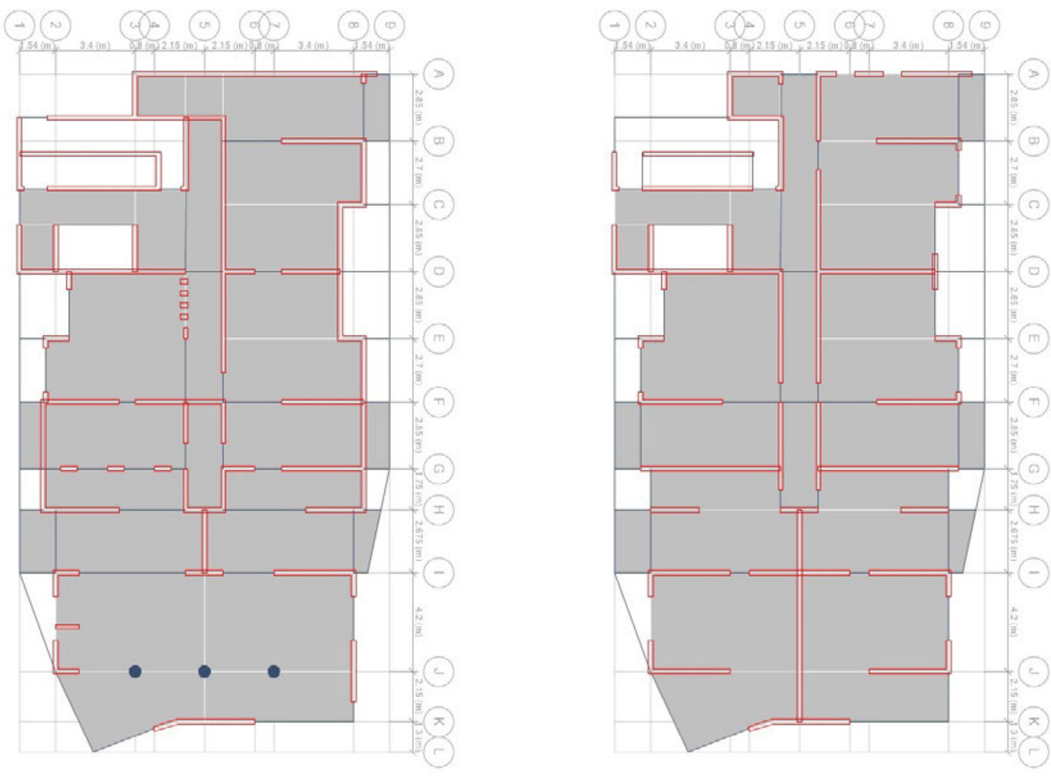

(a) Floorplan first 2 floors

(b) Floorplan floors 3 uptil 26

Figure 12.2: Floorplan configurations from Etabs

13
Forces

In this chapter the applied forces on the Altamar model are described. In section 13.1 the input records of the earthquake are determined and the nonlinear time history analysis is explained. In section 13.2 the different tsunami forces that are applicable are described and calculated using input data from the NEOWAVE numerical simulation from part I. Section 13.3 describes how these forces are modelled in Etabs.

13.1. Earthquake forces

In order to analyse the resistance of the Altamar building to earthquake loading, the old earthquake records from September 2015 are used. Appendix N.1 shows the records as they've been provided by Dr.Ir. Claudio Oyarzo and describes the procedure that was followed to scale the earthquake of 2015 to an earthquake that better matches the worst case scenario that was determined in appendix F as scenario 4. The final time-history functions that are used in Etabs to model the earthquake in x and y direction are shown in figure 13.1 and 13.2.

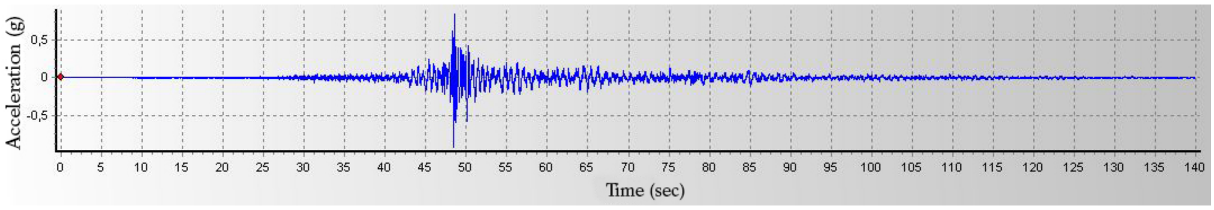

Figure 13.1: Time-history data after scaling in East - West direction

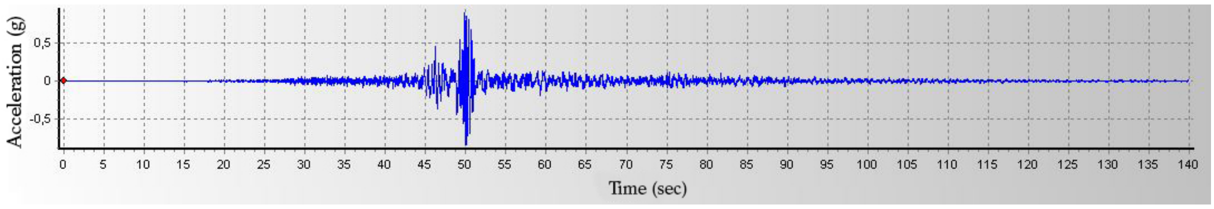

Figure 13.2: Time-history data after scaling in North - South direction

13.1.1. Nonlinear time history analysis

A full time history analysis will give the response of a structure over time during and after the application of a load. To find the full time history response of a structure, the structures equation of motion must be solved. The equilibrium equations of motion are of the form:

$$M\frac{d^2u(t)}{dt^2} + C\frac{du(t)}{dt} + Ku(t) = F(t) \tag{13.1}$$

Etabs solves these equation using direct-integration methods. This is a nonlinear dynamic analysis method which integrates the equilibrium equations of motion fully at every time step of the input, regardless of the output increment.

The direct-integration method in Etabs uses mass- and stiffness-proportional damping, which in fact is just another name for Rayleigh damping. The theory states that during formulation of the damping matrix it is assumed to be proportional to the mass and stiffness matrix. More information about this method and the calculation of the 2 coefficients is given in appendix N.2.

Etabs uses by default the Hilber-Hughes-Taylor method as a time stepping algorithm. Information about this method and the incorporated parameters are given in appendix N.2. The α-factor determines the amount of numerical damping. A variation study on the parameter α has been performed and the results will be compared. In this study the analysis was repeated for different values of α.

13.2. Tsunami forces

All the possible forces that are induced by a tsunami are mentioned in appendix O. These are obtained from Federal Emergency Management Agency [17, ch.6].

For the Altamar building a rather open structure on the ground level is observed, which is in accordance with tsunami regulations. Therefore hydrostatic forces and buoyant forces are not relevant for the analysis of the building.

13.2.1. Worst case scenario input from NEOWAVE model

Properties that have to be obtained in order to calculate the tsunami force are wave speed, wave direction and flow depth. These properties are determined by the numerical simulation done in NEOWAVE. In order to be conservative a worst case scenario is applied. Table 13.1 gives the relevant parameters obtained from the numerical simulation.

Parameter:	Value:
Run up height (R^*)	10,655 m
Ground elevation at Altamar location (z)	3,78 m
Horizontal flow velocity from coast to building (u_{x1})	337,7 cm/s
Horizontal flow velocity from building to coast (u_{x2})	464,5 cm/s
Largest horizontal flow velocity parallel to coast (u_y)	213,7 cm/s
Slope of grade at Altamar location (α)	$(4,0-2,867)/30 = 0,0378$

Table 13.1: Input parameters from NEOWAVE numerical simulation of the worst case scenario

13.2.2. Calculation results

In accordance with Federal Emergency Management Agency [17] calculations of the following forces had to be performed:

- Hydrodynamic forces
- Impulsive forces
- Debris impact forces
- Uplift forces on elevated floors
- Additional gravity loads on elevated floors

Hydrostatic forces and buoyant forces on the structure as a whole are not relevant for the Altamar building as an open structure of the ground level was observed. Because of the open structure a water level difference between the inside and the outside or between several compartments within the building is unlikely to occur and hydrostatic forces will be in equilibrium with each other. Furthermore because the water level difference can not occur buoyant forces will not affect the building. Damming of waterborne debris can be neglected as well because the building is wider than the width of the debris. Therefore the surface for hydrodynamic loading is not increased by the debris width.

An Excel sheet has been created to calculate the values that have to be applied to our building. In appendix O the calculations are elaborated in detail. Table 13.2 shows the results of these calculations.

Force:	Value:	Location of application:
Hydrodynamic force	12390,1 N/m^2	On all members that are passed by the leading edge of the tsunami surge, uniformly from z=0 uptil z=h_{max}
Impulsive force	18585,2 N/m^2	On members at the leading edge of the tsunami surge uniformly from z=0 uptil z=h_{max}
Debris impact forces	5344890,5 N/m	Locally on a single member at h_{max}
Uplift forces on elevated floors (buoyant) (hydrodynamic)	21795,9 N/m^2 29,3 N/m^2	Upward on highest submerged floor
Additional gravity loads on elevated floors	19676,9 N/m^2	Downward on submerged floor

Table 13.2: Results calculations of different tsunami forces

13.2.3. Tsunami force combinations

According to Federal Emergency Management Agency [17, p.82] the impulsive force only occurs at the leading edge of a tsunami surge and the structural elements that are already passed by the leading edge will only experience the hydrodynamic force. The worst case of this will be when the leading edge is at the last parts of the building and all parts in front experience the hydrodynamic force. Figure 13.3 shows figure 6-10 from Federal Emergency Management Agency [17], which clarifies the combined application of impulsive and drag forces.

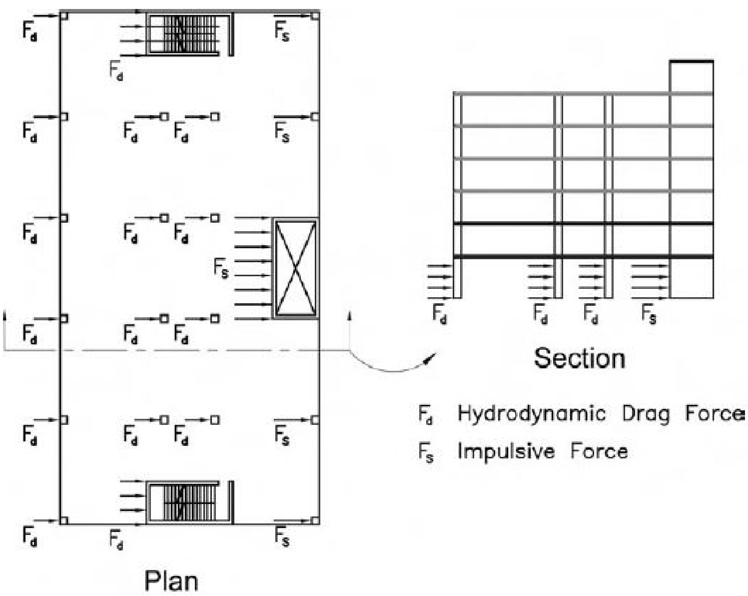

Figure 13.3: Impulsive and drag forces applied to an example building. Source: Federal Emergency Management Agency [17, p.83]

Debris impact forces won't occur at the leading edge of a tsunami surge as the leading edge doesn't carry large debris. The Federal Emergency Management Agency [17, p.82] states that the probability of multiple impacts at the same time is very small and therefor only 1 impact at any point in time needs to be considered. All structural components need to be designed to be able to withstand the hydrodynamic drag force in combination with an impact force.

Uplift forces on submerged floors have to be taken into account simultaneously with the hydrodynamic, impulsive and debris impact forces, as it reduces the weight of the structure. This may impact the overturning resistance of the building. Additional gravity loads due to retained water may be considered separatly. The way the different forces work simultaneously or not is summarised in table 8.1.

13.2.4. Load combinations

Federal Emergency Management Agency [17, p.85] states the following load combinations that should be taken into consideration when designing a vertical evacuation refuge:

Load Combination 1: $1,2D + 1,0T_s + 1,0L_{REF} + 0,25L$
Load Combination 2: $0,9D + 1,0T_s$

Here D is the dead load, T_s is the tsunami load, L_{REF} is the live load in refuge areas (4,788 kN/m^2) and L is the live load outside of the refuge areas.

Load combination 1 is for the refuge areas. All other floor areas will experience a reduced live load of 25% of the design live load, which is also the case during earthquake loading. Load combination 2 is for when gravity loads oppose the tsunami loads, so in case of uplift forces this load combination should be taken into consideration.

13.3. Modelling of forces in Etabs

As mentioned in section 13.1 the earthquake was modelled using the time-history function input in Etabs. Only the most severe one of the 2 records is used, this was the record in North - South direction. This is done, because the difference between the 2 records is negligible and the processing of the records in Etabs takes a very long time.

Two main load combinations have been modeled, EqX+TS and EqY+TS. EqX+TS contains the earthquake acceleration in x-direction, all tsunami loads, the dead load and the live load. EqY+TS is basically the same as EqX+TS but the earthquake now is modeled to act in y-direction.

The earthquake in x-direction is simulated first with the initial conditions set to zero, subsequently the earthquake in y-direction is simulated using the initial conditions of the state of the building after the x-earthquake. Unfortunately Etabs is not able to simulate both at the same time. The building is stiffest in x-direction, therefore the damage after the x-earthquake will be smaller than after the y-earthquake. As the damage is smaller after the x-earthquake the effect these initial conditions will have on the following earthquake will be smaller and the result obtained will be closer to reality.

All different tsunami forces are modelled in a nonlinear static load case with the initial conditions set after the y-earthquake. All the different load cases are put together in one load combination, to realise the effect that the hydrodynamic, impulsive, debris impact and uplift forces work simultaneously.

Unfortunately Etabs doesn't have an option to define area loads or line loads at a random location on a shell. It is only possible to put a load on a complete shell object. Due to this the hydrodynamic and impulsive force work from z=0 to z=10,0 m instead of $h_{max} = 10,0715\ m$ as it was rather difficult to split shell objects. The debris impact works on an area of width = 5,22 m and height = 1,2 m at a height of 8,8 to 10,0 m, instead of being a line load over a length of 6,096 m at a height of h_{max}. The value of the area load has been modelled as approximately 4500 kN/m^2.

14 Results

This chapter is an elaboration of the results obtained in the previously described investigations. First the general results of the modeling of the earthquake and tsunami forces will be discussed, followed by a review of the alteration of the alpha factor, reinforcement ratios, and mesh size.

14.1. Main results

Appendix P contains obtained results from Etabs for the different simulation runs that have been performed. The different runs have the following input differences:

Run 1:	reinforcement ratio = 1%,	alpha = 0,	mesh size = 1,25 m,	succeeded
Run 2:	reinforcement ratio = 3.5%,	alpha = 0,	mesh size = 1,25 m,	succeeded
Run 3:	reinforcement ratio = 3.5%,	alpha = -0,1,	mesh size = 1,25 m,	succeeded
Run 4:	reinforcement ratio = 1%,	alpha = 0,	mesh size = 0,625 m,	succeeded
Run 5:	reinforcement ratio = 1%,	alpha = 0,	mesh size = 0,3125 m,	not succeeded

The reinforcement ratio mentioned in the overview above is the ratio present in the shear walls. The most relevant results will be presented and discussed in this chapter. Run 5 has not succeeded due to a lack in hardware resources.

14.1.1. Stability

During the sub-sequential earthquake and tsunami loading on the building, the structure remains completely stable. Members do not fail and excessive displacement does not occur. This can be seen in table P.1, where the maximum displacements can be observed. Furthermore all steps have converged during the performance of the non linear (time history) analysis, which is an indication of complete stability as well.

14.1.2. Displacements

The displacements have been regarded in a x and a y-component and are presented in table 14.1. In x-direction the maximum displacement occurs on the third floor, denoted by the red dot in figure 14.1. This displacement has a value of 63 mm, which is quite high. This value will never occur in reality since this location is in a wall which separates the stairs. The stairs are not modeled which decreases the stiffness of this part of the structure drastically. The maximum displacement in x-direction which is actually considered to be realistic occurs on the fifth floor and has a value of 18,2 mm. This deformation is mainly induced by the debris impact force. The location of this deformation is denoted with the blue dot in figure 14.1. The maximum displacement in x-direction occurs when both the earthquake in x-direction and the tsunami occur.

In y-direction the tsunami forces have less influence and thus the displacements are significantly lower. The maximum displacement in y-direction occurs in the roof and has a value of 7.8 mm. This value is mainly induced by the earthquake acceleration forces. Although the tsunami forces mainly work in x-direction, they do influence the displacements in y-direction. The maximum displacement in y-direction occurs when both the earthquake in y-direction and the tsunami occur.

During the earthquake in x-direction with tsunami the maximum displacement in the top of the building is 3,5 mm in x-direction and 6,8 mm in y-direction. During the same earthquake in y-direction and the tsunami loading the maximum displacements are 3,1 mm in x-direction and 7,8 mm in y-direction.

The vertical deformations are minor, in the worst case the top of the building is 6,25 mm lower. This happens in case of the earthquake in y-direction and the tsunami loading. This is also not the final state but the maximum vertical displacement during the load cycle.

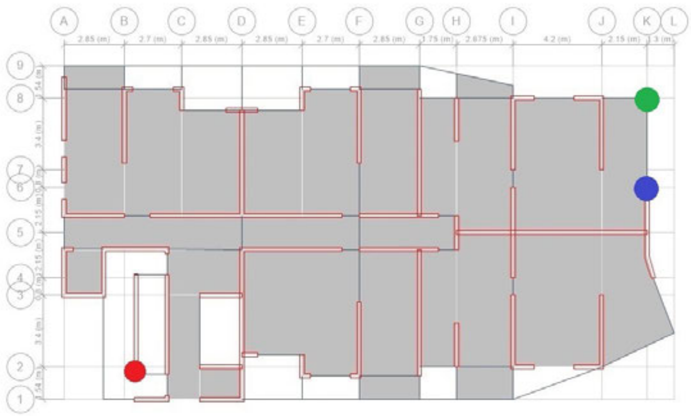

Figure 14.1: Locations of interest during interpretation of results

14.1.3. Interstory drift

The maximum interstory drift has to fulfill two demands in the serviceability limit state according to the Chilean building and design code.

$$\delta_0 / h < 0,2\% \tag{14.1}$$

$$\frac{\delta_{i;max} - \delta_0}{h} < 0.1\% \tag{14.2}$$

In equation 14.1 δ_0 is the drift in the center of mass of the story, h is the story height. In equation 14.2 $\delta_{i;max}$ is the extreme drift in the corner depicted with the green dot in figure 14.1. In paragraph P.1 in the appendices the results for the equations above are presented for the earthquake in X and Y-direction with accompanying tsunami. The story drifts in the center of mass are not nearly close to the maximum allowed value whereas for the story drift in the corner this is a close call. Due to the tsunami impact forces the story drift of the corner is 0,098, quite close to 0,01.

Figure 14.2 presents two plots of the results of equations 14.1 and 14.2 from left to right over the height of the building. The graphs represent the results for the earthquake in x-direction (which has the most severe consequences) and the tsunami. Drifts in x and y-direction are plotted against each other. On the right side of both graphs is a red line representing the maximum allowed value stated in the equations. The tsunami impact can clearly be seen in the lower floors. Even though the tsunami forces are working completely in x-direction it is interesting to see that also in y-direction the displacements, and thus the interstory drift, are significantly influenced.

14.2. Reinforcement ratio

Since reinforcement ratios for all structural elements appear to be unknown the ratios of the walls have been lowered from 3.5% to 1% with positive result, no stability issues occurred during the analysis. This conservative configuration of reinforcement should increase the likelihood of a reliable final conclusion.

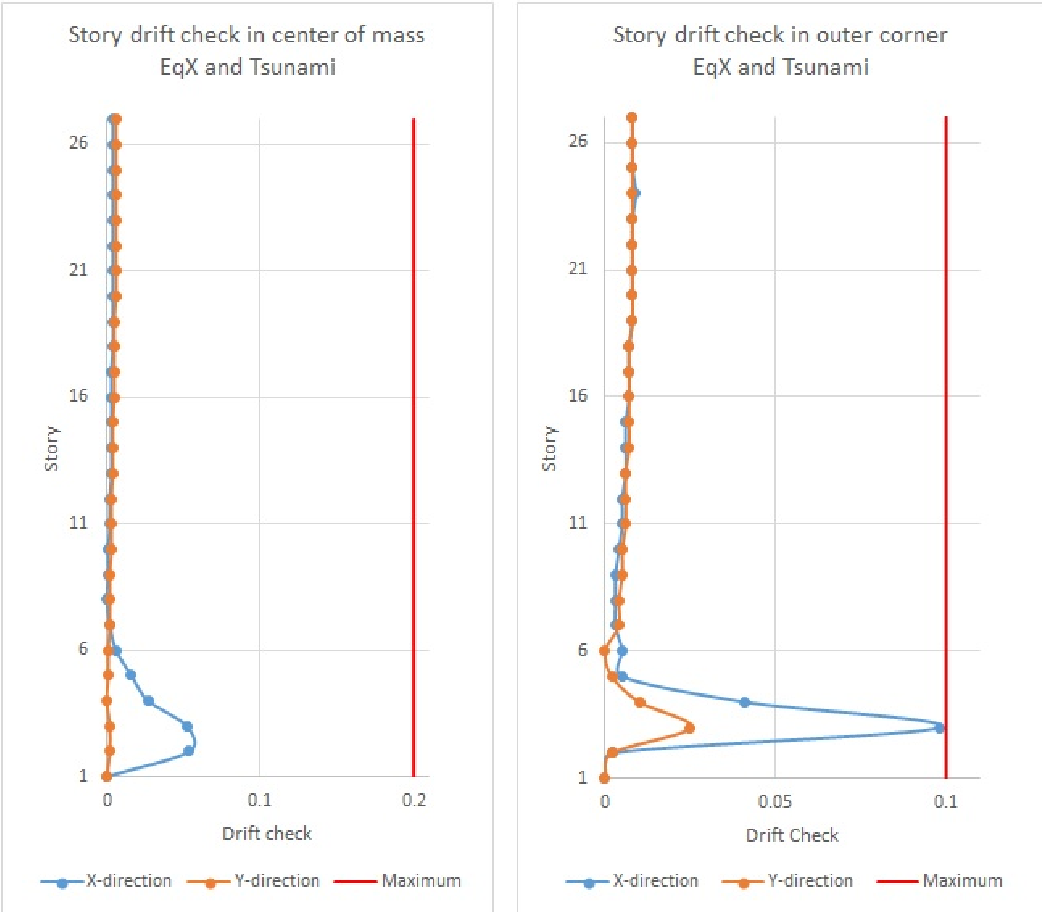

Figure 14.2: Story drift in center of mass and in outer corner due to earthquake in x-direction and tsunami

14.3. Alpha factor

The alpha factor, as described in appendix N.2, is of importance in the Hilber-Hughes-Taylor stepping algorithm for solving the nonlinear time history earthquake analysis. In short, for α between 0 and -1/3 the Hilber-Hughes-Taylor method is unconditionally stable and for α is 0 numerical damping of high frequency modes is not present. By increasing α from -0,1 to 0 it was investigated whether the model would still converge. A higher alpha would be beneficial for the reliability of the results. For the model of the Altamar building an α of 0 appeared to be sufficient.

14.4. Mesh size

A full mesh-refinement study would mean dividing the mesh size by 2 until the difference with the new results compared to the previous results is smaller than 1%. Table 14.1 shows the results of the simulation with different mesh sizes and the corresponding error percentages between the different mesh refinement steps.

As Fz and My are caused by the dead load, which is always the same and already accurate for the largest mesh size these are left out.

Overall the mesh refinement results in larger displacements, smaller forces and larger moments. A new refinement have been tried to run, named run 5 in the beginning of this chapter, but failed on time and hardware resource capacities.

14.5. Safety factors

The design of a vertical evacuation refuge according to Federal Emergency Management Agency [17] includes safety factors as mentioned in section 13.2.4. However these load combinations are primarily used to assess the safety of the floors (vertical forces). A more detailed floor assessment is pointless as there's no structural in-

	mesh = 1,25 m (1)	mesh = 0,625 m (2)	error (1) - (2)
ux-1	63,283 mm	63,164 mm	0,19%
ux-2	15,972 mm	18,232 mm	14,15%
uy	7,591 mm	7,82 mm	3,02%
uz	-6,105 mm	-6,254 mm	2,44%
Fx	34787,04 kN	34756,73 kN	0,09%
Fy	-661,33 kN	-647,41 kN	2,10%
Mx	840454,4 kNm	840654,9 kNm	0,02%
Mz	275044,0 kNm	274601,0 kNm	0,16%

Table 14.1: Mesh refinement study

formation about the floors available. The load combinations do not affect horizontal force because a relatively high safety has been incorporated in the determination of the tsunami forces according to Federal Emergency Management Agency [17].

14.6. Floors

As mentioned, due to lack of information about the floors (thickness, material, reinforcement ratio) it is meaningless to perform a detailed study on the floor capacity based on only assumptions.

To be able to operate as a vertical evacuation refuge the floors in refuge areas of the Altamar building need to be able to carry an additional live load of 4,788 kN/m^2. Furthermore, the floors that get submerged during a tsunami need to be checked on a load combination of 90% of the dead load with uplift forces and 100% of the dead load with the additional gravity forces. Unfortunately this could not be checked in this study.

15
Conclusion

This chapter presents the conclusions that are based on the results obtained thoughout this project and presented in the previous chapter. The subjects stability, displacements, story drift, mesh size, and alpha factor finally lead to a conclusion on the main research question in the general conclusion.

15.1. Stability

As has been elaborated in chapter 14 the model has not showed any stability issues. An important aspect of a vertical evacuation building of course is overall stability to facilitate a safe refuge. For the structural data taken into account it can be concluded that under the considered earthquake and tsunami loading the building remains stable.

15.2. Displacements

The displacements appear to be remarkably small even though the loading was considerable. The deformations at the location of the red dot in figure 14.1 are left out of consideration because of the low possibility of occurrence since in reality stairs are located there. A big deformation concentration is located in front of the building, the green dot in the picture, where waterborne debris might possibly hit the building and the first wave hits the building. This nonetheless does not influence overall stability. The relatively small deformations confirm the results of the modal analysis which showed low eigenperiods indication a stiff building, see paragraph 12.3. The small deformations under the loading are beneficial for the building and its coveted function.

15.3. Story drift

The story drift can have a significant influence on overall stability and damage issues. As presented in the results chapter the story drift has been checked in two locations, the center of mass and the extreme corner in front of the building. The tsunami loading puts the Altamar building to the test but it manages to keep the extreme story drift below the 0,1% mark, which results in the fact that for both the measurements in the center of mass and the extreme corner the building suffices the Chilean building and design code demands.

15.4. Mesh size

The mesh refinement study has showed that the differences in results between the coarse mesh (1,25m) and the firstly refined mesh (0,625m) are bigger than 1%. The next step was to refine the mesh with a factor 0,5 again to 0.325 m. Unfortunately the attempts on performing this run have failed due to hardware capacity. It thus has to be concluded that the applied mesh size has not been of proper size for achieving the coveted reliability. Figure 15.1 shows the difference between the several runs in terms of displacement. Run 4 is the run with the refined mesh. It appears that the refinement influences the results significantly.

15.5. Alpha factor

The final analysis (run 4) have been run with alpha having a value zero. The alpha factor being zero results in the absence of numerical damping and thus increasing the reliability of the result.

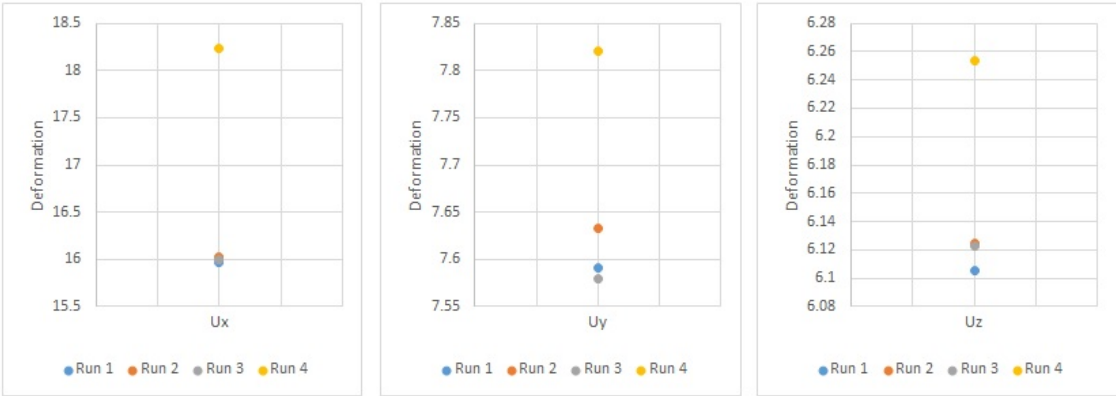

Figure 15.1: Differences in deformation results for different runs, run 4 (alpha=0) is governing. See chapter 14 for an overview of properties of each run

15.6. General conclusion

Altamar, being part of the total plan of making Coquimbo Bay a safer place, might function as a vertical evacuation location. This research has been performed according to the following research question:

> *To what extend is the Altamar building capable of resisting a possible future earthquake and tsunami load, requiring a vertical evacuation function remains possible?*

As mentioned before in paragraph 11.4.2, in Chile the building philosophy nowadays is focused on saving people, not buildings. This means that as long as the building remains stable and full collapse is prevented during earthquake and tsunami loading, damage is accepted. Even if the building loses the capability of fulfilling its primary function, in this case the residential function, completely due to the damage, this is accepted. The results obtained during this research project speak in favour of Altamar being capable of fulfilling this vertical refuge function in compliance with the Chilean building philosophy. Under the load of a fierce earthquake and tsunami the building will be damaged but full collapse is unlikely to happen. Thus for this research results it can be concluded that the Altamar building can be used as a vertical refuge building and thus can be incorporated in the integral plan for Coquimbo Bay.

IV

Master plan

16

Evacuation plan

In this chapter the total evacuation plan of the area is decribed. The chosen alternative is combined with the possibility to evacuate to the Altamar building.

16.1. Evacuation routes

In the area of Baquedano there is an existing evacuation plan for the neighbourhoods that surround the area (appendix Q). In the plan the safe area for tsunamis is given, here people can evacuate to via the main evacuation routes. The new evacuation routes in the final plan will be connected to the existing routes.

Figure 16.1: evacuation regions with the corresponding evacuation routes connecting to the existing evacuation routes, source: Mapbox.com [30]

Figure 16.1 shows that the Altamar building is integrated as a vertical evacuation point. Mostly the touristic area will evacuate to the Altamar Building. The red lines are big paths that function as evacuation routes and will be connected to the existing evacuation routes.

In appendix Q a maximum evacuation distance of 800 m is specified. This 800 m is based on the assumption that some people will not walk faster than 3,2 km/h. The average speed is considered to be 6,4 km/h but because also the slower people have to be able to reach safety the requirement is set more conservative. The requirement of 800 m is fulfilled in almost the whole area, only in the top right corner of the area the maximum distance to evacuate is exceeded. The evacuation distance at this location is approximately 1200 m. A decision was made not to implement extra measures for this area, as there are no people living there and the requirement of 800 m is very conservative. Additionally a time of arrival of 15 minutes has been chosen which is in accordance with the results from the numerical simulations. Nevertheless, FEMA states that a time of arrival of maximum 30 minutes can be maintained. Furthermore the first arriving wave is really small thus it is likely that the arrival time of a significant tsunami will be longer in reality. The wave which first arrives during the numerical simulation does not reach far inland which should give people enough time to find refuge. To warn people for an approaching tsunami extra signs and alarms will be placed. Of course the evacuation routes can also be used on a daily base in a regular way.

17

Conclusion

In part I an integral design is developed to improve the area of Coquimbo bay. The coastal protection from this integral plan is designed in part II and the possible function of the Altamar highrise as a vertical evacuation refuge is analysed. In the end an evacuation plan is created and presented. The final mapping of the area is given in figure 17.1.

Figure 17.1: Overview of the total area with the final arrangement , source: Mapbox.com [30]

Multiple aspects in the area have been improved with respect to the current situation. First, the safety has been improved. The new coastal protection will retain small tsunamis and for larger tsunamis the amount of inundation in the Baquedano neighbourhood is strongly reduced. Additionally the first wave is now fully retained by the new coastal protection, which increases the available evacuation time.

Subsequently, the possibilities for quick evacuation have been increased by the availability of the Altamar building as a vertical evacuation location. Especially with the increase in public activities close to the Altamar building this is an important improvement.

Finally, the whole area is more attractive due to the development of recreational space. A touristic area is created to stimulate tourism and to improve the environment of the local inhabitants. Besides the touristic area a natural area will be developed, which can also be used for recreational purposes. Additionally, the natural and ecological value of the area is increased due to the increase in wet surface and the increased interaction between the coast and the wetlands. Impressions of the integral plan are given in figure 17.2.

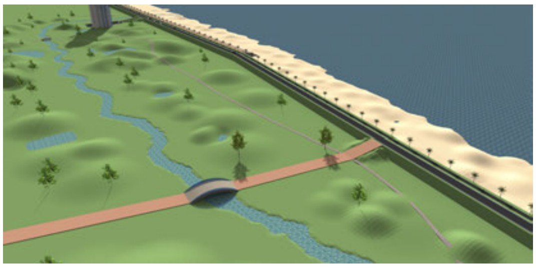

(a) Impression of the integral plan with the recreational area.

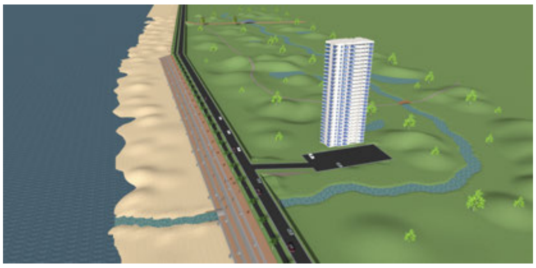

(b) Impression of the integral plan with the Altamar and boulevard.

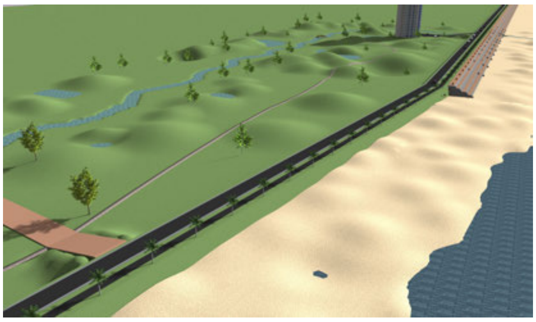

(c) Impression of the integral plan with the coastal road.

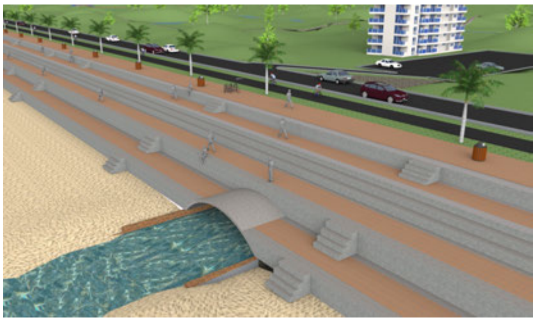

(d) Impression of the integral plan with the boulevard.

Figure 17.2: Different impressions of the integral plan.

18
Recommendations

18.1. Masterplan Coquimbo Bay

To perform the tsunami simulations only 1 earthquake scenario is used based on the expert judgment of dr. R. Aránguiz. However, in order to perform a full analysis different possible earthquake scenarios should be analysed and their probabilities of occurrence should be known. In combination with the value of the damage that would occur as a result of a certain scenario a better conclusion can be drawn about the economical feasibility of a solution.

An extensive social-economic research should be done to make sure that the solution is in line with the wishes of the people most influenced by it. A more detailed research should determine the true disposition of all stakeholders. The result can be used to do a less subjective Multi Criteria Analysis conforming the relevant criteria and values.

In this study it is assumed that it is possible to create a touristic area enlarging the welfare of the neighbourhood. However, it is unsure if there is need for more tourist facilities, as La Serena has many facilities already. The possibility for tourism in Coquimbo should be studied more carefully to determine if the investment is worth it.

The effects of the alterations on the wetlands should be studied. The alterations will influence the ecology of the wetlands and the morphology of the wetlands and adjacent coasts, but the exact effects are uncertain.

The determination of the costs of the different alternatives is based on a reference project and is rather approximate and incomplete. For instance the costs of construction and maintenance should be calculated in more detail.

18.2. Coastal protection

The NEOWAVE model used a grid size of 10 m. This grid size is rather large and inaccurate. To get a better understanding of the occuring processes, such as turbulance, refraction and shoaling, a more refined grid should be used. Likewise, the inundation height and flow velocity that are obtained using the NEOWAVE simulations would be more accurate using a refined grid. These values are used to calculate the tsunami forces on the structures and therefore relevant for an adequate design.

The application of non-hydrostatic flow in the NEOWAVE model should be studied. Due to a lack of project time it was not possible to perform all simulations of the model with non-hydrostatic properties. In the case of non-hydrostatic flow the inundation height and flow velocity might turn out lower. Therefore the tsunami forces that are applied to the structures will probably reduce as well and a more efficient design could be made.

In further research with the NEOWAVE numerical simulations also the tide should be included. The combination of high tide and a tsunami wave might increase the impact of the tsunami.

The design of the coastal protection can be done in more detail. In this project only the overall stability and the protection against scour were taken into account. However the internal structural stability and the resistance against earthquakes might be critical as well. Furthermore, the height of the protection can be optimized. A probabilistic approach can be used to determine the damage in Baquedano with a varying coastal protection height. This damage should be compared to the construction costs and an optimum should be found.

The level of uncertainty concerning the amount of scour protection is high. Additional research is recommended to determine the minimum diameter and the length of the protection. Due to the sole availability of empirical data the use of a scale model is preferred.

It is recommended to look into possibilities for the Baquedano neighbourhood to increase the safety. For instance it might be beneficial to rebuild the neighbourhood with elevated houses.

18.3. Altamar

The research on the Altamar highrise has initially been one containing many uncertainties and assumptions. Eventually a part of the official structural information about the building was obtained, but a lack of project time made it impossible to implement all gained knowledge. This situation has resulted in a set of recommendations for further research to improve the reliability of the final conclusion about the possibility of the Altamar building as a vertical refuge location in case of an earthquake with corresponding tsunami.

It is recommended to obtain more of the available structural information about the building and implement all structural details in the model. This includes dimensions of structural elements and material properties such as reinforcement ratios. This way a complete and realistic model can be created and most of the uncertainties can be removed.

Floor behaviour should be taken into account. As mentioned before the consideration of floor behaviour has been left out of this research because of a lack of information and resources. Especially the vertical components of the tsunami loading influences the lower floors significantly and the additional live load due to the evacuated people must be checked. For the building to satisfy all demands of Federal Emergency Management Agency [17] the floors should be checked on all associated forces thus the relevance of investigating this is high.

The staircases are not modeled resulting in very high local joint displacements. The highest joint displacement in x-direction is found in the wall which is supposed to be in between the stairs, location of red dot in figure 14.1. This is an unrealistic result of the displacements in this point and therefore it is recommended to create a more detailed model containing the stairs as well.

It appeared to be too difficult to amplify an earthquake from a Mw 8.3 to a Mw 8.5 earthquake. Unfortunately in both the project team and in Universidad Católica de la Santísima Concepción the expertise was missing. Since earthquake magnitude is presented in a log-scale the expectation is that the influence can be significant. Therefore it is highly recommended to do a more detailed study concerning the earthquake that might apply to the Altamar building in a future event.

In chapter 14 the results of the mesh refinement study are elaborated. The results were not satisfying yet, but unfortunately this study could not be finished due to time and resource limitations. It is recommended to finalize the mesh refinement study to increase the reliability of the research results.

Due to hardware limitations we have not been able to obtain element stresses and interstory shear forces. Although it is known that the building remains stable, this does not imply that none of the elements fails. Stressed could be locally redistributed without endangering overall stability. Locally failing elements can be determined using element stresses and interstory shear; the most heavily loaded elements can be found and checked using the structural information of that element. On the critical members of the structure the most unfortunate load combination should be applied and checked as well.

Bibliography

[1] Rafael Aránguiz. Lecture Origen of tsunamis; 11-07-2014. 2014.

[2] Rafael Aránguiz, Gabriel González, Juan González, Patricio A. Catalán, Rodrigo Cienfuegos, Yuji Yagi, Ryo Okuwaki, Luisa Urra, Karla Contreras, Ian Del Rio, and Camilo Rojas. The 16 September 2015 Chile Tsunami from the Post-Tsunami Survey and Numerical Modeling Perspectives. *Pure and Applied Geophysics*, 173:333–348, 2016. ISSN 14209136. doi: 10.1007/s00024-015-1225-4.

[3] Rafael Aránguiz, Luisa Urra, Ryo Okuwaki, and Yuji Yagi. Tsunami damage estimation based on fragility curves: Application to Coquimbo, Chile. *CENG*, 2016.

[4] Robert E Bachman and John F Silva. NCh-433-Of-1996 : Seismic Design of Buildings, 2010.

[5] Judith Bosboom and Marcel Stive. *Coastal Dynamics 1 - Lecture Notes CIE4305*. TU Delft, 2015.

[6] Elisabete Alberdi Celaya and Juan José Anza. BDF- α : A Multistep Method with Numerical Damping Control. 1(3):96–108, 2013.

[7] Juan Sebastián Alcayaga Claussen. “Los Espacios Naturales y sus Usos Urbanos” El Caso del humedal “El Culebrón” de la ciudad Coquimbo, Chile. 2014. Technical report, Universidad Nacional Autonoma de Mexico, 2014.

[8] cpsinmobiliaria.cl (13-09-2016). CPS Inmobiliaria, 2011. URL `www.cpsinmobiliaria.cl`.

[9] Daft Logic. Google Maps Area Calculator Tool (19-10-2016). URL `https://www.daftlogic.com/projects-google-maps-area-calculator-tool.htm`.

[10] M De Gunst. Stone stability in a turbulent flow behind a step. Technical report, TU Delft, Civil Engineering and Geosciences, 1999.

[11] H. de Vriend and M. van Koningsveld. *Building with Nature*. EcoShape, 2012. ISBN 9789461909572. URL `http://www.ecoshape.nl/nl{_}NL`.

[12] Robert George Dean and Robert A. Dalrymple. *Water Wave Mechanics for Engineers and Scientists*, volume 2. 1984. ISBN 9810204213. URL `http://books.google.co.uk/books/about/Water{_}Wave{_}Mechanics{_}for{_}Engineers{_}and{_}S.html?id=9-M4U{_}sfin8C{&}pgis=1`.

[13] DeltaresFilm. Stopping A Tsunami: A Membrane Tsunami Float Barrier Concept With Dyneema®, 2014. URL `https://www.youtube.com/watch?v=0eFU4KIezSc`.

[14] Dirección de Obras Portuarias. Construccion obras anexas muelle pesquero Tongoy, IV Region, 2015.

[15] Dsm.com. Tsunami Flood Barrier Concept (20-09-2016), 2014. URL `http://www.dsm.com/products/dyneema/en{_}GB/about/stories/the-tsunami-catcher.html`.

[16] E-pao.net. Engineers’ Worst Fear - When Earth Boils (26-09-2016). URL `http://www.e-pao.net/epSubPageExtractor.asp?src=education.Scientific{_}Papers.Engineers{_}Worst{_}Fear{_}When{_}Earth{_}Boils`.

[17] Federal Emergency Management Agency. *Guidelines for Design of Structures for Vertical Evacuation From Tsunamis*. Number June. FEMA, 2008. URL `ftp://jetty.ecn.purdue.edu/spujol/Andres/files/15-0021.pdf`.

[18] Geofun M R. Informe de mecánica de suelos, 2008.

[19] Google Earth. Overview Coquimbo Bay (15-09-2016), 2011. URL `https://www.google.nl/maps/@-29.779279,-71.5869856,26921a,20y,114.11h,48.32t/data=!3m1!1e3`.

[20] M.J.C.M Hertogh. Voorbeelden kentallen dd 25-04-2007. pages 5–7. TU Delft, 2007.

[21] Robert Hunziker. Chile's Plantation Economy (18-09-2016), 2014. URL `http://dissidentvoice.org/2014/12/chiles-plantation-economy/`.

[22] Instituto Nacional de Normalizacion. Diseño estructural de edificios - Cargas permanentes y sobrecargas de uso, 1986.

[23] Instituto Nacional de Normalizacion. Diseño sísmico de edificios, 2012.

[24] Ioc-sealevelmonitoring.org. ioc-sealevelmonitoring (15-09-2016). URL `http://www.ioc-sealevelmonitoring.org/station.php?code=coqu`.

[25] Bas Jonkman, Oswaldo Morales-napoles, and Raphael Steenbergen. Lecture CIE 4130, Probabilistic Design, TU Delft. Number January. TU Delft, 2016.

[26] S N Jonkman, A C W M Vrouwenvelder, R D J M Steenbergen, O Morales-nápoles, and J K Vrijling. *Probabilistic Design : Risk and Reliability Analysis in Civil Engineering*. TU Delft, 2015.

[27] Yu Ting Joanne Khew, Marcin Pawel Jarzebski, Fatma Dyah, Ricardo San Carlos, Jianping Gu, Miguel Esteban, Rafael Aránguiz, and Tomohiro Akiyama. Assessment of social perception on the contribution of hard-infrastructure for tsunami mitigation to coastal community resilience after the 2010 tsunami: Greater Concepcion area, Chile. *International Journal of Disaster Risk Reduction*, 13: 324–333, 2015. ISSN 22124209. URL `http://www.scopus.com/inward/record.url?eid=2-s2.0-84938323308{&}partnerID=tZOtx3y1`.

[28] Rene Lagos, Marianne Kupfer, Jorge Lindenberg, Patricio Bonelli, Rodolfo Saragoni, Tomas Guendelman, Leonardo Massone, Ruben Boroschek, and Fernando Yanez. Seismic Performance of High-rise Concrete Buildings in Chile Seismic Performance of High-rise Concrete Buildings in Chile. *International Journal of High-Rise Buildings*, 1(3):181–194, 2012. URL `http://global.ctbuh.org/resources/papers/download/1991-seismic-performance-of-high-rise-concrete-buildings-in-chile.pdf`.

[29] Mapbox.com. Project Location, 2016. URL `https://www.openstreetmap.org/{#}map=15/-29.9635/-71.3234`.

[30] Mapbox.com. Project Scope, 2016. URL `https://www.openstreetmap.org/{#}map=16/-29.9622/-71.3226`.

[31] Ministry of Housing and Urban Development. Master Plan Remodelling Urban Sector Baquedano Coquimbo. 2016.

[32] Ministry of Housing and Urban development. Masterplan region Baquedano, 2016.

[33] F Molenaar and Z Voorendt. *Manual Hydraulic Structures*. Number March. TU Delft, 2016.

[34] Municipalidaddecoquimbo.cl. Tourism in Coquimbo, Regional Economy (14-09-2016). URL `http://www.municipalidaddecoquimbo.cl/tourism/economia.aspx`.

[35] Ioan Nistor, Dan Palerma, Younes Nouri, Tad Murty, and Murat Saatcioglu. Handbook of Coastal and Ocean Engineering. In *Gulf Professional Publishing*, number August 2016, chapter Chapter 11, page 1340. 1992. ISBN 9789812819307. URL `https://www.researchgate.net/publication/259674497`.

[36] Yoshimitsu Okada. Surface deformation due to shear and tensile faults in a half-space, 1985.

[37] Oregongeology.org. Oregon Tsunami Clearinghouse / Resource Library (13-09-2016). URL `http://www.oregongeology.org/tsuclearinghouse/faq-tsunami.htm`.

[38] Photorator.com. Tsunami Wall Japan (22-09-2016). URL `http://photorator.com/photo/10097/tsunami-wall-under-construction-in-noda-iwate-japan-in-`.

[39] SATREPS. Tsunami Mitigation Measures Menu. 2(March), 2016. URL http://www.cigiden.cl/wp-content/uploads/2016/04/Vol.2-Tsunami-mitigation-measures-menu.pdf.

[40] G. J. Schiereck. *Introduction to Bed, Bank and Shore Protection*. CRC Press, London, 2004. URL http://search.ebscohost.com/login.aspx?direct=true{&}db=nlebk{&}AN=145614{&}site=ehost-live.

[41] Secretaria Regional Minesterial De Vivienda y Urbanismo Coquimbo. Diagnóstico Áreas De Riesgos Localidades Costeras, Región de Coquimbo. Technical report, 2008.

[42] Sepchile.cl. Empresa Portuaria Puerto de Coquimbo (14-09-2016). URL http://www.sepchile.cl/empresas-sep/portuario/empresa-portuaria-puerto-de-coquimbo-epco/?no{_}cache=1.

[43] Angelo Simone. Time-dependent problems. In *CIE5123 Introduction to the Finite Element Method*, volume 0, chapter 9, pages 113–124. TU Delft, 2015.

[44] J.M.J. Spijkers, A.W.C.M. Vrouwenvelder, and E.C. Klaver. *Structural Dynamics CT 4140*. Number January. TU Delft, Delft, 2005.

[45] Tensar. Tensartech systemen voor keermuren en steile taluds. URL http://www.tensarcorp.com/.

[46] Universidad Católica de Valparaiso Grupo de Geotecnia. Clasificación de suelos-Diapositivas. pages 1–20.

[47] Valuta.nl. Exchange rate currencies (20-10-2016), 2016. URL http://www.valuta.nl/chileense{_}peso.

[48] Van den Noort Innovations B.V. Twin-Wing Tsunami Barrier. 2013. URL http://www.noort-innovations.nl/.

[49] A.Q.C. Van der Horst. Information for cost comparison and estimate. In *Construction Technology of civil engineering structures, CIE4170*. TU Delft, 2015.

[50] B. K. van Wesenbeeck, M. D. van der Meulen, C. Pesch, H. de Vriend, S.N. Jonkman, and M. B. de Vries. Nature-based coastal defence: Physical restrictions and engineering challenges. In *Building with Nature: Design Construct*.

[51] Westfrieseomringdijk.nl. Dijk Friesland (22-09-2016). URL http://www.westfrieseomringdijk.nl/clientdata/images/handboek/crop/940x392//tmphomemedium.jpg.

[52] Patrick Winckler, Manuel Contreras-Lopez, Rodrigo Campos-Caba, Joseph F. Beya, and Mauricio Molina. The storm of August 8, 2015 in the regions of Valparaiso and Coquimbo, Chile Central. *Statewide Agricultural Land Use Baseline 2015*, 1:1–39, 2015.

[53] Wordpress.com. Dunes Lake Michigan (22-09-2016). URL https://toonecycling.files.wordpress.com/2010/11/dsc00030.jpg.

[54] Yoshiki Yamazaki. Depth-integrated, non-hydrostatic model with grid nesting for tsunami generation, propagation, and run-up. *International Journal for Numerical Methods in Fluids*, pages 2081–2107, 2010.

[55] Yoshiki Yamazaki, Zygmunt Kowalik, and Know Fai Cheung. Depth-integrated, non-hydrostatic model for wave breaking and run-up. *International journal for numerical methods in fluids*, pages 601–629, 2008.

Appendices

A

Boundary conditions

A.1. Coastline features

The coast of Chili is located near the fault line of two converging tectonic plates. The Nazca plate and the South American Plate. The movement of the Nazca plate is around 8 cm per year. This has had an enormous impact on the formation of the coastline and determines the broadest features of the coast. Where the oceanic and the continental plate meet, the denser oceanic plate dives under the continental plate. This process creates mountains and oceanic trenches and is often combined with seismic and volcanic activity.

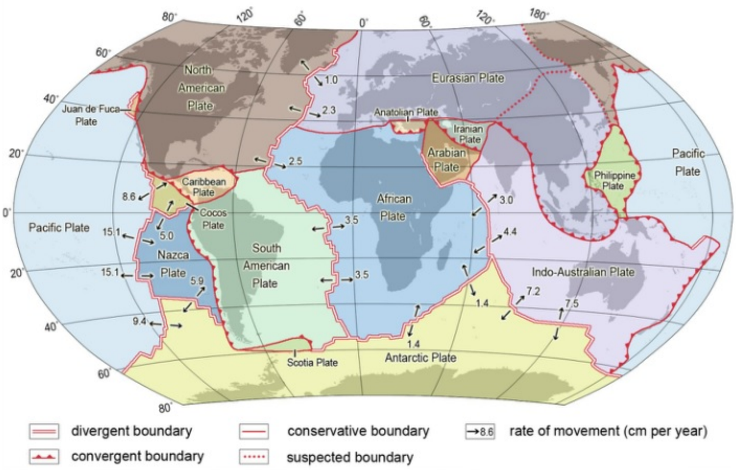

Figure A.1: Tectonic plates of the world, source: Bosboom and Stive [5]

Because of the converging plates the coast of Chili is categorised as a leading-edge or collision coast. This collision has resulted in narrow shelves, earthquakes, coastal uplift, and the formation of mountains immediately inland from the coast, resulting in a very small shelf width.

The shelf width has an effect on the hydrodynamic conditions. Narrow shelves have a lower potential for storm surge elevations but wind wave heights are higher because there is less dampening due to the deeper sea bottom. It has to be noted that the tidal amplitude can be strongly effected by resonance phenomena (Bosboom and Stive [5]).

A.2. Soil properties

Soil properties are used from soil properties that are taken for the Altamar building soil investigation [18]. CPT results are given in figure A.2.

Universidad Católica de Valparaiso Grupo de Geotecnia [46] gives the following descriptions of the soil types that are indicated left in figure A.2:

SP - Poorly graded sands, sands with little or fine gravel

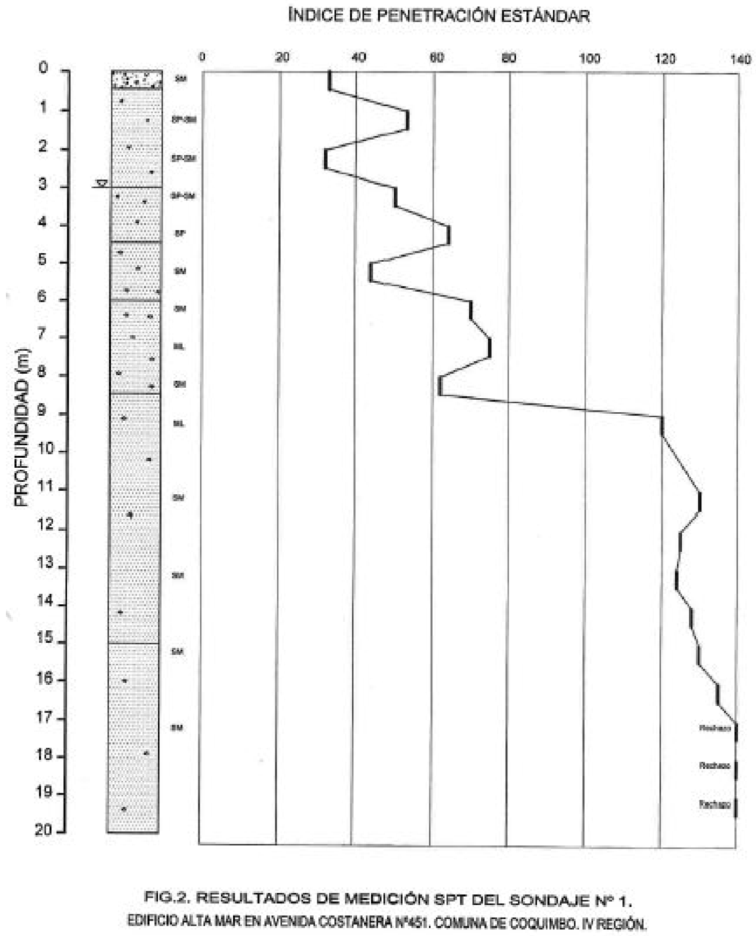

Figure A.2: CPT at Altamar building, source: Geofun M R [18]

SM - Silty sands, mixture of sand and silt, poorly graded
ML - Inorganic silts and very fine sand rock dust, clay or silty fine sand with slight elestic plasticity

Properties of these soil types are linked to the soil types stated in Molenaar and Voorendt [33, p.177]. From 0 to 7 meter, the soil type is SP-SM which corresponds with a slightly silty sand mixture (γ = 27 degrees, c' = 0, ρ = 18 kN/m^3). From 7 to 9,5 meter the soil type is ML which is mainly silty clay (γ = 22,5, c' = 5, ρ = 18 kN/m^3). From 9,5 meters and deeper is soil type SM and corresponds with a silty sand mixture (γ = 27, c' = 0, ρ = 18 kN/m^3).

A.3. Tides

The tidal character of the ocean in front of Coquimbo can be identified as mainly semidiurnal with a maximum tidal amplitude of 1 metre. This can be validated with figure A.3, displaying tidal elevations at Coquimbo in the last 30 days, which were comparable to the tidal elevations of the last year. Furthermore, figure A.4 shows that the tidal character of the region is indeed mainly semidiurnal.

A.4. Waves

The wave climate is dominated by swell waves propagating form the South West. These swell waves originate from the Southern storm wave belt at 55°S. But also swell from the North West is possible, which are generated at the Northern hemisphere. These generally only occur during the winter at the Northern hemisphere.

The swell consists of persistent waves with long periods, typically around 10 s. The waves are uniform in direction and size and the waves have a height of 1-2 m.

The project site is largely protected from the swell waves due to the location in the bay, only a small portion

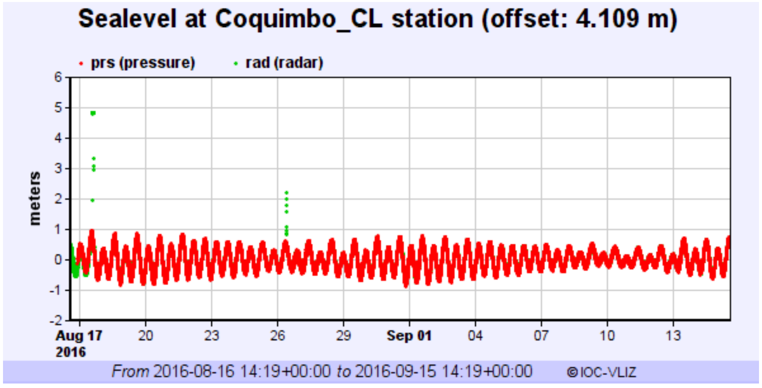

Figure A.3: Fault plane, source: Ioc-sealevelmonitoring.org [24]

.

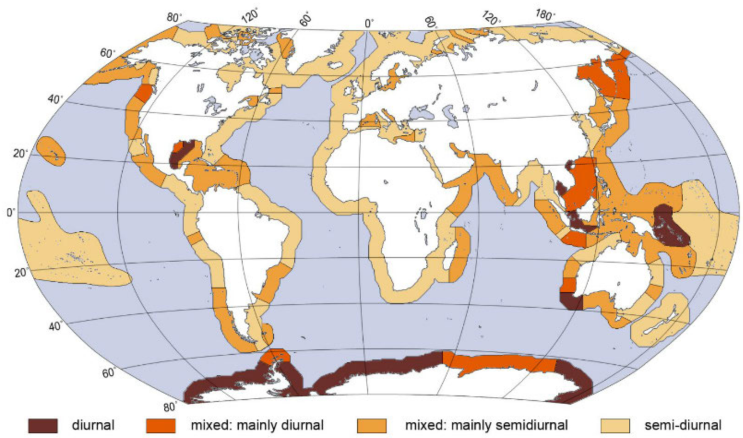

Figure A.4: Fault plane, source: Bosboom and Stive [5]

.

of the waves penetrates into the bay. The site is mostly affected by locally generated wind waves and on rare occasions by the swell waves from the North West (Bosboom and Stive [5]).

Storm surges also occur in the Coquimbo region. These storms propagate from the South West or the North West (Winckler et al. [52, p.28]). The last storm that occurred was at the 8^{th} of August 2015. This storm was characterized by a height of H_s = 7,23 m, and a period of 13,3 s (Winckler et al. [52, p.8]).

A.5. Wind

In La Serena mostly South East Trade winds occur.These winds are moderate but persistent throughout the year.They can vary spatially and temporally with the seasons, because of monsoons due to the heating of the continent (Bosboom and Stive [5]).

A.6. Climate

The region has a cool desert climate which is clearly seasonal. The region is permanently subjected to the Pacific anicyclone, which constantly blocks the despressions that cause rain in the central region. The climate is classified as a semi-desert coastal climate with plenty of cloud cover and reduced rainfall, about 80 mm per year. Temperatures are relatively homogeneous and rarely exceeds the temperature range of 7 to 18 °C.

Rainfall is concentrated in the winter months, with 60% of the annual rainfall recorded in the months June and July, and less than 1% registered between the months December and February. In the last 20 years Chile has seen periods of extended drought, sporadically interrupted by periods of intense rains. This phenomenon is associated with the presence of El Niño (Claussen [7]).

A.7. Morphology

The steepness of the beach varies over the year. During the project visit the beach was extremely flat. The beach grows flatter due to the swell waves that bring sediment toward the beach . During storms the smaller waves cause erosion. Which causes the beach to be steeper after a storm has occurred. In Google Earth can be seen that the shape of the coastline remains the same during multiple years, see figure A.5.

(a) 10-5-2005

(b) 20-2-2007

(c) 18-2-2010

(d) 20-4-2013

Figure A.5: Development of the coastline, source: Google Earth [19]

B
Stakeholders

In this section, the different stakeholders for the scope area are discussed. The amount of power and interest is elaborated here.

- **Ministry of Housing and Development**
  The ministry has a clear goal in creating a more social-economic valuable region for the scope area. The execution period is planned to start at the end of the year 2018 (Ministry of Housing and Urban Development [31]). Since the plans are in a far stage already, the interest in this area is of great importance.
- **People living on the wetlands**
  On the wetlands several houses built of corrugated sheets are present. Depending on the rights and privileges of these people living here, a possible change of landscape might be hard.
- **Altamar**
  This highrise building is located inside the scope of the project and therefore has a big interest in the development of the scope region. The residences in the building will become more valuable if the surroundings will be more social-economic developed. The Alta Mar could serve the purpose of an evacuation location.
- **Municipality Coquimbo**
  For the municipality of Coquimbo the development of Coquimbo bay is of major importance. The developments will create an opportunity to find an integrate solution for the different problems in this part of the city. Besides this, also the image of Coquimbo will be improved and the city can attract more tourists.
- **Municipality La Serena**
  The developments also play a role of importance for the municipality of La Serena, since the scope area is close to La Serena as well.
- **Public Works**
  The ministry of public works can benefit in the project by implementing their solutions for their shares. The new seawall and coastal road can be renewed in this project by finding an integrated solution.
- **Inhabitants / Companies of the area behind the wetlands**
  South from the wetlands a district with mainly residences and companies of the lower part of the society is established. These people/companies can benefit a lot from the future plans.
- **Insurance companies**
  Insurance companies will have a benefit with the future plans of the region, since they benefit with an area that is safer against future tsunamis and criminality. Their influence however is very limited.
- **Port of Coquimbo (Empresa Portuaria Coquimbo)**
  The Port of Coquimbo was formally established as an independent company on October 1, 1998[42]. By an increase in the value of the lower Coquimbo Bay, the value of the Port area will increase as well. Besides this, there are still potential possibilities in especially the coastal zone for port enlargements.

- **Conservation organisation** The wetlands function already partly as a nature reserve for different flora and fauna. From the viewpoint of the conservation organisations, this area should not deteriorate and preferably should be improved.

C
Historic events

The following list contains an overview of some major historic seismic events along the coast of Chile.

- 1730 ~9.0 Mw Coquimbo-Illapel region
- 1819 8.3 Mw Copiapó-Coquimbo region
- 1849 7.5 Mw Copiapó-Coquimbo region
- 1880 7.7 Mw Coquimbo-Illapel region
- 1922 8.3 Mw Copiapó-Coquimbo region
- 1943 7.9 Mw Coquimbo-Illapel region
- 27 February 2010 8.8 Mw Maule
- 16 September 2015 8.3 Mw Coquimbo-Illapel region

The 2015 earthquake closed the seismic gap that existed from 1943, therefore no major earthquake is expected to happen in that region in the near future. The region of interest is the Copiapó-Coquimbo region in which a seimic gap exists from 1922 on. Unfortunately no detailed data is available about the 1922 earthquake, therefore the detailed information about the 2015 earthquake and tsunami are used to analyse the effects on the region of Coquimbo Bay.

C.1. Tsunami 2015

On September 16, 2015 an earthquake with a magnitude Mw 8.3 took place in front off the coast of the Coquimbo Region, Chile (Aránguiz et al. [2]). The following tsunami brought significant damage to the lower parts of Coquimbo Bay. The inundation had a run-up reaching up to 6.4 m and a penetration distance of 700 m (Aránguiz et al. [3]). At certain places the water was retained by a vertical wall. In this section the analysis of the impact of the 2015 tsunami is described. In the first part the visual analysis that is conducted during the field survey is elaborated. In the secondly part, different previous analysis on the impact on the lower part of Coquimbo bay are considered.

C.2. Field survey

From Sunday the 4th of September until Tuesday the 6th of September a field survey was carried out by Tsunami Project Coquimbo, supervised by Dr. R. Aránguiz. Main occupations in this survey involved visual inspection of the scope area and interviewing stakeholders. Different important issues concerning the tsunami of 2015 were:

- the prior earthquake that damaged tsunami retaining structures and evacuation buildings
- the scour created by high flow velocity of the tsunami wave
- the debris that comes along with the wave
- the retreating water from the tsunami that causes an impact in opposite direction to the direction of the initial wave
- the reopening of former waterstreams

C.3. Wetlands

The 2015 tsunami flooded the wetlands completely, since the seawall couldn't retain the whole tsunami wave. Impact analysis on Coquimbo bay showed a function of the wetlands as a buffer zone for the tsunami flood [3]. Damage to the wetlands remained limited because of the unused grounds. Figure C.1 shows the wetlands directly after the tsunami of 2015. And in figure C.2 there can be seen how much debris has been brought to the area due to the tsunami.

Figure C.1: Flooded wetlands. Picture taken one day after the 2015 tsunami, photo provided by Mr. Rene Andras Vergas

C.4. Seawall

The seawall was originally designed as a reinforced concrete talud up to a hight of approximately 1,5 m relative to the beach level (see figure C.3 in section 2.1). This is resting on a upside down T-shaped foundation block. Under the concrete talud, stone rocks acted as foundation. Approximately over half of the length of the seawall, the seawall isn't in its original shape anymore. On top of the seawall remains of a small stone wall can be seen. Considering the thickness of the wall, the function was probably not to retain the tsunami wave. Behind this wal, the Av. Costanera is located. This road is a single lane road, with a bike lane and sidewalks. After the tsunami, concrete parts of the foundation of the seawall were found 30 meters land inwards.

C.5. Damage to buildings

Immediately after the tsunami of September 2015 a team conducted a thorough field survey in the affected area. During this survey they indicated 568 mixed buildings made of wood and masonry, 4 reinforced concrete structures of 8 or more stories and 13 houses that did not meet minimal building standards. Only the 568 mixed buildings were analysed in more detail and used for a fragility curve that was created. Two damage levels were determined; the first level was named "surviving" and the second level "destroyed".

Figure C.4 shows a map with the analysed buildings and the corresponding damage levels. Most destroyed buildings were found in the region near the intersection of the railway with the coastal road. However, the Altamar highrise is located near this region and has survived the earthquake and tsunami. This emphasizes the potential of this building as a vertical evacuation location. Figure C.5 shows the Altamar building and the coastal road directly after the 2015 tsunami and the current situation.

C.5.1. Causes of the damage and implications for design

Structural damage can be caused by direct hydrostatic and hydrodynamic forces from water inundation, impact forces from water-borne debris, fire spread by floating debris and combustible liquids, scour and slope/foundation failure and wind forces induced by wave motion (Federal Emergency Management Agency [17, p.16]).

Earlier studies have shown that buildings with wooden supporting structures end up more damaged than reinforced concrete structures. Also it has been suggested that some buildings survived a large tsunami because the lower floors of the structure were relatively open. The panels and windows didn't give much resistance when the water came in, so the forces on the buildings didn't exceed the loading capacity.

Figure C.2: The tsunami took debris with it, such as cars, boats and wooden structures, photo provided by Mr. Rene Andras Vergas

Figure C.3: Cross section of the damaged seawall, photo made by Chris Heuberger, date: 04-09-2016

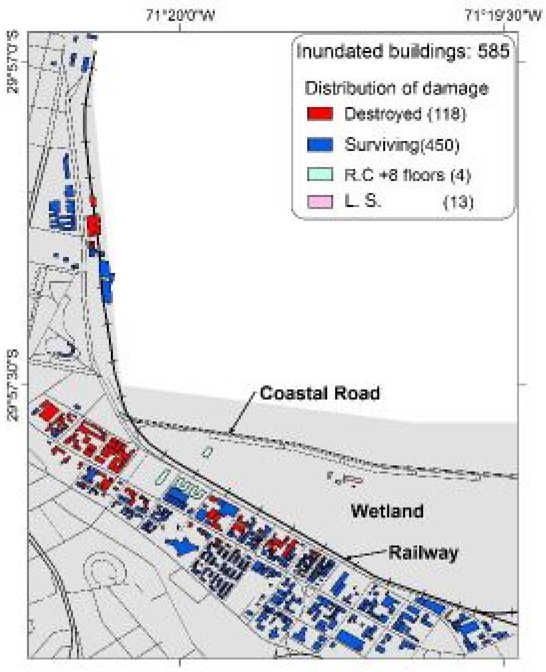

Figure C.4: Surveyed damage to structures due to the 2015 tsunami, source: Aránguiz et al. [3]

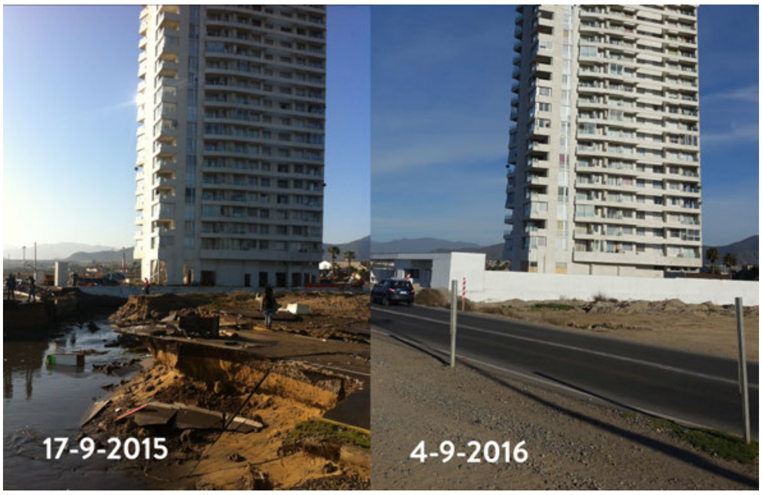

Figure C.5: Picture taken one day after the 2015 tsunami (left) and the current situation (right), photo provided by Mr. Rene Andras Vergas

As a result from historic tsunami events and studies that were performed afterwards, the following implications for structural design are stated by Federal Emergency Management Agency [17, p.28]:

- Vertical evacuation structures should be well-engineered reinforced concrete or steel frame structures.
- In the case of near-source generated tsunami hazards, vertical evacuation structures must be designed for seismic loading in addition to tsunami load effects.
- Vertical evacuation structures should be located away from the wave breaking zone.
- Impact forces and damming effects from water-borne debris are significant and must be considered.
- When elevated floor levels are subject to inundation, uplift forces from added buoyancy due to trapped air and vertical hydrodynamic forces on the floor slab must be considered.
- Scour around the foundations must be considered.

- Because of uncertainty in the nature of water-borne debris and the potential for very large forces due to impact, progressive collapse concepts should be employed in the design of vertical evacuation structures to minimize the possibility of disproportionate collapse of thestructural system.

This are all factors that need to be taken into consideration for new and existing buildings that could serve as a vertical evacuation location.

D

Ecological value and building with nature

The concept of building with nature is an interesting approach for the coastal and wetland zone.The wetlands serve a highly natural function. Besides this, the wetland area should also function as a bufferzone.

Wetlands are considered to be the “kidneys” of the planet, since they can filter and absorb contaminants out of natural or artificial waters. They are also important regulators of hydrological cycles and events like floods of tsunamis. They allow the generation of water for human use and agricultural development and are a habitat for many forms of plant and animal life. This induces that the wetlands have a great economic, cultural and recreational value. Despite all these benefits that wetlands provide, the public considers the wetlands to be dangerous “flooded land” without any economic value of production. This has caused misuse, abuse and a lack of management of the wetlands and their resources. With the increasing awareness for natural areas, a profitable relationship between urban development and natural areas is pursued.

D.1. Coquimbo wetlands

The region of Coquimbo has a very valuable network of coastal wetlands, all in proximity of population and therefore also known as the “urban wetland”. These wetlands are especially important because they are in a semi-arid region where wetlands are scarce. The total network in the Coquimbo region consists of 8 wetlands which are characterized by a high biodiversity. They generate a biological corridor for a variety of migratory birds and offer a place for resting and nesting. The wetland at the lower Coquimbo Bay area is the most important wetland in this system.

The location of the wetland within the urban area of the city Coquimbo has led in the recent decades to cause a serious threat to this ecosystem. This is caused by the growth of urban sprawl and intensified activities in the development of projects along the coastal edge. For these reasons the current wetlands are strongly deteriorated and has lost its landscape quality. Therefore it is perceived by the public as a vacant site without any function or use, which only enlarges its deterioration.

Figure D.1: State of wetlands previous of the coastal road, source: Claussen [7]

One of the causes for a lot of damage to the wetlands is the Av. Costanera. This road crosses the wetlands and has affected the normal functioning of the estuary due to this physical barrier. By reducing the flow of water during flooding and separating the wetland vegetation from the beach the ecosystem has been transformed. In figure D.1 can be seen how the wetlands used to be. In combination with the growth of the city, a progressive loss of wet surface has taken place. If it continues this way the wetlands will be distinguished and become urban land (Claussen [7]).

D.2. Building with nature

Building with nature is a concept that is based on a integrated, sustainable and flexible solution. With the global climate change ecology gets more and more important. At the same time the world population grows and urban spaces get more and more developed. This leads to more need for recreational spaces such as nature inside urban cities.

Originally, civil projects have a given design lifetime and once built they are not flexible anymore for different and new scenarios. Building with Nature initiatives are likely to affect the interest of the various stakeholders more, especially in densely populated urban areas. During the design process, three different perspectives are taken into account: natural environment perspective, the project perspective and the governance perspective. ([11]) In Appendix D, the bigger background of building with nature is discussed.

Following Ecoshape [11], the five general design steps in Building with Nature, usually in a cyclical processes, are:

- Step 1: Understand the system (including ecosystem services, values and interests).
- Step 2: Identify realistic alternatives that use and/or provide ecosystem services.
- Step 3: Evaluate the qualities of each alternative and preselect an integral solution.
- Step 4: Fine-tune the selected solution (practical restrictions and the governance context).
- Step 5: Prepare the solution for implementation in the next project phase.

The concepts for building with nature that can be applied in the coastal zone are given in table D.1.

Ecosystem	Coastal defense property	Value	Reference
Beach & dunes	Block waves	Waves up to 3.7 m	(Mascarenhas & Jayakumar 2008)
Coral reefs	Reduce waves, reduce tidal current speed	20-50% wave reduction, 30% reduction current speeds	(Harborneet al. 2006)
Mangroves	Wave attenuation	20-60%	(Mazda et al. 1997; Gedan et al. 2011a)
Salt marshes	Wave attenuation, foreshore stabilization	1.1-2.1 % per m of marsh	(Möller & Spencer 2002)
Shellfish reefs	Wave breaking	40 % with low water levels and wave heights	(Borsjeet al. 2011)
Kelp	Wave attenuation and reducing current speeds	No reference found	
Sea grass	Wave attenuation	40%; 7,3 mm of wave attenuation per m of seagrass	(Fonseca & Cahalan 1992; Bouma et al. 2005)
Intertidal flats	Wave height reduction, foreshore stabilization	Depending on incident wave height, water depth and sediment type. Decay coefficients of waves over intertidal flats vary between 0,002 and 0,0008.	(Le Hir et al. 2000; Houser & Hill 2010)

Table D.1: Quantitative overview of flood defensive properties of different ecosystems, source: van Wesenbeeck et al. [50]

Because a tsunami wave far more energetic than normal waves it is not possible to reduce the height of this wave by natural wave reduction methods. It is however possible to stop the tsunami from progressing by use of dunes.

E

NEOWAVE

NEOWAVE (Non-hydrostatic Evolution of Ocean WAVE) is a long wave model for tsunami numerical analysis according to Yamazaki et al. [55]. Long waves, such as tsunami waves, are generally modeled as shallow-water waves with a spherical coordinate system for the propagation around the globe. The shallow water wave assumption allows us to simplify the wave celerity to $\sqrt{gh}$, which is an important assumption when the propagation of these waves is predicted. The finite difference method is an effective way to numerically solve the depth-integrated equations. NEOWAVE can model three aspects of a tsunami: the generation, the propagation and the inundation on land. In this explanation of the model the focus will lie on the propagation of the tsunami. Usually hydrostatic pressure is assumed in these kind of propagation models (Dean and Dalrymple [12]). Compared to other long wave models, NEOWAVE distinguishes itself because it can also generate non-hydrostatic solutions. This should lead to improved results.

Firstly the governing equations are explained. After that the numerical scheme is exemplified and finally important input of the model is explained. Also earlier verifications of the model for the Coquimbo region are showed.

E.1. Governing equations

The governing equations are derived from the momentum (E.1) and continuity (E.2) equations.

$$\begin{aligned}
\frac{\partial u}{\partial t} + u\frac{\partial u}{\partial x} + v\frac{\partial u}{\partial y} + w\frac{\partial u}{\partial z} &= -\frac{1}{\rho}\frac{\partial p}{\partial x} + \nu\left(\frac{\partial^2 u}{\partial x^2} + \frac{\partial^2 u}{\partial y^2} + \frac{\partial^2 u}{\partial z^2}\right) \\
\frac{\partial v}{\partial t} + u\frac{\partial v}{\partial x} + v\frac{\partial v}{\partial y} + w\frac{\partial v}{\partial z} &= -\frac{1}{\rho}\frac{\partial p}{\partial x} + \nu\left(\frac{\partial^2 v}{\partial x^2} + \frac{\partial^2 v}{\partial y^2} + \frac{\partial^2 v}{\partial z^2}\right) \\
\frac{\partial w}{\partial t} + u\frac{\partial w}{\partial x} + v\frac{\partial w}{\partial y} + w\frac{\partial w}{\partial z} &= -\frac{1}{\rho}\frac{\partial p}{\partial x} + \nu\left(\frac{\partial^2 w}{\partial x^2} + \frac{\partial^2 w}{\partial y^2} + \frac{\partial^2 w}{\partial z^2}\right) - g
\end{aligned} \tag{E.1}$$

$$\frac{\partial u}{\partial x} + \frac{\partial u}{\partial y} + \frac{\partial u}{\partial z} = 0 \tag{E.2}$$

Where x, y, z are Cartesian coordinates and u, v, w are the velocities in the corresponding directions; t is time; p is pressure; g is gravitational acceleration and ν is the kinematic viscosity coefficient. These directions are illustrated in figure E.1.

To solve these equations boundary conditions are required. Firstly, the vertical velocity at the bottom and the surface are used (E.3) . Next to that also the non-hydrostatic pressure as a function of the depth is a boundary condition (E.4). The pressure is divided into a hydrostatic component and a non-hydrostatic component.

$$\begin{aligned}
w &= \frac{D(\zeta)}{Dt} = \frac{\partial \zeta}{\partial t} + u\frac{\partial \zeta}{\partial x} + v\frac{\partial \zeta}{\partial y} \quad \text{at z} = \zeta \\
w &= \frac{D(-h)}{Dt} = -u\frac{\partial h}{\partial x} - v\frac{\partial h}{\partial y} \quad \text{at } z = -h
\end{aligned} \tag{E.3}$$

$$p = \rho g(\zeta - z) + q \tag{E.4}$$

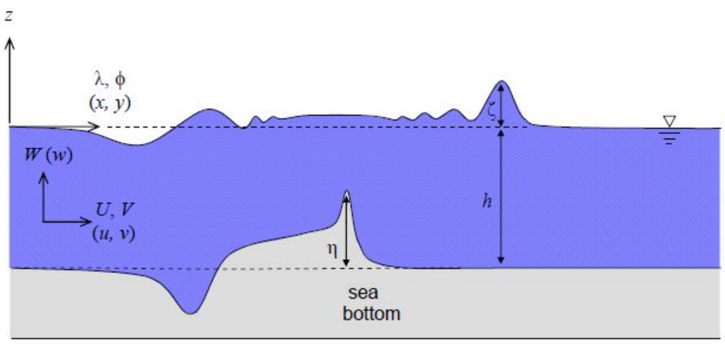

Figure E.1: Illustration of the governing equations. Source: Yamazaki [54].

Where ζ is the surface elevation; h is the water depth; D = ζ + h; q is the non hydrostatic pressure. At z = ζ both the pressure components become zero. When (E.1) and (E.2) are integrated over depth and the third momentum equation is linearised, taking boundary conditions (E.3) and (E.4) into account, provides the governing non-hydrostatic equations of the propagation which can be used in numerical calculations (E.5).

$$\begin{aligned}
\frac{\partial U}{\partial t} + U\frac{\partial U}{\partial x} + V\frac{\partial U}{\partial y} &= -g\frac{\partial \zeta}{\partial x} - \frac{1}{2}\frac{1}{\rho}\frac{\partial q}{\partial x} - \frac{1}{2}\frac{q}{D\rho}\frac{\partial}{\partial x}(\zeta - h) - n^2\frac{g}{D^{\frac{1}{3}}}\frac{U\sqrt{U^2+V^2}}{\rho D} \\
\frac{\partial V}{\partial t} + U\frac{\partial V}{\partial x} + V\frac{\partial V}{\partial y} &= -g\frac{\partial \zeta}{\partial y} - \frac{1}{2}\frac{1}{\rho}\frac{\partial q}{\partial y} - \frac{1}{2}\frac{q}{D\rho}\frac{\partial}{\partial y}(\zeta - h) - n^2\frac{g}{D^{\frac{1}{3}}}\frac{V\sqrt{U^2+V^2}}{\rho D} \\
\frac{\partial W}{\partial t} &= \frac{q}{\rho D} \\
\frac{\partial \zeta}{\partial t} + \frac{\partial (UD)}{\partial x} + \frac{\partial (VD)}{\partial y} &= 0
\end{aligned} \tag{E.5}$$

Where U, V and W are the depth-averaged velocities in the corresponding directions and n is the Manning coefficient introducing bottom friction. A linear distribution of w is assumed over the vertical. Thus W is the average of w at the surface and w at the seabed given in equation E.3. Solving these equations step by step for a numerical grid is the basis of the numerical modeling.

E.2. Numerical scheme

There are two solution schemes implemented in NEOWAVE. The hydrostatic and the non-hydrostatic solutions are obtained with different numerical computations. First the numerical scheme of the hydrostatic variant of NEOWAVE will be treated. Then the adaptations to receive non-hydrostatic results are explained. Both schemes are based on the finite difference method as mentioned before. The model makes use of a staggered spacial grid as illustrated in figure E.2. NEOWAVE calculates velocity components U and V in both horizontal directions at the cell interface and the surface elevation ζ at the cell center where the water depth h is known.

The hydrostatic variant works with an explicit scheme for the solution. A value of the surface elevation is computed by the integration of the continuity equation at the center of a cell in terms of fluxes as can be seen in equation E.6. The fluxes in x and y direction are denoted with FLX and FLY.

$$\zeta_{j,k}^{m+1} = \zeta_{j,k}^{m} + (\eta_{j,k}^{m+1} - \eta_{j,k}^{m}) - \Delta t\frac{FLX_{j+1,k} - FLX_{j,k}}{R\Delta\lambda cos(\phi_k)} - \Delta t\frac{FLY_{j,k}cos\left(\phi_k + \frac{\Delta\phi}{2}\right) - FLY_{j,k-1}cos\left(\phi_{k-1} + \frac{\Delta\phi}{2}\right)}{R\Delta\phi cos(\phi_k)} \tag{E.6}$$

Where m denotes the time step, Δt the size of the time step, $\Delta\lambda$ and $\Delta\phi$ the grid sizes in corresponding directions. The fluxes are defined in the following way:

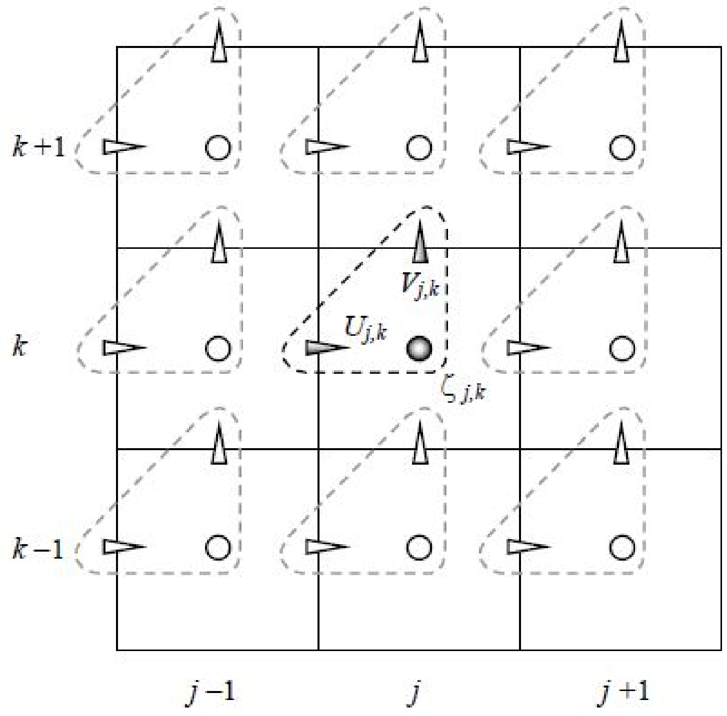

Figure E.2: Numerical spacial grid. Source: Yamazaki [54].

$$
\begin{aligned}
FLX_{j,k} &= U_{j,k}^{m+1}\frac{\zeta_{j-1,k}^{m}-\zeta_{j,k}^{m}}{2}+U_{j,k}^{*m+1}\frac{\left(h_{j-1,k}-\eta_{j-1,k}^{m}\right)+\left(h_{j,k}-\eta_{j,k}^{m}\right)}{2}\\
FLY_{j,k} &= V_{j,k}^{m+1}\frac{\zeta_{j-1,k}^{m}-\zeta_{j,k}^{m}}{2}+V_{j,k}^{*m+1}\frac{\left(h_{j-1,k}-\eta_{j-1,k}^{m}\right)+\left(h_{j,k}-\eta_{j,k}^{m}\right)}{2}
\end{aligned}
\tag{E.7}
$$

Equations E.6 and E.7 are used to compute all the velocities and surface elevations at the different time steps in the entire spacial grid. This formulation is actually a simplification of the complete scheme as different approximations of the velocity should be included. The * in equation E.7 indicates the simplification in the equations above. A detailed description can be found in the paper of Yamazaki [54]. However, these equations are the most important principle behind the numerical calculations.

When the non-hydrostatic variant is used, also the bottom pressure and the vertical velocity are included. Again a reference is made to the paper of Yamazaki [54] for a detailed description. It is important to note that while the hydrostatic variant is explicit, the adjusting to the non-hydrostatic scheme leads to an implicit scheme.

E.3. Input of the model

There is more to numerical modeling than just pushing the run button. Useful results can only be obtained when all the input is carefully prepared. The most important input parameters in this model are the earthquake source, the different grids, different physical parameters and the bathymetry. Different earthquake scenarios were proposed by Dr. R. Aránguiz in Aránguiz et al. [3]. These 6 earthquake scenarios are illustrated in figure E.3. The 2 most important tsunami source areas (S1 and S2) were determined through statistics. Apart from the geography, the interseismic coupling is varied in these scenarios. In case 1 (C1) a heterogeneous interseismic coupling is used, whereas in case 2 (C2) a spatially-constant 100% coupling is assumed. The six different scenarios can be computed with these 2 variables. From top left to bottom right in figure E.3 these scenarios will be addressed as scenario 1 up to scenario 6. The earthquake source is implemented in the model with the OKADA model (Okada [36]).

Up to 5 grids can be implemented in the current version of NEOWAVE. The coordinates, grid size and time step of the different grids are given in table E.1. The highest resolution which is used is approximately 10 m.

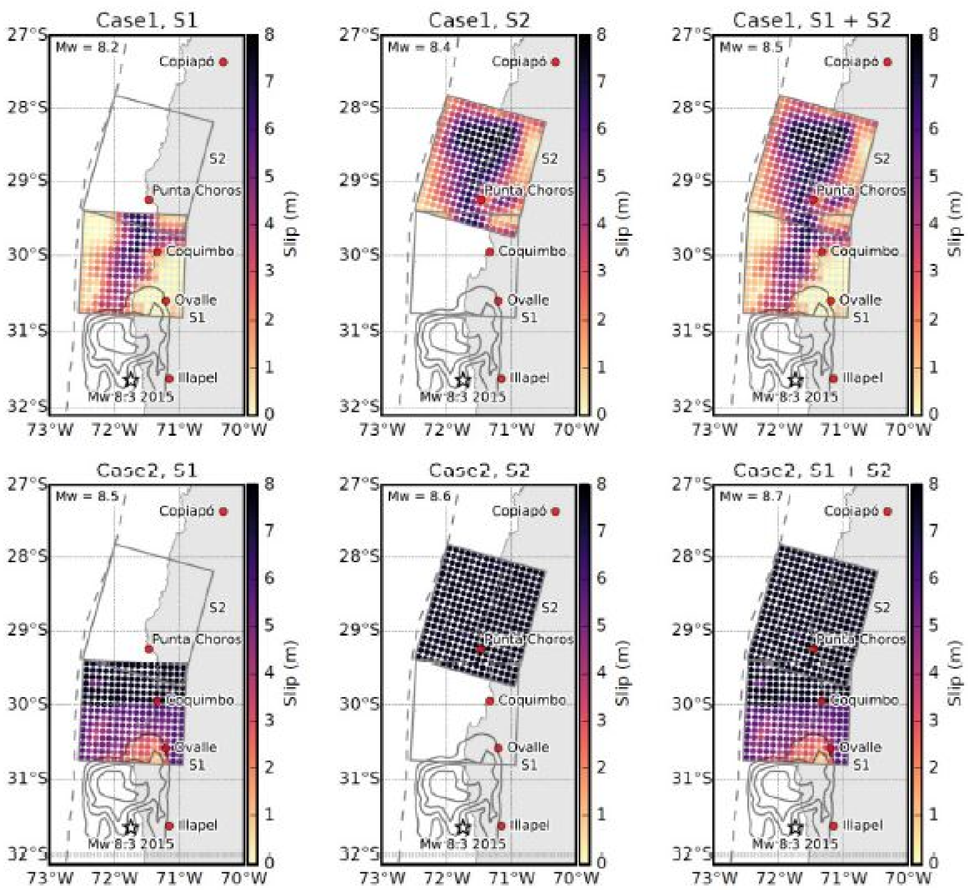

Figure E.3: Different earthquake scenarios. Source: Aránguiz et al. [3].

There will always be a trade-off between the grid size and the total amount of time to compute a run. An overview of the 5 grids which are used in the model is given in E.4 Different time steps are used varying from 1 second for the first grid to 0,125 seconds for the smallest grid. In some cases even a smaller time step of 0,0625 s is used. This way the Courant number is always smaller than 1 and the scheme should be stable.

Grid number	northern latitude (°)	southern latitude (°)	western longitude (°)	eastern longitude (°)	grid size dx (m)	time step dt (s)
1	-12	-41	-89	-66	3700	1
2	-28,8	-32,0	-72,5	-71,0	925	0,5
3	-29,2	-30,35	-71,75	-71,25	185	0,25
4	-29,82	-30,00	-71,40	-71,26	33,83	0,125
5	-29,95	-29,97	-71,34	-71,31	10,28	0,125

Table E.1: Grid information

The Manning coefficient is the most important parameter of the earlier mentioned physical parameters, which could be modified. This coefficient is determined by the structure of the soil. Given that most of the run-up will occur on the wetlands, a value of 0,025 is chosen which corresponds to materials like waste lands, parks and roads (Aránguiz et al. [2]).

The data of the original bathymetry of the area was provided by Dr. R. Aránguiz. With the help of Sjoerd van der Meulen, Matlab was used to modify the original bathymetry. An overview of the script is given in figure E.5. This way the different alternatives are implemented in the model. The modifications in the original bathymetry to implement the alternatives are given in figures E.6, E.7, E.8, E.9, and E.10.

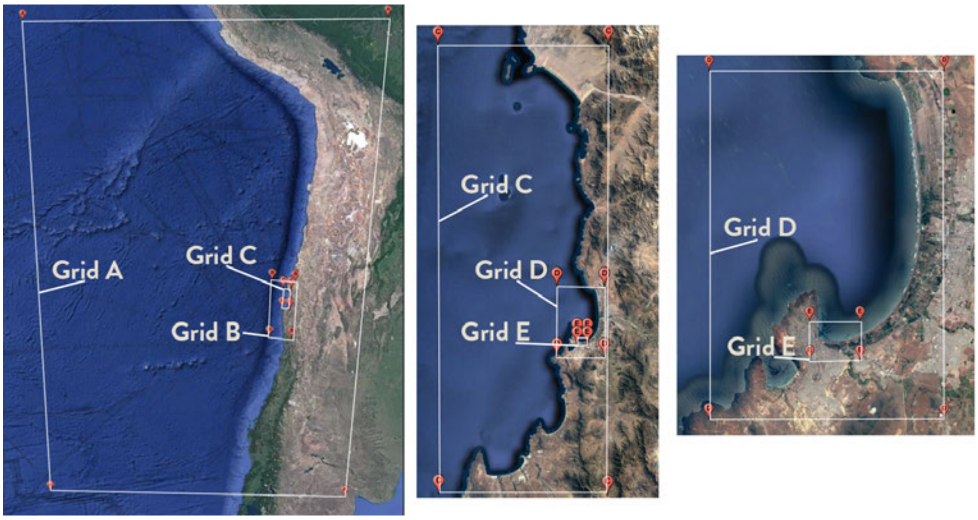

Figure E.4: The location of the 5 grids.

E.4. Verification of the model

Water level measurements of the 2015 tsunami are used to verify the NEOWAVE model for the bay of Coquimbo. In the second graph in figure E.11 a comparison is made between the measurements which were taken during the tsunami in 2015 and the results of the NEOWAVE model. Great similarity can be seen in both the arrival time of the tsunami as the wave amplitude. From these data it was concluded that the NEOWAVE model gives reasonable results for Coquimbo bay and can be used to predict a realistic impact of different tsunami scenarios. A detailed description of the NEOWAVE model can be found in Aránguiz et al. [2].

E.5. Identified errors

During the simulations different errors were encountered. The most important error was the 'overshoot flow' error. This error appears most of the time at the transition from the 4th to the 5th grid at the location of the changed bathymetry. Probably it is due to an abrupt change in bathymetry causing a large change in momentum. The model has difficulties with this large change in momentum resulting in the overshoot flow error. Possible solutions are smoothing the bathymetry, decreasing the grid size, or time step. Another acknowledged error can be seen in the aftermath of a tsunami. Water does not retreat completely resulting in a constant water level which does not match the water level prior to the tsunami. Also the velocities do not decrease to 0 at this stage, which can not be correct.

```matlab
% CC Sjoerd van der Meulen
close all
clear all

hoogte = 3;
heightD = ones(20)*hoogte;
LD = 217;
WD = 325;
y=[1:10.28:LD*10.28];
x=[1:10.28:WD*10.28];
C = load('grid_e.dat');
E=flipud(C);
D=fliplr(E);
filename = 'points3.xlsx';
sheet = 1;
xlRange = 'C17:C21';
xlRange2 = 'D17:D21';

CL = xlsread(filename,sheet,xlRange);
CLo = xlsread(filename,sheet,xlRange2);
CLong = [-29.950,-29.970];
CLat = [288.69,288.66];

StepLong = abs((CLong(1)-CLong(2))/LD);
StepLat = abs((CLat(1)-CLat(2))/WD);
for i = 1:length(CL)
    PosCL(i) = round(abs(CLong(1)-CL(i))/StepLong);
    PosCLo(i) = round(abs((CLat(1)-CLo(i))/StepLat));
end

for i = 1:(length(CL)-1)
    DiffL(i) = abs(PosCL(i)-PosCL(i+1));
    DiffLo(i)= abs(PosCLo(i)-PosCLo(i+1));
    lengthL(i) = max(abs(DiffLo(i)),(abs(DiffL(i))));
    D(PosCL(i),PosCLo(i)) = heightD(i);
    h= abs(DiffLo(i)/DiffL(i));
    g= abs(DiffL(i)/DiffLo(i));
    for j = 1:lengthL(i)
        if DiffL(i)>DiffLo(i)
            if PosCL(i)<PosCL(i+1)
                J = ((PosCL(i) + j));
            else
                J = ((PosCL(i) - j));
            end
            if PosCLo(i)<PosCLo(i+1)
                K = round((PosCLo(i) + h*j));
            else
                K = round((PosCLo(i) - h*j));
            end
            if DiffLo(i) ==0 && DiffL(i)~=0
                if PosCL(i)<PosCL(i+1)
                    J = ((PosCL(i) + j));
                else
```

(a) First part of the matlab script to modify the bathymetry

```matlab
                    J = ((PosCL(i) - j));
                end
            if DiffLo(i) ~=0 && DiffL(i)==0
                HY = 1
                if PosCLo(i)<PosCLo(i+1)
                    K = round((PosCLo(i) + h*j));
                else
                    K = round((PosCLo(i) - h*j));
                end
            end
        end
        if DiffLo(i)>DiffL(i)
            if PosCL(i)<PosCL(i+1)
                J = round(((PosCL(i) + g*j)));
            else
                J = round(((PosCL(i) - g*j)));
            end
            if PosCLo(i)<PosCLo(i+1)
                K = round((PosCLo(i) + j));
            else
                K = round((PosCLo(i) - j));
            end
            if DiffLo(i) ==0 && DiffL(i)~=0
                if PosCL(i)<PosCL(i+1)
                    J = round(((PosCL(i) + g*j)));
                else
                    J = round(((PosCL(i) - g*j)));
                end
            end
            if DiffLo(i) ~=0 && DiffL(i)==0
                HY = 1
                if PosCLo(i)<PosCLo(i+1)
                    K = round((PosCLo(i) + j));
                else
                    K = round((PosCLo(i) - j));
                end
            end
        end
        if D(J,K) < heightD(i)
            D(J,K) = D(J,K)+heightD(i);
        end
    end
end
F=fliplr(D);
G=flipud(F);
figure
mesh(x,y,G);
colorbar
colormap
hold on
contour(x,y,G,[0 0],'k');
save('grid_e_var3_h3.dat','G', '-ascii')
```

(b) Second part of the matlab script to modify the bathymetry

Figure E.5: Matlab script to modify the bathymetry.

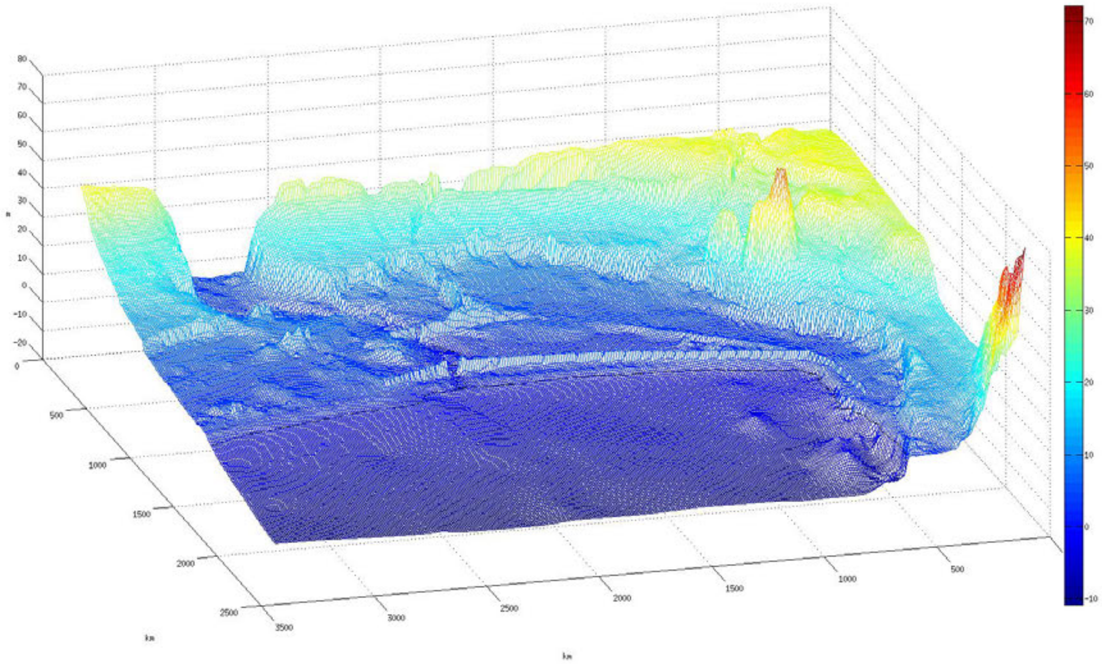

Figure E.6: Modifications in bathymerty to analyse alternative 1.

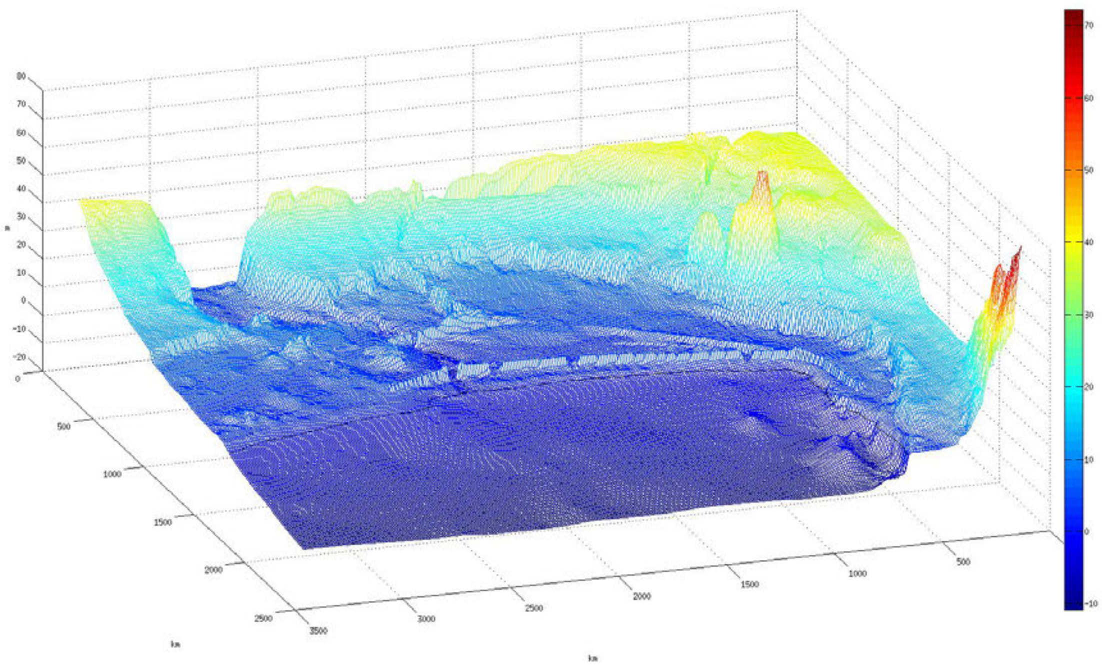

Figure E.7: Modifications in bathymerty to analyse alternative 2.

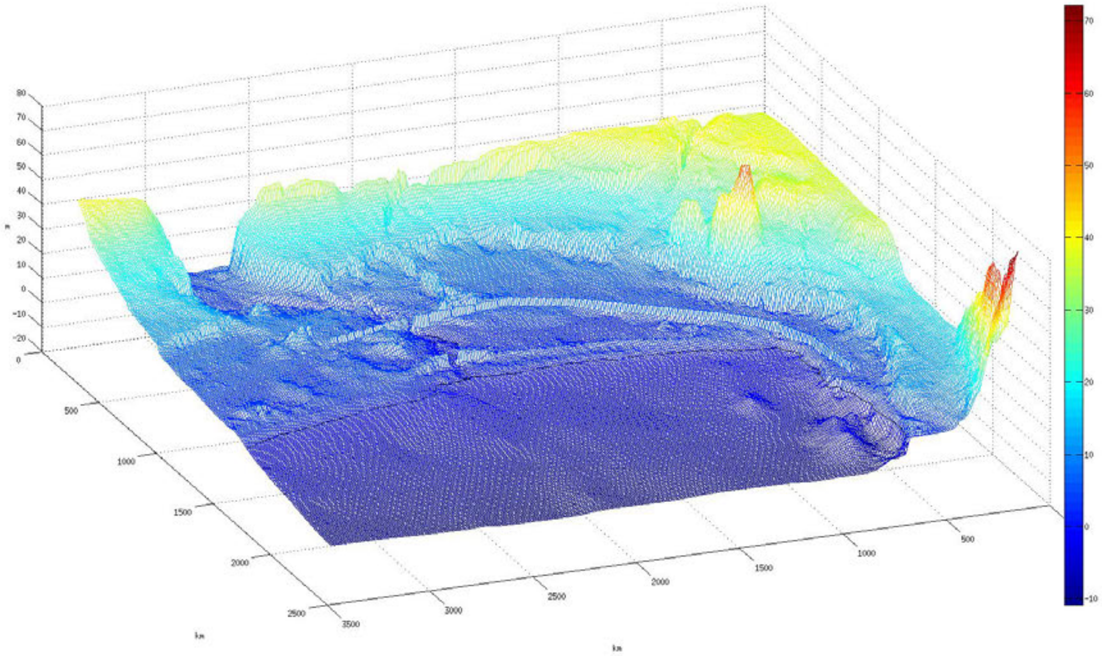

Figure E.8: Modifications in bathymerty to analyse alternative 3.

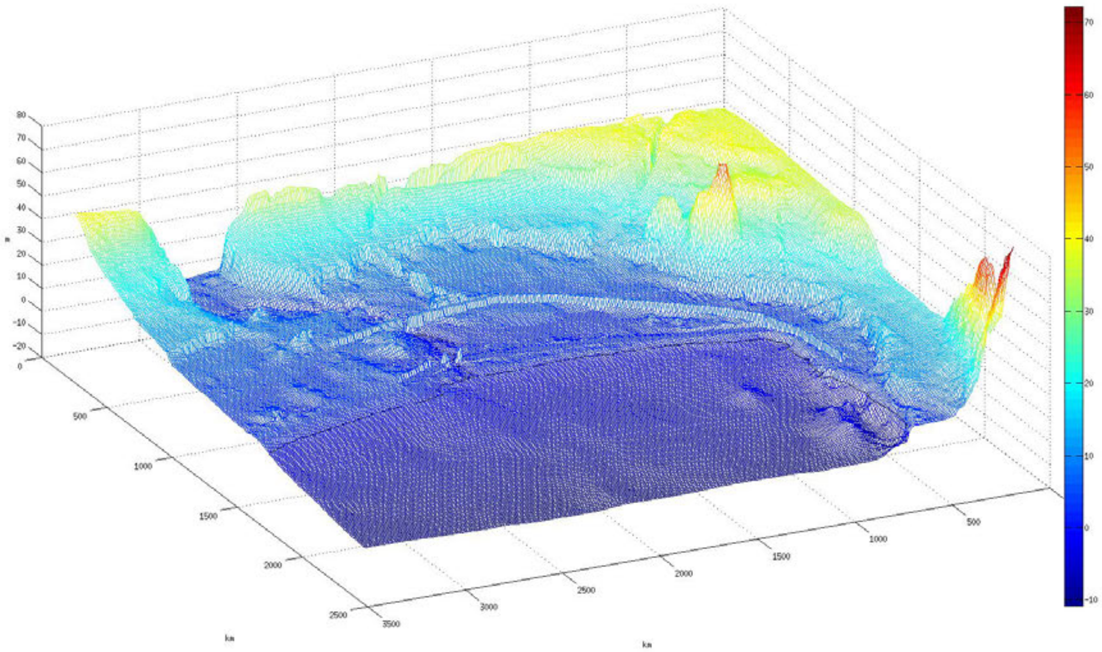

Figure E.9: Modifications in bathymerty to analyse alternative 4.

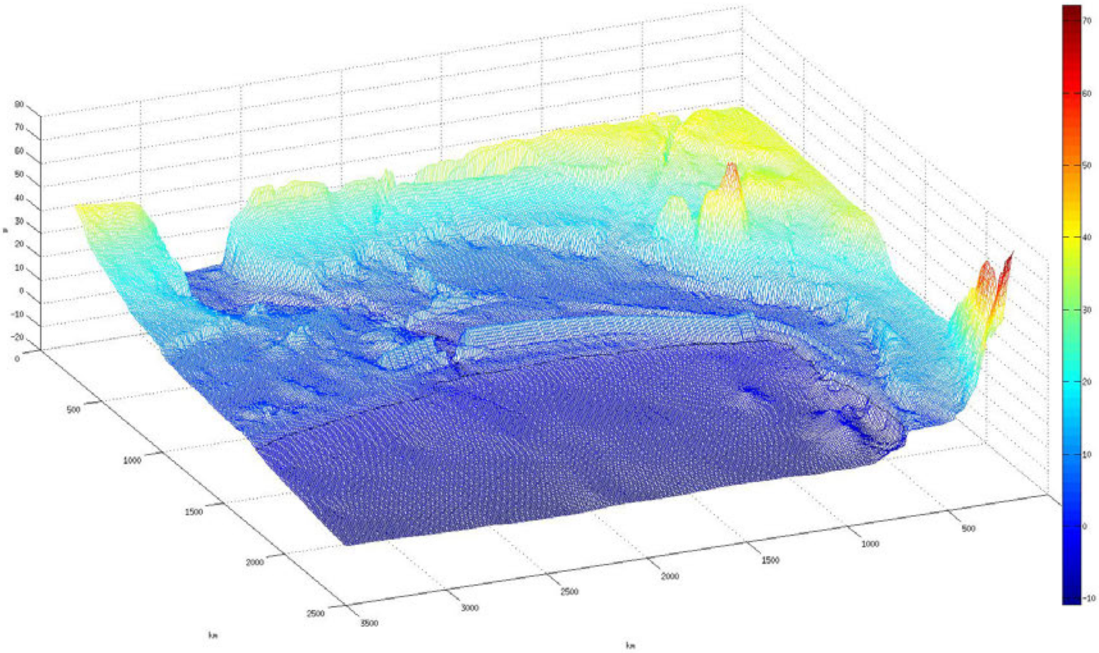

Figure E.10: Modifications in bathymerty to analyse alternative 5.

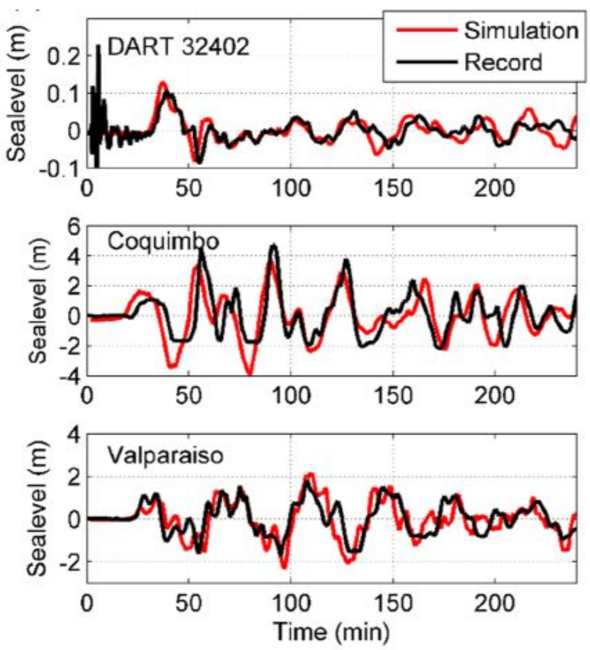

Figure E.11: Water level measurements compared with simulation results. Source: Aránguiz et al. [2].

F

Tsunami simulation results

F.1. Earthquake scenarios

The different earthquake scenarios mentioned in appendix E can be used as input to model the propagation and inundation of a tsunami in the different grids. It is possible to assign specific locations in the grids where the NEOWAVE model can provide specific data. The locations which were assigned into the model are given in figure 4.1. The inundation maps and tide gauges at the location of the Altamar building of the six different scenarios are given below in figures F.1 and F.2. Besides flow depths, flow velocities are required to make design calculations. The flow velocities of the different scenarios at the Altamar building are plotted against time in figure F.3.

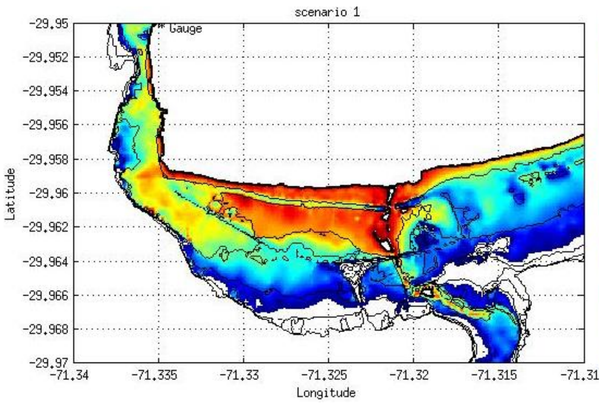

(a) Inundation map of scenario 1 with the original bathymetry.

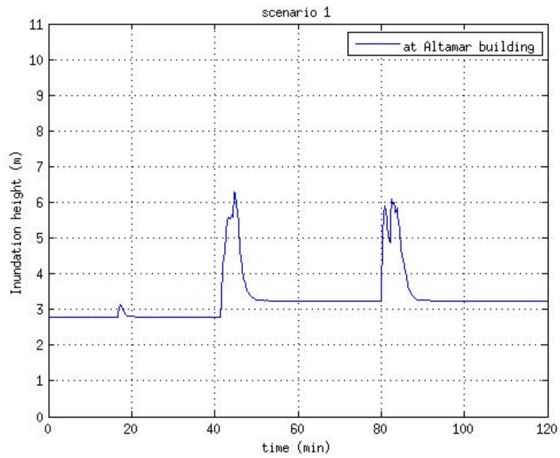

(b) Tide gauge of the inundation height at the altamar building of scenario 1.

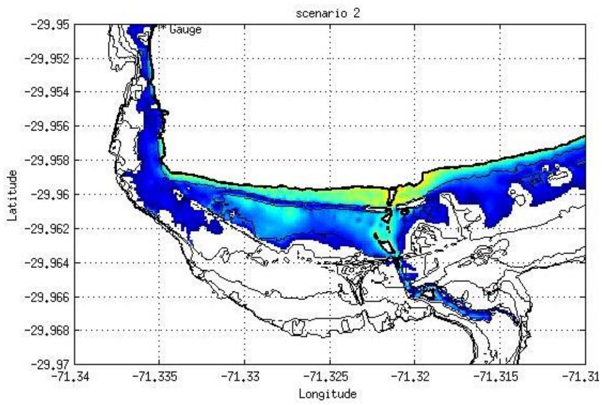

(c) Inundation map of scenario 2 with the original bathymetry.

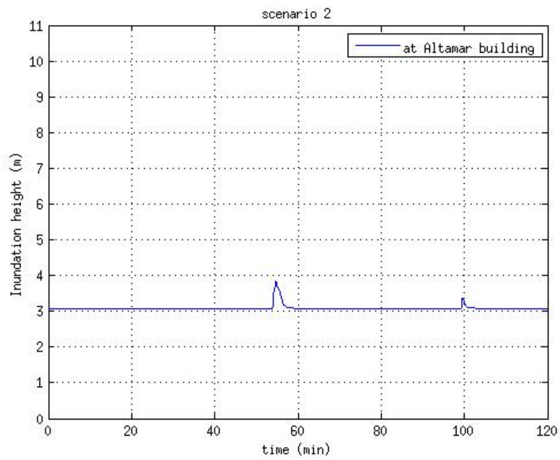

(d) Tide gauge of the inundation height at the altamar building of scenario 2.

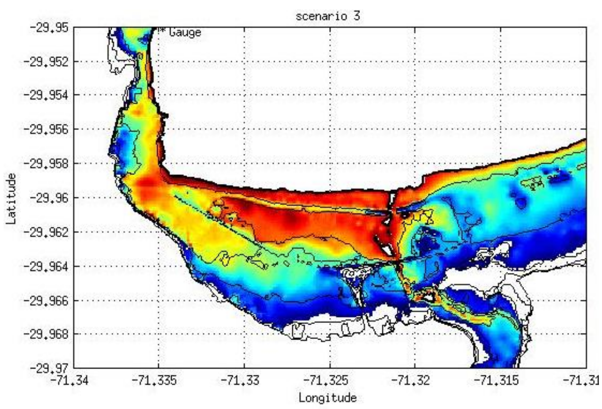

(e) Inundation map of scenario 3 with the original bathymetry.

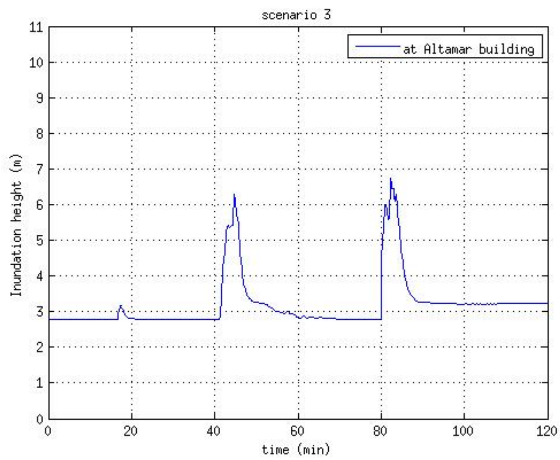

(f) Tide gauge of the inundation height at the altamar building of scenario 3.

Figure F.1: Inundation maps of the different earthquake scenarios with the corresponding tide gauges at the location of the Altamar building.

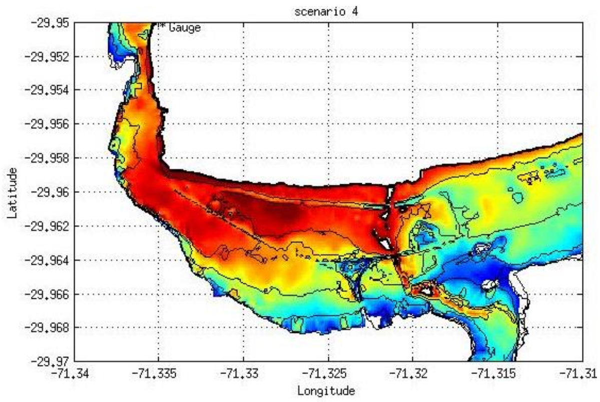

(a) Inundation map of scenario 4 with the original bathymetry.

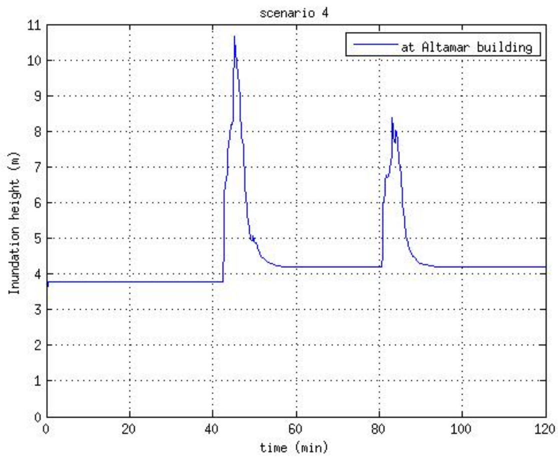

(b) Tide gauge of the inundation height at the altamar building of scenario 4.

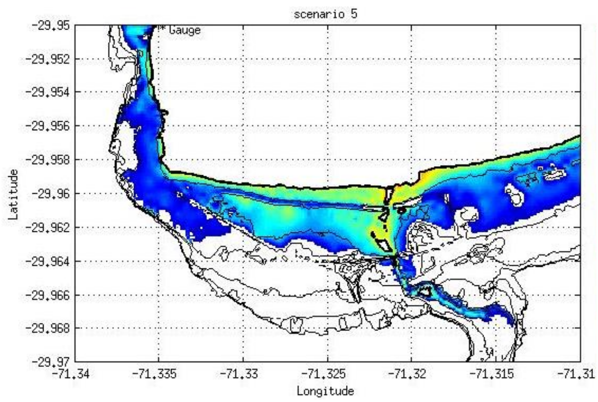

(c) Inundation map of scenario 5 with the original bathymetry.

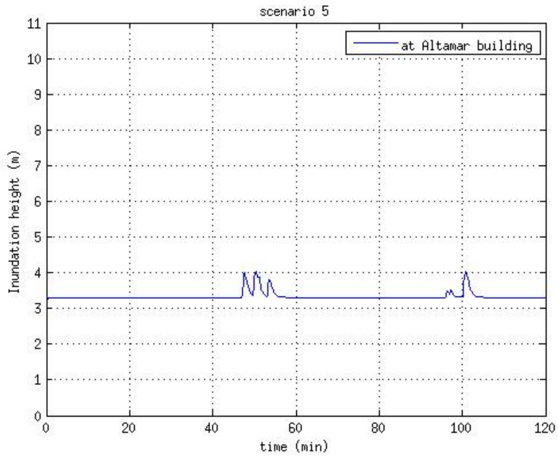

(d) Tide gauge of the inundation height at the altamar building of scenario 5.

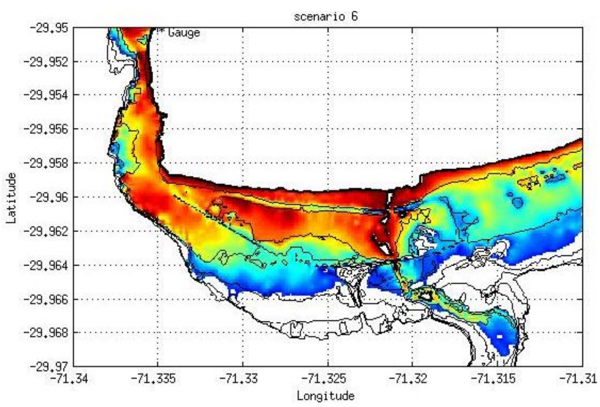

(e) Inundation map of scenario 6 with the original bathymetry.

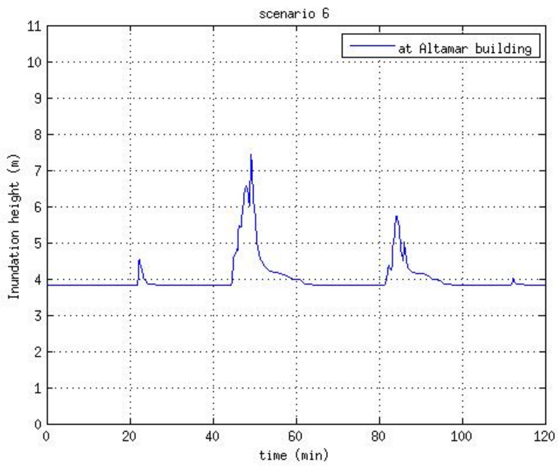

(f) Tide gauge of the inundation height at the altamar building of scenario 6.

Figure F.2: Inundation maps of the different earthquake scenarios with the corresponding tide gauges at the location of the Altamar building.

F.2. Simulating alternatives

To judge the effectiveness of the coastal protection of the different alternatives, the inundation maps in section 4.1 and tide gauges of both inundation height and flow velocities are taken into account. The tide gauges represent the values at the location which is marked with 'corner' in figure 4.1. The location 'corner' was used because it is positioned at the beginning of the neighbourhood Baquedano. This way it gives a global overview of the impact of the tsunami on the most important areas. In figures F.4 and F.5 these tide gauges are presented.

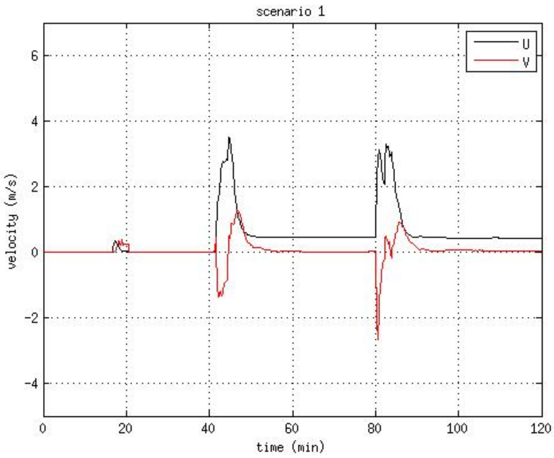

(a) Tide gauge of the velocities at the altamar building of scenario 1.

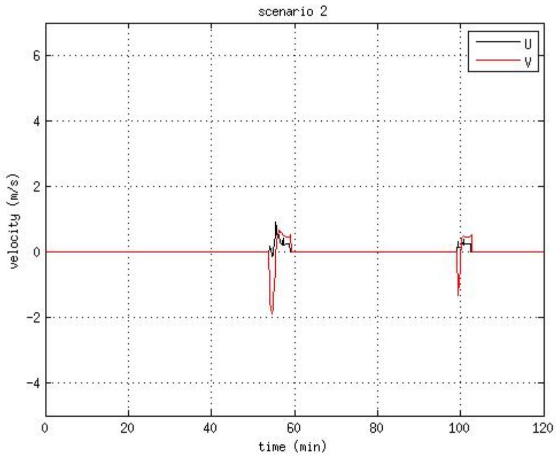

(b) Tide gauge of the velocities at the altamar building of scenario 2.

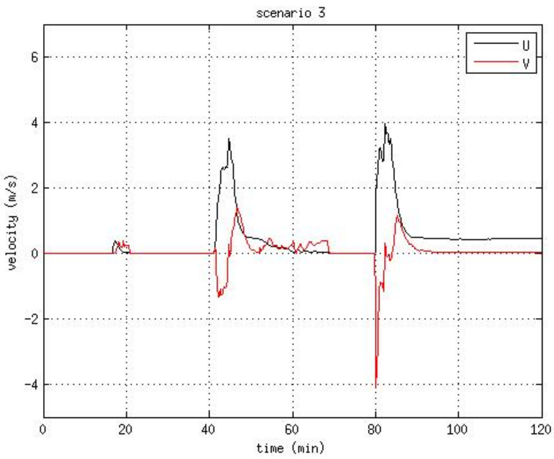

(c) Tide gauge of the velocities at the altamar building of scenario 3.

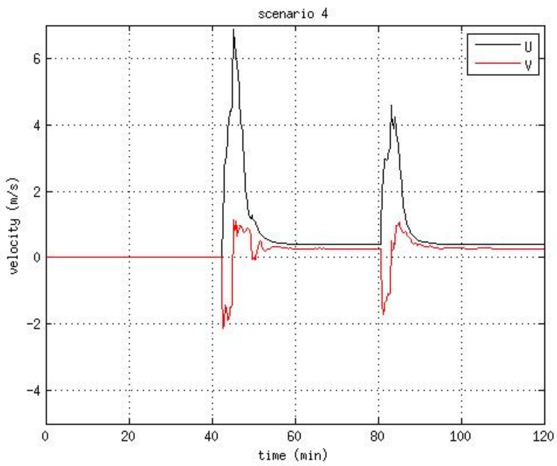

(d) Tide gauge of the velocities at the altamar building of scenario 4.

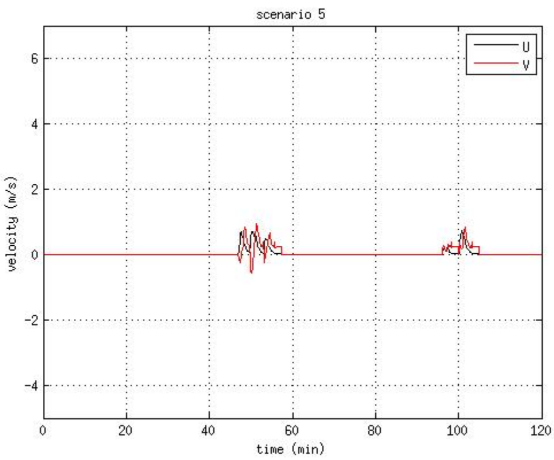

(e) Tide gauge of the velocities at the altamar building of scenario 5.

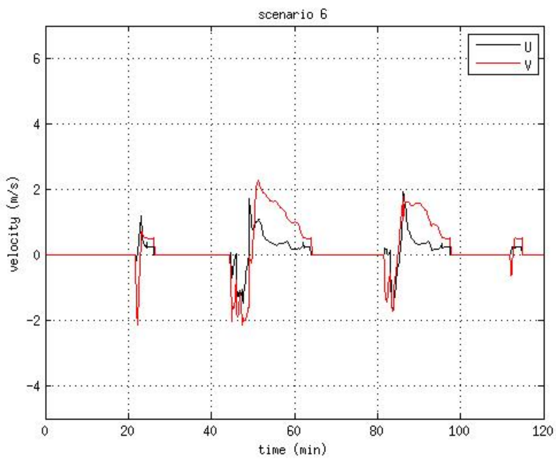

(f) Tide gauge of the velocities at the altamar building of scenario 6.

Figure F.3: Inundation maps of the different earthquake scenarios with the corresponding tide gauges at the location of the Altamar building.

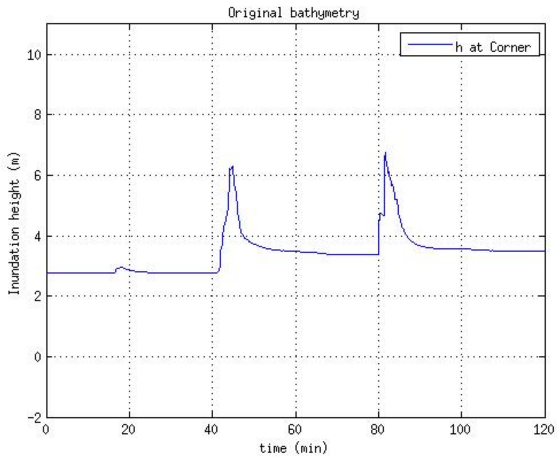

(a) Flow depth at location corner in original bathymetry.

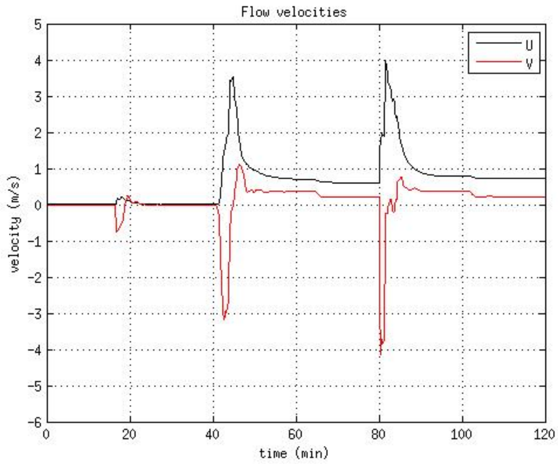

(b) Flow velocties at location corner in original bathymetry.

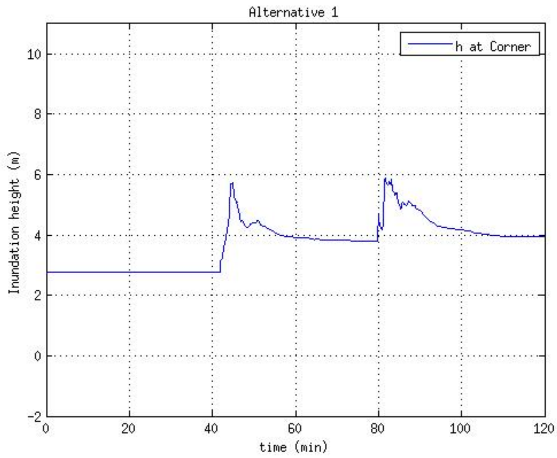

(c) Flow depth at location corner in alternative 1.

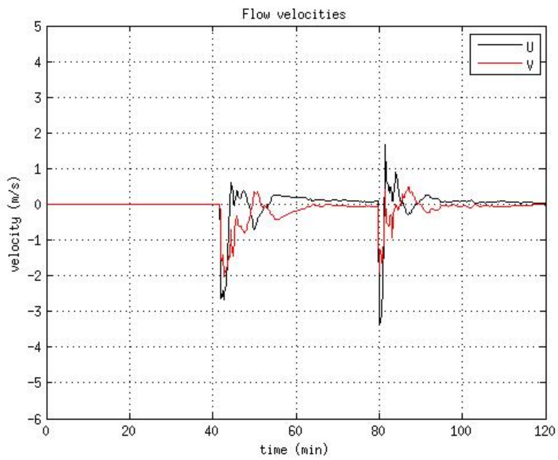

(d) Flow velocties at location corner in alternative 1.

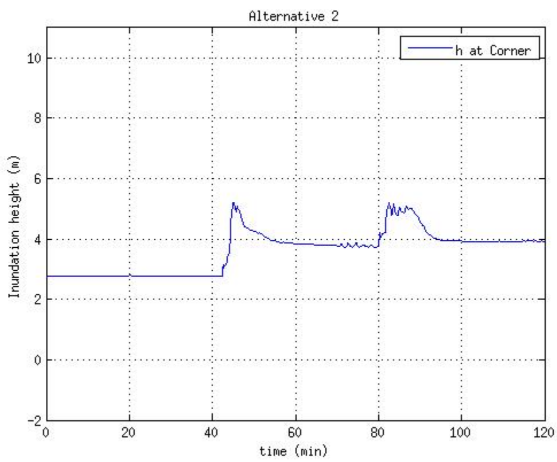

(e) Flow depth at location corner in alternative 2.

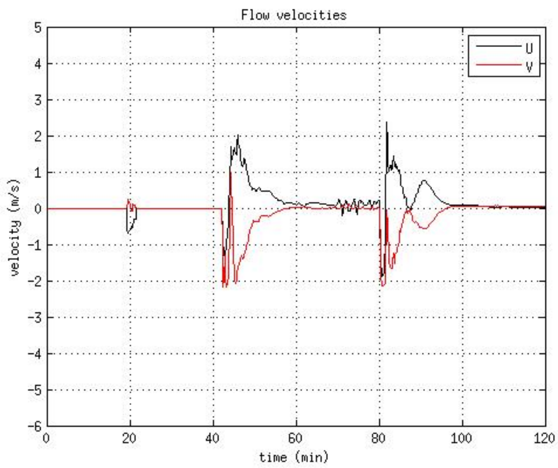

(f) Flow velocties at location corner in alternative 2.

Figure F.4: Tide gauges of inundation height and flow velocities at location corner of different alternatives.

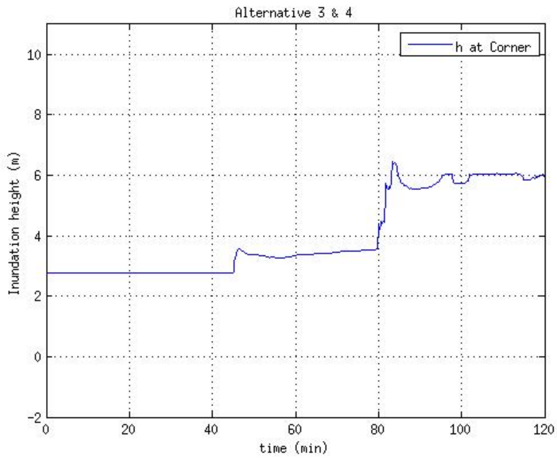

(a) Flow depth at location corner in alternative 3 and 4.

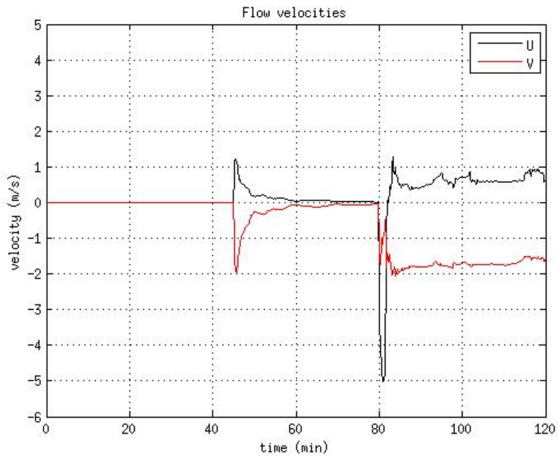

(b) Flow velocties at location corner in alternative 3 and 4.

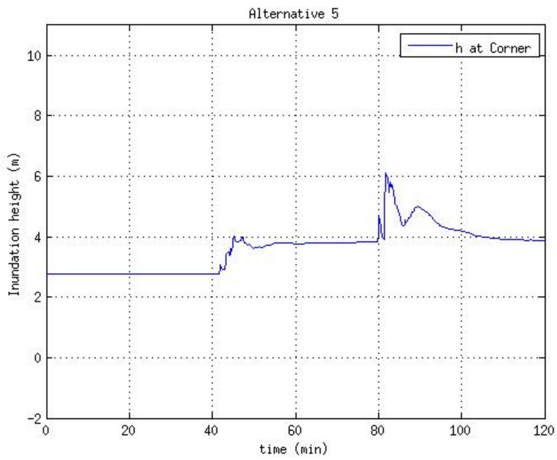

(c) Flow depth at location corner in alternative 5.

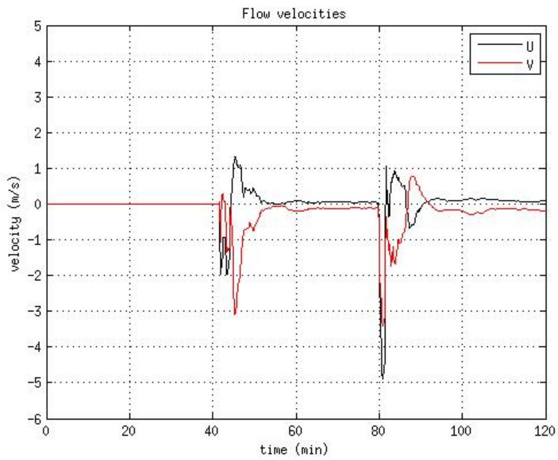

(d) Flow velocties at location corner in alternative 5.

Figure F.5: Tide gauges of inundation height and flow velocities at location corner of different alternatives.

F.3. Optimising alternative II

To find the optimum height of the coastal road of alternative II, tsunami simulations were performed with different elevations of the road. The most important results of these simulations are the inundation height and flow velocities in the neighbourhood Baquedano. The inundation maps of the proposed alternatives are given in figures F.6, F.7, and F.8. The results of the tide gauges at different locations in Baquedano of the different simulations are also presented below. The locations of the tide gauges are mentioned in section 4.1.

Besides that, the unity checks of the failure mechanisms require flow velocities and inundation heights in front of the structures. The tide gauges of beach2 were used as input for these calculations. The results of these tide gauges are presented in figure F.15.

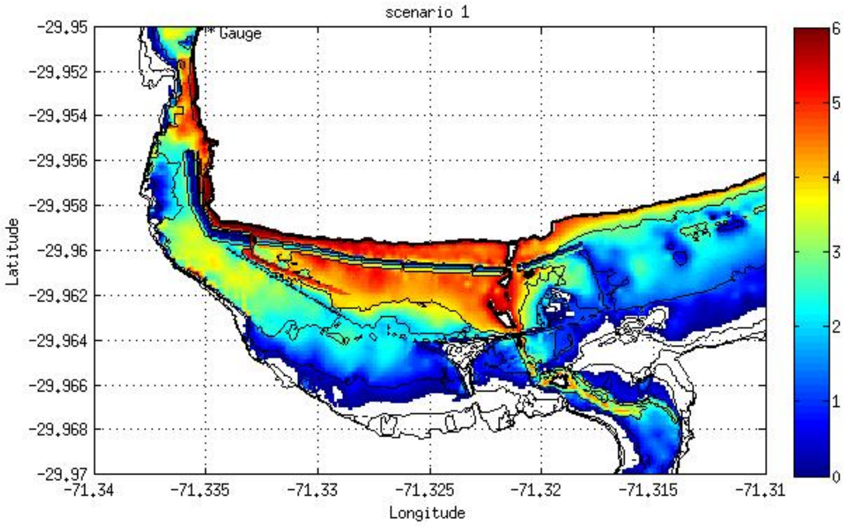

Figure F.6: Inundation map of alternative 2b with scenario 1.

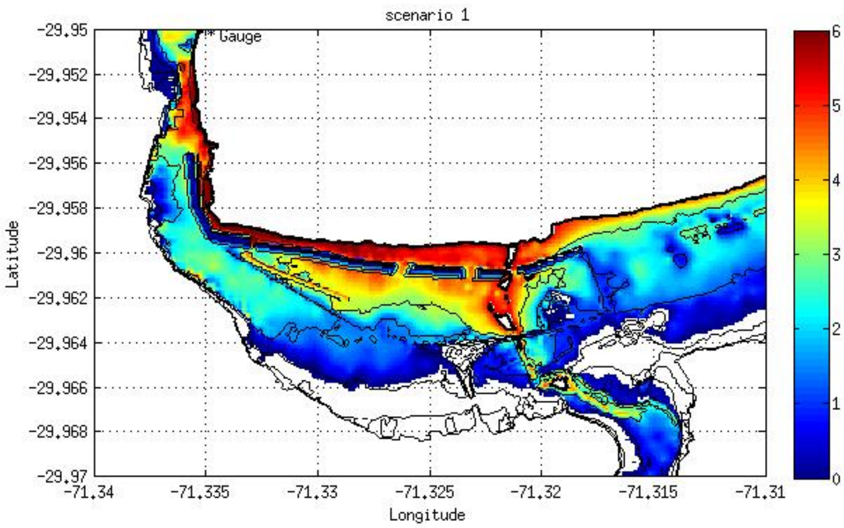

Figure F.7: Inundation map of alternative 2c with scenario 1.

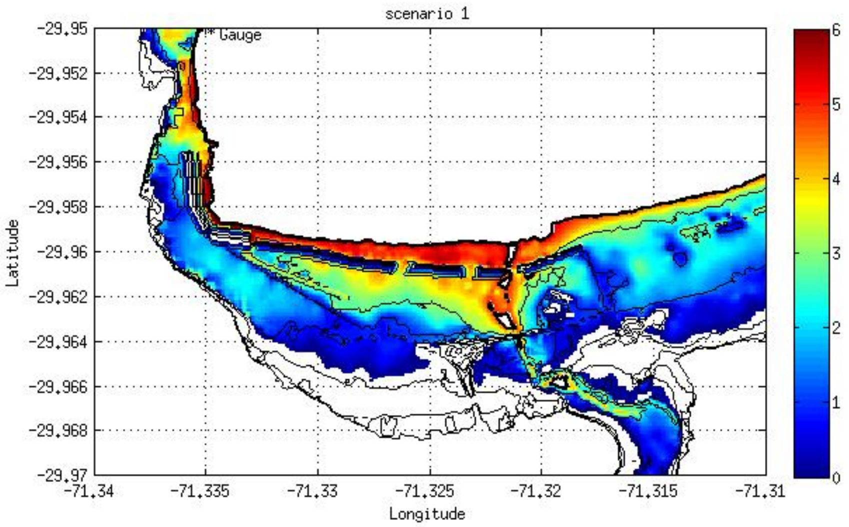

Figure F.8: Inundation map of alternative 2d with scenario 1.

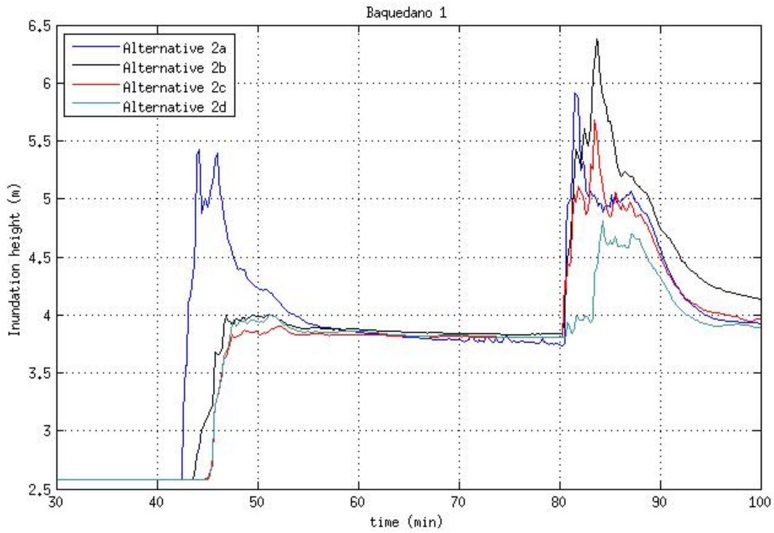

(a) Flow depth of different alternatives at location Baquedano 1.

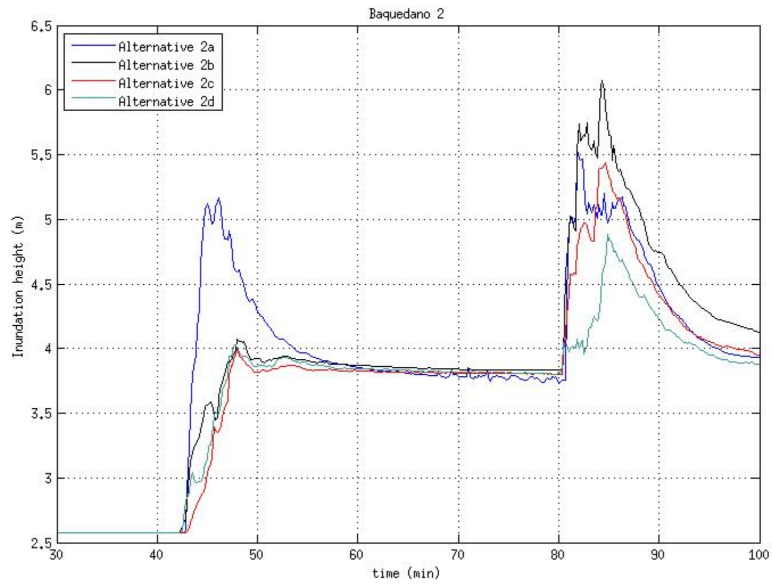

(b) Flow depth of different alternatives at location Baquedano 2.

Figure F.9: Tide gauges of inundation height at 4 locations in Baquedano.

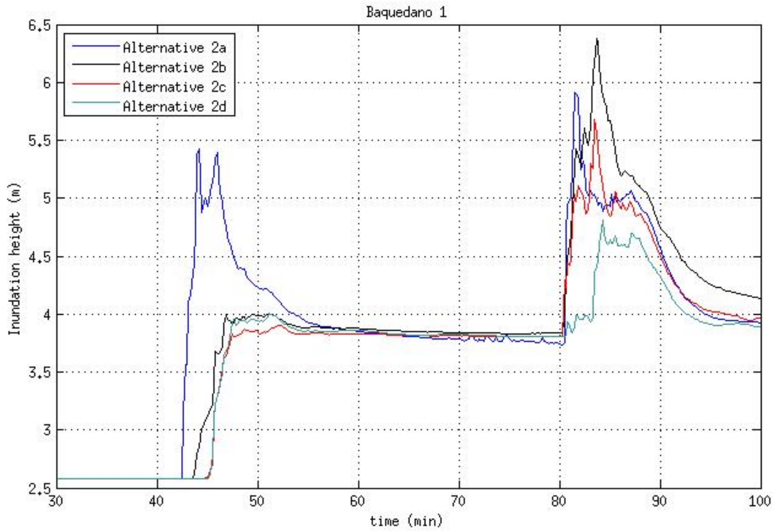

(a) Flow depth of different alternatives at location Baquedano 3.

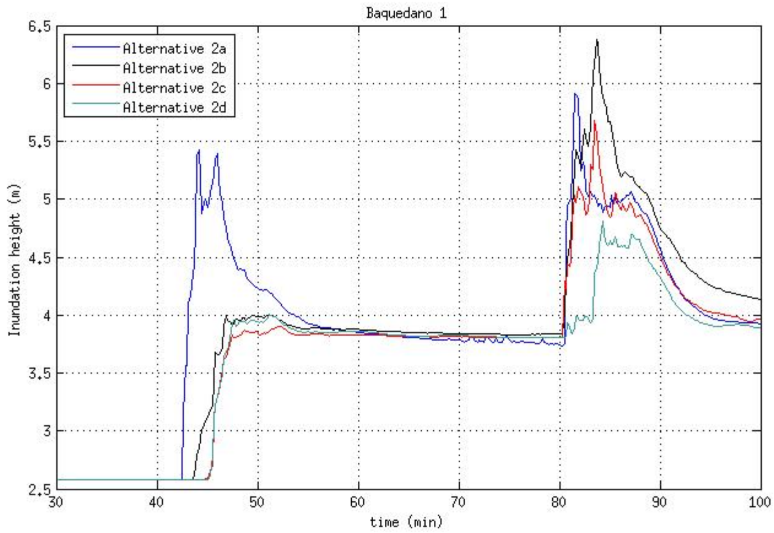

(b) Flow depth different alternatives at location Baquedano 4.

Figure F.10: Tide gauges of inundation height at 4 locations in Baquedano.

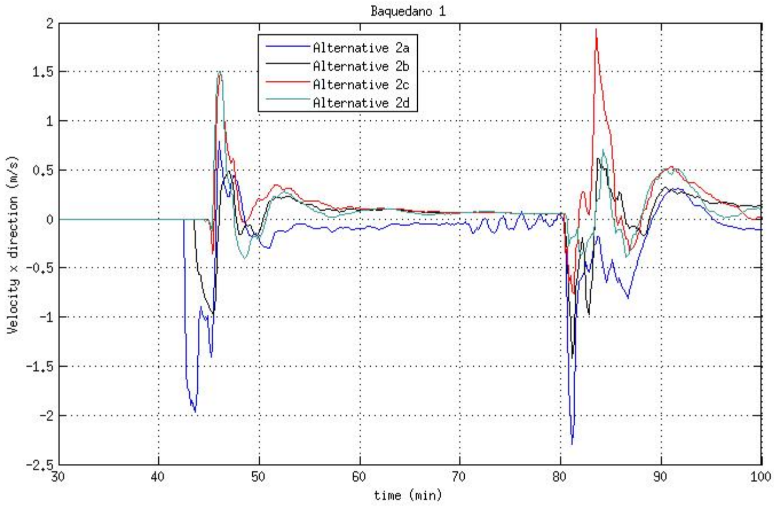

(a) Flow velocties in x direction of different alternatives at location Baquedano 1.

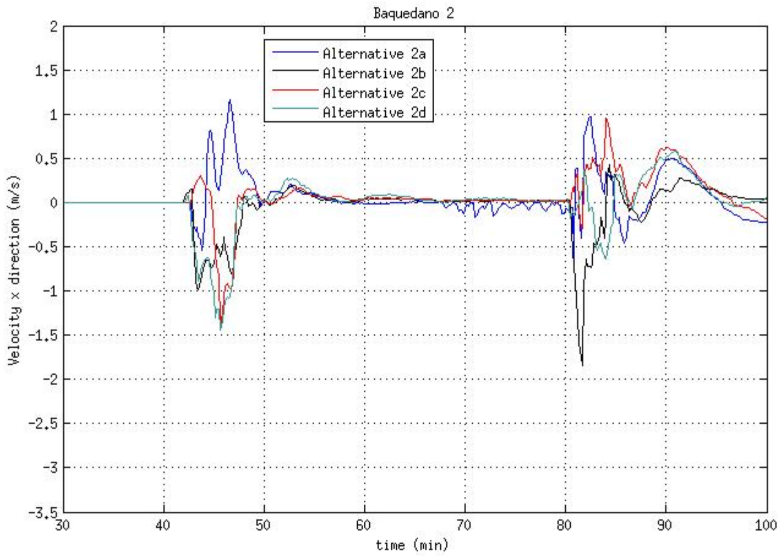

(b) Flow velocties in x direction of different alternatives at location Baquedano 2.

Figure F.11: Tide gauges of flow velocties in x direction at 4 locations in Baquedano.

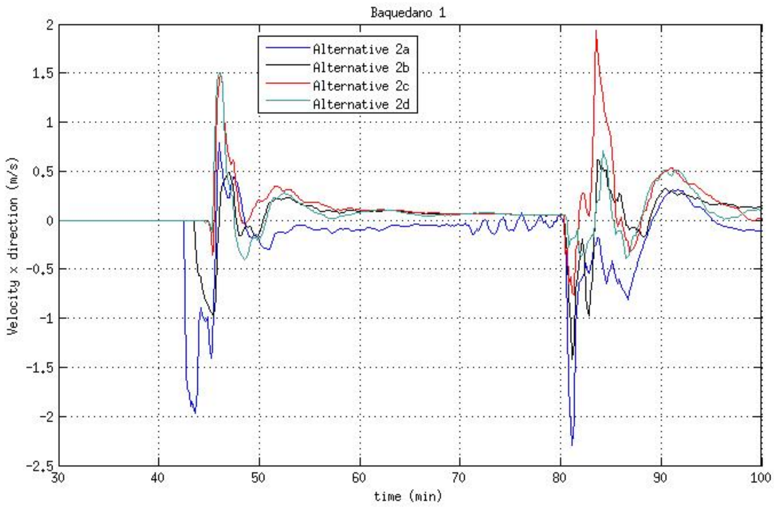

(a) Flow velocties in x direction of different alternatives at location Baquedano 3.

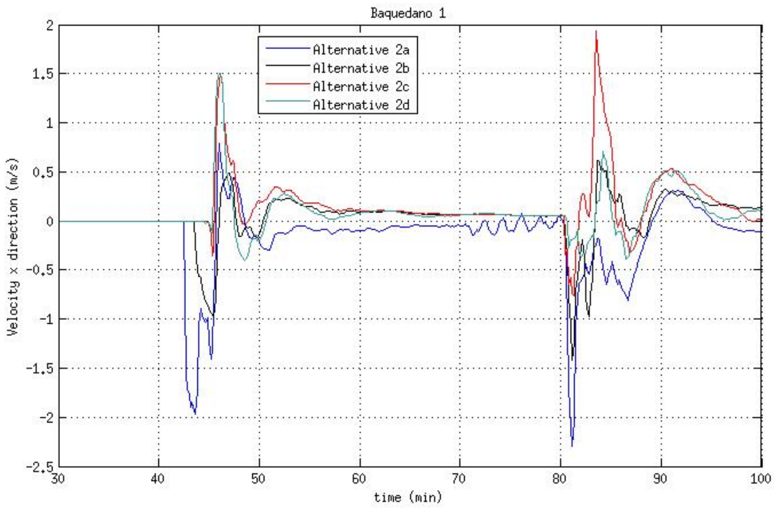

(b) Flow velocties in x direction of different alternatives at location Baquedano 4.

Figure F.12: Tide gauges of flow velocties in x direction at 4 locations in Baquedano.

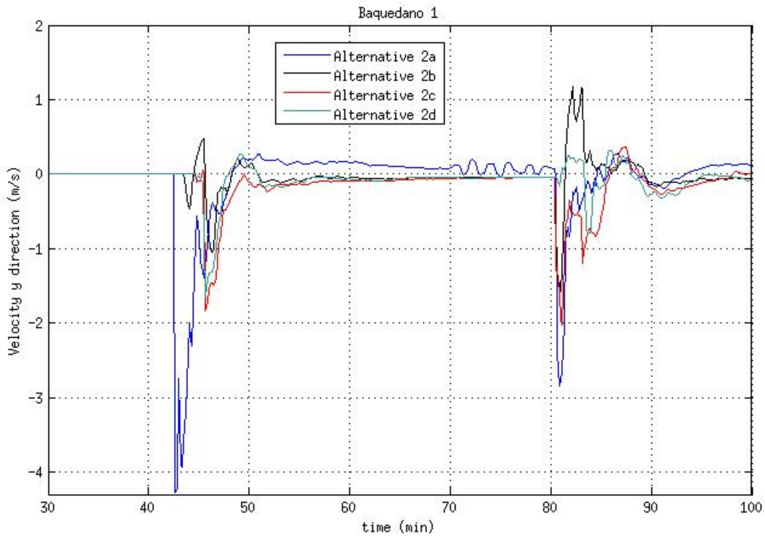

(a) Flow velocties in y direction of different alternatives at location Baquedano 1.

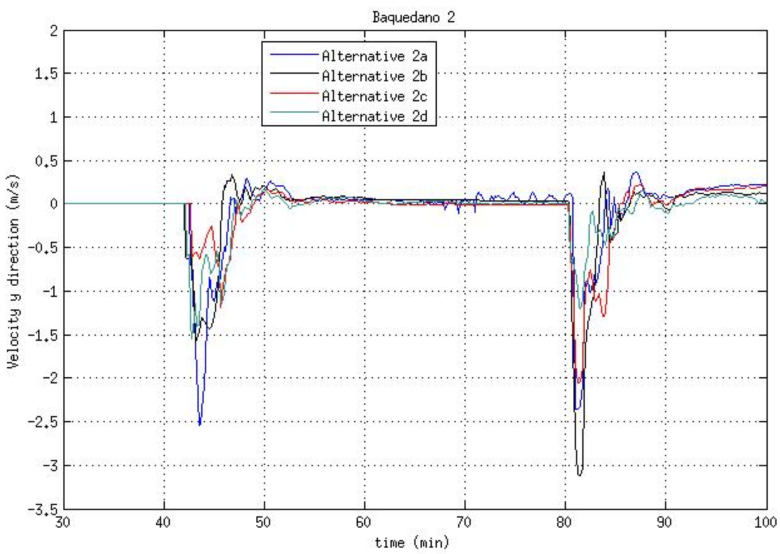

(b) Flow velocties in y direction of different alternatives at location Baquedano 2.

Figure F.13: Tide gauges of flow velocties in y direction at 4 locations in Baquedano.

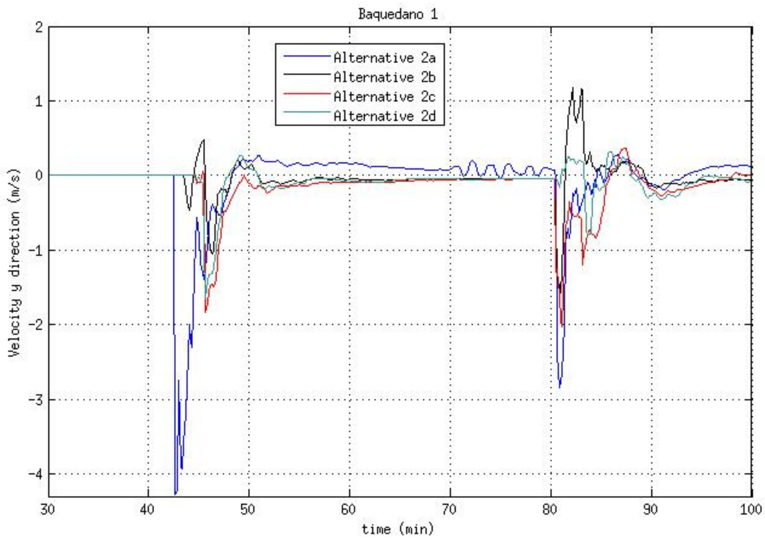

(a) Flow velocties in y direction of different alternatives at location Baquedano 3.

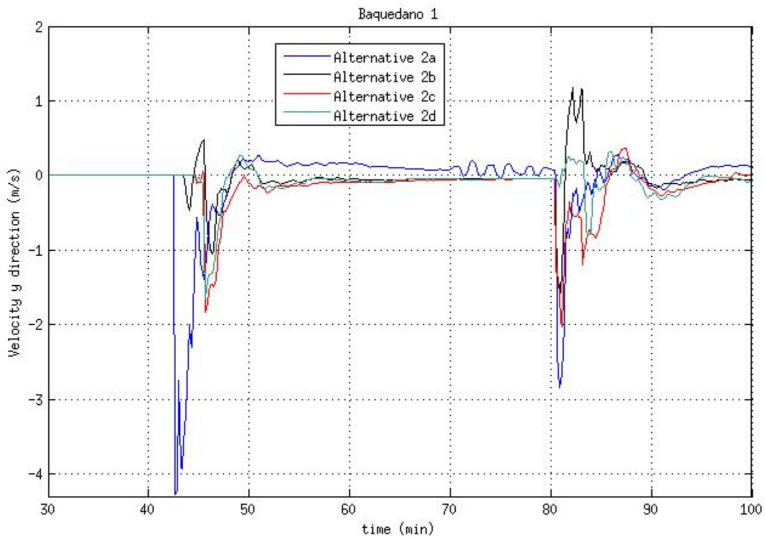

(b) Flow velocties in y direction of different alternatives at location Baquedano 4.

Figure F.14: Tide gauges of flow velocties in y direction at 4 locations in Baquedano.

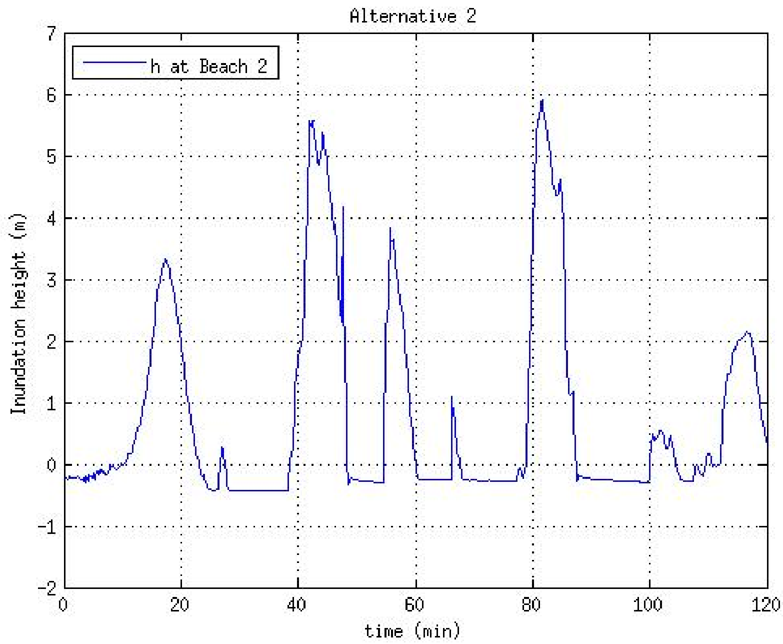

(a) Inundation height at beach 2 in alternative 2 with an elevation of 5 m from sea level.

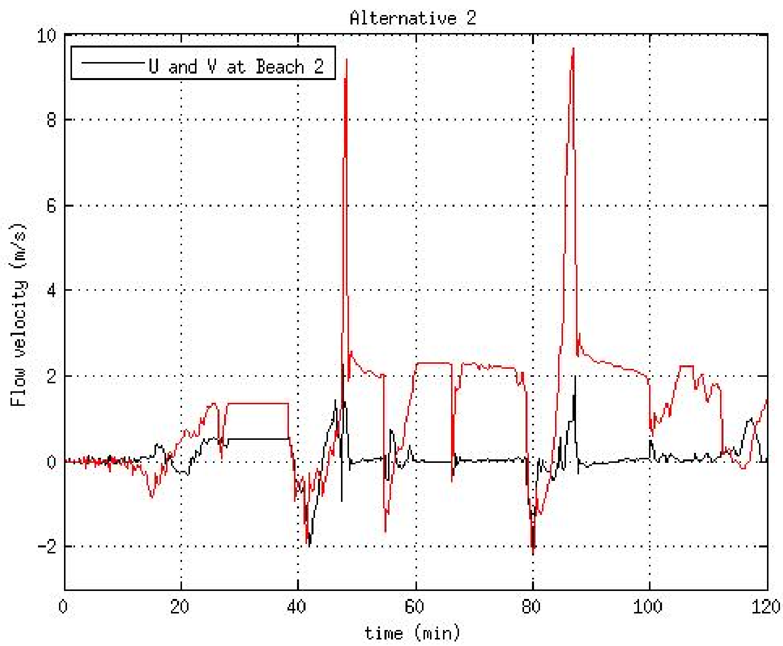

(b) Flow velocities at beach 2 in alternative 2 with an elevation of 5 m from sea level.

Figure F.15: Tide gauges of inundation height and flow velocties at Beach 2 in alternative 2 with an elevation of 5 m from sea level.

G Multi Criteria Analysis

A multi criteria analysis is a method to define a value to certain alternatives. The first step in this analysis is to define the criteria that define the value. These selected criteria are given a weight factor and a score. With these values the total value is determined.

G.1. Criteria

During the selection of the criteria it is important that the different aspects of importance are well balanced. When certain aspects are valued in multiple criteria the outcome is biased.

The costs can not be a criteria because this analysis is about the values. Values and costs should be evaluated separate from each other. The selected criteria are listed bellow.

Safety
The amount of safety depends on multiple aspects that are all considered in this criterion. A decrease of the original inundation, flow depth, the amount of retreating water and the financial damage are taken into account. Furthermore the risk of failure of the structures is an important aspect of this criteria.

Nature and recreation
This criterion represents the application of building with nature and the redevelopment of the wetlands. The redevelopment of the wetlands consists of restoring the ecosystem and creating a park for recreation.

Welfare neighbourhood
The welfare of the neighbourhood can be increased due to an increase of tourism. Next to that an increase in the economic resilience of the neighbourhood can cause an increase in welfare.

Visual hindrance
A high coastal protection will cause visual hindrance. This hindrance can be reduced by smart implementation into the surroundings.

Infrastructure
This criterion represents the impact of the solution on the local infrastructure and accessibility of Coquimbo.

Construction
Judged by the length of the building time, the hindrance for the surroundings can be measured. Also the level of difficulty of the construction process and the additional risks during construction are included in this criterion.

Durability
Durability is dependent of the lifetime of the structure and the amount of maintenance that is required. The amount of maintenance is not only based on the return period of the maintenance but also on the costs.

G.2. Weight factors

The weight that is given to a certain criterion is determined the following way. The criteria are placed in a matrix and for every combination of criteria there is stated which criterion is more important. If the row-criterion is more important a 1 will be placed in the joint box. If the column-criterion is more important a 0 will be placed. When the criteria are equally important there will be placed a 1 in both boxes. See table G.1 for an example of this system.

Criteria		a.	b.	c.	d.	e.	f.	g.
Safety	a.	-	1	1	1	1	1	1
Nature & recreation	b.	0	-	1	0	1	1	1
Welfare neigbourhood	c.	0	1	-	0	1	1	1
Visual hindrance	d.	0	1	1	-	1	1	1
Infrastructure	e.	0	0	0	0	-	1	0
Construction process	f.	0	0	0	0	1	-	0
Durability & maintenance	g.	0	1	0	1	1	1	-

Table G.1: Example of weight factor system

After this the total of the horizontal rows will be calculated. To determine the weight factor this amount will be divided by the total amount of ones in the whole matrix.

Because the priority someone gives to a criterion is very personal every person in the project group has made such a matrix. This has been done individually without a group discussion. However, the criteria have been stated upfront so everyone would apply the same aspects. Also it was the goal to fill in the matrices from the prospect of the stakeholders as a whole. Of all these matrices a the weight factors have been determined. The final weight factors of the criteria is determined by the average of the weight factors that followed from the individual matrices.

G.3. Scores

For this part of the analysis the approach is different. The scores are not determined individually but by means of a group discussion. This to ensure that all aspects will be taken into account and no arguments are forgotten. For each criteria the important aspects are determined by the whole group. After this a score is given per aspect for each alternative, these scores can be a ++, +, +-, - or - -. When all aspects have been given a score the score per alternative is determined as a number. This is done by giving values to the original scores from 10 to 0. When one aspect was considered to be extra important this score is weighted double in the calculation.

Safety

The amount of inundation and the maximum flow velocities in Baquedano are based on the numerical simulations (Appendix F). Here it can be seen that for alternatives I, II and V the inundation is the lowest and for alternatives III and IV it is the highest. Because the inundation is considered to be an important aspect it is weighed double in the calculation of the score. The flow velocities are determined from the velocity vector. From the numerical simulations it can be seen that alternative II has the lowest velocities and alternative V the highest.

The risk of failure is considered to be high for the dunes because there is a large risk of failure due to erosion. For alternatives I, III and IV the risk is assumed to be less. For alternative II the risk of overtopping is lower due to the extra openings which reduces the risk. However the flow velocities around the structure are higher which will again increase the risk. Therefore the amount of risk is considered to be the same as the previous alternatives.

The drainage of the water is dependent of two aspects. Firstly there is the amount of time it takes for the water to be drained from the area, here fast drainage is seen as a positive thing. However when flow velocities are high this will cause scour. In that case too fast drainage is judged negatively. For alternative II the drainage is fast due to the openings, also the velocities are not higher than 0,5 m/s. Which means that this alternatives scores good on both points. Alternatives I and V have slow drainage, but also low flow velocities. Alternatives III and IV have almost no drainage. This causes low flow velocities but the remaining water will cause a lot of nuisance.

The individual scores per aspect and the total score of the alternatives is summarised in table G.2.

Aspect	I	II	III	IV	V
Amount of inundation in Baquedano	+	+	-	-	+
Flow velocities in Baquedano	+	++	-	-	- -
Risk of failure	+	+	+	+	-
Drainage of water after tsunami	+	++	+-	+-	+
Scores	75	85	40	40	50

Table G.2: Overview scores safety

Nature and recreation
In alternative IV the wetlands are fully restored by removing the road. In alternative V the road is removed but the dunes form a new barrier which obstructs a full restoration. In the other alternatives the road remains an obstruction. In alternatives I and II the obstruction is even higher because of the heightening of the road. However, in alternative II the openings provide some interaction between the sea and the wetlands, which helps the wetlands to restore.

In all alternatives a park area is created. However in alternative IV the park area is larger due to the removal of the coastal road. In alternative V this area is not used for a park but to create a new natural environment. The individual scores per aspect and the total score of the alternatives is summarised in table G.3.

Aspect	I	II	III	IV	V
Restoration of ecosystem wetlands	- -	+	-	++	+-
Creation of park area	+	+	+	++	+
Creation of new nature	+-	+-	+-	+-	++
Scores	40	70	50	85	75

Table G.3: Overview scores nature & recreation

Welfare neighbourhood
The welfare of the neighbourhood can be positively influenced by an increase of tourism. A multi-functional boulevard will increase the economic resilience of the area and make it more attractive for tourists. Alternative I includes the largest boulevard. Alternative II also contains a boulevard but due to the openings the area will be less. The other alternatives do not contain a boulevard. Additionally in alternative IV the accessibility of the beach area is reduced and in alternative V the accessibility is reduced and the size of the dunes reduces the space available for tourism. The individual scores per aspect and the total score of the alternatives is summarised in table G.4.

Aspect	I	II	III	IV	V
Amount of touristic area	++	+	+-	+-	-
Accessibility of touristic area	+	+	+-	- -	- -
Scores	90	75	50	25	15

Table G.4: Overview scores welfare neighbourhood

Visual hindrance
The height of the protection is the highest in alternative V and the least high in alternative III and IV. An obstruction in the view is of less hindrance when the exterior is in line with the surroundings. On this alternatives I, II and V score better. This because the boulevard of alternatives I and II have a function in the surroundings and alternative V has a high natural value. For the visual hindrance it is considered that the hindrance is less when the object is further away from the beach. Therefore alternatives III and IV score better on the location of the protection and alternatives IV and V better on the location of the road. The individual scores per aspect and the total score of the alternatives is summarised in table G.5.

Aspect	I	II	III	IV	V
Height of the protection	+-	+-	+	+	-
Exterior of the protection	+	+	+-	+-	+
Location of protection	-	-	+	+	-
Location of the road	-	-	-	+	+
Scores	45	45	55	70	50

Table G.5: Overview scores visual hindrance

Infrastructure
Due to the replacement of the road the accessibility of Coquimbo will be less in alternatives IV and V. However the accessibility of the Baquedano neighbourhood will increase. Because the centre of Coquimbo is considered more important than the neighbourhood of Baquedano the alternatives I, II and III are given a higher score.The individual scores per aspect and the total score of the alternatives is summarised in table G.6.

Aspect	I	II	III	IV	V
Accessibility Coquimbo	+	+	+	-	-
Accessibility Baquedano	+-	+-	+-	+	+
Scores	65	65	65	50	50

Table G.6: Overview scores infrastructure

Construction
The construction time of the dunes is the longest because a lot of sand has to be placed for the creation of the dunes. Alternative III can be build the quickest because no mayor alteration are made to the surroundings. Which is also the reason why the hindrance during the construction is the lowest for this alternative. For the other alternatives there is a lot of construction on or near the road which will cause a lot of hindrance for the traffic. The individual scores per aspect and the total score of the alternatives is summarised in table G.7.

Aspect	I	II	III	IV	V
Construction time	+	+	++	+-	- -
Hindrance for traffic	-	-	+	+-	-
Scores	50	50	90	50	15

Table G.7: Overview scores construction

Durability & maintenance
After a tsunami alternative V is prone to have a lot of erosion. The other alternatives are made of more robust materials and are less vulnerable for damage. Additionally alternative V will need more maintenance because the dunes can also be eroded due to wind. For alternative II the openings could be closed due to the dynamics of the beach and the streams from the wetland. The individual scores per aspect and the total score of the alternatives is summarised in table G.8.

Aspect	I	II	III	IV	V
Amount of damage after tsunami	+	+	+	+	-
Amount of maintenance	+	+-	+	+	-
Scores	75	65	75	75	25

Table G.8: Overview scores durability & maintenance

H Costs

In this chapter, for each alternative the costs are given. First, the different cost drivers with the costs rates are given. These are extracted out of a similar construction project of a fishing pier in Tongoy in 2015 [14] and can be seen in table H.1. The total costs of each alternative is presented in Chilean pesos and in euros. The exchange rate from euro to Chilean pesos is taken as 1:750 [47].

Construction activity	Unit	Costs per unit (in Chilean pesos)
Removing concrete pavement	m^2	20.351
Removing concrete (sea)wall	m^3	186.900
Ground excavation	m^3	8.811
Construction road	m^2	30.633
Construction sub base (0,3 m)	m^2	7.190
Rubble sand	m^3	19.029
Construction concrete foundation (in situ)	m^3	205.280
Construction concrete wall (in situ)	m^3	629.013
Construction concrete slab (in situ)	m^3	425.567
Construction L block (prefab)	m^3	395.296
Placement L block (prefab)	m^3	84.957
Geo textile (including placement)	m^2	2.727
Bedrock 10 to 30 kg	m^3	38.784
Bedrock 100 to 300 kg	m^3	42.065
Bedrock 1200 to 2000 kg	m^3	46.652
*Bedrock 3000 to 6000 kg	m^3	50.000

Table H.1: Cost rates for different materials and construction activities, source: [14]. *: Costs are a rough extrapolation from the given bedrock costs.

In figure H.1 different sections of the new roads/coastal protection are indicated by numbers. The corresponding numbers are the distances in meters and are multiplied with the costs per running meter of the cross section.

Figure H.2 gives the schematized dimensions of the different cross sections used in the alternatives. The boulevard from alternative I and II is schematized by a concrete block with dimensions 5 m x 15 m and a wall thickness of 0.5 m. The reflective T-wall can be seen as a L block constructed as a straight seawall with on the land side a slope of excavated ground. The inland coastal wall from alternative III and IV is designed as a concrete reflective wall in a trapezium form. The base is 3 meter, the height is 4 meter and the top width is 0,5 meter. The dunes are schematized by a triangular shape with a base of 40 meter and top of the crest at 6 meter. A road consist of a sub base of 30 cm thickness and a top layer of asphalt of 20 cm, both calculated with a total width of 7 meter. In case a certain structure is not completely demolished or built, but only repair took place, half of the respective costs are taken into account.

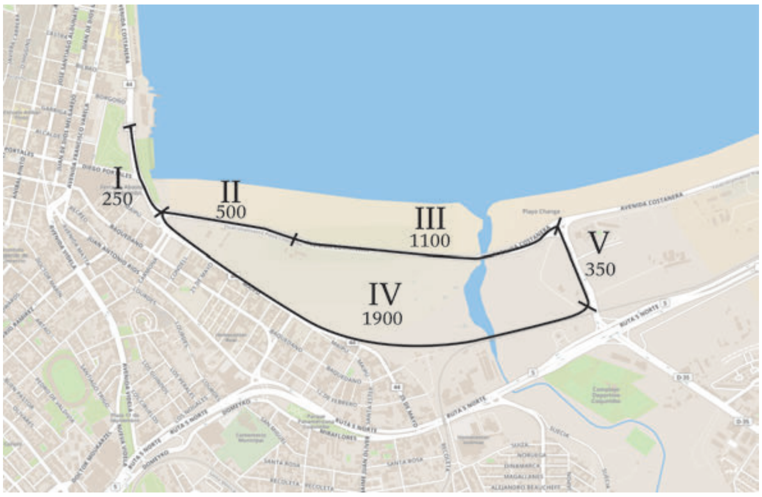

Figure H.1: Division of different sections along which the cross sections vary

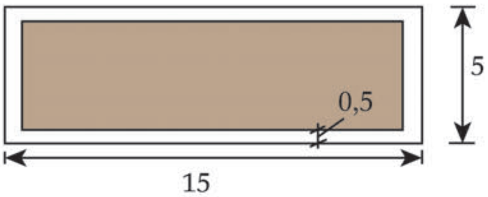

(a) Schematization of the boulevard

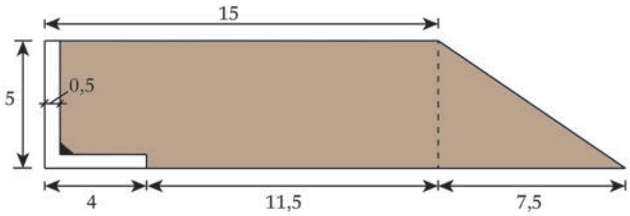

(b) Schematization of the reflective wall

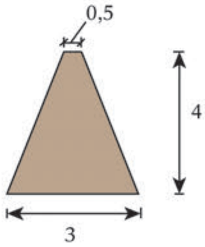

(c) Schematization of the inland reflective wall

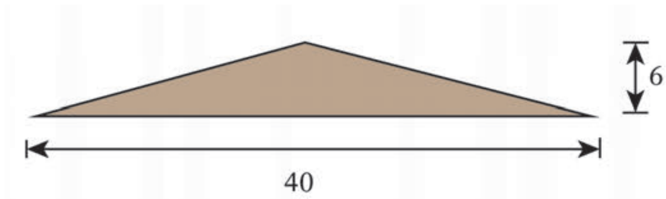

(d) Schematization of the dunes

Figure H.2: Schemaitizations used for the different cross sections

H.1. Costs part I

Alternative I

The concrete boulevard is constructed along the entire coastline (section I, II, and III). Before this can be placed, the current road, seawall and embankment has to be removed. On top of the concrete boulevard a new road is constructed. The boulevard is filled with rubble sand. Table H.2 gives the overview of the costs of alternative I.

Alternative II

The concrete boulevard is only build along a part of the coastline (section I and II). Section III is dimensioned with a reflective L-Wall, which makes the costs lower. The costs of the drainage openings are based on Dutch standards for a polder drainage channel [20]. In total there will be 4 openings built with costs of 50.000 euro per sluice. This is converted to Chilean pesos with an exchange rate of 1:750 [47]. This with the Table H.3 gives the overview of the costs of alternative II.

Alternative III

The removal of the original road, seawall and embankment are relative cheaper since they are not completely

Construction activity	Costs (in million Chilean pesos)
Remove road	263
Remove seawall	598
Remove embankment	338
Construct road	489
Construct boulevard	13.407
Fill boulevard	1.971
Total	17.069
Total (in million euros)	22,8

Table H.2: Costs overview alternative I

Construction activity	Costs (in million Chilean pesos)
Remove road	263
Remove seawall	598
Remove embankment	105
Construct road	489
Construct boulevard	5.435
Fill boulevard	799
Drainage openings	150
Reflective wall	2.641
Embankment behind wall	1.460
Total	11.943
Total (in million euros)	15,8

Table H.3: Costs overview alternative II

removed, but just renewed. Big cost driver in this alternative is the inland reflective wall along section I and IV. Table H.4 gives the overview of the costs of alternative III.

Construction activity	Costs (in million Chilean pesos)
Remove road	114
Remove seawall	299
Construct road	211
Repair original seawall	1.006
Construction reflective wall	7.227
Total	8.859
Total (in million euros)	11,8

Table H.4: Costs overview alternative III

Alternative IV
The road and seawall along the coastline (II and III) are removed. Along part I and IV there is a inland reflective wall constructed. The road capacity is extended along section I, IV and V. Table H.5 gives the overview of the costs of alternative IV.

Alternative V
The dunes are places along section II and III. The road capacity is extended along section I, IV and V. Along section I, an inland reflective wall has to be placed. Table H.6 gives the overview of the costs of alternative V.

Overview
Table H.7 gives for each alternative the total costs, which is a sum of the specific costs per alternative, general costs and the overhead costs. The general costs include renewal of the park and smaller structures and

Construction activity	Costs (in million Chilean pesos)
Remove road	227
Remove wall	598
Remove embankment	338
Construct road	595
Construct reflective walll	7.227
Total	8.988
Total (in million euros)	12,0

Table H.5: Costs overview alternative IV

Construction activity	Costs (in million Chilean pesos)
Remove road	227
Remove seawall	598
Remove embankment	338
Construct road	595
Construct dunes	3.653
Construct reflective wall	840
Total	6.254
Total (in million euros)	8,3

Table H.6: Costs overview alternative V

components, such as fences, lights, benches and evacuation signs. The general costs are estimated to be approximately 2 billion Chilean Pesos. In the end, 10 % of overhead costs (equipment and running site costs) are added [49].

Alternative	Alternative specific costs*	General costs*	Overhead costs*	Total costs*	Total costs**
I	17.069	2.000	1.907	20.976	28,0
II	11.942	2.000	1.394	15.214	20,3
III	8.859	2.000	1.086	11.945	15,9
IV	8.988	2.000	1.099	12.087	16,1
V	6.254	2.000	825	9.079	12,1

Table H.7: Total costs overview. *Costs given in million Chilean pesos. **Costs given in million euros

H.2. Costs part II

This section elaborates the costs of alternative II. Three different options for section III of the seawall are added: the L-wall, the ground dam and the reinforced soil. Additional to the elaboration from the different options for section III the scour protection is determined which brings the costs to a significant higher level.

The scour protection is elaborated in 8.4.5 and the design of the layers are given in 8.3. Since the costs of bedrock 3000 - 6000 kg was not familiar a rough extrapolation is done with the costs of the other bedrocks. Costs per m^3 is taken as 50.000 CLP. In FIGURES it can be seen how the scour protection is dimensioned.

L-Wall

In this option the L-Wall is constructed over a long part of the coastal protection. In table H.8 an overview is given of all the cost.

Ground wall

This option is executed with a ground wall along section III. The big cost driver of this option is the scour layer over the talud of the ground wall. In table H.9 an overview is given of all the cost.

Construction activity	Costs (in million Chilean pesos)
Remove road	264
Remove wall	598
Remove embankment	106
Build road	490
Build boulevard	3.658
Sand boulevard	1.201
Drainage openings	150
L-Wall	4.101
Sand behind L-Wall	2.030
Bedrock 10-30 kg	894
Bedrock 100-300 kg	2.457
Bedrock 1200-2000 kg	5.524
Bedrock 3000-6000 kg	9.728
Total	31.200

Table H.8: Costs overview option L-wall

Construction activity	Costs (in million Chilean pesos)
Remove road	264
Remove wall	598
Remove embankment	106
Build road	490
Build boulevard	3.658
Sand boulevard	1.201
Drainage openings	150
Ground embankment	2.533
Bedrock 10-30 kg	996
Bedrock 100-300 kg	2.757
Bedrock 1200-2000 kg	6.242
Bedrock 3000-6000 kg	11.136
Total	30.131

Table H.9: Costs overview option ground wall

Reinforced soil

Option reinforced soil is executed with Tensar Geogrids for section III and the backside of the boulevard along section II. This gives the possibility to create a steep talud with a natural visual aspect. Appendix K gives the elaboration of the calculations made for the design of the reinforced soil. In table H.10 an overview is given of all the cost given by Tensar [45]. The costs of the different geogrids are based on the Dutch prices of the geogrids. The transfer rate of 1:750 is used to find costs in Chilean Pesos.

Tensar Geogrid	Unit	Costs per unit (in Chilean pesos)
RE510	m^2	2.025
RE520	m^2	2.363
RE570	m^2	3.900
RE500 Bodkins	per unit (1,3 m width)	1.313
Erosiemat (Vmax)	m^2	2.250

Table H.10: Cost rates for different Tensar Geogrids, source:

In table H.11 an overview is given of all the cost of option reinforced soil.

Overview

Construction activity	Costs (in million Chilean pesos)
Remove road	264
Remove wall	598
Remove embankment	106
Build road	490
Build boulevard	3.658
Fill boulevard and behind	1.101
Drainage openings	150
Ground embankment	1.277
Bedrock 10-30 kg	745
Bedrock 100-300 kg	2.019
Bedrock 1200-2000 kg	4.479
Bedrock 3000-6000 kg	7.680
Tensar geogrids	455
Total	23.021

Table H.11: Costs overview option reinforce soil

In table H.12 an overview is given of all the cost of option reinforced soil. It can be seen that the option with reinforced soil is the most economic option.

Option	Option specific costs*	General costs*	Overhead costs*	Total costs*	Total costs**
L-wall	31.200	2.000	3.320	36.520	48,7
Ground wall	30.131	2.000	3.213	35.344	47,1
Reinforced soil	23.021	2.000	2.502	27.523	36,7

Table H.12: Total costs overview. *Costs given in million Chilean pesos. **Costs given in million euros

I

Reference projects

In this section different reference projects are highlighted that overlap with possible solutions for the project. During a field survey on September 14th 2016 the cities Dichato, Tomé and Penco in the Concepcíon area were visited as reference projects on tsunami mitigation measures. On February 27th 2010 a tsunami hit Chile's Maule region. This was denoted as the biggest tsunami hazard of South-America since 1979(Khew et al. [27]). After this tsunami a lot of different mitigation measures were taken in the Concepcíon region. Mitigation measures proposed here are likely to be accepted in other Chilean regions like Coquimbo as well.

I.1. Protection in Concepcion area

Small sea-walls are often used in the Concepcion area, which have a height of less than five metres above sea level. These seawalls provide basic protection against far field tsunamis or storm surges. Additionally evacuation warning signs and evacuation routes are implemented in almost all coastal zones.

In Dichato a large part of the coastal zone was rebuilt. First of all, the boulevard was increased 2 to 3 meters in height. Also concrete reflection walls were placed in front of the boulevard as can be seen in figure I.1).

Figure I.1: Concrete reflection wall in Dichato, picture made by: Reinier Daals

Rubble mound is placed along the coastline at places where there is no beach to protect the shore.

Planting trees in the coastal region is also used as a mitigation measure. The trees are still young and small, but in time they will become stronger. The function of the trees is to decrease the kinetic propagation energy of a tsunami wave. Additionally, a dense field of trees could function as a sieve against debris. The risk of this measure is that when the trees are still young they can easily be flushed away. Floating trees will function as debris and cause damage on buildings and structures. The functioning of the trees is further explained in figure I.3.

Finally the governement has raised the houses which are located in proximity of the coast. These elevated houses provide space for the tsunami to flow underneath the houses.

Figure I.2: Scourprotection in Dichato, picture made by: Reinier Daals

Figure I.3: Explanation of function of trees, picture made by: Reinier Daals

Figure I.4: Raised house on piles, picture made by: Reinier Daals

The promenades of Penco have had a positive influence on the community because it enabled a faster rebound of the tourist-related food businesses. Besides boosting the economic resilience the promenade also has the function of increasing awareness. It contains prominent tsunami warning signage and a memorial to the victims of the 2010 tsunami.

Figure I.5: A multifunctional solution for the raised boulevard, picture made by: Reinier Daals

According to Dr. R. Aránguiz the public is not very positive about the measures that have been taken. This is because in case of a major tsunami there is no substantial physical protection due to the insufficient height of the walls. The new housing arrangements do not suffice because the wooden houses will not offer sufficient protection. Additionally, the raised houses decrease the evacuation speed due to hindrance by the extra stairs, and a lack of a door at higher levels. The one thing that was well received by the local people was the multi-functional boulevard. This contributed to the economic resilience of the community.

I.2. Innovative tsunami structures

In this section, different innovative tsunami structures are discussed. These solutions have all in common that they are not realized yet on a realistic scale. Therefore, there is a big risk included in the functioning of these measures. Also costs of such solutions will be high.

The Tsunami Catcher by Dyneema and Deltares
The Dyneema Tsunami Catcher works by a mechanism where a water tight membrane connected between ground level and a buoyancy tube protects the shore from the tsunami. In normal resting stage the tube is hidden under the ground. When a tsunami hits, water flows into the basin where the tube is located. Due to an upward buoyancy force, the water pushes the tube upward. A strong watertight membrane of approximately 1 cm thick can restrain the most of the incoming tsunami wave. The tube is consequently kept horizontally in place by a strong cable connected in seaside.Dsm.com [15]

(a) Concept of the Dyneema Tsunami Catcher, source: DeltaresFilm [13]

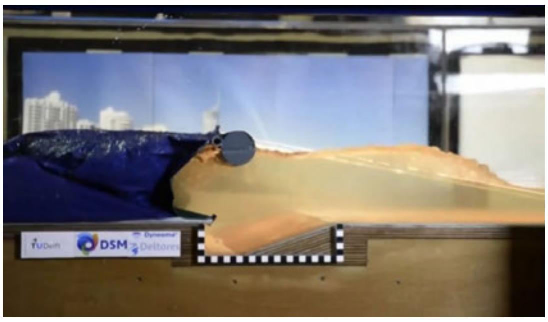

(b) Scale tests performed at Deltaras, source: DeltaresFilm [13]

Figure I.6: Dyneema Tsunami Catcher

Twin Wing Tsunami Barrier by Van den Noort Innovations B.V.
A tsunami is characterized by retreating water first, this is the so called negative tsunami. When the tsunami will propagate in the coastal direction it can be called a positive tsunami. The Twin-Wing Tsunami Barrier has been developed in order to disrupt and neutraliseboth negative and positive tsunami

1. In its resting position, the barrier wings are positioned horizontally on the sea bed, ready to swing up like a wall from their piled foundations as soon as the coastal waters retreat. This gives the possibility for ships and wind waves to pass the barrier.

2. On either side of the foundation, the barrier wing is instantly pushed up into a vertical position once a strong upcoming onshore or offshore directed water stream starts to emerge. If a negative tsunami wave strikes, the barrier wing on the shore side is swung into its vertical position and it closes off the shore water that would feed the tsunami.

3. During the positive tsunami impact, the wave will be reflected back. However, due to the huge amount of water, there could still be a certain amount of overtopping. A lot of the wave energy will be dissipated bt this process. Through their hinges, the barrier wings can swing back and forth from their horizontal positions into a vertical position, picking up the impact of secondary waves as well [48]. In figure I.7 the mechanism of the Twin Wing barrier is explained.

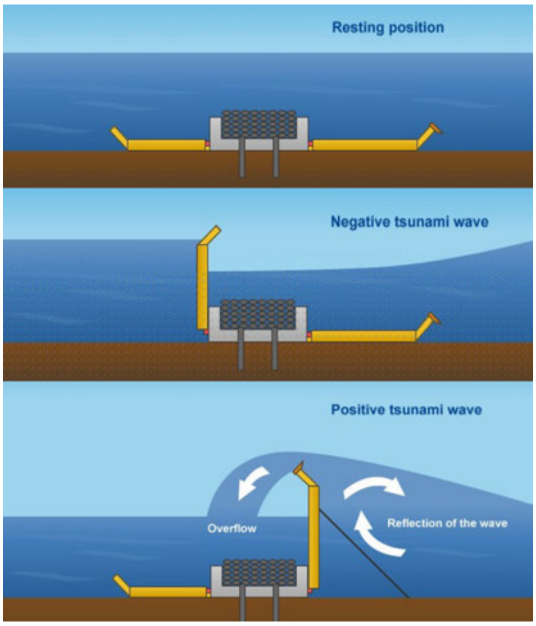

Figure I.7: Concept of the Twin Wing Tsunami Barrier, source:Van den Noort Innovations B.V. [48]

J

Selection of mitigation measures

In the project scope the focus is mainly on hard mitigation measures. In section J.1 the known mitigation measures from (SATREPS [39]) are discussed. For different reasons, a selection is made out of this lists and described in section J.2.

J.1. Possible mitigation measures

- **Coastal structures**
  - Coastal levees: Dike or revetment with the function of preventing overtopping waves of immersion of hinterlands. Relative expensive measure and often ground improvement needed.
  - Breakwaters: Securing calmness inside harbour against ocean waves. Rarely used for tsunamis. Expensive measure.
  - Floodgates: Used to restrain inundation when still able to drain inside water. Can restrain wave run up. Expensive measure and risk on not functioning whithout tsunami warning or earthquake damage.

- **Secondary barriers**
  - Elevated road: Used as restraint for tsunami inundation. Incorporated in transportation planning.

- **Tsunami control forest**
  - Coastal prevention forest: Effect on mitigation on water current strength and blocking of floating objects (proved for inundation of 3 m or less). When inundation is higher lodging or grubbing of trees might occur and driftwoods might cause secondary damage. The costs of this measure are relatively low but it takes time to fulfil an energy dissipation function (trees need time to grow).
  - Roadside trees and premises forest: Can capture floating objects (debris) to control secondary damage.

- **Canals**
  - Artificial channel for water transportation. Mitigation of water current strength due to energy loss in hydraulic jump. Could lead to magnifying tsunami inundation.

- **Evacuation facilities**
  - Evacuation buildings or towers: Shelter for areas where tsunamis arrive quickly or plain areas where there is less evacuation time.
  - Embankments: Plateau of hill, used for temporary evacuation. Can easily be integrated in a natural environment
  - Evacuation decks: Comparatively wide bridge

- **Town planning**
  - Relocation to plateaus: relocation of community. Community consensus is a difficult issue. Land-use restriction of empty area needed to prevent future use.
  - Land-use regulation: Designating high risk areas with land-use restrictions.
  - Miyagi Model (Multiple defense): Multilayereddefense facilities.
  - Warning Areas: Additional safety of buildings is het zone with higher risk.

- **Other**
  - Evacuation drills and exercises (Current evacuation plan for Coquimbo can be found in Q)
  - Public awareness
  - Warning systems
  - Evacuation information

In Chile hard measures can have multiple functions. It can decrease the direct damage, it can be multi-functional and facilitate the social and/or economic recovery of the affected areas, or it can serve as a physical reminder to reinforce tsunami awareness. These different functions can be separated in soft and hard measures, see figure J.1.

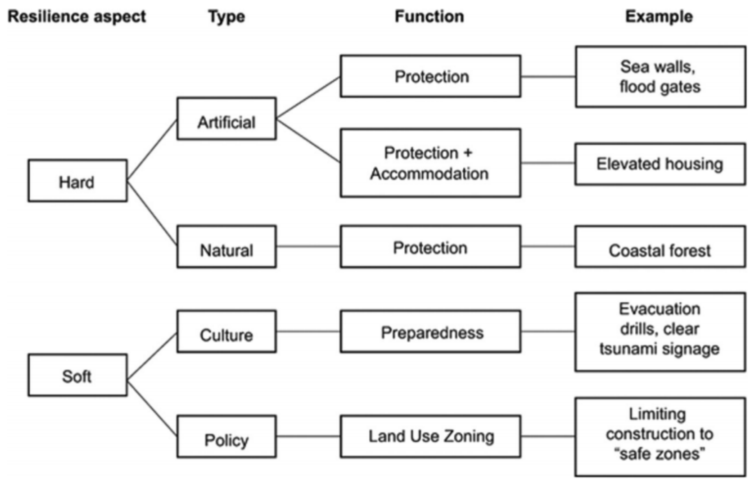

Figure J.1: Function of different migitation measures, source: Khew et al. [27]

A measure like a very high retaining wall, which is used in Japan, is not considered as a good solution in Chile. The building costs of such a wall are high and the population find such a barrier between them and the sea very unwanted Khew et al. [27]. A more integrated solution in the environment is likely to gain more public support.

J.2. Selected measures

Below the different options that are possible for the alternatives in part I are visualised and their most important failure mechanisms are given.

J.2.1. Concrete boulevard

When the road is heightened the structure can be given different shapes. One of the possible options is to create a multifunctional boulevard. In figure J.2 an impression of such a boulevard is given. Of this kind of construction the overall stability and failure due to scouring of the foundation are the most important failure mechanisms.

Figure J.2: Impression of multifunctional boulevard, photo made by: Reinier Daals

J.2.2. Wall

In the case that the protection is located at the end of the wetlands a wall as a protection is an option. Because it is not directly at the seaside the visual hindrance will be less. This is the case in alternatives III and IV. An example of such a wall can be seen in figure J.3. The wall is schematized as a straight and solid wall. Made of concrete and possibly with additional reinforcement. The most important failure mechanisms are falling over and structural damage to the wall itself.

Figure J.3: Example of a concrete wall, source: Photorator.com [38]

J.2.3. Dam of normal ground

A normal dam made of soil possessing a natural slope can be used in alternatives I to IV. It can be applied with and without the road on top of it. An example of such a dam can be seen in figure J.4. Because of the high flow velocities that can occur during a tsunami it might be necessary to apply a protection to avoid failure due to scour. Also failure of the soil stability is probable to occur.

J.2.4. Dam of reinforced ground

This measure is in exterior similar to the previous option. However due to the extra strength that is given through the mats that are added inside the ground. The dam has a better resistance against the high flow velocities and thus can keep its natural appearance. An impression of the functioning of this construction is given in figure J.5. Failure mechanisms that are to be taken into account are the overall stability of the dam and failure of the geogrids of the reinforcement.

Figure J.4: Example a dam made out of ground, source: [51]

Figure J.5: Example a dam made with reinforced ground, source: [45]

J.2.5. Dunes

In alternative V the coastal protection will consist of dunes. This to give the area a fully natural character. In figure J.6 an example of such dunes is given. The most important failure mechanism of the dunes is scour. This can occur due to scour at the toe of the dune or due to overtopping.

Figure J.6: Example of dunes, source: [53]

K

Calculations mitigation measures

This appendix gives the specific values and calculations of the tsunami forces and failure mechanisms that work on the different proposed mitigation measures.

K.1. Tsunami loading

The formulas stated in Federal Emergency Management Agency [17, ch.6] are valid for vertical onshore evacuation buildings. These approximations for the load can also be used for the hard mitigation structures, since the structures are designed as onshore retaining structures. The tsunami retaining structure is in normal situation not exposed to seawater and can therefore be excluded from forces such as tides, wind waves, wind set-up and ice loads.

To understand the derivation of the loads used, understanding of a tsunami wave is necessary. Despite the name "wave" a tsunami impact can not be seen as a big progressive wind wave. Due to the shape of the continental edge of Chile, it is highly probable that tsunami waves break offshore or at the shoreline. Therefore, calculations for a breaking wave on a structure does not have to be considered.

The shape of the tsunami wave can be considered as a bore. The front of the tsunami wave is turbulent. After this there is an abrupt increase in water depth which gives a high impact on the structure. This impact can be seen as a plunging-type of wave. After this there is a longer period of flow with a peak in wave speed and a peak in flow depth [35]. Properties that are to be obtained in order to calculate the tsunami force are wave speed, wave direction and flow depth. These properties will be determined by the numerical simulation.

The forces that are relevant to take into account in the calculations are:

- Weight
- Hydrostatic forces
- Buoyant forces
- Hydrodynamic forces
- Impulsive forces
- Debris impact forces

All of these forces are dependent on the height of $\left(hu^2\right)_{max}$. This can be determined by using the simulation results or with a formula of the FEMA. The calculation of this term is given in K.1.

K.1.1. Assumptions

In section 6.5.1 of Federal Emergency Management Agency [17, p.69] 3 main assumptions are made. Summarised they entail the following:

- As the water of a tsunami doesn't only consist of fresh water, but also contains some sediment the fluid density should be taken as ρ_s = 1200 kg/m^3.
- The design run-up elevation (R) should be taken as 1,3*R*, where R* is the predicted maximum run-up elevation. This due to uncertainty in numerical simulation and variability in local run-up heights.
- Equation 6-6, Equation 6-9, and Figure 6-7 contain approximations for design parameters, such as flow velocity and depth. Results obtained using numerical simulations should not be less than 80% of these approximations.

These assumptions are incorporated in the application of the formulas presented by Federal Emergency Management Agency [17].

K.1.2. Calculation of $(hu^2)_{max}$

For the tsunami forces the value of $(hu^2)_{max}$ is needed. This value can be taken from Equation 6-6 from Federal Emergency Management Agency [17, p. 73, ch.6] or can be obtained using data from a numerical simulation. As a numerical simulation has been done this data can be used. During the simulation the flow height and flow velocities are measured at two locations on the beach, see figure 4.1. The values extracted from this simulation are displayed in table K.1.

Parameter	Beach 1	Beach 2
Run up height (R*)	6,55 m	6,17 m
Ground elevation	-1,01 m	-0,19 m
Maximum flow velocity	4,24 m/s	2,15 m/s
Minimum flow velocity	-7,95 m/s	-9,66 m/s

Table K.1: Values extracted from NEOWAVE simulation of scenario1

Location Beach 1

The scenario for which the coastal protection must be designed results on the first location in a water height and flow velocity over time as shown in figure K.1.

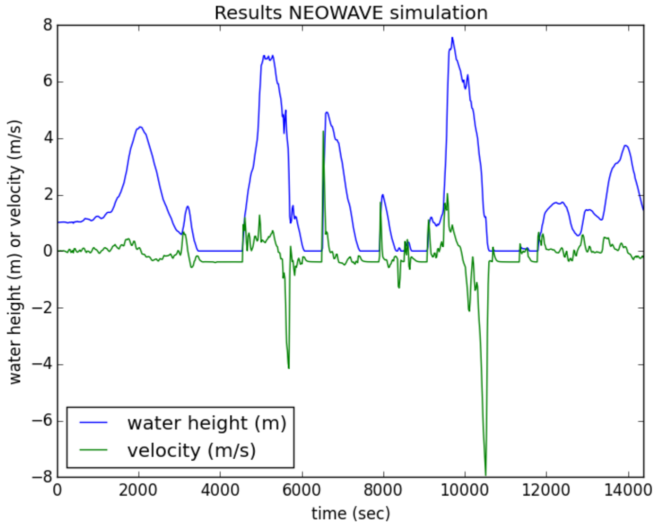

Figure K.1: Plot results water height and flow velocity

The green line shows a numerical error as the flow velocity should be zero when the water height remains the same. However, this does not have impact on the computation of $(hu^2)_{max}$ as this value will probably occur in one of the peaks.

Using this data the value of $(hu^2)_{max}$ can be plotted over time as well. This is shown in figure K.4. The maximum value has been determined using a python script and has determined to be $(hu^2)_{max} = 76,2606223959\ m^3/s^2$.

The obtained value from the numerical simulation shouldn't be less than 80% of the value obtained using Equation 6-6. Equation 6-6 is given by:

$$(hu^2)_{max} = gR^2\left(0,125 - 0,235\frac{z}{R} + 0,11\left(\frac{z}{R}\right)^2\right) \tag{K.1}$$

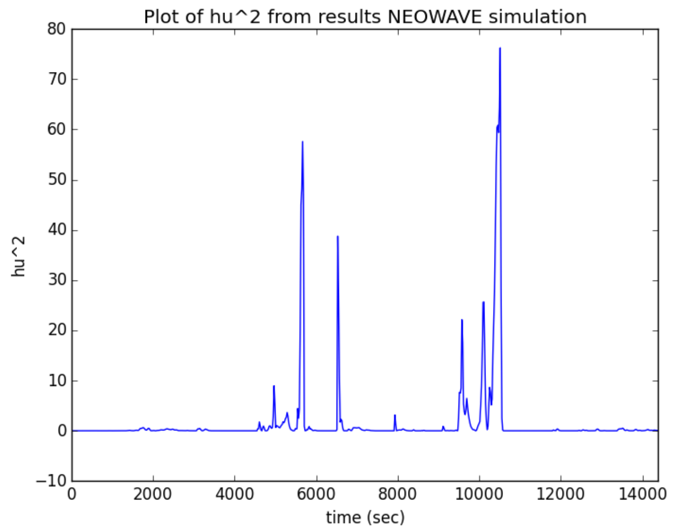

Figure K.2: Plot of $\left(hu^2\right)_{max}$ over time

Using the values of z and R^* from table K.1 the result is:

$$
\begin{aligned}
R &= 1,3 * R^* = 6,55\ m \\
(hu^2)_{max} &= 9,81 * 6,55^2 \left(0,125 - 0,235 \frac{-1,01}{6,55} + 0.11 \left(\frac{-1,01}{6,55}\right)^2\right) \\
&= 109,85\ m^3/s^2
\end{aligned} \tag{K.2}
$$

80% of this value is $0,80 * 109,85 = 87,88\ m^3/s^2$. The value obtained using numerical simulation is slightly too low. In order to meet the criteria of the Federal Emergency Management Agency [17] the value of $\left(hu^2\right)_{max} = 76,2606223959\ m^3/s^2$ needs to be adjusted up to $\left(hu^2\right)_{max} = 87,88\ m^3/s^2$.

Location Beach 2

The scenario for which the coastal protection must be designed results on the second location in a water height and flow velocity over time as shown in figure K.3.

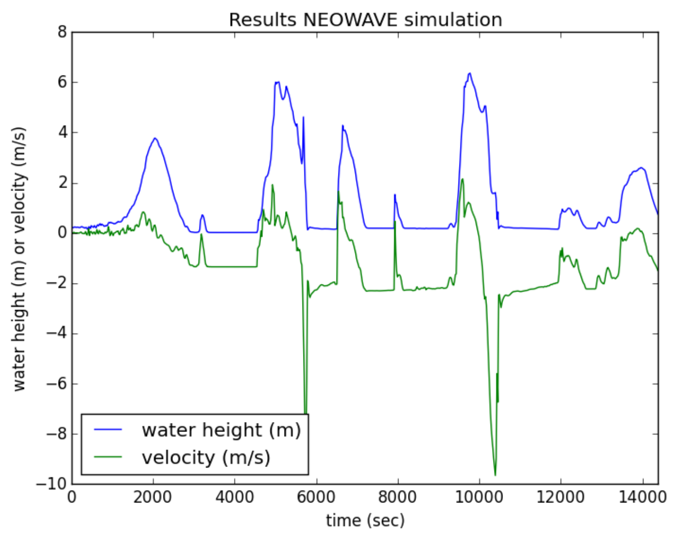

Figure K.3: Plot results water height and flow velocity

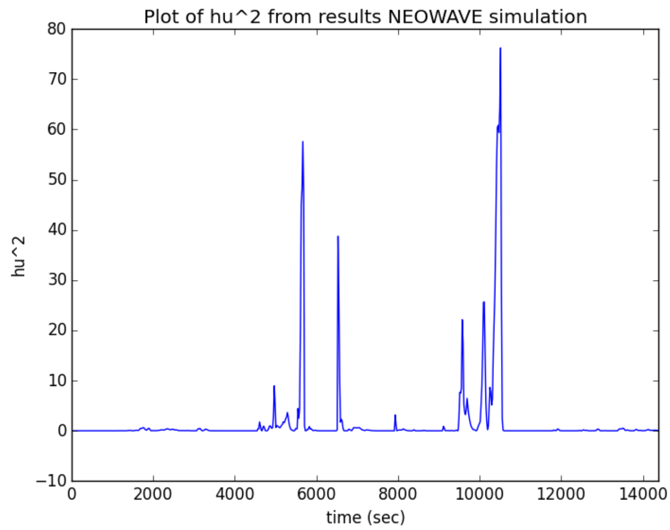

Figure K.4: Plot of $(hu^2)_{max}$ over time

Using this data the value of $(hu^2)_{max}$ can be plotted over time as well. This is shown in figure K.4. The maximum value has been determined using a python script and has determined to be $(hu^2)_{max} = 149,864349383\ m^3/s^2$.

The obtained value from the numerical simulation shouldn't be less than 80% of the value obtained using Equation 6-6. Equation 6-6 is given by:

$$(hu^2)_{max} = gR^2\left(0,125 - 0,235\frac{z}{R} + 0,11\left(\frac{z}{R}\right)^2\right) \tag{K.3}$$

Using the values of z and R^* from table K.1 the result is:

$$\begin{aligned} R &= 1,3 * R^* = 6,17\ m \\ (hu^2)_{max} &= 9,81 * 6,17^2\left(0,125 - 0,235\frac{-0,19}{6,17} + 0.11\left(\frac{-0,19}{6,17}\right)^2\right) \\ &= 82,48\ m^3/s^2 \end{aligned} \tag{K.4}$$

In this case the value that result from the simulation is far higher than that of the FEMA. However this value is the result of a high velocity away from the coast and thus will not be acting on the structure. When only the positive velocities are taken into account this results in a value of $(hu^2)_{max} = 20,4146\ m^3/s^2$. This is far lower than the value of the FEMA.

Because the value resulting from the FEMA of the first measure point is higher than that of the second. The value of the first measure point will be used. This is a value of $(hu^2)_{max} = 87,88\ m^3/s^2$.

K.1.3. Velocity of debris

A small container is assumed to be possible debris in the area of Coquimbo Bay. There is a harbour situated in the bay, but the containers that are used are not very large. Table 6-1 in Federal Emergency Management Agency [17] shows the mass and stiffness properties of common waterborne debris. A 20-ft container has a mass of 2200 kg and a stiffness of 1,5*10^9 N/m. We've chosen to apply the debris impact force as a line load with the length of the assumed container, which is 20 $ft = 6,096\ m$. The width of such a standard container is 8 ft = 2,44 m.

Large and heavy debris has a certain depth to flow, this is the draft. This draft influences the velocity with which the debris hits the structure. Federal Emergency Management Agency [17] proposes the following approximation of u_{max} to calculate the debris impact force:

$$\begin{aligned} d &= \frac{W}{\rho_s g A_f} \\ &= \frac{2200 * 9,81}{1200 * 9,81 * 2,44 * 6,096} \\ &= 0,123\ m \end{aligned} \tag{K.5}$$

Now using $\frac{z}{R} = 0,273$ and $\frac{d}{R} = 0,00890$ it can be read from figure 6-7 in Federal Emergency Management Agency [17, p.77] that $\upsilon = \frac{u_{max}}{\sqrt{2gR}} = 0,68$ approximately. This is shown in figure K.5.

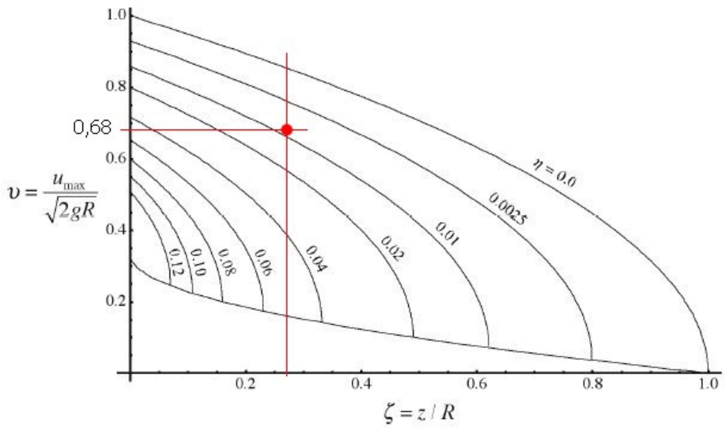

Figure K.5: Figure 6-7 from Federal Emergency Management Agency [17]

u_{max} is then calculated as follows:

$$\begin{aligned} u_{max} &= 0,68 * \sqrt{2 * 9,81 * 13,852} \\ &= 11,210\ m/s \\ 80\% * u_{max} &= 8,968\ m/s \end{aligned} \tag{K.6}$$

Again it turns out that the results from the numerical simulations with NEOWAVE don't provide a sufficient result. Federal Emergency Management Agency [17] states that a lowerbound value of 80% of u_{max} from figure 6-7 must be used in case of insufficient results from numerical simulations.

K.2. Failure mechanisms

In Molenaar and Voorendt [33] the different possible failure mechanisms are discussed. The further design of the barrier will be based on preventing the most relevant failure mechanisms. Failure mechanisms due to an earthquake load are of great importance as well. Therefore the soil failure mechanisms such as liquefaction are considered. The relevant failure mechanisms that are taken into account are:

- Horizontal stability
- Rotational stability
- Vertical stability
- Piping
- Vertical bearing capacity
- Horizontal bearing capacity
- Stability of slopes
- Liquefaction due to an earthquake
- Scour

For the first 7 failure mechanisms the procedure from Molenaar and Voorendt [33] is followed. The later 2 failure mechanisms are discussed in the next sections.

Figure K.6 gives an overview of different failure mechanisms of dikes (Jonkman et al. [25]). Even though the dam and dune elaborated in the various variants is not exposed to a constant high water level, still some of the failure mechanisms can possibly occur.

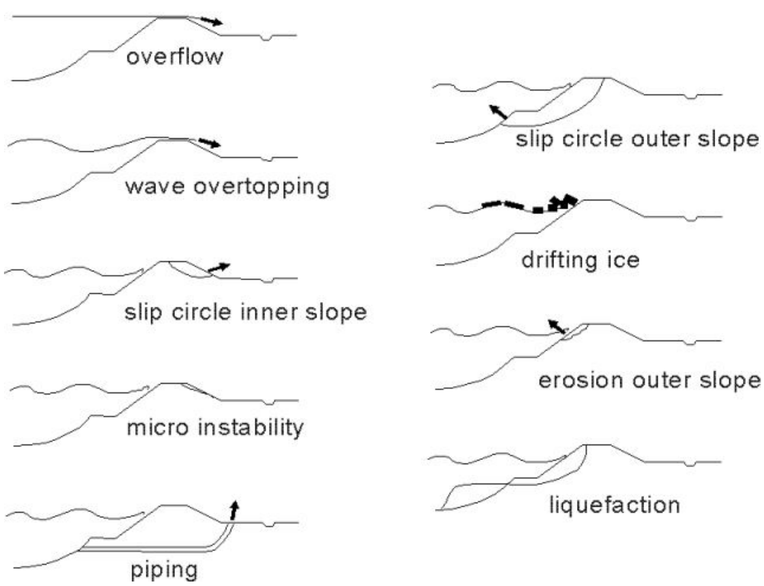

Figure K.6: Failure mechanisms of dikes, source: Jonkman et al. [25]

K.2.1. Liquefaction due to an earthquake

Liquefaction is a risk during earthquakes and can cause the structure to fail even before the tsunami arrives. It can also weaken the structure which makes it more vulnerable for failure during the tsunami.

The shaking of an earthquake is vibrating a water saturated soil or unconsolidated soil. As a result the soil shows properties of water of a liquid. The water pressure in a soil can carry the structure on their own which makes the soil very unstable. Figure gives an animation of the behavior of the soil particles during liquefaction. Solution to this problem is a creating a dense non-porous soil foundation. It is recommended to apply a densely packed soil as foundation of the structure and do more research into the risk of liquefaction.

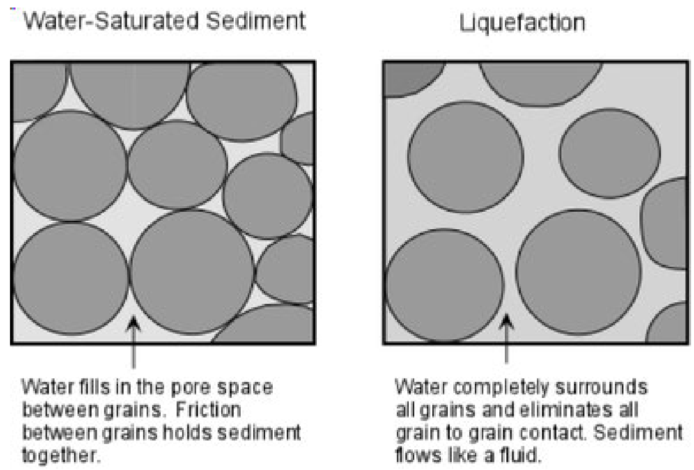

Figure K.7: Interaction between soil particle in case of liquefaction, source: E-pao.net [16]

K.2.2. Scour

Because of the high flow velocities that occur around structures during a tsunami scour is an important failure mechanism. The structure will become unstable when it's foundation is eroded away. It will not be possible to reduce the forces of the tsunami enough to prevent scouring. Therefore the soil must be strengthened by the application of scour protection. The possibilities of application are further discussed in section K.2.

It is not possible to prevent scour to occur but with the protection the scour can be kept away far enough from the structure to prevent failure. During the tsunami a scour hole will form at the end of the protection.

When the slope of this hole becomes too large the ground will slip. Therefore the length of the protection should be long enough to prevent this slip from reaching the structure. This is visualised in figure K.8.

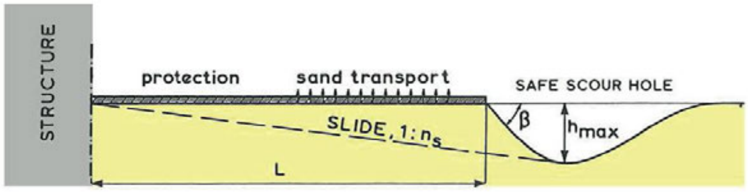

Figure K.8: Required length of a scour protection, source: Molenaar and Voorendt [33]

K.2.3. Scour protection

The diameter of the scour protection that is necessary depends on multiple factors. The most important factors are the slope and the local flow velocity. This local velocity depends on the amount of turbulence and the accelerations due to the velocity. It is calculated with the use of Chezy and the Shields parameter. The formula used for the calculation of the diameter is the following (Schiereck [40]):

$$d = \frac{K_v^2 \bar{u}_c^2}{K_s \psi_c \Delta C^2} \tag{K.7}$$

Where:

$$\begin{aligned} K_v &= \text{Velocity and turbulence facto, indication a load deviation from uniform flow} \\ \bar{u}_c &= \text{Depth average critical velocity in uniform flow} \\ K_s &= \text{Reduction parameter for slopes} \\ \psi_c &= \text{Shield threshold of motion parameter} \\ \Delta &= \text{Relative density} \\ C &= \text{Chezy coefficient} \\ &= 18 log\left(\frac{12R}{k_r}\right) \end{aligned}$$

After the determination of the necessary diameter. The grading of the rock can be determined withfigure K.9.

Filter layer

When scour protection is used it is necessary to apply a filter between the soil and the top layer of the protection. This top layer is the layer with the largest diameter and has to resist the largest flow velocity. The filter layer has smaller diameters and has to protect the soil from being flushed away underneath the rocks.

This filter layer can consist of one or multiple layers of loose rocks. Another option is the use of geotextile with one layer of smaller rocks to protect the geotextile from puncture. When the filter layer consists of only rock there are to options for design. One option is a geometrically closed filter. The design of this filter is based on the sieve curves of the material. Its stability is based on the fact that the grains can not move within the filter. In order to attain this it is often needed to use a lot of layers and the design is very conservative. The other option is a geometrically open filter. In this case it is physically possible for a grain to move through the filter but this is prevented by ensuring that the velocities to not reach the critical value. This critical value is the value of the velocity on which the grain will be lifted from its place (Schiereck [40]).

Because the tsunami is a rare event and for a short period it is acceptable when a little loss of material occurs. Therefore a geometrically closed is to conservative for this purpose. Also a geotextile is more expensive then a geometrically open filter. This because a geotextile is more difficult to install and rock has a good availability in Chile.

K.3. Concrete boulevard

The maple sheet of the calculation of the stability of the concrete boulevard:

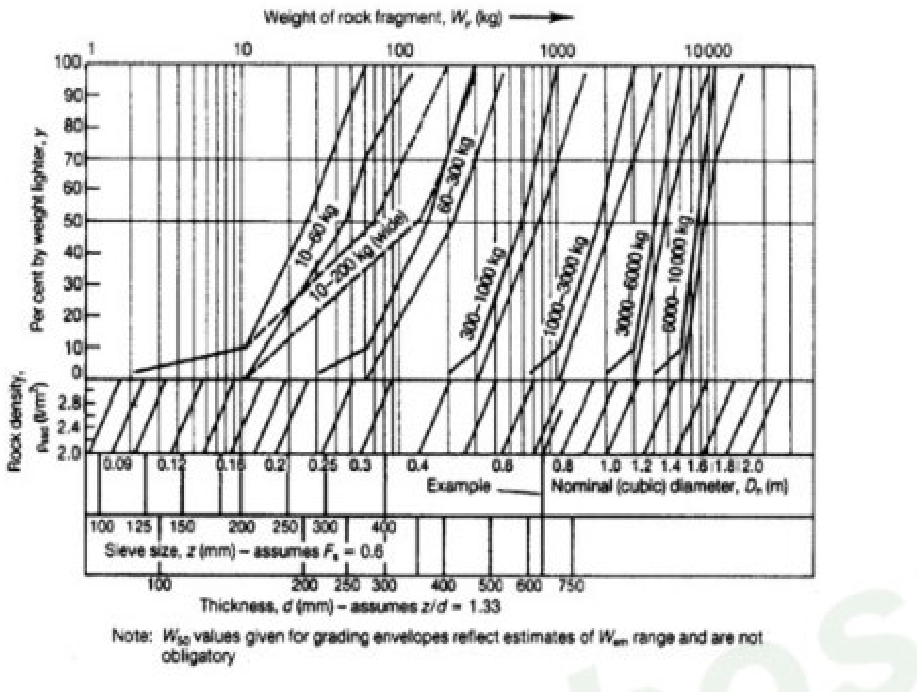

Figure K.9: Rock gradings, source: Schiereck [40]

Calculation stability concrete boulevard

> restart;

> $h := 5 : b := 17 : t\_r := 0.3 : t\_s := 0.3 :$

>

Horizontal stability: sum horizontal forces < fiction coefficient * sum vertical forces

> $\text{rho}[sw] := 1200 : g := 9.81 : \text{rho}[c] := 2400 : \text{rho}[s\_dry] := 1650 : \text{phi} := evalf\left(\frac{22.5}{180} \cdot \text{Pi}\right) : f := \min(\tan(\text{phi}), 0.5) :$

> $Fh\_hpressure := 0.5 \cdot \text{rho}[sw] \cdot g \cdot h^2;$

$$Fh\_hpressure := 1.47150000\ 10^5 \tag{1}$$

(no safety factor because force can not be bigger because of limiting height)

> $C[d] := 2.0 : hu[\max] := 87.88 : u[\max] := 8.968 : C[m] := 2.0 : K := 1.5 \cdot 10^9 : M := 2200 : B\_i := 200 :$

> $F\_d := \text{rho}[sw] \cdot C[d] \cdot hu[\max];$

$$F\_d := 2.10912000\ 10^5 \tag{2}$$

> $F\_s := 1.5 \cdot F\_d;$

$$F\_s := 3.163680000\ 10^5 \tag{3}$$

> $F\_i := \frac{C[m] \cdot u[\max] \cdot \text{sqrt}(K \cdot M)}{B\_i};$

$$F\_i := 1.629118102\ 10^5 \tag{4}$$

F_i is the only force that is inflicted in one point instead of over a line. That is why it is devided over a certain length.

> $F\_dm := 0.5 \cdot \text{rho}[sw] \cdot C[d] \cdot hu[\max];$

$$F\_dm := 1.054560000\ 10^5 \tag{5}$$

> $Fh\_tsunami1 := F\_s;$

$$Fh\_tsunami1 := 3.163680000\ 10^5 \tag{6}$$

> $Fh\_tsunami2 := F\_d + F\_i;$

$$Fh\_tsunami2 := 3.738238102\ 10^5 \tag{7}$$

(According to the FEMA no safety factors have to be taken into account)

> $Fh1 := Fh\_hpressure + Fh\_tsunami1;$

$$Fh1 := 4.635180000\ 10^5 \quad (8)$$

> $Fh2 := Fh\_hpressure + Fh\_tsunami2;$

$$Fh2 := 5.209738102\ 10^5 \quad (9)$$

> $Fv\_weight := 2 \cdot h \cdot t\_s \cdot \text{rho}[c] \cdot g + b \cdot t\_r \cdot \text{rho}[c] \cdot g + (b - 2 \cdot t\_s) \cdot (h - t\_r) \cdot \text{rho}[s\_dry] \cdot g;$

$$Fv\_weight := 1.438361820\ 10^6 \quad (10)$$

(beneficial so safety factor of 0.9)

> $Fv\_ben := Fv\_weight \cdot 0.9$

$$Fv\_ben := 1.294525638\ 10^6 \quad (11)$$

> $f \cdot Fv\_ben;$

$$5.362100763\ 10^5 \quad (12)$$

> **if** $Fh1 < f \cdot Fv\_ben$ **then** $print(Sufficient)$ **elif** $Fh1 \geq f \cdot Fv\_ben$ **then** $print(FAILURE)$ **end if**

Sufficient (13)

> **if** $Fh2 < f \cdot Fv\_ben$ **then** $print(Sufficient)$ **elif** $Fh2 \geq f \cdot Fv\_ben$ **then** $print(FAILURE)$ **end if**

Sufficient (14)

>

Rotational stability: sum of moments devided by sum of vertical forces =< 1/6 * b

> $Fv := Fv\_weight \cdot 0.9;$

$$Fv := 1.294525638\ 10^6 \quad (15)$$

> $M\_sum1 := Fh\_hpressure \cdot \left(\frac{1}{3}\right) \cdot h + F\_s \cdot 0.5 \cdot h;$

$$M\_sum1 := 1.036170000\ 10^6 \quad (16)$$

> $M\_sum2 := Fh\_hpressure \cdot \left(\frac{1}{3}\right) \cdot h + F\_d \cdot 0.5 \cdot h + F\_i \cdot h;$

$$M\_sum2 := 1.587089051\ 10^6 \quad (17)$$

> $\frac{M\_sum1}{Fv}; \frac{M\_sum2}{Fv};$

$$0.8004244718$$
$$1.226000478 \quad (18)$$

> $evalf\left(\left(\frac{1}{6}\right) \cdot b\right);$

$$2.833333333 \quad (19)$$

> **if** $\frac{M\_sum1}{Fv} \leq \left(\frac{1}{6}\right) \cdot b$ **then** $print(Sufficient)$ **elif** $\frac{M\_sum1}{Fv} > \left(\frac{1}{6}\right) \cdot b$ **then** $print(FAILURE)$
end if

Sufficient (20)

> **if** $\frac{M\_sum2}{Fv} \leq \left(\frac{1}{6}\right) \cdot b$ **then** $print(Sufficient)$ **elif** $\frac{M\_sum2}{Fv} > \left(\frac{1}{6}\right) \cdot b$ **then** $print(FAILURE)$
end if

Sufficient (21)

>

Vertical stability: Bearing capacity soil = sum vertical forces/ (b*l) +sum moments/(1/6*l*b^2)

Bearing capacity soil:

> $c := 5 \cdot 10^3 : \gamma := (18 - 10) \cdot 10^3 : q := 0 : Fh := \max(Fh1, Fh2) :$

> $Nq := evalf\left(\frac{1 + \sin(\text{phi})}{1 - \sin(\text{phi})} \exp(\text{Pi} \cdot \tan(\text{phi})) \right) : Nc := (Nq - 1)\cot(\text{phi}) : N\gamma := 2(Nq - 1)\tan(\text{phi}) :$

> $sc := 1 + 0.2 : s\gamma := 1 - 0.3 : sq := 1 + \sin(\text{phi}) :$

>

> $iq := \left(1 - \frac{0.7 \cdot Fh}{Fv + b \cdot c \cdot \cot(\text{phi})}\right)^3 : ic := \frac{(iq \cdot Nq - 1)}{Nq - 1} : i\gamma := \left(1 - \frac{Fh}{Fv + b \cdot c \cdot \cot(\text{phi})}\right)^3 :$

>

> $\text{sigma}[k, \max] := (c \cdot Nc \cdot sc \cdot ic + q \cdot Nq \cdot sq \cdot iq + 0.5 \cdot \gamma \cdot b \cdot N\gamma \cdot s\gamma \cdot i\gamma) :$

>

Maximal vertical effective soil stress:

> $\frac{Fh1}{b} + \frac{M\_sum1}{\left(\frac{1}{6}\right) \cdot b^2}; \frac{Fh2}{b} + \frac{M\_sum2}{\left(\frac{1}{6}\right) \cdot b^2};$

$$48777.94464$$

$$63595.46395 \tag{22}$$

> if $\text{sigma}[k, \max] \geq \frac{Fh1}{b} + \frac{M\_sum1}{\left(\frac{1}{6}\right) \cdot b^2}$ **then** *print*(*Sufficient*) **elif** $\text{sigma}[k, \max] < \frac{Fh1}{b} + \frac{M\_sum1}{\left(\frac{1}{6}\right) \cdot b^2}$ **then** *print*(*FAILURE*) **end if**

$$\textit{Sufficient} \tag{23}$$

> if $\text{sigma}[k, \max] \geq \frac{Fh2}{b} + \frac{M\_sum2}{\left(\frac{1}{6}\right) \cdot b^2}$ **then** *print*(*Sufficient*) **elif** $\text{sigma}[k, \max] < \frac{Fh2}{b} + \frac{M\_sum2}{\left(\frac{1}{6}\right) \cdot b^2}$ **then** *print*(*FAILURE*) **end if**

$$\textit{Sufficient} \tag{24}$$

K.4. Ground dam protection

The maple sheet of the necessary protection for the dam of soil:

Calculation stability ground dam

> $restart;$

> $h := 5 : b\_t := 14 : b\_b := 44 :$

>

Horizontal stability: sum horizontal forces < fiction coefficient * sum vertical forces

> $\text{rho}[sw] := 1200 : g := 9.81 : \text{rho}[c] := 2400 : \text{rho}[s\_dry] := 1650 : \text{phi} := evalf\left(\frac{22.5}{180} \cdot \text{Pi}\right) : f := 0.5 :$

> $Fh\_hpressure := 0.5 \cdot \text{rho}[sw] \cdot g \cdot h^2;$

$$Fh\_hpressure := 1.47150000\ 10^5 \quad \textbf{(1)}$$

(no safety factor because force can not be bigger because of limiting height)

> $C[d] := 2.0 : hu[\max] := 87.88 : u[\max] := 8.968 : C[m] := 2.0 : K := 1.5 \cdot 10^9 : M := 2200 : B\_i := 200 :$

> $F\_d := \text{rho}[sw] \cdot C[d] \cdot hu[\max];$

$$F\_d := 2.10912000\ 10^5 \quad \textbf{(2)}$$

> $F\_s := 1.5 \cdot F\_d;$

$$F\_s := 3.163680000\ 10^5 \quad \textbf{(3)}$$

> $F\_i := \frac{C[m] \cdot u[\max] \cdot \text{sqrt}(K \cdot M)}{B\_i};$

$$F\_i := 1.629118102\ 10^5 \quad \textbf{(4)}$$

F_i is the only force that is inflicted in one point instead of over a line. That is why it is devided over a certain length.

> $Fh\_tsunami1 := F\_s;$

$$Fh\_tsunami1 := 3.163680000\ 10^5 \quad \textbf{(5)}$$

> $Fh\_tsunami2 := F\_d + F\_i;$

$$Fh\_tsunami2 := 3.738238102\ 10^5 \quad \textbf{(6)}$$

(According to the FEMA no safety factors have to be taken into account)

> $Fh1 := Fh\_hpressure + Fh\_tsunami1;$

$$Fh1 := 4.635180000\ 10^5 \quad \textbf{(7)}$$

> $Fh2 := Fh\_hpressure + Fh\_tsunami2;$

$$Fh2 := 5.209738102\ 10^5 \quad \textbf{(8)}$$

> $Fv\_weight := \frac{(b\_b + b\_t) \cdot h}{2} \cdot \text{rho}[s\_dry] \cdot g;$

$$Fv\_weight := 2.347042500\ 10^6 \quad \textbf{(9)}$$

(beneficial so safety factor of 0.9)

> $Fv\_ben := Fv\_weight \cdot 0.9$

$$Fv\_ben := 2.112338250\ 10^6 \quad \textbf{(10)}$$

> $f \cdot Fv\_ben;$

$$1.056169125\ 10^6 \quad \textbf{(11)}$$

>

> **if** $Fh1 < f \cdot Fv\_ben$ **then** $print(Sufficient)$ **elif** $Fh1 \geq f \cdot Fv\_ben$ **then** $print(FAILURE)$ **end if**

Sufficient **(12)**

> **if** $Fh2 < f \cdot Fv\_ben$ **then** $print(Sufficient)$ **elif** $Fh2 \geq f \cdot Fv\_ben$ **then** $print(FAILURE)$ **end if**

Sufficient **(13)**

Calculation protection ground dam

> $restart;$

> $dn50 := 1.2$

$$dn50 := 1.2 \quad (1)$$

> $h := 5; b\_b := 35; b\_t := 5; \text{phi} := evalf\left(\frac{30}{180}\cdot\text{Pi}\right); \text{alpha}[s] := \arctan\left(\frac{h}{(b\_b - b\_t)\cdot 0.5}\right);$
> $\text{k\_r} := 2\cdot\text{dn50};$

$$h := 5$$
$$b\_b := 35$$
$$b\_t := 5$$
$$\phi := 0.5235987758$$
$$\alpha_s := 0.3217505544$$
$$k\_r := 2.4 \quad (2)$$

> $Kv := 1.3$

$$Kv := 1.3 \quad (3)$$

Fig 3.13 in BBSP shows that this factor has a maximum of 3

> $Ks := \frac{\sin(\text{phi} - \text{alpha}[s])}{\sin(\text{phi})};$

$$Ks := 0.4009607408 \quad (4)$$

> $C := 18\cdot\log10\left(\frac{12\cdot h}{k\_r}\right)$

$$C := 25.16292016 \quad (5)$$

> $u[c] := 4.24; \text{psi}[c] := 0.06; \text{Delta} := 1.650;$

$$u_c := 4.24$$
$$\psi_c := 0.06$$
$$\Delta := 1.650 \quad (6)$$

> $d := \frac{Kv^2\cdot u[c]^2}{Ks\cdot\text{psi}[c]\cdot\text{Delta}\cdot C^2};$

$$d := 1.208813474 \quad (7)$$

> $qs := \frac{13\cdot\text{psi}[c]^{2.5}\cdot 60\cdot 8}{\text{d}^3};$

$$qs := 3.115192144 \quad (8)$$

> $evalf\left(\frac{Kv^2}{Ks}\right);$

$$4.214876490 \quad (9)$$

K.5. L-wall

The maple sheet of the stability of the L-wall:

Calculation Stability "L-wall"

> *restart*;

> $h := 5 : b := 14 : t\_w := 0.5 : t\_f := 0.75 :$

>

Horizontal stability: sum horizontal forces < fiction coefficient * sum vertical forces

> $\text{rho}[sw] := 1200 : g := 9.81 : \text{rho}[c] := 2400 : \text{rho}[s\_dry] := 1650 : \text{phi} := evalf\left(\frac{22.5}{180} \cdot \text{Pi}\right) : f := \min(\tan(\text{phi}), 0.5) :$

> $Fh\_hpressure := 0.5 \cdot \text{rho}[sw] \cdot g \cdot h^2;$

$$Fh\_hpressure := 1.47150000\ 10^5 \quad (1)$$

(no safety factor because force can not be bigger because of limiting height)

> $C[d] := 2.0 : hu[\max] := 87.88 : u[\max] := 8.968 : C[m] := 2.0 : K := 1.5 \cdot 10^9 : M := 2200 : B\_i := 200 :$

> $F\_d := \text{rho}[sw] \cdot C[d] \cdot hu[\max];$

$$F\_d := 2.10912000\ 10^5 \quad (2)$$

> $F\_s := 1.5 \cdot F\_d;$

$$F\_s := 3.163680000\ 10^5 \quad (3)$$

> $F\_i := \frac{C[m] \cdot u[\max] \cdot \text{sqrt}(K \cdot M)}{B\_i};$

$$F\_i := 1.629118102\ 10^5 \quad (4)$$

F_i is the only force that is inflicted in one point instead of over a line. That is why it is devided over a certain length.

> $Fh\_tsunami1 := F\_s;$

$$Fh\_tsunami1 := 3.163680000\ 10^5 \quad (5)$$

> $Fh\_tsunami2 := F\_d + F\_i;$

$$Fh\_tsunami2 := 3.738238102\ 10^5 \quad (6)$$

(According to the FEMA no safety factors have to be taken into account)

> $Fh1 := Fh\_hpressure + Fh\_tsunami1;$

$$Fh1 := 4.635180000\ 10^5 \quad (7)$$

> $Fh2 := Fh\_hpressure + Fh\_tsunami2;$

$$Fh2 := 5.209738102\ 10^5 \quad (8)$$

> $Fv\_weight := h \cdot t\_w \cdot \text{rho}[c] \cdot g + b \cdot t\_f \cdot \text{rho}[c] \cdot g + (b - t\_w) \cdot h \cdot \text{rho}[s\_dry] \cdot g;$

$$Fv\_weight := 1.398660750\ 10^6 \quad (9)$$

(beneficial so safety factor of 0.9)

> $Fv\_ben := Fv\_weight \cdot 0.9$

$$Fv\_ben := 1.258794675\ 10^6 \quad (10)$$

> $f \cdot Fv\_ben;$

$$5.214098268\ 10^5 \quad (11)$$

> **if** $Fh1 < f \cdot Fv\_ben$ **then** *print*(*Sufficient*) **elif** $Fh1 \geq f \cdot Fv\_ben$ **then** *print*(*FAILURE*) **end if**

Sufficient (12)

> **if** $Fh2 < f \cdot Fv\_ben$ **then** *print*(*Sufficient*) **elif** $Fh2 \geq f \cdot Fv\_ben$ **then** *print*(*FAILURE*) **end if**

Sufficient (13)

Rotational stability: sum of moments devided by sum of vertical forces =< 1/6 * b

> $Fv := Fv\_weight \cdot 0.9;$

$$Fv := 1.258794675\ 10^{6} \tag{14}$$

> $a\_r := (\mathrm{rho}[c] \cdot h \cdot t\_w \cdot 0.5 \cdot t\_w + \mathrm{rho}[c] \cdot b \cdot t\_f \cdot 0.5 \cdot b + \mathrm{rho}[s\_dry] \cdot (h - t\_f) \cdot (b - t\_w) \cdot (0.5(b - t\_w) + t\_w)) / (\mathrm{rho}[c] \cdot h \cdot t\_w + \mathrm{rho}[c] \cdot b \cdot t\_f + \mathrm{rho}[s\_dry] \cdot (h - t\_f) \cdot (b - t\_w))$

$$a\_r := 6.866266945 \tag{15}$$

> $M\_sum1 := Fh\_hpressure \cdot \left(\frac{1}{3}\right) \cdot h + (b - t\_w) \cdot (h - t\_f) \cdot \mathrm{rho}[s\_dry] \cdot g \cdot ((0.5 \cdot (b - t\_w) + t\_w) - a\_r) + (b - t\_w) \cdot t\_f \cdot \mathrm{rho}[c] \cdot g \cdot ((0.5 \cdot (b - t\_w) + t\_w) - a\_r) - t\_w \cdot h \cdot \mathrm{rho}[c] \cdot g \cdot (a\_r - 0.5 \cdot t\_w) + F\_s \cdot 0.5 \cdot h;$

$$M\_sum1 := 1.094585021\ 10^{6} \tag{16}$$

> $M\_sum2 := Fh\_hpressure \cdot \left(\frac{1}{3}\right) \cdot h + (b - t\_w) \cdot (h - t\_f) \cdot \mathrm{rho}[s\_dry] \cdot g \cdot ((0.5 \cdot (b - t\_w) + t\_w) - a\_r) + (b - t\_w) \cdot t\_f \cdot \mathrm{rho}[c] \cdot g \cdot ((0.5 \cdot (b - t\_w) + t\_w) - a\_r) - t\_w \cdot h \cdot \mathrm{rho}[c] \cdot g \cdot (a\_r - 0.5 \cdot t\_w) + F\_d \cdot 0.5 \cdot h + F\_i \cdot h;$

$$M\_sum2 := 1.645504072\ 10^{6} \tag{17}$$

> $\frac{M\_sum1}{Fv}; \frac{M\_sum2}{Fv};$

$$0.8695500885$$
$$1.307206095 \tag{18}$$

> $evalf\left(\left(\frac{1}{6}\right) \cdot b\right);$

$$2.333333333 \tag{19}$$

> $\textbf{if}\ \mathrm{abs}\left(\frac{M\_sum1}{Fv}\right) \le \left(\frac{1}{6}\right) \cdot b\ \textbf{then}\ print(\mathit{Sufficient})\ \textbf{elif}\ \mathrm{abs}\left(\frac{M\_sum1}{Fv}\right) > \left(\frac{1}{6}\right) \cdot b\ \textbf{then}\ print(\mathit{FAILURE})\ \textbf{end if}$

$$\mathit{Sufficient} \tag{20}$$

> $\textbf{if}\ \mathrm{abs}\left(\frac{M\_sum2}{Fv}\right) \le \left(\frac{1}{6}\right) \cdot b\ \textbf{then}\ print(\mathit{Sufficient})\ \textbf{elif}\ \mathrm{abs}\left(\frac{M\_sum2}{Fv}\right) > \left(\frac{1}{6}\right) \cdot b\ \textbf{then}\ print(\mathit{FAILURE})\ \textbf{end if}$

$$\mathit{Sufficient} \tag{21}$$

Vertical stability: Bearing capacity soil = sum vertical forces/ (b*1) +sum moments/(1/6*1*b^2)

Bearing capacity soil:

$> c := 5 \cdot 10^3 : y := (18 - 10) \cdot 10^3 : q := 0 : Fh := \max(Fh1, Fh2) :$

$> Nq := evalf\left(\frac{1 + \sin(\phi)}{1 - \sin(\phi)} \exp(\text{Pi} \cdot \tan(\phi))\right) : Nc := (Nq - 1)\cot(\phi) : Ny := 2(Nq - 1)\tan(\phi) :$

$> sc := 1 + 0.2 : sy := 1 - 0.3 : sq := 1 + \sin(\phi) :$

>

$> iq := \left(1 - \frac{0.7 \cdot Fh}{Fv + b \cdot c \cdot \cot(\phi)}\right)^3 : ic := \frac{(iq \cdot Nq - 1)}{Nq - 1} : iy := \left(1 - \frac{Fh}{Fv + b \cdot c \cdot \cot(\phi)}\right)^3 :$

>

$> \text{sigma}[k, \max] := (c \cdot Nc \cdot sc \cdot ic + q \cdot Nq \cdot sq \cdot iq + 0.5 \cdot y \cdot b \cdot Ny \cdot sy \cdot iy);$

$$\sigma_{k,\max} := 94865.90044 \qquad \textbf{(22)}$$

>

Maximal vertical effective soil stress:

$> \frac{Fh1}{b} + \frac{M\_sum1}{\left(\frac{1}{6}\right) \cdot b^2}; \frac{Fh2}{b} + \frac{M\_sum2}{\left(\frac{1}{6}\right) \cdot b^2};$

$$66616.13329$$
$$87584.98864 \qquad \textbf{(23)}$$

$> \textbf{if } \text{sigma}[k, \max] \geq \frac{Fh1}{b} + \frac{M\_sum1}{\left(\frac{1}{6}\right) \cdot b^2} \textbf{ then } print(Sufficient) \textbf{ elif } \text{sigma}[k, \max] < \frac{Fh1}{b} + \frac{M\_sum1}{\left(\frac{1}{6}\right) \cdot b^2} \textbf{ then } print(FAILURE) \textbf{ end if}$

$$Sufficient \qquad \textbf{(24)}$$

$> \textbf{if } \text{sigma}[k, \max] \geq \frac{Fh2}{b} + \frac{M\_sum2}{\left(\frac{1}{6}\right) \cdot b^2} \textbf{ then } print(Sufficient) \textbf{ elif } \text{sigma}[k, \max] < \frac{Fh2}{b} + \frac{M\_sum2}{\left(\frac{1}{6}\right) \cdot b^2} \textbf{ then } print(FAILURE) \textbf{ end if}$

$$Sufficient \qquad \textbf{(25)}$$

K.6. Reinforced soil

The maple sheet of the horizontal stability of the dam of reinforced soil and the documents produced by the Tensar software. The first document is of the situation without a tsunami and the second of the situation after the tsunami has been.

Calculation stability reinforced soil

> restart;

> $h := 5 : b\_t := 14 : b\_b := 18 :$

>

Horizontal stability: sum horizontal forces < fiction coefficient * sum vertical forces

> $\text{rho}[sw] := 1200 : g := 9.81 : \text{rho}[c] := 2400 : \text{rho}[s\_dry] := 1650 : \text{phi} := evalf\left(\frac{22.5}{180} \cdot \text{Pi}\right) : f := 0.5 :$

> $Fh\_hpressure := 0.5 \cdot \text{rho}[sw] \cdot g \cdot h^2;$

$$Fh\_hpressure := 1.47150000\ 10^5 \quad (1)$$

(no safety factor because force can not be bigger because of limiting height)

> $C[d] := 2.0 : hu[\max] := 87.88 : u[\max] := 8.968 : C[m] := 2.0 : K := 1.5 \cdot 10^9 : M := 2200 : B\_i := 200 :$

> $F\_d := \text{rho}[sw] \cdot C[d] \cdot hu[\max];$

$$F\_d := 2.10912000\ 10^5 \quad (2)$$

> $F\_s := 1.5 \cdot F\_d;$

$$F\_s := 3.163680000\ 10^5 \quad (3)$$

> $F\_i := \frac{C[m] \cdot u[\max] \cdot \text{sqrt}(K \cdot M)}{B\_i};$

$$F\_i := 1.629118102\ 10^5 \quad (4)$$

F_i is the only force that is inflicted in one point instead of over a line. That is why it is devided over a certain length.

> $Fh\_tsunami1 := F\_s;$

$$Fh\_tsunami1 := 3.163680000\ 10^5 \quad (5)$$

> $Fh\_tsunami2 := F\_d + F\_i;$

$$Fh\_tsunami2 := 3.738238102\ 10^5 \quad (6)$$

(According to the FEMA no safety factors have to be taken into account)

> $Fh1 := Fh\_hpressure + Fh\_tsunami1;$

$$Fh1 := 4.635180000\ 10^5 \quad (7)$$

> $Fh2 := Fh\_hpressure + Fh\_tsunami2;$

$$Fh2 := 5.209738102\ 10^5 \quad (8)$$

> $Fv\_weight := \frac{(b\_b + b\_t) \cdot h}{2} \cdot \text{rho}[s\_dry] \cdot g;$

$$Fv\_weight := 1.294920000\ 10^6 \quad (9)$$

(beneficial so safety factor of 0.9)

> $Fv\_ben := Fv\_weight \cdot 0.9$

$$Fv\_ben := 1.165428000\ 10^6 \quad (10)$$

> $f \cdot Fv\_ben;$

$$5.827140000\ 10^5 \quad (11)$$

>

> **if** $Fh1 < f \cdot Fv\_ben$ **then** *print*(Sufficient) **elif** $Fh1 \geq f \cdot Fv\_ben$ **then** *print*(FAILURE) **end if**

Sufficient (12)

> **if** $Fh2 < f \cdot Fv\_ben$ **then** *print*(Sufficient) **elif** $Fh2 \geq f \cdot Fv\_ben$ **then** *print*(FAILURE) **end if**

Sufficient (13)

Calculations in accordance with:Bishop's method of slices (static loading)

Client:	
Project:	

Tensar
Structural Systems

Tensar *tech*
Wraparound Facing System

IMPORTANT NOTES

This document contains an Application Suggestion which has been prepared byTensar International Limited on a confidential basis, to enable the application of **Tensar** geogrids to be evaluated. The Application Suggestion is merely illustrative and is not a detailed design.It is specific to the unique characteristics of the **Tensar** geogrids which are referenced within the calculations.

The information provided in this document is supplied without charge. It does not form part of any contract orintended contract with the recipient. No liability in negligence will arise from the construction of any projectbased on such information or material. Final determination of the suitability of any information or material forthe use contemplated and the manner of use is the sole responsibility of the user and its professional advisors,who must assume all risk and liability in connection therewith. Tensar International Limited assumes no responsibilityto the recipient or any third party for the whole or any part of the content of this document.

Method of analysis	The calculation method used to create this Application Suggestionis the simplified method of slices using a circular slip surface following the method given by Bishop (Géotechnique, Vol 5, No 1, 1955) modified to take into account the stabilising effect of layers of geogrid reinforcement

Reference		**Date**	22 Oct 2016	**Page**	1 of 5

Tensar International BV

Tel:**+31 73 6241916**
Fax:**+31 73 6240652**
E-mail:**info@tensar.nl**
www.tensar.nl

Helftheuvelweg 11
5222 AV 's-Hertogenbosch
Netherlands

Input data and Section **Project:**

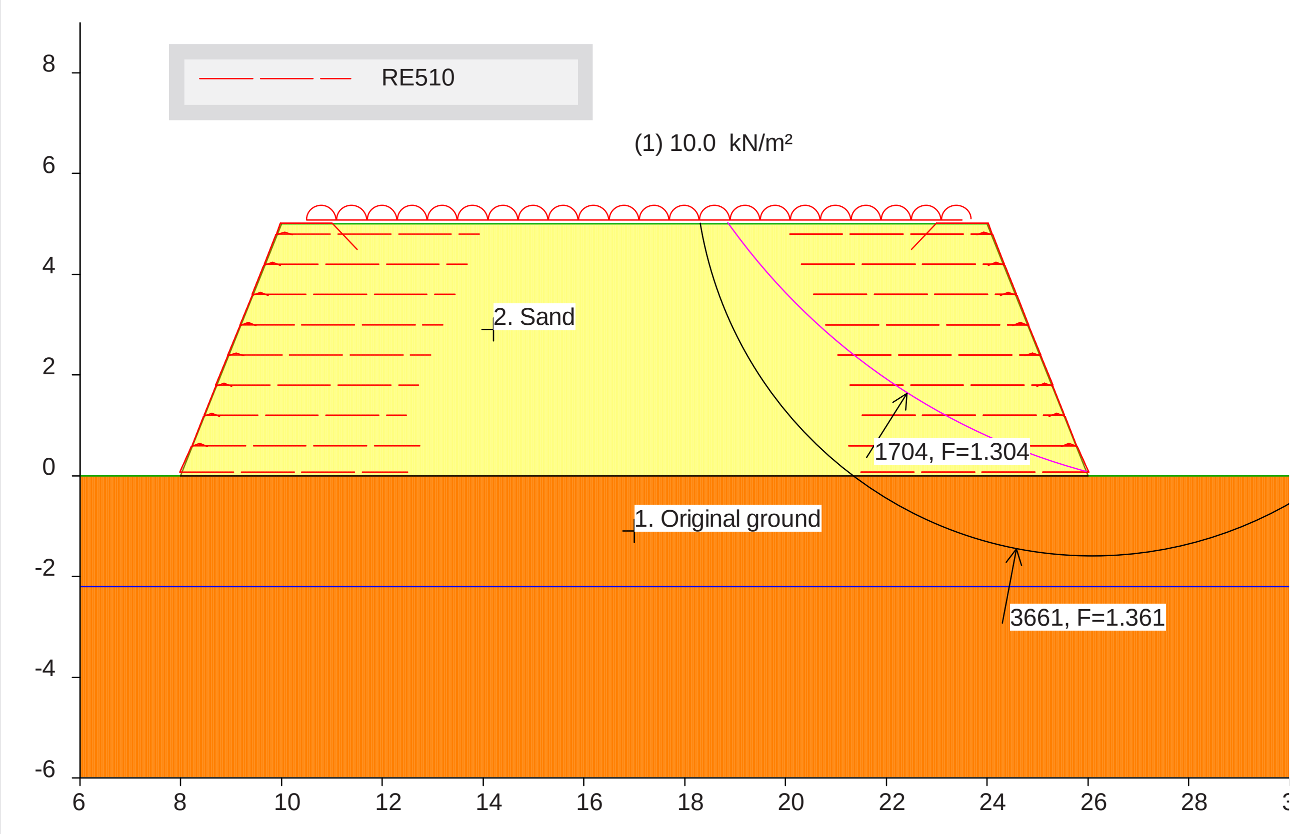

Tensar Structural Systems Tensar *tech* **Wraparound Facing System**

Static loading case

All dimensions in metres Scale 1:150

Soil properties

Soil zone	Drained/ undrained	c (kN/m²)	ϕ (°)	γbulk (kN/m³)
1, Original ground	Drained	5.0	22.5 (cv)	18.0
2, Sand	Drained	0.0	30.0 (cv)	20.0

Surcharges

Load	Load acts from x (m)	To x (m)	Load (kN/m²)	Live/Dead
1	10.500	23.500	10.00	Live

x values are measured from X=0

Tensar software output
TensarSlope Version1.14

Calculations in accordance with:Bishop's method of slices (static loading)

Client:	
Project:	

Tensar
Structural Systems

Tensar *tech*
Wraparound Facing System

IMPORTANT NOTES

Method of analysis	The calculation method used to create this Application Suggestionis the simplified method of slices using a circular slip surface following the method given by Bishop (Géotechnique, Vol 5, No 1, 1955) modified to take into account the stabilising effect of layers of geogrid reinforcement

Reference		**Date**	22 Oct 2016	**Page**	

Tensar International BV
Helftheuvelweg 11
5222 AV 's-Hertogenbosch
Netherlands

Tel:**+31 73 6241916**
Fax:**+31 73 6240652**
E-mail:**info@tensar.nl**
www.tensar.nl

Q 05288
ISO 9001:2008

EMS 86463
ISO 14001:2004

Input data and Section **Project:**

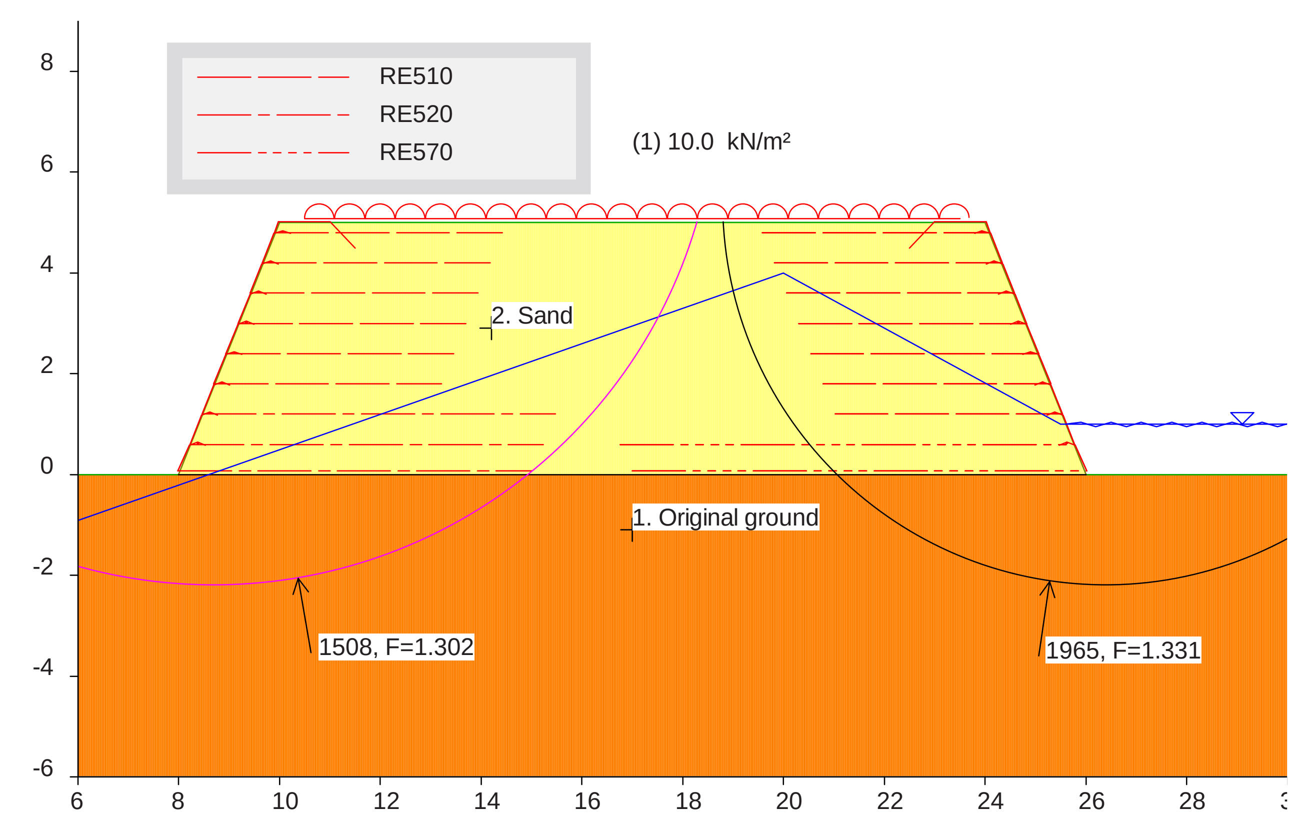

Tensar Structural Systems Tensar *tech* **Wraparound Facing System**

Static loading case

All dimensions in metres Scale 1:150

Soil properties

Soil zone	Drained/ undrained	c (kN/m²)	ϕ (°)	γ_{bulk} (kN/m³)
1, Original ground	Drained	5.0	22.5 (cv)	18.0
2, Sand	Drained	0.0	30.0 (cv)	20.0

Surcharges

Load	Load acts from x (m)	To x (m)	Load (kN/m²)	Live/Dead
1	10.500	23.500	10.00	Live

x values are measured from X=0

L

Initial process and calculations Altamar building

Initially unwillingness of the local authorities of Coquimbo forced us to generate a model of the Altamar building without any structural information. For educational purposes our initial assumptions, model and process is presented in this appendix. Fortunately the official structural drawings have been provided to us eventually, therefore most of the information in this appendix is not used for our final model and results.

L.1. Floorplan

The Altamar highrise is a residential building counting 26 stories. Due to initial lack of cooperation of the local authorities it turned out to be impossible to obtain the structural documents of the building in time. A solution has been found in generating a floor plan out of the single floor plans presented on the website of the housing agency [8]. Combining these architectural floor plans with the observations made during the visit at the building results in the complete floor plan presented in figure L.1. Each floor consists of five different apartments, a corridor, a lift shaft with 2 elevators and 2 stairs. The outer red line in the floor plan represents the edge of the facade.

Figure L.1: Estimated floor plan Altamar

L.2. Supporting structure

The supporting structure had to be based completely on assumptions. This is described in the next section.

L.2.1. Model assumptions

In Chile residential buildings are mostly supported by shear walls, whereas office buildings consist mostly out of columns. Figure L.2 from Lagos et al. [28, p.183] confirms this statement. In the Altamar building this is also the case.

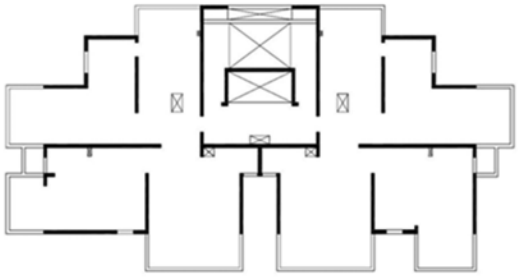

Figure L.2: Typical shear wall configuration for residential buildings. Source: Lagos et al. [28]

In the same article a rule of thumb for floor thicknesses of high-rise residential buildings is stated, namely 14 to 18 centimeters. Using pictures of our visit to the building and Dr.Ir. Claudio Oyarzo's experience it has initially been estimated that the thickness of the supporting shear walls is 25 cm for the lower 7 levels and 20 cm for the upper 19 levels.

The first 2 levels of the building do not have a residential purpose and therefore the configuration of these levels will probably differ from the configuration of the residential levels. Unfortunately there's no information available that could help determine the configuration of the lowest 2 levels. Therefore the position of the shear walls and beams will be extrapolated to these levels. Also, there's no continuous floor in between the first two levels, which makes them 1 very high level without the possibility of a diaphragm function of the floor.

The concrete quality is assumed to be H30, which is the same as C25/30 in terms of Eurocode 2. Both concrete qualities poses a characteristic cube compressive strength at 28 days of 30 N/mm^2 or 300 kg/cm^2. This is the most commonly applied concrete quality for highrise buildings like Altamar in Chile.

The reinforcement ratios in Chile range from 1 to 8 %. These high ratios can be explained by the fact that high ductility is needed to resist seismic loading, as earthquakes are common in Chile. To be conservative an assumption of 1% will be used in the model.

The locations of the structural components have been determined in compliance with Dr.Ir. Claudio Oyarzo, the result is presented in figure L.4. The applied initial dimensions of the structural elements can be found in table L.1.

Element	Floors	Dimensions
Floors		18 cm
Walls	1-7	25 cm
	8-26	20 cm
Beams	1-7	40x25 cm
	8-26	40x20 cm

Table L.1: Overview dimensional assumptions Altamar model

L.3. Model verification

The procedure of modeling and verifying the building in Etabs has been one of trial and error. The first assumed structural configuration, figure L.3, has been modeled and a modal analysis has been performed to obtain a response spectrum and a scale factor. The building has been modeled with its seismic weight instead of the normal weight, this is explained in appendix M.1.

L.3.1. Stiffness verification

For the verification of the stiffness of the model the period of the mode with the highest mass participation is used (T^*). In Chile buildings are designed with this period being in between N/23 - N/15, where N is the

Figure L.3: Initial structural plan Altamar

number of stories. Regarding the number of stories in the Altamar building that range is $1.13 \leq T^* \leq 1,73$.

After the first run of the modal analysis T* appears to be 0,568 seconds in x-direction and 0,891 sec in y-direction. Conclusion is that the periods are far below the range which means the building is too stiff. It could be the case that Altamar actually is designed too stiff but according to Oyarzo this is highly unlikely. ‘Building this stiff is too expensive for Chilean standards’. The building is most likely modeled too stiff because of the high number of assumptions on dimensions and locations of structural elements. It has been decided to take a critical look at the elements, apply changes, and work up to more reasonable periods. The steps and results of this method are presented in table L.2.

Alteration	T*	
	x-direction [s]	y-direction [s]
Initial model	0,568	0,891
All walls t=200 mm	0,603	0,953
Delete several walls in x-direction	0,749	0,943
Subdivide long walls, alter lengths	1,06	0,946
Delete several walls in y-direction	1,118	1,002

Table L.2: Overview alterations to reduce stiffness of building

After the modifications the structural plan became as presented in figure L.4. The periods of the modes with the biggest mass participation are still low, but they have reached acceptable values, as can be seen in the last row of table L.2. Reducing the stiffness of the building even more would cause many other problems. The structural elements are modeled as presented in table L.3 in paragraph L.2. The values for the most important periods indicate that the model now is a more realistic interpretation of the actual building.

Element	Dimensions [mm]
Beams	400 x 200
Walls	200
Floors	180

Table L.3: Overview final dimensional assumptions structural elements

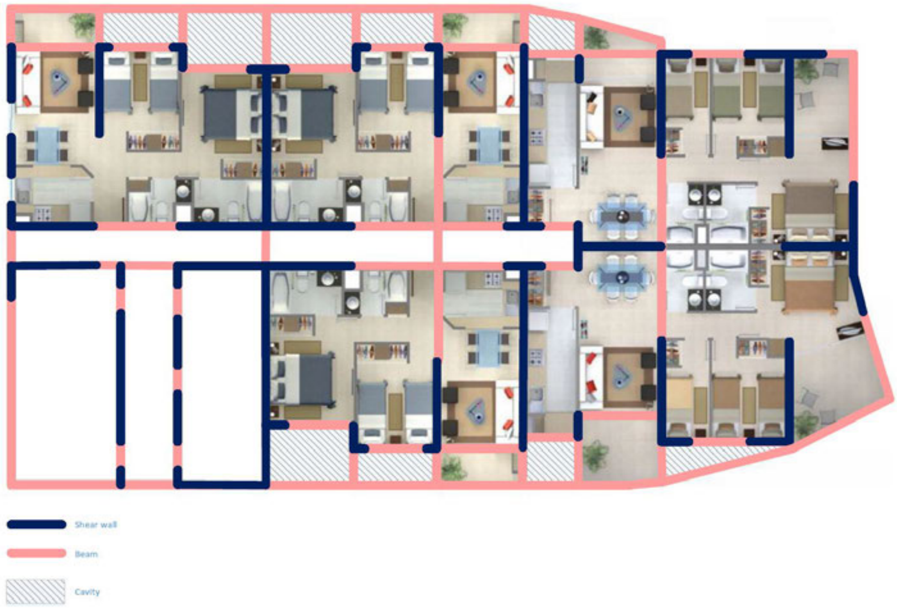

Figure L.4: Final configuration of structural elements

L.4. Final model

An impression of the final model can be found in figure L.5.

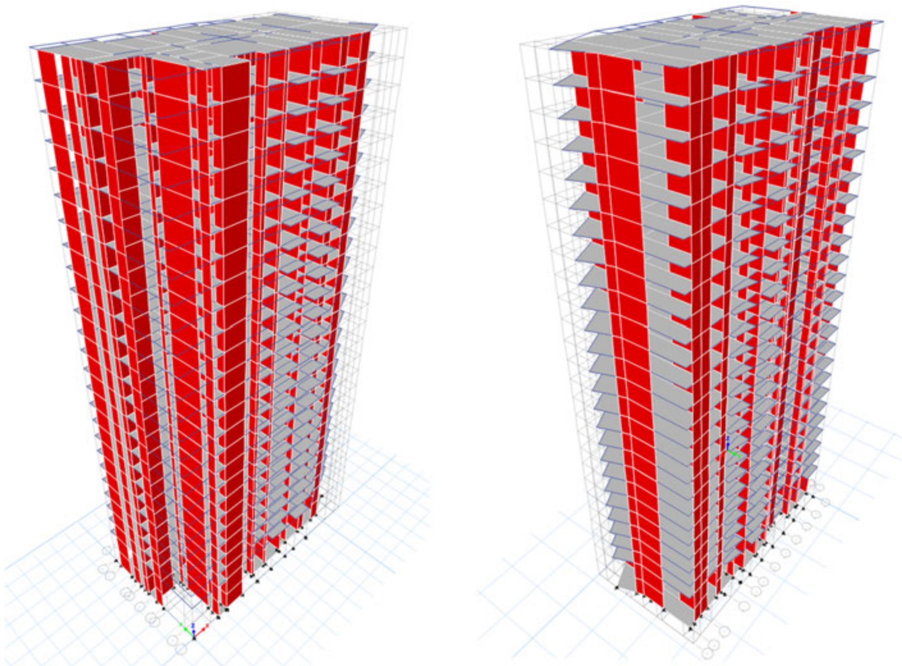

Figure L.5: Two elevations final Altamar model

L.5. Response Spectrum Analysis

The design response spectrum of the Altamar building can be determined using the following parameters and formulas.

L.5.1. Parameters

The project area is situated in seismic zone 3, for which $A_0 = 0,4g$ applies according to table 6.2 in Instituto Nacional de Normalizacion [23] . A conservative assumption of soil category D was made. Table 6.3 in Instituto Nacional de Normalizacion [23] gives the values for parameters S, T_0, T', n and p.

According to table 4.3 in Instituto Nacional de Normalizacion [23] the Altamar building falls in category II at the moment, as it is only a ordinary residential building, not used as an official evacuation refuge. As the building is considered as an evacuation refuge the building would be in category III. Values of 1,0 and 1,2 for I (coeficiente de importancia) will both be evaluated in the analysis.

The building consists of shear walls of reinforced concrete. Table 5.1 in Instituto Nacional de Normalizacion [23] gives the corresponding reduction factors that should be used.

Additionally in Instituto Nacional de Normalizacion [23] it can be found that a damping ratio of 5% is reasonable for reinforced concrete buildings.
A summary of all the relevant parameters is given in table L.4.

Parameter:	Value:
A_0 (m/s^2)	$0,4g = 3,924$
S	1,20
T_0 (s)	0,75
p	1,0
I	1,0 or 1,2
R	7
R_0	11
ζ	0,05

Table L.4: Relevant parameters for the modal analysis

L.5.2. Formulas

The following formulas are all obtained from Instituto Nacional de Normalizacion [23].

$$S_a = \frac{S * A_0 * \alpha}{R^* / I} \tag{L.1}$$

$$\alpha = \frac{1 + 4.5 * \left(\frac{T_n}{T_0}\right)^p}{1 + \left(\frac{T_n}{T_0}\right)^3} \tag{L.2}$$

$$R^* = 1 + \frac{T^*}{0.1 * T_0 + \left(\frac{T^*}{R_0}\right)} \tag{L.3}$$

Where T^* is the period of the mode with the highest translational equivalent mass in the direction of analysis, which can be obtained from Etabs after running the modal analysis.

L.5.3. Design response spectrum of the building

Etabs can generate the response spectrum using the Chilean code itself, however for the sake of apprehension and verification the spectrum has also been formed using Excel. Etabs uses a scale factor which is defined by $\left[\frac{1}{R^*} * g\right]$ and it plots $S * \frac{A_0}{g} * I * \alpha$, which together makes S_a. This is done because R^* is the only term that depends on T^*, which depends on the model; all the other terms are fixed.

Figure L.6 shows the spectrum that is generated by Excel using the parameters from section L.5. The two lines show the difference between the use of parameter I, which describes the importance category of the building. $I = 1,0$ describes a ordinary residential building as the Altamar building is at the moment and $I = 1,2$ describes a building with a evacuation function.

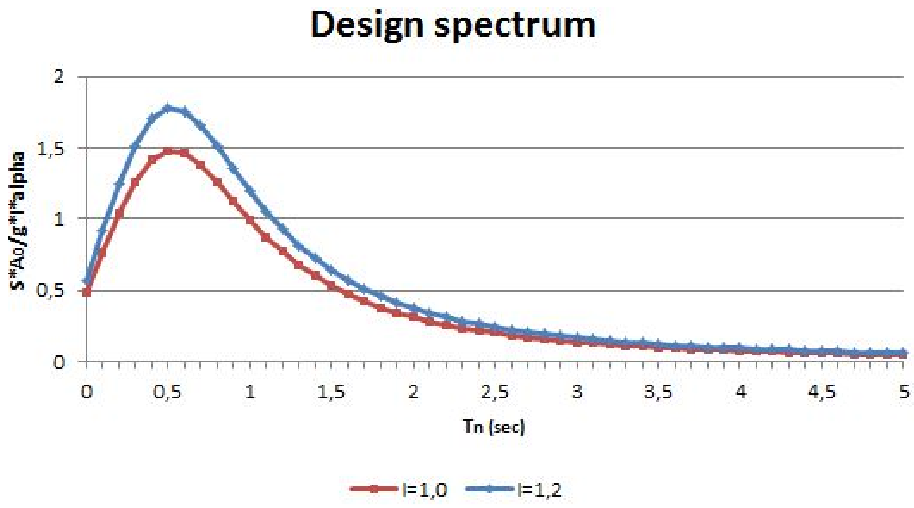

Figure L.6: Response spectrum generated using Excel

L.5.4. Scale factor

The scale factor defined by $[\frac{1}{R^*} * g]$ depends on T^*. After running the modal analysis the mode with the highest mass participation ratio can be determined, both in x and in y direction. The period of this mode is given by Etabs and must be used to determine the scale factor. In appendix L the iterative procedure to optimize the model of the building is described. The final model has a T_x^* value of 1,116 s and a T_y^* value of 1,002 s. Table L.5 shows the scale factors for the x and y direction.

	T^* (s)	R^*	Scale factor (mm/s^2)
x	1,116	7,329388	1338,447
y	1,002	7,032841	1394,884

Table L.5: Determination of the scale factor

M

Final model Altamar building

On the 7th of October 2016 Dr. Rafael Aranguiz provided us with the official structural drawings and information from the local authorities. Although, this was almost too late to incooperate in our project, we did incooperate some of it anyway.

M.1. Response Spectrum Analysis

Following the same procedure as in appendix L.5 the response spectrum analysis was performed again using the new soil information. The soil category was initially assumed to be D, which was a conservative assumption. However, in the official structural information about the building it states that soil category B is used.

M.1.1. Modal Analysis

A modal analysis is performed to determine the natural mode shapes and eigenfrequencies of a structure during free vibration, for it is assumed that during forced vibrations the mode shape will be a superposition of the eigenvectors multiplied with a certain unknown time function. Eigenvectors describe the natural mode shapes, therefore the particular solution (response of forced vibrations) is assumed to be a summation of eigenvectors each weighed with an unknown time function:

$$\underline{x}(t) = \sum_{i=1}^{n} \underline{\hat{x}} u_i(t) = E\underline{u}(t) \tag{M.1}$$

Where E is the eigenmatrix which contains all the eigenvectors as collumns. This information has been obtained from Spijkers et al. [44].

If the eigenvectors and eigenvalues of a structure are known the response of the building to a certain earthquake can be estimated. In order to do this the earthquake is represented as a spectrum which depends on the seismic region, the soil category and the building category. This is described in section L.5.

M.1.2. Seismic weight

The modal analysis needs to be carried out using the seismic weight of the building. In the Chilean code the seismic weight of a structure is defined as:

$$P = PP + 0,5 * SC \tag{M.2}$$

Where PP is the permanent load and SC is the live load.

The dead weight of the total building can be extracted from the model in Etabs and has appeared to be 105.470,9 kN.

From table 3 in Instituto Nacional de Normalizacion [22] live loads for several uses can be retrieved. For an ordinary living space a maximum live load of 2,5 kPa is mentioned. When many people seek refuge in the Altamar building during a tsunami the live load might turn out to be higher than this value, therefore a value of 3 kPa (=300 kg/m^2) is used from now on. The model of the Altamar building has a floor area of 341,91 m^2.

This gives a total live load on the building of:

$$\begin{aligned} 341,91 * 26 &= 8889,66\ m^2 \\ \frac{8889,66 * 300 * 9,81}{1000} &= 26.162,27\ kN \end{aligned} \tag{M.3}$$

To add 0,5*SC to the structure for the modal analysis the thickness of the floors has been adjusted as follows:

$$\begin{aligned} \frac{0,5 * SC}{26} = \frac{26.162,27 * 0,5}{26} &= 503,121\ kN \\ \frac{503,121}{25 * 341,91} &= 0,05886\ m \\ &= 58,86\ mm \end{aligned} \tag{M.4}$$

Where $\rho_c = 25\ kN/m^3$ is the weight of concrete. The original floor thickness is 18 cm. To add 0,5*SC every floor needs an increased thickness of $180 + 58,86 = 238,86\ mm$.

M.1.3. Parameters

Table M.1 shows the altered parameters based on the new information. Only S, T_0, and p are changed because of the different soil category.

Parameter:	Value:
A_0 (m/s^2)	$0,4g = 3,924$
S	1,0
T_0 (s)	0,30
p	1,5
I	1,0 or 1,2
R	7
R_0	11
ζ	0,05

Table M.1: Relevant parameters for the modal analysis

M.1.4. Design response spectrum of the building

Etabs can generate the response spectrum using the Chilean code itself, however for the sake of apprehension and verification the spectrum has also been formed using Excel. Etabs uses a scale factor which is defined by $\left[\frac{1}{R^*} * g\right]$ and it plots $S * \frac{A_0}{g} * I * \alpha$, which together makes S_a. This is done because R^* is the only term that depends on T^*, which depends on the model; all the other terms are fixed.

Figure M.1 shows the spectrum that is generated by Excel using the parameters from section M.1. The two lines show the difference between the use of parameter I, which describes the importance category of the building. $I = 1,0$ describes a ordinary residential building as the Altamar building is at the moment and $I = 1,2$ describes a building with a evacuation function.

M.1.5. Scale factor

The scale factor defined by $\left[\frac{1}{R^*} * g\right]$ depends on T^*. After running the modal analysis the mode with the highest mass participation ratio can be determined, both in x and in y direction. The period of this mode is given by Etabs and must be used to determine the scale factor. Values of $T_x^* = 0,651s$ and $T_y^* = 0,996s$ have been found. Table M.2 shows the scale factors for the x and y direction.

	T^* (s)	R^*	Scale factor (mm/s^2)
x	0,651	8,2997	1181,971
y	0,996	9,262	1059,116

Table M.2: Determination of the scale factor

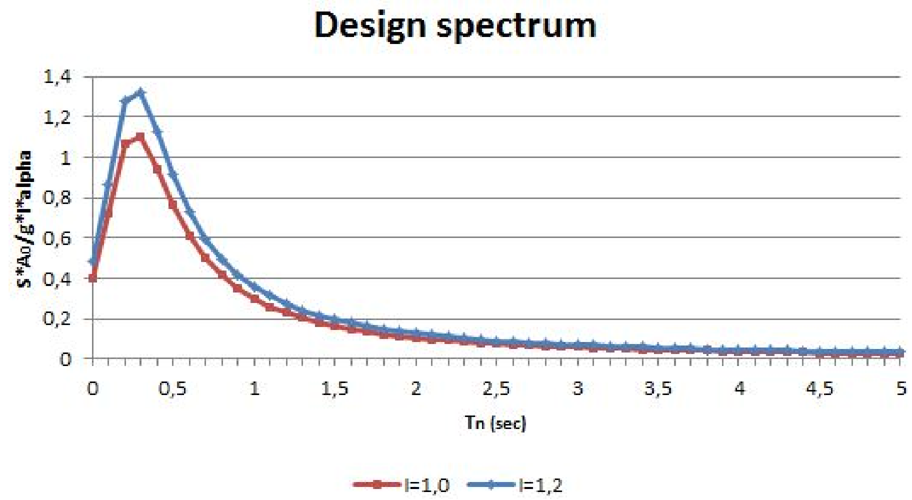

Figure M.1: Design response spectrum generated using Excel

N
Earthquake forces

N.1. Earthquake records

At first the earthquake records from the September 2015 earthquake are used as input for the time-history function in Etabs. The used records come from the measurement station that is indicated in figure N.1. This is less than a kilometer from the location of the Altamar building.

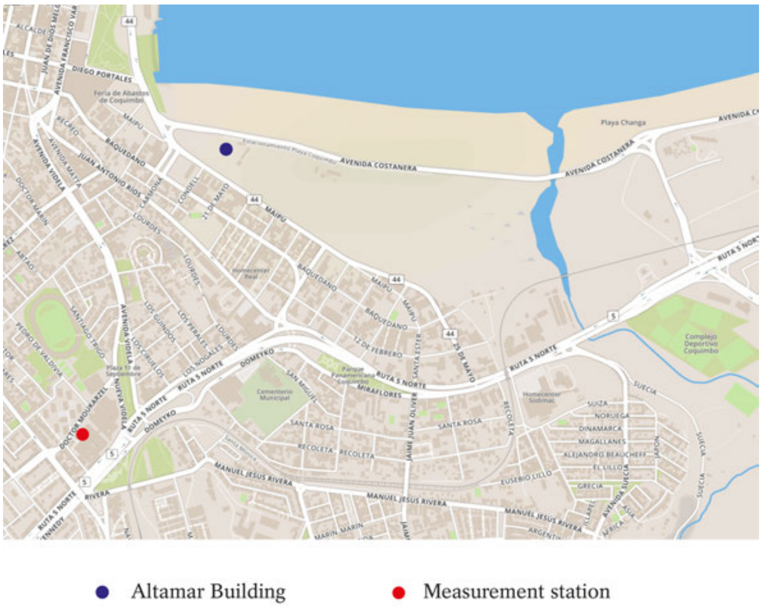

Figure N.1: The location of the measurement station

Figures N.2 and N.3 show the time-history records of the earthquake of September 2015.

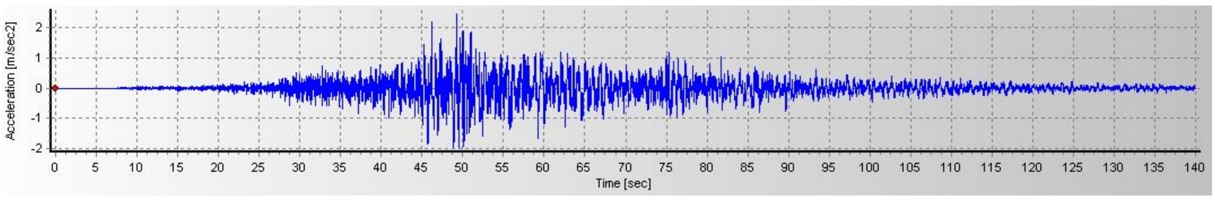

Figure N.2: Earthquake records in the direction from North to South

The records in North to South direction will be the input in U1 direction. The short side of the building is approximately parallel to the beach and the long side is approximately perpendicular to the beach and the x-

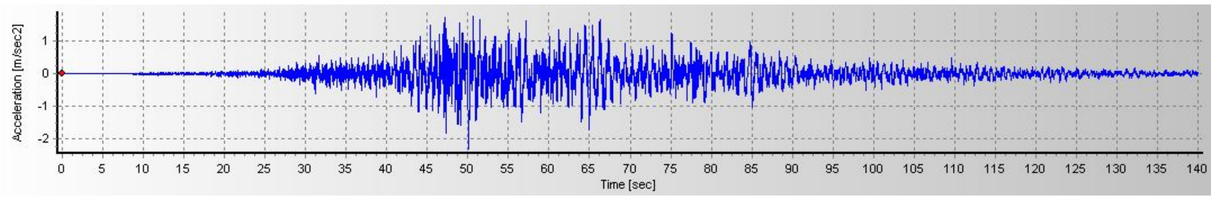

Figure N.3: Earthquake records in the direction from East to West

direction in the model is the long side, which makes the direction North to South coincide with the U1 direction in the model. The records in East to West direction will therefore be used as input in the U2 direction.

N.1.1. Upscaling of earthquake records

These records need to be upscaled to better match the worst case scenario as mentioned in appendix E. The epicentre of the earthquake of September 2015 was close to Illapel, which lies approximately 250 km South of Coquimbo. The distance from the epicentre has an influence on the intensity of the earthquake felt at a specific location. A measurement station closer to Illapel was located, as shown in figure N.4. Unfortunately, no information closer to Illapel could be retrieved. It is not possible to simply use these records, but we have

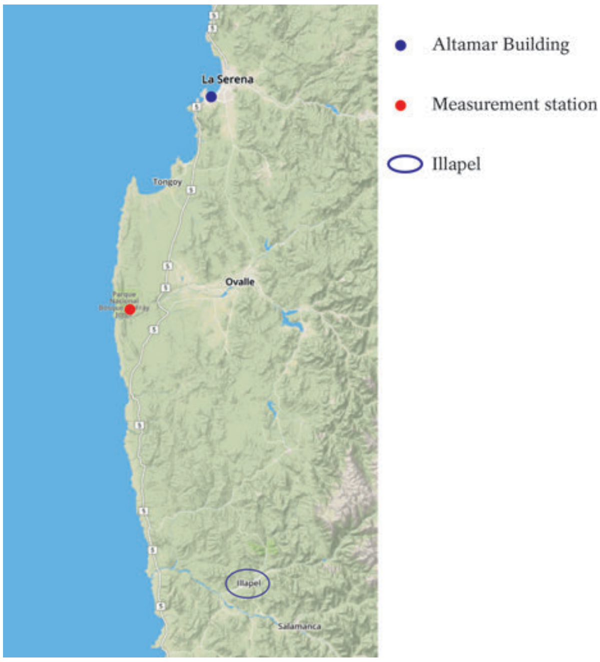

Figure N.4: Location of the measurement station closest to Illapel

to match the spectrum of the Coquimbo records to the records closer to Illapel. This is because of geological differences of the locations, for example the soiltype has an influence on the way the effects of an earthquake are felt at a certain location.

To match the spectrum of the earthquake records from this location to the spectrum of the records from the Coquimbo measurement station SeismoMatch software was used.

> "*SeismoMatch is an application capable of adjusting earthquake accelerograms to match a specific target response spectrum, using the wavelets algorithm proposed by Abrahamson [1992] and Hancock et al. [2006].*" Source: http://seismosoft.com/seismomatch

According to Eurocode 8 the matching should be done between periods of $0,2T_1$ and $2,0T_1$ in each direction. For T_1 the generated T^* values can be used. This means that for x-direction a span of 0,1302 up to 1,302 is taken into account and in y-direction a span of 0,1992 up to 1,992. The matched spectra are shown in figure N.5. It is clear that between the mentioned spans of periods the spectra match rather well.

The earthquake also needs to be upgraded from a 8.3 Mw. to a 8.5 Mw. earthquake. An 8.5 Mw. earthquake releases twice as much energy as an 8.3 Mw. earthquake, which is significant. Unfortunately the process of upscaling the magnitude of an earthquake is very extensive and difficult, therefore we haven't been able to do this.

The SeismoMatch software is able to generate the final time-history data files. These are shown in figure 13.1 and 13.2. For the time-history function in Etabs only the most severe one is used as input, because the difference is negligible and the processing of the input files takes a long time.

N.2. Nonlinear time-history analysis

For the nonlinear time-history analysis some parameters needed to be considered and adapted to the correct values.

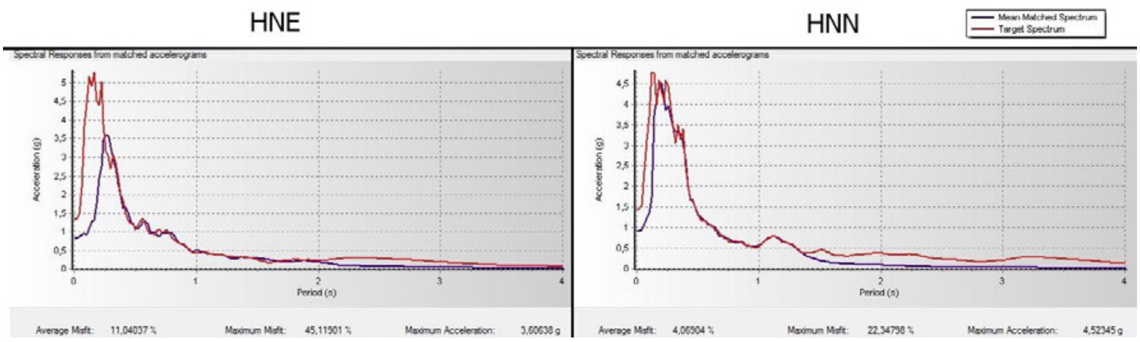

Figure N.5: Matched spectra using SeismoMatch

N.2.1. Damping

The direct-integration method in Etabs uses mass- and stiffness-proportional damping, which in fact is just another name for Rayleigh damping. The theory states that during formulation of the damping matrix it is assumed to be proportional to the mass and stiffness matrix like:

$$C = \eta M + \delta K \tag{N.1}$$

Where η is the mass-proportional damping coefficient and δ is the stiffness-proportional damping coefficient. With this formulation the damping ratio is the same for axial, bending and torsional response. Rayleigh damping results in different damping ratios for different response frequencies according to:

$$\xi = \frac{1}{2}\left(\frac{\eta}{\omega_n} + \delta\omega_n\right) \tag{N.2}$$

Where ξ is the critical damping ratio, where 1 is critical damping and ω is the response frequency.

So, the critical damping ratio depends on the natural frequency. The values of the coefficients η and δ are usually selected according to engineering judgement. A damping ratio must be given to 2 known frequencies and then Etabs will be able to calculate the corresponding values for the coefficients. The 2 eigenmodes that have the highest mass participation ratios have been used, these are shown in table N.2. Table N.1 shows the obtained damping coefficients.

	x-direction:	y-direction:
Mass-proportional coefficient	0,7672	0,5253
Stiffness-proportional coefficient	0,00225	0,002887

Table N.1: Damping coefficients

N.2.2. Time-stepping algorithm

The following information is mainly obtained from Simone [43].

For dynamic simulations that include numerical damping often the Hilber-Hughes-Taylor method is used, also known as the α-method. This is also the method that Etabs has as a default setting.

The method uses the Newmark algorithm, which gives a_{n+1} and $\dot{a}_{n+1}$ as:

$$\begin{aligned} a_{n+1} &= a_n + \Delta t \dot{a}_n + \frac{\Delta t^2}{2}\left(\left(1-2\beta\right)\ddot{a}_n + 2\beta\ddot{a}_{n+1}\right) \\ \dot{a}_{n+1} &= \dot{a}_n + \Delta t\left(\left(1-\gamma\right)\ddot{a}_n + \gamma\ddot{a}_{n+1}\right) \end{aligned} \tag{N.3}$$

Subsequently the Hilber-Hughes-Taylor method solves:

$$M\ddot{a}_{n+1} + (1+\alpha)C\dot{a}_{n+1} - \alpha C\dot{a}_n + (1+\alpha)Ka_{n+1} - \alpha Ka_n = f_{n+1+\alpha} \tag{N.4}$$

Where $f_{n+1+\alpha} = f_{n+1+\theta\Delta t}$. Clearly this is an implicit scheme.

For $\alpha = 0$ the Hilber-Hughes-Taylor method is equal to the Newmark scheme with $\beta = 1/4$ and $\gamma = 1/2$, which is also called the trapezoidal rule. This scheme solves:

$$M\ddot{a}_{n+1} + C\dot{a}_{n+1} + Ka_{n+1} = f_{n+1} \tag{N.5}$$

To include numerical damping γ needs to be higher than $\frac{1}{2}$. For $\gamma > \frac{1}{2}$ the Newmark scheme reduces to first order accuracy. The Hilber-Hughes-Taylor method has second-order accuracy while allowing for numerical damping, therefore this method is preferred.

The Hilber-Hugher-Taylor method is unconditionally stable for:

$$\begin{aligned} -\frac{1}{3} &< \alpha < 0 \\ \gamma &= \frac{(1-2\alpha)}{2} \\ \beta &= \frac{(1-\alpha)^2}{4} \end{aligned} \tag{N.6}$$

Etabs has these formulas in-cooperated; when the value for α is changed, it automatically changes the values for γ and β as well. The method is always unconditionally stable that way.

Concerning the α value that should be used, the eigenmodes of the model must be evaluated. Figure N.6 shows a graph from Celaya and Anza [6]. h is the time-step size of the time-history function, T is the period of an eigenmode of the structure, ρ can be interpreted as the amount of numerical damping, where 1,0 is no numerical damping. The 5 eigenmodes with the highest mass participation ratio shouldn't be damped out.

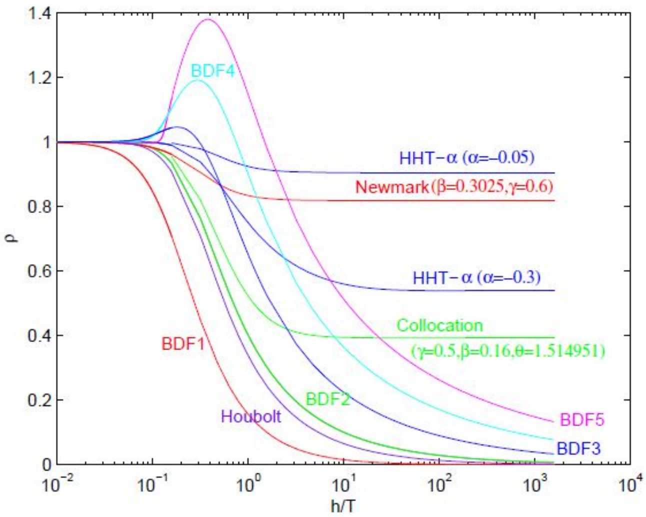

Figure N.6: Celaya and Anza [6]

Table N.2 shows these periods in both x and y direction. Together these modes make up to 95% of the complete

	x-direction:	y-direction:
T_1	0,637 s	0,973 s
T_2	0,182 s	0,223 s
T_3	0,599 s	0,847 s
T_4	0,095 s	0,248 s
T_5	0,064 s	0,106 s

Table N.2: Periods of 5 eigenmodes with highest mass participation in both directions

mass participation. The smallest period is 0,064 s. To not damp this mode out h/T should be lower than 10^{-1}. This gives a maximum time-step size of:

$$\begin{aligned} h/T &< 10^{-1} \\ h/0,064 &= 10^{-1} \\ h &= 0,0064\ s \end{aligned} \tag{N.7}$$

We have data with a stepsize of 0,005 s, which is sufficient. From this it is concluded that for the model of the Altamar building it doesn't matter what value for α is used in the range of $0 < \alpha < -1/3$.

O

Tsunami forces on the Altamar building

In Federal Emergency Management Agency [17, ch.6] the different tsunami forces are elaborated in detail. This appendix only gives the specific values and calculations of the tsunami forces that work on the Altamar building.

O.1. Hydrodynamic force

For the hydrodynamic force the value of $(hu^2)_{max}$ is needed. This value can be taken from Equation 6-6 from Federal Emergency Management Agency [17, p. 73, ch.6] or can be obtained using data from a numerical simulation. As a numerical simulation has been done this data can be used. The worst case scenario has resulted in a water height and flow velocity over time as shown in figure O.1. The green line shows a numerical error as the flow velocity should be zero when the water height remains the same. However, this does not have impact on the computation of $(hu^2)_{max}$ as this value will probably occur in one of the peaks.

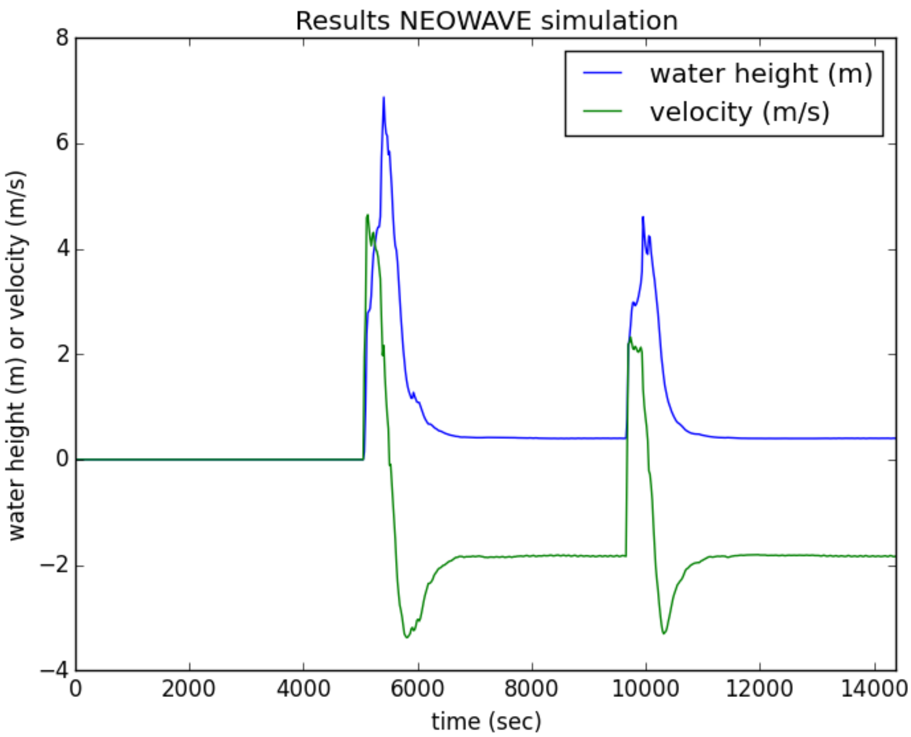

Figure O.1: Plot results water height and flow velocity

Using this data the value of $(hu^2)_{max}$ can be plotted over time as well. This is shown in figure O.2. The maxi-

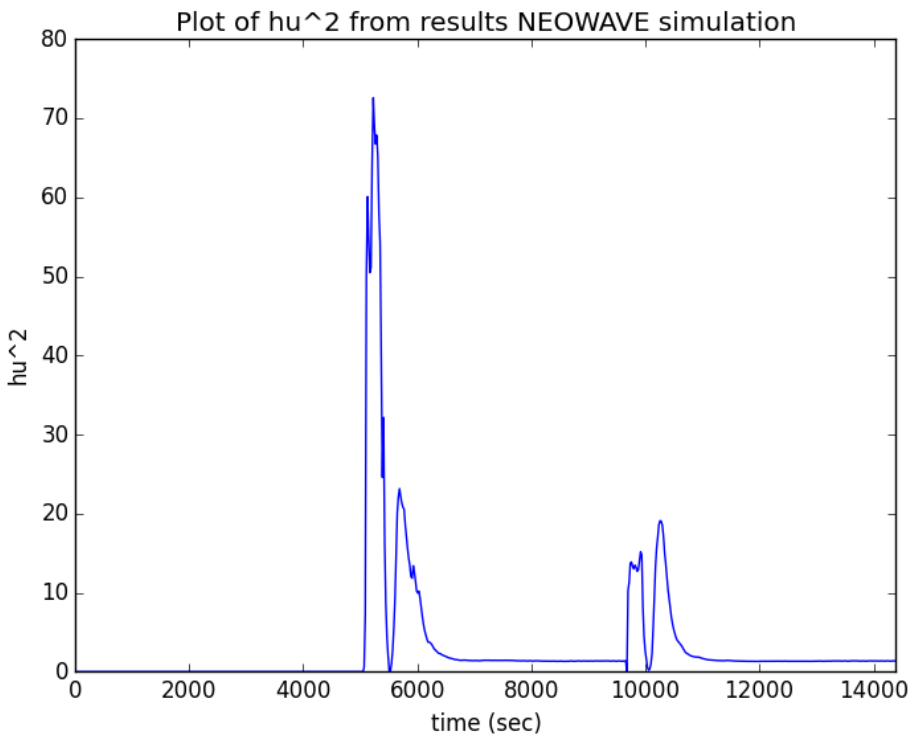

Figure O.2: Plot of $(hu^2)_{max}$ over time

mum value has been determined using a python script and has determined to be $(hu^2)_{max} = 72,5880899587\ m^3/s^4$.

The obtained value from the numerical simulation shouldn't be less than 80% of the value obtained using Equation 6-6. Equation 6-6 is given by:

$$(hu^2)_{max} = gR^2\left(0,125 - 0,235\frac{z}{R} + 0,11\left(\frac{z}{R}\right)^2\right) \tag{O.1}$$

Using the values of z and R^* from table 13.1 the result is:

$$\begin{aligned} R &= 1,3 * R^* = 13,852\ m \\ (hu^2)_{max} &= 9,81 * 13,852^2\left(0,125 - 0,235\frac{3,78}{13,852} + 0.11\left(\frac{3,78}{13,852}\right)^2\right) \\ &= 129,986\ m^3/s^4 \end{aligned} \tag{O.2}$$

80% of this value is $0,80 * 129,986 = 103,989\ m^3/s^4$. Clearly the value obtained using numerical simulation is too low. In order to meet the criteria of the Federal Emergency Management Agency [17] the value of $(hu^2)_{max} = 72,5880899587\ m^3/s^4$ needs to be adjusted up to $(hu^2)_{max} = 103,989\ m^3/s^4$. This is the value that will be used from now on.

The calculation of the hydrodynamic force is as follows:

$$\begin{aligned} F_d &= \frac{1}{2}\rho_s C_d (hu^2)_{max} \\ &= \frac{1}{2} * 1200 * 2,0 * 103,989 \\ &= 124787,3728\ N/m \\ \frac{F_d}{h_{max}} &= 12390,148\ N/m^2 \end{aligned} \tag{O.3}$$

O.1.1. Location of application

According to Federal Emergency Management Agency [17, p.73] the resultant force is applied approximately at half the height of h_{max}, which is the height of the wetted surface. However, in this case a surface load as has been computed. This load works uniformly from z=0 uptil z=h_{max}. The force works only on members, which the leading edge of the surge of the tsunami has already passed.

O.2. Impulsive force

The impulsive force is formulated and calculated as follows:

$$\begin{aligned} F_s &= 1,5F_d \\ &= 1,5 * 124787,3728 \\ &= 187181,0591\ N/m \\ \frac{F_s}{h_{max}} &= 18585,222\ N/m^2 \end{aligned} \tag{O.4}$$

O.2.1. Location of application

According to Federal Emergency Management Agency [17] the resultant force is applied approximately at half the height of h_{max}. However, similar to the application of the hydrodynamic force a uniform distribution of the surface load is assumed that works from z=0 uptil z=h_{max}. The impulsive force only work on members at the leading edge of the tsunami surge.

O.3. Debris impact force

In appendix K.1 the velocity of a standard ship container of 20ft is calculated. 80% of this velocity is used to calculate the Debris impact force, which is: $80\% * u_{max} = 8,968\ m/s$.

Again it turns out that the results from the numerical simulations with NEOWAVE don't provide a sufficient result. Federal Emergency Management Agency [17] states that a lowerbound value of 80% of u_{max} from figure 6-7 must be used in case of insufficient results from numerical simulations. This is used to calculate the debris impact force:

$$\begin{aligned} F_i &= \frac{C_m u_{max}\sqrt{km}}{L} \\ &= \frac{2,0 * 8,968 * \sqrt{1,5 * 10^9 * 2200}}{6,096} \\ &= 5344890,492\ N/m \end{aligned} \tag{O.5}$$

O.3.1. Location of application

The debris impact force only works locally on a single member. The resultant force works at the height of h_{max}, as the debris is assumed to be floating.

O.4. Damming of waterborne debris

The assumed debris is a 20-ft standard shipping container. This is approximately 6 m and therefore a lot smaller than the 15,75 m width of the front of the Altamar building. Therefore damming of waterborne debris has no relevant impact on the hydrodynamic force on the Altamar building.

O.5. Uplift forces on elevated floors

The first floor of the Altamar building is located at a height of 6 m and the second floor is located at a height of 8,4 m. When the water flow depth is higher than the height of the floor, it will prevent water from rising higher. In that case the water will push against the floor, this is a buoyant force. As h_{max} is 10,0715 m the second floor will flood completely as well as the first one, therefore the buoyant force works on the second floor with $h_b = 10,0715 - 6 - 2,4 + 0,18 = 1,8515\ m$. Federal Emergency Management Agency [17] states the following formula to calculate this force, which simply states the law of Archimedes:

$$\begin{aligned} f_b &= \rho_s g h_b \\ &= 1200 * 9,81 * (10,078 - 6 - 2,4 + 0,18) \\ &= 21795,858\ N/m^2 \end{aligned} \tag{O.6}$$

Where 0,18 meter is the thickness of the floor.

Furthermore, hydrodynamic forces can work vertically during rapid flooding. To calculate the resulting force the vertical flow velocity is necessary. This can be estimated using:

$$\begin{aligned} u_v &= u\ tan\alpha \\ &= 3,337 * tan(0,0378) \\ &= 0,127598705\ m/s \end{aligned} \tag{O.7}$$

Federal Emergency Management Agency [17] gives a formula that estimates the resulting vertical uplift force on the floor system:

$$\begin{aligned} f_u &= \frac{1}{2} C_u \rho_s u_v^2 \\ &= \frac{1}{2} * 3,0 * 1200 * 0,127598705^2 \\ &= 29,30657298\ N/m^2 \end{aligned} \tag{O.8}$$

O.6. Additional gravity loads on elevated floors

When the water of the tsunami is drawn back, there might be some water retained at the second floor of the Altamar building. According to Federal Emergency Management Agency [17] the retained water can have a maximum height of:

$$\begin{aligned} h_r &= h_{max} - 6 - 2,4 \\ &= 10,078 - 6 - 2,4 = 1,672\ m \end{aligned} \tag{O.9}$$

The maximum additional gravity load will then be:

$$\begin{aligned} f_r &= \rho_s g h_r \\ &= 1200 * 9,81 * 1,672 \\ &= 19676,898\ N/m^2 \end{aligned} \tag{O.10}$$

P

Results simulation of the Altamar building

Table P.1 shows the maximum displacement and base reactions for several different simulation runs of the model in Etabs.

For the displacement results in x and y-direction and the base moments in all directions are presented as the absolute maximum value found during all load cases and load combinations.

ux-1 is the maximum value of the displacement in x-direction, which is found in the wall in the middle of the stairs. This wall is in our model on one side only supported by a beam and not by a floor. In reality there's a staircase, the expectation is that this staircase makes this part of the building behave slightly stiffer than the model. Therefore also ux-2 is presented, which is the largest displacement in x-direction found in other parts of the building. For all different results this happens to be at the location where the debris impact force hits the building. As this force is rather large, this is not unexpected.

A remark should be made by the value of My which is largest for the dead load loadcase. As the building is not symmetrical it rotates slightly under its selfweight, which causes a rather large base moment.

P.1. Story Drift

In the tables P.2 upto P.5 story drifts on several locations are presented. Tables P.2 and P.3 present the story drifts measured in a point near the center om mass of each story. Tables P.4 and P.5 present the maximum story drift in the outer corner of the building.

in the tables P.2 and P.3 the drift percentages are obtained through equation 14.1. In the tables P.4 and P.5 the drift check percentages are obtained through equation 14.2.

	Joint displacements				Base reactions					
	ux-1 [mm]	ux-2 [mm]	uy [mm]	uz [mm]	Fx [kN]	Fy [kN]	Fz [kN]	Mx [kNm]	My [kNm]	Mz [kNm]
Run 1										
Value:	63,283	15,972	7,591	-6,105	34787,03	-661,33	105470,90	840454,40	1441772,0	275044,0
Location:	Story 3	Story 5	Roof	Roof						
Load combination:	EqX+TS		EqY+TS	EqY+TS	EqX+TS	EqY+TS	Dead load	EqY+TS	Dead load	EqY+TS
Run 2										
Value:	63,774	16,019	7,633	-6,125	35111,15	-830,22	105470,90	840454,40	1441772,0	276026,0
Location:	Story 3	Story 5	Roof	Roof						
Load combination:	EqX+TS		EqY+TS	EqX+TS	EqX+TS	EqY+TS	Dead load	EqY+TS	Dead load	EqY+TS
Run 3										
Value:	63,62	15,993	7,579	-6,123	34913,48	-731,71	105470,90	839638,65	1441772,0	274962,0
Location:	Story 3	Story 5	Roof	Roof						
Load combination:	EqX+TS		EqY+TS	EqX+TS	EqX+TS	EqY+TS	Dead load	EqY+TS	Dead load	EqY+TS
Run 4										
Value:	63,164	18,232	7,82	-6,254	34756,73	-647,41	105470,90	840654,90	1441772,0	274601,0
Location:	Story 3	Story 5	Roof	Roof						
Load combination:	EqX+TS		EqY+TS	EqY+TS	EqX+TS	EqY+TS	Dead load	EqY+TS	Dead load	EqY+TS

Table P.1: Overview results different runs

Story	UX [mm]	Drift [mm]	Drift check [%]	UY [mm]	Drift [mm]	Drift check [%]
1	0.000	0.000	0.000	0.000	0.000	0.000
2	-1.297	0.054	0.054	-0.054	-0.054	0.002
3	-2.554	-0.002	0.052	-0.103	-0.049	0.002
4	-3.194	-0.026	0.027	-0.113	-0.010	0.000
5	-3.576	-0.011	0.016	-0.085	0.028	0.001
6	-3.721	-0.010	0.006	-0.050	0.035	0.001
7	-3.770	-0.004	0.002	-0.011	0.039	0.002
8	-3.777	-0.002	0.000	0.034	0.045	0.002
9	-3.761	0.000	0.001	0.088	0.054	0.002
10	-3.730	0.001	0.001	0.151	0.063	0.003
11	-3.687	0.001	0.002	0.223	0.072	0.003
12	-3.636	0.000	0.002	0.305	0.082	0.003
13	-3.576	0.000	0.003	0.395	0.090	0.004
14	-3.510	0.000	0.003	0.494	0.099	0.004
15	-3.438	0.000	0.003	0.600	0.106	0.004
16	-3.360	0.000	0.003	0.713	0.113	0.005
17	-3.278	0.000	0.003	0.833	0.120	0.005
18	-3.191	0.000	0.004	0.958	0.125	0.005
19	-3.100	0.000	0.004	1.089	0.131	0.005
20	-3.005	0.000	0.004	1.225	0.136	0.006
21	-2.906	0.000	0.004	1.365	0.140	0.006
22	-2.804	0.000	0.004	1.509	0.144	0.006
23	-2.708	0.000	0.004	1.655	0.146	0.006
24	-2.617	0.000	0.004	1.805	0.150	0.006
25	-2.521	0.000	0.004	1.955	0.150	0.006
26	-2.421	0.000	0.004	2.107	0.152	0.006
Roof	-2.315	0.000	0.004	2.257	0.150	0.006

Table P.2: Story drift per story in center of mass triggered by the earthquake in X-direction and the tsunami forces

Story	UX [mm]	Drift [mm]	Drift check [%]	UY [mm]	Drift [mm]	Drift check [%]
1	0.000	0.000	0.000	0.000	0.000	0.000
2	-1.289	-1.289	0.054	-0.019	-0.019	0.001
3	-2.533	-1.244	0.052	-0.028	-0.009	0.000
4	-3.160	-0.627	0.026	0.009	0.037	0.002
5	-3.525	-0.365	0.015	0.094	0.085	0.004
6	-3.653	-0.128	0.005	0.192	0.098	0.004
7	-3.684	-0.031	0.001	0.299	0.107	0.004
8	-3.673	0.011	0.000	0.415	0.116	0.005
9	-3.638	0.035	0.001	0.539	0.124	0.005
10	-3.587	0.051	0.002	0.673	0.134	0.006
11	-3.443	0.144	0.006	0.815	0.142	0.006
12	-3.358	0.085	0.004	0.963	0.148	0.006
13	-3.369	-0.011	0.000	1.116	0.153	0.006
14	-3.281	0.088	0.004	1.293	0.177	0.007
15	-3.186	0.095	0.004	1.484	0.191	0.008
16	-3.085	0.101	0.004	1.683	0.199	0.008
17	-2.980	0.105	0.004	1.888	0.205	0.009
18	-2.870	0.110	0.005	2.098	0.210	0.009
19	-2.756	0.114	0.005	2.312	0.214	0.009
20	-2.638	0.118	0.005	2.531	0.219	0.009
21	-2.518	0.120	0.005	2.753	0.222	0.009
22	-2.394	0.124	0.005	2.977	0.224	0.009
23	-2.269	0.125	0.005	3.203	0.226	0.009
24	-2.142	0.127	0.005	3.430	0.227	0.009
25	-2.013	0.129	0.005	3.658	0.228	0.009
26	-1.883	0.130	0.005	3.885	0.227	0.009
Roof	-1.749	0.134	0.006	4.111	0.226	0.009

Table P.3: Story drift per story in center of mass triggered by the earthquake in Y-direction and the tsunami forces

Story	UX [mm]	Drift [mm]	Drift [%]	Drift check [%]	UY [mm]	Drift [mm]	Drift [%]	Drift check [%]
1	0.000	0.000	0.000	0.000	0.000	0.000	0.000	0.000
2	0.000	0.000	0.000	0.002	0.000	0.000	0.000	0.002
3	-2.361	-2.361	-0.098	0.098	-0.659	-0.659	-0.027	0.025
4	-3.375	-1.014	-0.042	0.041	-0.912	-0.253	-0.011	0.010
5	-3.507	-0.132	-0.006	0.005	-0.825	0.087	0.004	0.002
6	-3.408	0.099	0.004	0.005	-0.791	0.034	0.001	0.000
7	-3.335	0.073	0.003	0.003	-0.849	-0.058	-0.002	0.004
8	-3.268	0.067	0.003	0.003	-0.909	-0.060	-0.003	0.004
9	-3.188	0.080	0.003	0.003	-0.972	-0.063	-0.003	0.005
10	-3.092	0.096	0.004	0.004	-1.035	-0.063	-0.003	0.005
11	-2.981	0.111	0.005	0.005	-1.098	-0.063	-0.003	0.006
12	-2.858	0.123	0.005	0.005	-1.160	-0.062	-0.003	0.006
13	-2.723	0.135	0.006	0.006	-1.221	-0.061	-0.003	0.006
14	-2.577	0.146	0.006	0.006	-1.281	-0.060	-0.002	0.007
15	-2.423	0.154	0.006	0.006	-1.339	-0.058	-0.002	0.007
16	-2.261	0.162	0.007	0.007	-1.395	-0.056	-0.002	0.007
17	-2.091	0.170	0.007	0.007	-1.448	-0.053	-0.002	0.007
18	-1.914	0.177	0.007	0.007	-1.500	-0.052	-0.002	0.007
19	-1.731	0.183	0.008	0.008	-1.550	-0.050	-0.002	0.008
20	-1.542	0.189	0.008	0.008	-1.598	-0.048	-0.002	0.008
21	-1.348	0.194	0.008	0.008	-1.645	-0.047	-0.002	0.008
22	-1.149	0.199	0.008	0.008	-1.691	-0.046	-0.002	0.008
23	-0.946	0.203	0.008	0.008	-1.735	-0.044	-0.002	0.008
24	-0.739	0.207	0.009	0.009	-1.779	-0.044	-0.002	0.008
25	-0.539	0.200	0.008	0.008	-1.821	-0.042	-0.002	0.008
26	-0.344	0.195	0.008	0.008	-1.862	-0.041	-0.002	0.008
27	-0.151	0.193	0.008	0.008	-1.901	-0.039	-0.002	0.008

Table P.4: Story drift per story in extreme corner triggered by the earthquake in X-direction and the tsunami forces, control of demand

Story	UX [mm]	Drift [mm]	Drift [%]	Drift check [%]	UY [mm]	Drift [mm]	Drift [%]	Drift check [%]
1	0.000	0.000	0.000	0.000	0.000	0.000	0.000	0.000
2	0.000	0.000	0.000	0.054	0.000	0.000	0.000	0.001
3	-2.360	-2.360	0.098	0.047	-0.719	-0.719	0.030	0.030
4	-3.368	-1.008	0.042	0.016	-1.013	-0.294	0.012	0.014
5	-3.494	-0.126	0.005	0.010	-0.976	0.037	0.002	0.002
6	-3.388	0.106	0.004	0.010	-1.001	-0.025	0.001	0.005
7	-3.307	0.081	0.003	0.005	-1.124	-0.123	0.005	0.010
8	-3.232	0.075	0.003	0.003	-1.255	-0.131	0.005	0.010
9	-3.142	0.090	0.004	0.002	-1.392	-0.137	0.006	0.011
10	-3.036	0.106	0.004	0.002	-1.534	-0.142	0.006	0.012
11	-2.914	0.122	0.005	0.001	-1.680	-0.146	0.006	0.012
12	-2.779	0.135	0.006	0.002	-1.827	-0.147	0.006	0.012
13	-2.631	0.148	0.006	0.007	-1.975	-0.148	0.006	0.013
14	-2.472	0.159	0.007	0.003	-2.123	-0.148	0.006	0.014
15	-2.304	0.168	0.007	0.003	-2.270	-0.147	0.006	0.014
16	-2.127	0.177	0.007	0.003	-2.416	-0.146	0.006	0.014
17	-1.942	0.185	0.008	0.003	-2.560	-0.144	0.006	0.015
18	-1.750	0.192	0.008	0.003	-2.701	-0.141	0.006	0.015
19	-1.552	0.198	0.008	0.003	-2.841	-0.140	0.006	0.015
20	-1.347	0.205	0.009	0.004	-2.977	-0.136	0.006	0.015
21	-1.138	0.209	0.009	0.004	-3.111	-0.134	0.006	0.015
22	-0.924	0.214	0.009	0.004	-3.242	-0.131	0.005	0.015
23	-0.707	0.217	0.009	0.004	-3.371	-0.129	0.005	0.015
24	-0.488	0.219	0.009	0.004	-3.496	-0.125	0.005	0.015
25	-0.269	0.219	0.009	0.004	-3.618	-0.122	0.005	0.015
26	-0.051	0.218	0.009	0.004	-3.737	-0.119	0.005	0.014
27	0.162	0.213	0.009	0.003	-3.852	-0.115	0.005	0.014

Table P.5: Story drift per story in extreme corner triggered by the earthquake in Y-direction and the tsunami forces, control of demand

Q

Evacuation Routes

Evacuation Routes
Within the city of Coquimbo there is a micro-zoning evacuation system, which divides the city in different sectors. This division gives more structure in the tsunami mitigation and evacuation routes. The most relevant sectors for the scope of the project given by Secretaria Regional Minesterial De Vivienda y Urbanismo Coquimbo [41] are:

- Baquedano, Victoria and Porvenir
  This area contains inhabitants with a lower income. Main occupations are garages, tankstations, schools, colleges and a revalidation centre. Evacution is established by south directed avenues.
- Centro, Avenida Costanera, Puerto and Caleta Coquimbo
  In this area there is a lot of employment, tourism and education. This includes a market, fisshing port, bus terminal, different schools and different public buildings. Multiple evacuation routes gives the option to reach uphill.

In figure Q.1, an inundation map of Coquimbo is given, together with the evacuation routes.

Figure Q.1: The inundation level and different evacuation routes along the Coquimbo Bay, source: Secretaria Regional Minesterial De Vivienda y Urbanismo Coquimbo [41]

siting of evacuation routes
In the Federal Emergency Management Agency [17] there is a distinction made between three types of tsunamis: far-source-generated tsunami, mid-source-generated tsunami, and near-source tsunami. For the design of

the evacuation routes in the master plan only the near-source-tsunami will be considered. This because this tsunami has an approximate warning time of less than 30 min Federal Emergency Management Agency [17]. From the scenario where the design of the master plan is based on the warning time will be 15 min B. The lowest warning time in the Federal Emergency Management Agency [17] is also 15 min. Based on these times this will be the warning time where the evacuation routes will be based on. Based on the average walking speed of a mobility impaired population the average walking speed is assumed as 2-mph or 3,2 km/h Federal Emergency Management Agency [17]. With a warning time of 15 min a person can travel a distance of 800 meters in that time. This distance will be the maximum of what someone has to travel to arrive at a safe location.